Reinterpreting vintage geophysical data from the Algoa and Gamtoos Basins, South Africa: an integrated sequence stratigraphic framework since the middle Mesozoic

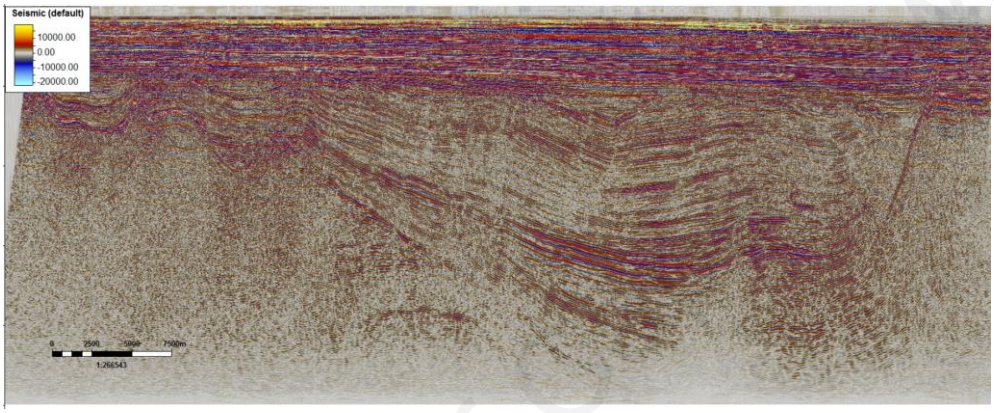

Marvel Hope Makhubele

A thesis submitted to the Faculty of Science, University of Cape Town, in fulfilment of the requirements for the
degree of Doctor of Philosophy

Supervisor: **Associate Professor Emese M Bordy**

Plagiarism declaration

I, **Marvel Hope Makhubele** hereby declare that the work on which this thesis is based is my original work (except where acknowledgements indicate otherwise) and that neither the whole work nor any part of it has been, is being, or is to be submitted for another degree in this or any other university. I authorise the University to reproduce for the purpose of research either the whole or any portion of the contents in any manner whatsoever.

Abstract

Sequence stratigraphy is a branch of stratigraphy that is concerned with how genetically related geological successions are deposited in time and space. This requires the integration of diverse types of datasets (drill core, outcrop, wireline, reflection seismic surveys, etc.) to build robust depositional models, the cornerstones of stratigraphic frameworks. Although the application of sequence stratigraphy has been a successful tool to predict the lithology of geobodies in the petroleum industry, terminology is inconsistently used by the different schools of thought to define stratigraphic surfaces. This has resulted in multiple sequence stratigraphic models that interpret the same data differently. The limited exploration, to-date, and poor dataset quality have impeded the understanding of the geological evolution of the offshore Algoa and Gamtoos Basins in the southern Cape region of South Africa. To reconstruct the main geological events in the area since the late Early Jurassic, we integrated vintage borehole and seismic data as well as key outcrop observations, generated contemporary gross depositional environment models for the basin fill, and tested the applicability of different sequence stratigraphic models. The studied stratigraphic interval formed since the inception of Gondwana break-up, in syn- and post-rift systems that were increasingly dominated by marine processes, especially in the distal hanging walls. Marine incursions are detected in the Upper and Middle Jurassic in the Algoa and Gamtoos Basins, respectively. However, the severely eroded Algoa Basin syn-rift succession, exacerbated by poor data quality, makes it challenging to understand the timing of the marine incursion in this compartmentalized half-graben. Sedimentation within these half-grabens primarily occurred above the hanging walls, whilst the footwalls (i.e., basement highs) formed the dominant sediment source areas. The geological characteristics of the studied syn-rift succession prevents the application of the depositional sequence stratigraphic or the tectonic system tracts models. Because subaerial unconformities (SUs) in the distal syn-rift sequence are not detectable, a diachronous, northward advancement of the shoreline until the late Valanginian can be postulated. The observations in the syn-rift sequence, which is bound by a basal SU, followed by third and fourth-order transgressive and regressive cycles and a second-order maximum flooding surface at the top, can be explained with a modified genetic sequence stratigraphic model. In the transitional to drift phase interval, from Hauterivian to Holocene, the successions are bound by third-order SUs and their correlative conformities. In the successions without evidence for subaerial exposure in the drift successions, flooding surfaces are used as sequence-bounding stratigraphic contacts, validating the applicability of the genetic and transgressive-regressive sequence stratigraphic models for this upper part of the studied stratigraphic interval. This study reaffirms the notion that while the sequence stratigraphic concept is model independent, sequence models are sensitive to depositional scale and data resolution. Moreover, it also reiterates that sequence boundaries should not be limited to subaerial unconformities, but rather to correlative surfaces that bound genetically related sedimentary successions.

Acknowledgements

First of all, I would like to acknowledge the strong-as-a-rock ladies in my life. Here, I would like to thank my supervisor, who took a chance on me as a part-time student and went out her way to make sure I complete my PhD in three years, despite having to juggle between professional commitments, (COVID) school and family. I could not have done this without your support, mentorship, friendship and guidance; I am forever indebted to you, thank you. I would also like to thank my incredible super-wife, Mulanga Makhubele who unwaveringly encouraged me every waking minute of this PhD. I would also like to express my sincere gratitude to my mother and sister, who never stopped praying, supporting and believing in me. To my smart, beautiful, funny and courageous daughter, Šīlōh Makhubele, thank you for being my light and inspiration, I love you greatly. To my amazing in-laws, I am very blessed and grateful for the love and care you showed me through-out this PhD journey.

To all my friends and extended family, thank you for being so patient with me, and for listening to me while I complain about the toughness of doing this PhD part time while working full time, having a young family and pulling off an intercontinental relocation in the middle of a pandemic. And thank you for being so understanding when I could not make it to your events or if I did, I had to leave early.

A special thanks to Chris Malaver, David Holmes, Richard Paterson, Gerhard Brinks, Duncan Barkwith and Richard Harris for reviewing various drafts of this thesis.

I would also like to acknowledge the Geological Society of South Africa for the REI funding of the dataset used in this project. I would also like to thank my current employer Tullow Oil allowing me the flexibility to concentrate on my studies and professional development. A sincere thanks to the Petroleum Agency SA for the provision of the dataset used in this study and permission to publish my results based on their data.

Lastly, to my lifelong academic mentor Uncle Dave Reid of UCT, I am endlessly grateful for all that you have done for me, and for your continuous support, I love you.

To the many women and men who helped me to be where I am today, thank you.

"I come as one, but I stand as ten thousand." – Maya Angelou

Content

1 Introduction

1.1 Aims and objectives

This thesis will reinterpret vintage dataset from the Algoa and Gamtoos Basins, with an aim to build an integrated sequence stratigraphic framework to understand mechanisms responsible for basin formation and development in these passive margin basins located near Port Elizabeth (renamed to Gqeberha in February 2021) in South Africa (Figure 1.1). Globally, in the past few decades, sequence stratigraphic models have been derived and tested, with a view to predict and build depositional models away from data control, especially in frontier basins. Using desktop-based interpretational software (i.e., Petrel E&P Software Platform), the following objectives are addressed:

1. Analyse and interpret the geological record in the Algoa and Gamtoos Basins, firstly by using basic principles of stratigraphy and process sedimentology (i.e., independent of any sequence stratigraphic school).

2. Understand the depositional mechanisms (autocyclic and/or allocyclic) responsible for seismic reflector geometries and sequence generation in these two basins in the southern Cape.

3. Compare stratal architecture defined by reflection seismic terminations observed in the dataset to stratigraphic boundaries and geometries defined by different sequence stratigraphic models.

4. Use the most appropriate sequence stratigraphic models to predict facies distribution in the basins, by testing the robustness of current models and highlighting their advantages and limitations in the study area.

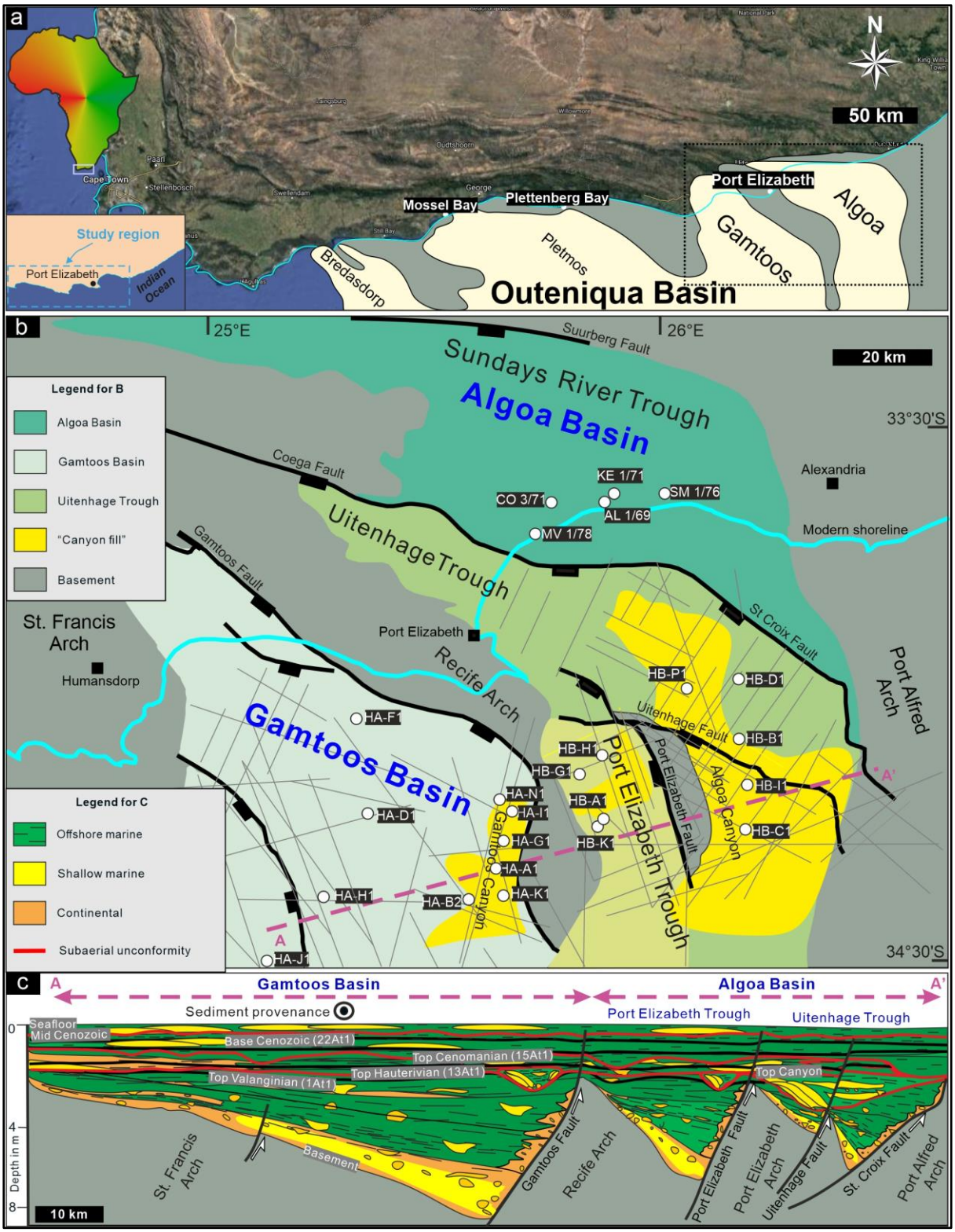

Figure 1.1 Simplified geological map and cross-section of the Algoa and Gamtoos Basins of South Africa (modified from McMillan et al., 1997; Broad et al., 2012; Muir at al., 2020). Base map data ©2020 Google, Maxar Technologies, AfriGIS (Pty) Ltd.).

1.2 The key problems

1.2.1 Standardising concepts and terminology used in sequence stratigraphy

This thesis uses datasets from the Algoa and the Gamtoos Basins of South Africa to test the advantages and limitations of some sequence stratigraphic models to understand the basin evolution of the study area. Sequence stratigraphy is a relatively modern branch of stratigraphy commonly used to understand the depositional history of a basin and often applied in the petroleum industry (Catuneanu, 2006, p.2). Sequence stratigraphy emphasises how genetically related successions were deposited in time and space, independent of scale (Mitchum et al., 1977; Neal et al., 1993; Catuneanu et al., 2011; Catuneanu, 2019a,b; Catuneanu and Zecchin, 2020). Despite serious collaborative scientific efforts in the past decade (e.g., Catuneanu et al., 2011) to stabilize the burgeoning terminology in the sequence stratigraphic method, the key terms are still inconsistently used by different schools not only to define stratigraphic surfaces but also to interpret the geological history of stratigraphic successions.

There are currently six conventional sequence stratigraphic models grouped into depositional, genetic and transgressive-regressive (T-R) sequence stratigraphic models (Embry et al., 2007; Catuneanu, 2002; Catuneanu et al., 2011). Depositional sequence models use subaerial unconformities and correlative conformities as sequence boundaries, while the genetic and T-R sequence stratigraphic models use shoreline trajectories (MFS and MRS) to define a sequence boundary (Catuneanu, 2006, p. 235-241; Embry et al., 2007; Catuneanu et al., 2011). Unlike other disciplines of stratigraphy (litho-, chrono-, magneto-, etc.), terminology in sequence stratigraphy has not yet been formalised (Catuneanu, 2002; Catuneanu et al., 2011). While North American Commission on Stratigraphic Nomenclature (NACSN) and the International Sub-commission on Stratigraphic Classification (ISSC) have in the past tried to formalise the nomenclature and terminology used in sequence stratigraphy, the various schools seem a bit inflexible (Catuneanu, 2007). However, Embry et al. (2007) argues that terminology should not be standardized, due to the already existing complex terminology. Dialogs and debates surrounding sequence stratigraphy terminology and concepts can be found on the Society for Sedimentary Geology (SEPM) website (http://www.sepmstrata.org).

1.2.2 Algoa and Gamtoos Basins summary

To-date, although 41 wells (22 onshore and 19 offshore) have been drilled between 1968 and 1990, there has been limited exploration success in the Algoa and Gamtoos Basins of South Africa (Malan, 1993; McMillan et al., 1997; Davids et al., 2017; New Age Energy Report, 2018). Additionally, over 5 000 km of 2D reflection seismic lines and two 3D reflection seismic surveys have been acquired in the study area (Malan, 1993; McMillan et al., 1997; New Age Energy Report, 2010; Davids et al., 2017; Petroleum Agency SA, 2020). Although extensive datasets have been acquired in the region in the past few decades, this, by-far vintage dataset ranges from poor to good quality, requiring reprocessing to improve imaging, especially in the deeper successions. Despite the discouraging drilling results to date, New Age Global Energy Company reported in 2018 that the Algoa Canyon, the syn-rift slope petroleum plays in the Gamtoos and Outeniqua Basins (Figure 1.1) could contain ~510 MMBOE (million barrels of oil equivalent) in-place resources (New Age Global Energy, 2018). Consequently, coupled with limited exploration success, contemporary basin development models for offshore Algoa and Gamtoos region are not available to date (e.g., Ayodele et al., 2020; Caku et al., 2020). This is partially due to the lack of robust data, but also due to the lack of re-interpretation of the existing data within a modern sequence stratigraphic paradigm. Herein, by combining the available data (seismic, wireline and some outcrop data), we generate conceptual models of the gross depositional environments (GDE), which are shown as maps. These GDE maps were derived from studying facies change, the vertical stacking pattern of facies in available wireline data, seismic geometries, and also by incorporating recent results from field studies conducted onshore from the study area. The results were then integrated into the updated sequence stratigraphic framework for these two basins situated along the southern Cape of South Africa.

1.3 Layout of the thesis

This thesis contains nine connected chapters, and their brief content is presented below. The current *Chapter 1* introduces the thesis and problems to be addressed, and briefly summarizes the main challenges, debates and conversations within the sequence stratigraphic community. This chapter also gives a brief overview on the geological and data limitations within the two basins and the implications of hydrocarbon potential in the study area.

Chapter 2 is the geological background of the Mesozoic Algoa and Gamtoos Basins. The geological and tectonic evolution of each basin is summarised to understand how and when basin infill was generated

from the late Early Jurassic to Holocene. This chapter also reviews the lithostratigraphy of the Enon, Kirkwood and Sundays River Formations, as well as the Cenozoic Algoa Group based on the outcrop and subsurface studies published to-date (e.g.,; Le Roux, 1987; McMillan, 1990; Illenberger, 1992; Muir et al., 2017a, b, 2020).

Chapter 3 covers the fundamental principles of the dataset used in this study, and addresses what seismic data is, how different lithologies respond to seismic energy, and the advantages and disadvantages of seismic data applied to sequence stratigraphy. It explains the process of well-to-seismic tie, showing how wireline and seismic data can be correlated to relate geological welltops with seismic reflectors. The chapter then reviews the variation of velocities in clastic successions, and how the frequency and velocity are used to estimate the resolution of the data. It also gives a summary on how gamma ray (GR), density (RHO), sonic (DT), spontaneous potential (SP) and photoelectric factor (PEF) logs respond to different lithologies in a borehole. In the overview of wireline logs, an explanation is given to how these logging tools operate, what they measure in formation, also highlighting the limitation and advantages of using wireline data. Although this thesis does not include new field data, the points on: 1) the importance of incorporating core and outcrop data, and 2) the role these datasets in building robust geological models are made. Field data are extracted from already published work (Hattingh, 2001; Muir et al., 2015, 2017a, b; Muir, 2019, etc.) conducted onshore the Algoa and Gamtoos Basins. Moreover, this chapter introduces the workflow use to build depositional models of the Algoa and Gamtoos Basins. This workflow was presented at the 2018 GeoCongress of the Geological Society of South Africa in Johannesburg, and at the 2018 ICE AAPG meeting in Cape Town.

Chapter 4 is a summary of key concepts, terminology and models used in sequence stratigraphy. It reviews parameters controlling relative and eustatic sea level as well as shoreline trajectories. It gives an overview of the 'global sea level chart' by Haq et al. (1987) and why this chart is not used in this study. Since different schools of thought use different surfaces to define a sequence, an overview of stratigraphic surfaces, highlighting their limitations and advantages, are given together with how these surfaces are used to package strata. The chapter also reviews stratal terminations to understand the association of stratal geometries to geological settings, and how stratal geometries can be used to restore shoreline trajectories. A summary of current sequence models (i.e., depositional, T-R and genetic sequence stratigraphic models), highlighting the main surfaces, similarities and difference between system tracts, and the limitations and strength of each model is also given. The chapter concludes with a high-level overview on how hierarchy is applied in sequence stratigraphy, and the constraints used to define and classify these hierarchical orders.

Chapters 0 and 6 present results and observations from wireline and seismic data. In this chapter, gamma ray, sonic and photo electric wireline logs are interpreted based on stratal stacking pattern to infer shoreline trajectories and possible depositional settings. Isopach maps are also derived from seismic interpretation to understand the changes in depocenter during deposition. Moreover, internal seismic stratal geometries are interpreted based on stratal terminations, to understand provenance direction, shoreline trajectories, tectonic movement, etc.

Chapter 7 integrates the observations shown in chapters 5 and 6, with the onshore studies presented in Chapter 2 in order to develop a series of gross depositional environment (GDE) maps from the Early Jurassic to the Holocene. These GDEs are based on observation using basic principles of stratigraphy and process sedimentology without inferring any school of thought or stratigraphic models. This chapter also highlights which mechanisms are responsible for depositional trends and stratal geometries, to understand shoreline trajectories and RSL fluctuations. Based on the GDE maps, modern-day analogues for the Algoa and Gamtoos Basins are also presented. Lastly, using the sequence boundaries to define system tracts, this chapter justify the lateral facies variation in the GDE models and contrast the stratigraphic boundaries observed in this dataset with current stratigraphic models.

Chapter 8 is a summary/conclusion of the main findings of this study, and their implications for the sequence stratigraphy and basin development of the Algoa and Gamtoos Basins.

Chapter 9 is the reference list for citations in this thesis.

The *Appendix* is a summary of this doctoral thesis in form of a revised manuscript that has been submitted to Geo-Marine Letters (manuscript number EMID:4787406fa4983ae4). The manuscript has been fully peer reviewed by two anonymous reviewers in early 2021 and is under editorial decision at the time of the submission of the PhD thesis. If it is accepted for publication in the special issue entitled “Coastal and marine geology in southern Africa: alluvial, abyssal and everything in between”, the full citation will be: “Makhubele, M.H. and Bordy, E.M. 2021. Sequence stratigraphy in the Algoa and Gamtoos Basins (South Africa): a shoreline’s journey since the Middle Mesozoic. *Geo-Marine Letters*".

2 Geological background

2.1 Geological setting

The Algoa Basin, together with the Gamtoos, Pletmos and Bredasdorp Basins are collectively known as the Outeniqua Basin and are located along the southern coast of South Africa (Figure 1.1; Malan, 1993; Brown et al., 1995; McMillan et al., 1997; Singh et al., 2005; Thompson et al., 2019; Muir et al., 2020). The Outeniqua Basin is a remnant of an extensional basin system that formed in southern Africa during Gondwana break-up in the Early Jurassic (McLachlan and McMillan, 1976; Dingle et al., 1983; Malan, 1993; McMillan et al., 1997; Thompson et al., 2019; Muir et al., 2020). Seismic stratigraphic studies from the Bredasdorp and Pletmos Basins, situated SW of the Algoa and Gamtoos Basins, showed that the sedimentary succession offshore the S-SE coast of South Africa is stratigraphically subdivided by up to 22 major unconformities namely: Basement D, 1At1, 5At1/6At1, 13At1, 15At1 and 22At1 (Figure 2.1; Malan, 1993; Brown et al., 1995; McMillan et al., 1997; Petroleum Agency SA, 2012). The first letter of each of these codes represents the hierarchy order (e.g., A is first order, B is second order), while ‘t1’ or ‘t2’ represent unconformity types as defined by Posamentier et al. (1988).

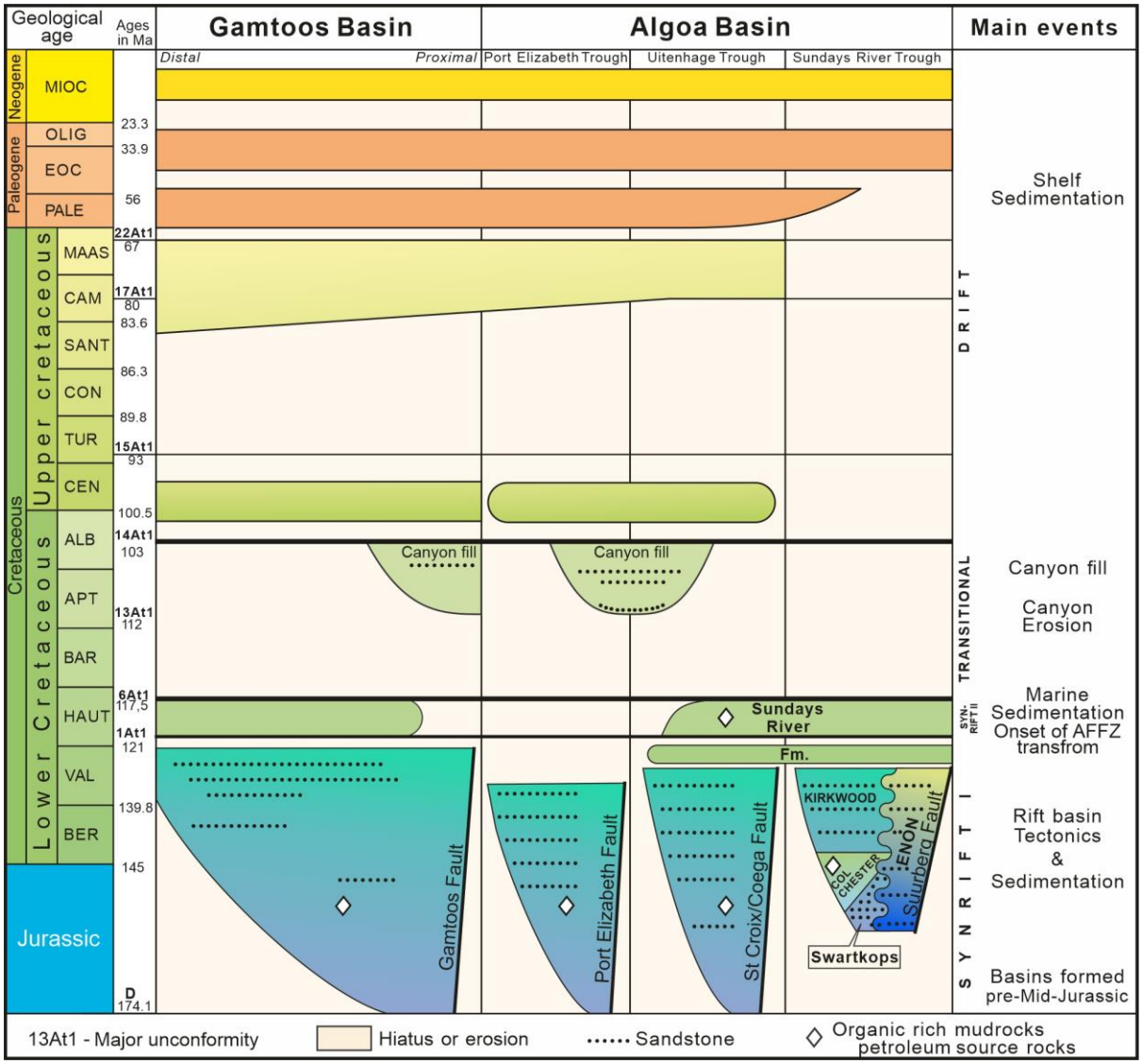

Figure 2.1 Stratigraphic succession and major geological events in the Algoa and Gamtoos Basins (modified from McMillan et al., 1997; Broad et al., 2012).

The oldest rocks are conglomerates and subordinate sandstones that belong to the Enon Formation, deposited as alluvial fans developed from high-energy rivers during the early Middle Jurassic (or earlier) to the Early Cretaceous (Figure 2.1; McLachlan and McMillan, 1976; Dingle et al., 1983; Malan, 1993; McMillan, et al., 1997; Muir et al., 2017a, 2020). This basal conglomeritic unit, with thickest accumulations in the deepest portions of the sub-basins adjacent to the bounding fault traces (Muir et al., 2017a) is coeval with, but occasionally overlain by the variegated mudstones and sandstones of the Kirkwood Formation (Figure 2.1; McLachlan and McMillan, 1976; Dingle et al., 1983; McMillan et al., 1997; Muir et al., 2015, 2017b, 2020). The Kirkwood Formation was deposited by meandering rivers and floodplains along the dipping landscape of the hanging walls of the rift normal faults (Figure 2.1; McLachlan and McMillan, 1976; Dingle et al., 1983; McMillan et al., 1997; Muir et al., 2015, 2017b, 2020). Onshore, the continental deposits of the Enon and Kirkwood Formations are overlain by the Sundays River Formation. In outcrops, this marine, regionally extensive unit is well known for its age-

diagnostic Valanginian foraminifera (McMillan et al., 1997, 2003; Broad et al., 2012; Muir et al., 2017a, b, 2020). Unlike the Enon and Kirkwood Formations, the age of the Sundays River Formation has not been determined with radioisotopic dating methods (see Muir et al., 2020 for discussion). Based on biostratigraphic proxies, its lower part is considered coeval with the upper Kirkwood and potentially Enon Formations. Despite lacking robust age constraints, the Sundays River Formation is widely considered to mark the end of syn-rift deposition in the study region, chiefly because it is overlain by the Hauterivian to Albian transitional phase succession (Figure 2.1; McLachlan and McMillan, 1976; Dingle et al., 1983; McMillan et al., 1997). The syn-rift and transitional phase sediments are well preserved in the offshore Gamtoos Basin but not in the Algoa Basin, where they have been eroded during the late Aptian uplift. Aero-magnetic studies shows that the Uitenhage Group in the Algoa Basin can reach thicknesses of up to 6 km, especially towards the SW part of the basin (Caku et al., 2020). The Aptian uplift resulted in the Algoa and Gamtoos Canyons (Figures 1.1 and 2.1; McLachlan and McMillan, 1976; Dingle et al., 1983; Malan et al., 1990; Bate and Malan, 1992; McMillan et al., 1997; Paton and Underhill, 2004), which were subsequently, filled with transitional phase late Aptian (13At1) to early Albian (possible early Cenomanian) inner to middle shelf marine claystones with sandstone interbeds (McMillan et al., 1997). The transitional phase succession is truncated by the regionally extensive Top Cenomanian (15At1) unconformity, which is onlapped by marine-dominated Upper Cretaceous drift phase sediments (Figure 2.1; McMillan et al., 1997; Broad et al., 2012). Unconformably overlying the Mesozoic successions onshore are various Cenozoic formations comprising of the: Bathurst, Alexandria, Nanaga, Salnova, Nahoon, and Schelm Hoek Formations, which mostly belong to the Eocene to Holocene-age Algoa Group (e.g., McMillan and McMillan, 1976; Du Toit, 1979; Le Roux, 1987, 1989, 1990, Illenberger, 1992; McMillan, 1990; McMillan et al., 1997; Hattingh, 2001; Broad et al., 2012).

2.2 Tectonic setting and basin evolution

In the long-lived rift-basin system of the southern Cape, two main rifting episodes were recorded: 1) the opening of west Gondwana during the Early Jurassic, and 2) the Early Cretaceous strike-slip movement along the Agulhas-Falkland Fracture Zone (AFFZ; Figure 2.1; Baby et al., 2018 their fig. 12; Muir et al., 2020). Based on recent U-Pb radioisotopic dating of pyroclastics and resedimented volcaniclastics in the southern Cape, Muir et al. (2020) showed that the Uitenhage Group was deposited over a 40 myr-long-period, from the Early Jurassic to the Early Cretaceous. This age assessment suggests that the initial rifting in the region occurred pre-Aalenian, during the Early Jurassic, when the region was part of the rift system that was generated during the separation of East and West Gondwana, in the initial Gondwana break-up interval (Jungslager, 1996; Muir et al., 2020).

The second rifting phase (late Valanginian transitional phase) occurred in the Early Cretaceous due to transform rifting, which is linked to the initiation of the AFFZ and the opening of the South Atlantic (McLachlan and McMillan, 1976; Martin et al., 1981; Dingle et al., 1983; Broad, 1990; Bate and Malan, 1992; Ben-Avraham et al., 1993; Paton and Underhill, 2004; Muir et al., 2020). This second rift phase was shown to correspond to the M21-M10 magnetic signatures with a radioisotopic age of ~145−122 Ma (Martin and Hartnady, 1986). During the post-rifting phase, the basin underwent several uplift events, the first of which occurred during the Barremian−Aptian (6At1 to 13At1; Figure 2.1; McLachlan and McMillan, 1976; Dingle et al., 1983; Malan, 1993; Brown et al., 1995; Thomson, 1999; Paton and Underhill, 2004). This uplift was followed by the final separation between the Falkland (Malvinas) Margin and the southern tip of Africa, which occurred during the Albian to lower Cenomanian, and connected the Indian and South Atlantic Oceans (Figure 2.1; Martin et al., 1981; McMillan et al., 1997; Brown et al., 1995; Reeves, 2018; Baby et al., 2018 their fig. 13). The final separation of the Falkland Margin from Africa resulted in a passive margin along the south coast of South Africa (Brown et al., 1995). After the transitional phase, the second major erosional event resulted from “Drift Sequence” (*sensu* Broad et al., 2012; thermal subsidence driven) that caused the uplift of the shelf. It took place in the distal/offshore part of the basin in the Late Cretaceous (15At1 to 22At1; Figure 2.1; Malan, 1993; Baby et al., 2018). The last notable uplift event occurred during the Oligocene, when the basin tilted to the N, eroding much of the drift sediments on the shelf (Hattingh, 2001; Baby et al., 2018).

2.2.1 Algoa Basin

The reactivation of Palaeozoic Cape Supergroup lineaments during early rifting resulted in structurally controlled sub-basins separated by the St. Croix, Port Elizabeth, and Uitenhage Faults, which are the three major bounding faults (Figures 1.1 and 2.1; McLachlan and McMillan, 1976; Dingle et al., 1983; Broad et al., 1990; Bate and Milan, 1992; Malan, 1993; Broad et al., 2012; McMillan et al., 1997). The Jurassic St. Croix Fault is the most laterally extensive and only fault in the Algoa Basin to extend from onshore to offshore regions, separating the Sundays River Trough from the Uitenhage Trough (Figures 1.1 and 2.1; Broad et al., 1990; Bate and Malan, 1992; Malan, 1993; McMillan et al., 1997; Broad et al., 2012). The Port Elizabeth Fault, which is also Jurassic in age, is the most laterally restricted of the three Algoa main faults, separating the Uitenhage and the Port Elizabeth Troughs (Figures 1.1 and 2.1; Broad et al., 1990; Broad et al., 2012; McMillan et al., 1997). Contrary to the other two faults, which show a preferred NW-SE strike, the Port Elizabeth Fault appears to have a N-S strike (Figures 1.1 and 2.1; Broad et al., 1990; Broad et al., 2012; McMillan et al., 1997). The Uitenhage Fault, which is localised in the offshore part of the basin, formed in the late Valanginian to Hauterivian (1At1 to 6At1).

It separates the Uitenhage Trough from the Port Elizabeth Trough, and also subdivides the Uitenhage Trough into two mini basins (Figures 1.1 and 2.1; Broad et al., 1990; 2012; McMillan et al., 1997).

These structurally complex Algoa Basin troughs (or sub-basins) have unique sedimentation histories and are separated from each other and the other basins by the Ordovician to Silurian Cape Supergroup basement highs (Figure 2.1; Dingle et al., 1983; Bate and Malan, 1992; Malan, 1993; McMillan et al., 1997; Broad et al., 2012). The predominately onshore-located Sundays River Trough is the largest of the three Algoa sub-basins, has a Devonian basement (Bokkeveld Group) that is overlain by ~200 m of continental conglomerates (Enon Formation; Broad et al., 1990; McMillan et al., 1997). The Uitenhage Trough is partially filled with continental conglomeritic sandstones (Enon Formation) and contains the Algoa Canyon, which is its most prominent feature, found between unconformities 6At1 and 13At1 (Figures 1.1 and 2.1; McMillan et al., 1997; Broad et al., 2012). In contrast to the other troughs, the oldest rocks intersected by boreholes in the Port Elizabeth Trough are Kimmeridgian shallow marine to transitional deposits (McMillan et al., 1997; Broad et al., 2012).

2.2.2 Gamtoos Basin

The Gamtoos Fault, which has been identified as a listric-type fault, is the largest and most prominent syn-rift fault on seismic data in the Gamtoos Basin, with a throw of 3 km onshore and 12 km offshore, (Figures 1.1 and 2.1; Malan et al., 1990; Bate and Malan, 1992; Malan, 1993; McMillan et al., 1997; Paton and Underhill, 2004). Although the exact age of the Gamtoos Fault is uncertain, it is believed to form part of the Early to Late Jurassic south Gondwana rifting episodes (Malan et al., 1990; McMillan et al., 1997; Paton and Underhill, 2004; Muir et al., 2020). Unlike the Algoa Basin, which is structurally more complex, the Gamtoos Basin is made up of a simple half graben, striking at NW-SE towards the NW part of the basin, changing to N-S strike towards the E (Figures 1.1 and 2.1; Malan et al., 1990; Malan, 1993; McMillan et al., 1997; Paton and Underhill, 2004). This change in geometry could be related to the right-lateral strike slip motion of the Agulhas-Falkland Fracture Zone (AFFZ; Broad, 1990; Bate and Malan, 1992; Ben-Avraham et al., 1993). However, others (e.g., Martin et al.,1981; de Wit, 1992; Paton and Underhill, 2004) argue that the change in geometry was caused by crustal-scale anisotropy of the basin, meaning that the Gamtoos Fault was following pre-existing crustal-scale Palaeozoic Cape Supergroup lineaments. The oldest sediments, which are at least Aalenian in age (Muir at al., 2020), were deposited in a continental setting (Broad et al., 1990; McMillan et al., 1997). However, during the Kimmeridgian to Tithonian, a rapid displacement across the Gamtoos Fault resulted in a lacustrine environment, favouring the deposition of anoxic shales, which are the main source rocks in the basin (Broad et al., 1990; McMillan et al., 1997; Paton and Underhill, 2004). The

maximum displacement of the fault is along the N-S part of the fault, indicating that the basin underwent a WSW-ENE extensional regime (Paton and Underhill, 2004). The basin went through a period of compression sometime between the late Valanginian and early Hauterivian, which resulted the Gamtoos Anticline, most notably along a dip line near the N-S trending part of the Gamtoos Fault (Bate and Malan, 1992; McMillan et al., 1997; Thomson, 1999). Although the development of the Gamtoos Anticline is documented in Thomson (1999, his fig. 9), the origin of the stress field responsible for the tectonic inversion is poorly understood (Thomson, 1999). The compressional phase was followed by a period of uplift and erosion during the Hauterivian to Aptian, resulting in the Gamtoos Canyon (and Algoa Canyon; Figure 2.1; McMillan et al., 1997; Broad et al., 2012). Although significantly smaller in size relative to the Algoa Canyon, the Gamtoos Canyon was also formed as a result of uplift and subaerial erosion of the shelf due to the dextral Agulhas/Falkland transform motion during the break-up of Gondwana (Figure 2.1; Malan, 1993; McMillan et al., 1997; Paton and Underhill, 2004; Broad et al., 2012). The Gamtoos Canyon sediment fill is mostly early Aptian to middle Albian age (13At1 to 14At1; Figure 2.1; Malan, 1993; McMillan et al., 1997; Paton and Underhill, 2004).

2.3 Onshore Algoa Basin field studies

2.3.1 Enon Formation

The conglomeritic Enon Formation, which is the oldest succession in the Uitenhage Group was first mapped by Atherstone (1857) in the Algoa Basin (Dingle et al., 1983). This formation crop out in multiple locations in the basin, as a primarily immature, poorly sorted, white to orange-red coloured, pebble to cobble conglomerate with very rare sandstone intercalations (Figures 2.1 and 2.2a; McLachlan and McMillan, 1976; Dingle et al., 1983; Malan, 1993; McMillan et al., 1997; Singh et al., 2005; Muir et al., 2017a). In contrast to the heavily red stained conglomerates observed in the Algoa Basin (Figure 2.2a; Muir et al., 2017b), the Enon Formation near Andrieskraal in the Gamtoos Basin is predominantly grey, with some orange staining (Figure 2.2b; Muir et al., 2017b). In the Gamtoos Basin these Cape (and to a lesser extent Karoo) Supergroups derived conglomerates are also thickly bedded, poorly sorted, immature to mature deposits (Figure 2.2b; Muir et al., 2017a). Core log reports from boreholes KE 1/71 and CO 3/71 (Figures 1.1 and 2.1) also describe the Enon Formation as a pebbly conglomerate, sourced locally from the underlying Bokkeveld Group (Fletcher, 1971a, b). Although bone fragments and wood fossils have been encountered in the Enon Formation (Muir et al., 2017a their fig. 3), these fossils do not provide a diagnostic depositional age for this stratigraphic unit (McLachlan and McMillan, 1976). Recent radioisotopic dating however suggests that the deposition

of the Enon Formation was already active by the Aalenian (i.e., late Early Jurassic) and was ongoing until the Early Cretaceous (Muir, 2019; Muir et al., 2020).

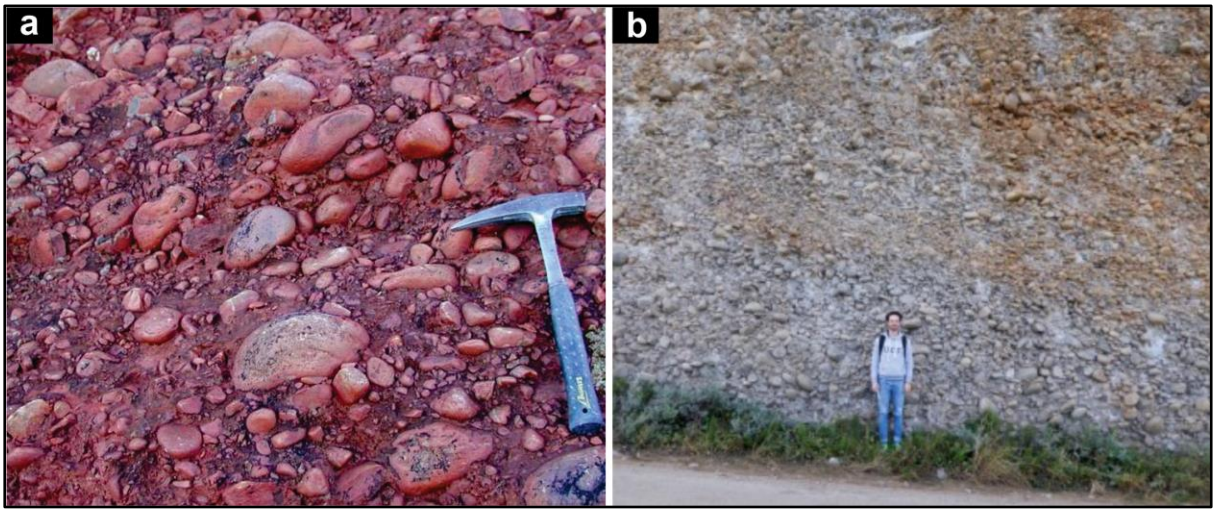

Figure 2.2 a Conglomeritic Enon Formation near Enon in the Algoa Basin. **b** Conglomeritic Enon Formation in the Gamtoos Basin, near Andrieskraal (taken from Muir et al., 2017b with permission from the author).

The sedimentary characteristics of the Enon Formation imply deposition in high-energy debris flow processes, which eroded the quarzitic basement rocks that built the Palaeozoic-Mesozoic Cape Fold Belt (McLachlan and McMillan, 1976; Dingle et al., 1983; McMillan et al., 1997; Muir et al., 2017a, b; Muir, 2019). This imbricated conglomerate indicates a S-SW paleocurrent direction (Shone, 1976; Muir et al., 2017a). Moreover, because the formation is more prominent along the footwalls of the main extensional faults (see Martins-Neto and Catuneanu, 2010; Holz et al., 2017), fault movements were most likely responsible for generating high gradients necessary for the sediment transport during the Enon depositional phase (Muir et al., 2017a). The variation in thickness of the Enon Formation is high in the Algoa Basin with a maximum thickness of 480 m measured by Dingle et al. (1983) in the more proximal setting. Additionally, the Enon Formation appears to be diachronous across the basin and has a gradational/conformable contact with the overlying Kirkwood Formation (Figure 2.1; McLachlan and McMillan, 1976; Dingle et al., 1983; McMillan et al., 1997; Muir et al., 2017a).

2.3.2 Kirkwood Formation

Conformably overlying the Enon Formation, the variegated mudstones with palaeosols and sandstones with subordinate conglomerates from part of the Kirkwood Formation (Figures 2.1 and 2.3a; Muir et al., 2017b). In the Gamtoos Basin, the Kirkwood Formation outcrops on riverbanks of the Gamtoos River, onshore the Gamtoos Basin (Figure 2.3b; Muir, 2019). In this location, the Kirkwood Formation is primarily sandstone, with some claystone interbeds (Figure 2.3b; Muir, 2019). Based on field sedimentological evidence, these rocks have been interpreted as deposits of: a) low-energy, likely meandering rivers; b) with persistent freshwater lakes with at least episodic anoxia, and c) intermittent and likely short-lived shallow marine conditions (Figure 2.3a; McLachlan and McMillan, 1976; Shone, 1976; Dingle et al., 1983; Malan, 1993; McMillan et al., 1997; Singh et al., 2005; Shone, 2006; McMillan, 2010; Muir et al., 2015; 2017b). The Kirkwood Formation shows variable thickness across the Algoa Basin with borehole AL 1/69 (Figures 1.1 and 2.1) intersecting up to 2210-m-thick unit, while attaining a maximum thickness of 1900 m onshore the Gamtoos Basin (Dingle et al., 1983).

The Colchester Member, which was initially named the 'Colchester Formation' by Rigassi and Dixon (1972), has been recently reclassified as a member of the Kirkwood Formation (Muir et al., 2017b) to represent the organic matter-rich, exclusively continental lake deposits in the formation (Figure 2.1). The same authors also proposed that the Bethelsdorp Member, which is largely limited to the offshore areas of the Algoa Basin, has a likely marine origin. Core log reports from boreholes KE 1/71 and CO 3/71 also describes the Colchester Member as mostly shales with thin sandstone interbeds (Fletcher, 1971a, b). These organic-rich lacustrine shales are recorded with a maximum thickness of 140 m in boreholes CO 1/69 and CO 3/71 (Figure 1.1b; McLachlan and McMillan, 1976) and are postulated to have acted as the main source rocks for the hydrocarbons detected in the basin (McLachlan and McMillan, 1976; Malan, 1993; McMillan et al., 1997; Muir et al., 2017b). The grey mudstones of marine affinity in the Bethelsdorp Member are very poorly exposed (Figure 2.3c) in the Port Elizabeth and the Uitenhage Troughs (McMillan, 2010; Muir et al., 2017b).

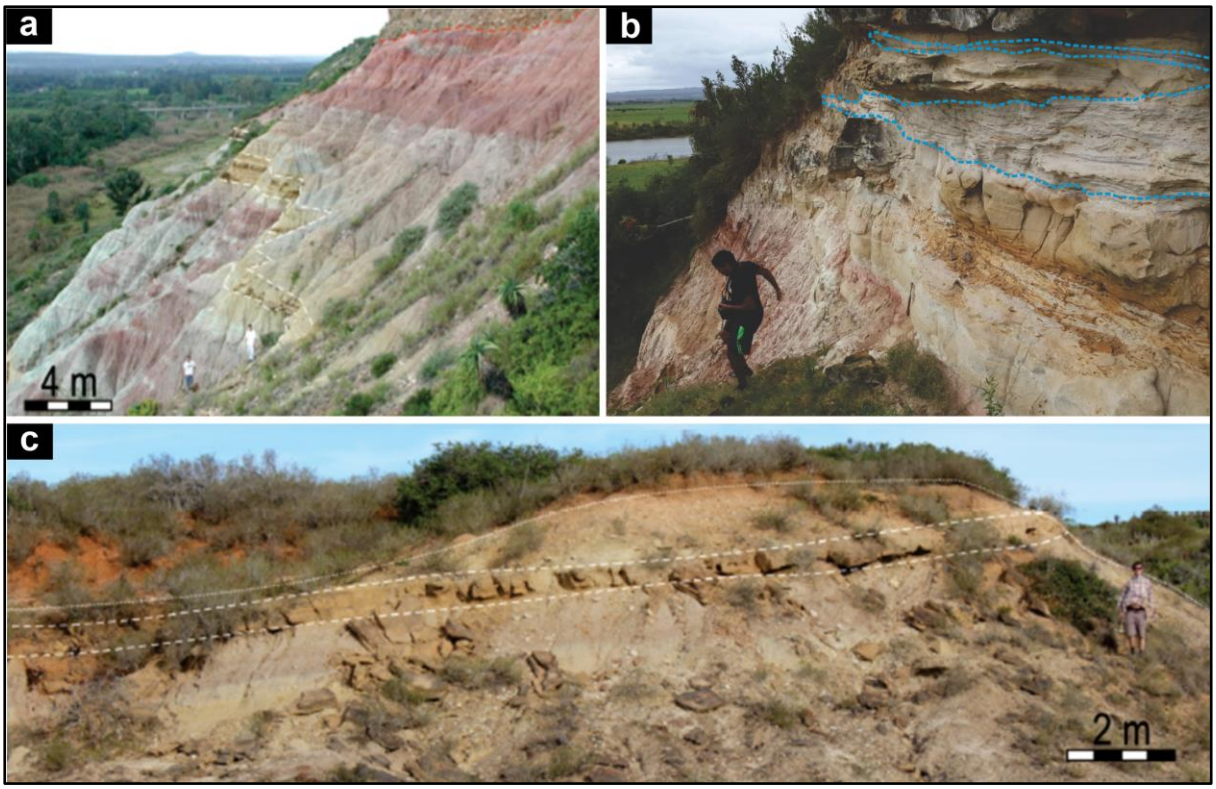

Figure 2.3 Kirkwood Formation outcrops in the Algoa and Gamtoos Basins. **a** The white interbeds in the red- to purple-coloured mudstones are palaeosols, and together with the tetrapod rich fauna, they indicate a terrestrial depositional environment. **b** Kirkwood Formation along the banks of the Gamtoos River. **c** Bethelsdorp Member exposed in the Uitenhage Trough (taken from Muir, 2019; Muir et al., 2017b with permission from the authors)

Although a rich and diverse continental fossil biota of theropod dinosaurs, freshwater fish, plants, etc. has been discovered in the Kirkwood Formation, the lack of age-diagnostic macrofossils the age for this unit was estimated to be Late Jurassic to Early Cretaceous (Figure 2.1; McLachlan and McMillan, 1976; Dingle et al., 1983) until the robust radioisotopic dating work by Muir (2019) and Muir et al. (2020). The Late Jurassic age was suggested based on a Tithonian microfossil assemblage from the Bethelsdorp and Colchester Members (McMillan et al., 1997; McMillan, 2010; Muir et al., 2017b). While the Early Cretaceous age of the upper Kirkwood Formation was estimated based on the overlying Valanginian to Hauterivian Sundays River Formation (McLachlan and McMillan, 1976; Dingle et al., 1983; McMillan et al., 1997; McMillan, 2010). Recent radioisotopic dating established a late Early Jurassic to Early Cretaceous age for the Kirkwood Formation (Muir, 2019; Muir et al., 2020). Although the Kirkwood Formation could be the distal facies of the Enon Formation (Dingle et al., 1983), Muir (2019) recognises that there is a large section of the Kirkwood Formation that remains undrilled and untested, even with the deepest boreholes that were drilled offshore (Figure 1.1b), as such, the Kirkwood Formation could be older than the reported late Early Jurassic (Aalenian) age (see Muir et al., 2020 their fig. 6).

2.3.3 Sundays River Formation

Overlying the Kirkwood and Enon Formations, the regionally extensive Sundays River Formation (which only outcrops in the Uitenhage Trough; Muir, 2019) is characterised by green-grey laminated mudstones, interbedded with very fine- to medium-grained sandstone beds (Figure 2.1 and 2.4; Muir, 2019). Core log reports from boreholes KE 1/71 and CO 3/71 (Figure 1.1b) also describes the unit as shales and siltstones with subordinate argillaceous sandy interbeds (Fletcher, 1971a, b). Unlike the palaeosol- and continental fossil-rich, variegated mudstones of the underlying Kirkwood Formation, the Sundays River Formation contains marine fossil invertebrates that indicate a suite of shallow marine, estuarine and tidal-flat habitats, with ages ranging from the Valanginian to Hauterivian in the Early Cretaceous (McLachlan and McMillan, 1976; Dingle et al., 1983; Malan, 1993; McMillan et al., 1997; Singh et al., 2005; Muir, 2019; Muir et al., 2020). The nature of the basal contact between the Kirkwood and Sundays River Formations is ambiguous (McLachlan and McMillan, 1976; Muir, 2019), but Shone (1978) argues that in some parts of the basin (e.g., near Dunbrody in the Algoa Basin; Muir, 2019), the Sundays River Formation interfingers with the Kirkwood Formation. This supposed gradational contact contradicts Winter's (1973) postulation for an unconformable contact between the two formations. Although the Sundays River Formation has a highly variable thickness across the Algoa Basin, it is the thickest stratigraphic unit in the Uitenhage Group (Muir, 2019), with a thickness of over 1400 m intersected onshore borehole KE 1/71 (Figure 1.1b; Fletcher, 1971a).

Figure 2.4: Outcrop of the marine Sundays River Formation near Sunland in the Algoa Basin (taken from Muir, 2019 with permission from the author).

2.3.4 Algoa Group

Unconformably overlying the Mesozoic Sundays River Formation are various Cenozoic formations comprising calcareous sandstones, coquinite (coarse-grained, cemented shell debris), sandy and shelly limestones, and conglomerates, which mostly belong to the Eocene to Holocene Algoa Group (Figure 2.5; e.g., McMillan and McMillan, 1976; Du Toit, 1979; Le Roux, 1987, 1989, 1990, 1991, 1992, 2000; Illenberger, 1992; McMillan, 1990; McMillan et al., 1997; Hattingh, 2001; Broad et al., 2012; Roberts et al., 2006; Claassen, 2014; Lockley et al., 2021). The Algoa Group consists of a series of transgressive and regressive deposits [i.e., calcareous sandstones, coquinite, sandy and shelly limestones, and conglomerates] that formed during glacio-eustatic sea-level fluctuations in aeolian, coastal and shallow marine settings (Le Roux, 1987, 1989, 1990, 1991, 1992, 2000; Illenberger, 1992; Roberts et al., 2006; Claassen, 2014). Stratigraphically the group is subdivided into the: Bathurst, Alexandria, Nanaga, Salnova, Nahoon, and Schelm Hoek Formations (Figure 2.5; Le Roux, 1987, 1989, 1990, 1991, 1992, 2000; Illenberger, 1992; Roberts et al., 2006; Claassen, 2014).

The Bathurst Formation, which is the oldest of the Algoa Group, comprises primarily a fully-marine, shark-teeth-bearing limestone that is overlain by thin pebbly coquinite and conglomerate at the top (Figure 2.5; Claassen, 2014). These Eocene deposits are ~20-m-thick, and unconformably overlie the Palaeozoic/Mesozoic successions onshore the Algoa Basin (Figure 2.5; Le Roux, 1990, his fig.2).

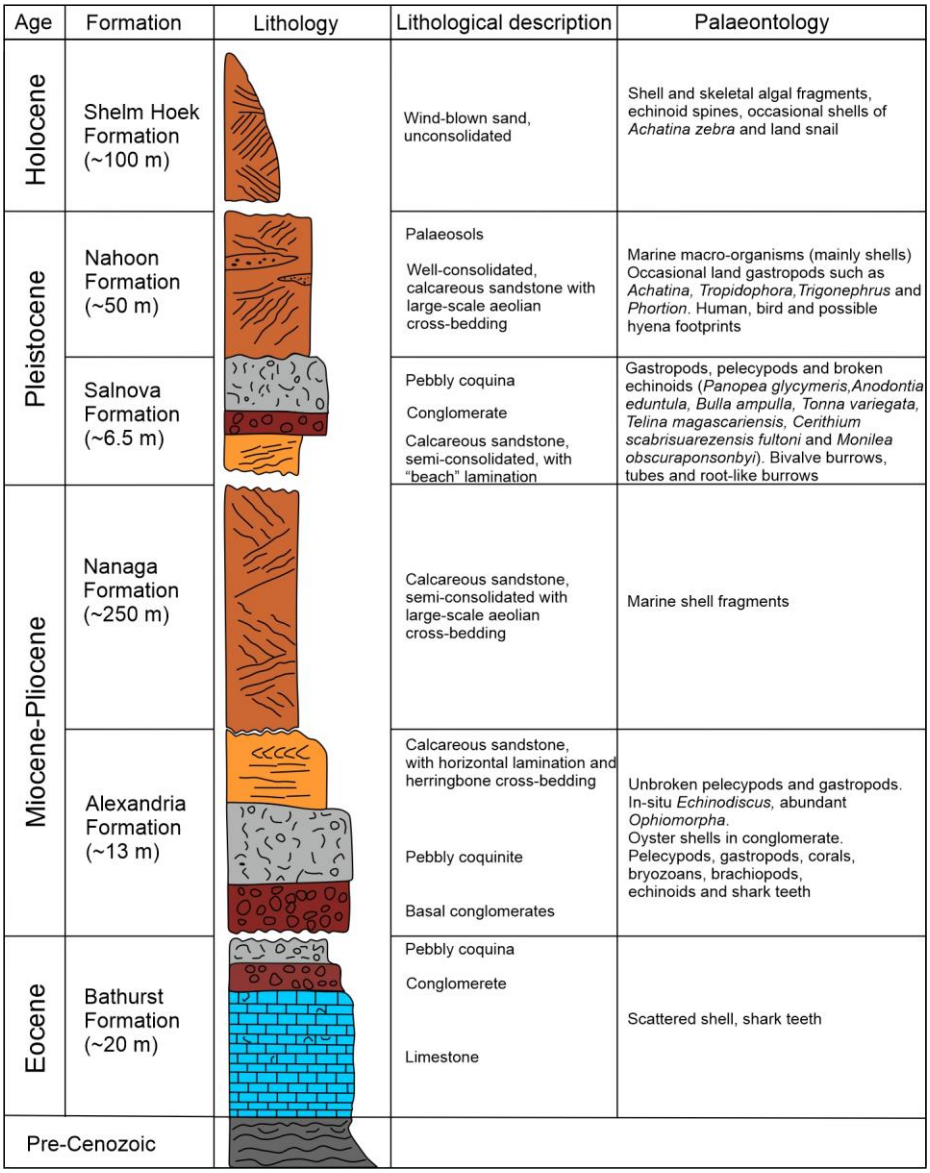

Figure 2.5: The Algoa Group succession based on outcrop studies onshore the Algoa Basin (modified after Le Roux, 1990; Roberts et al., 2006).

Unconformably overlying the Bathurst Formation is the Alexandria Formation, which is dominated by quartzite-clast bearing, shell-debris-rich conglomerates at the base, which give way to an interbedded succession of pebbly coquinite and calcareous sandstones with herringbone cross-bedding (Figure 2.5; Le Roux, 1987; Roberts et al., 2006; Claassen, 2014). This 3 to 13-m-thick, highly calcareous succession (Figure 2.5; Le Roux, 1987 his Figs. 2 and 5-8) contains fossil assemblages typical in shoreface, foreshore, lagoonal and estuarine depositional settings (Le Roux, 1987; McMillan, 1990; Hattingh, 2001), and likely resulted from a major transgressive event in the early Miocene. The Mio-Pliocene age estimate for the Alexandria Formation is based on *Toddinella lenticularis* (Gudina; Le Roux, 1987; McMillan, 1990).

Overlying the Alexandra Formation is the semi-consolidated calcareous sandstone, sandy limestone, palaeosols and calcrete dominated Nanaga Formation, which shows evidence of aeolian cross-bedding (Figure 2.5), signalling that at least part of the unit was deposited in a nearshore, continental setting (Le Roux, 1992 his figs.7-9). In contrast to the underlying succession, there is no evidence of conglomerates or large marine fossils in the Nanaga Formation and it thus can be associated with a major regressive event in this region. The Pliocene to early Pleistocene age was based on the similarity of the Nanaga Formation to the overlying Salnova Formation (McMillan, 1990), which contains more age diagnostic foraminifera. The Nanaga Formation shows highly variable thickness and attain a thickness of up to 250 m locally (Le Roux, 1992).

The Pleistocene Salnova Formation is dominated by basal conglomerates that give way to fine- to coarse-grained calcareous sandstones (Figure 2.5; Le Roux, 1991 his figs. 2-5; Roberts et al., 2006; Claassen, 2014). The fossil assemblage suggests an intertidal to estuarine depositional setting, with a marine incursion that occurred in the late Pliocene to early Quaternary (Le Roux, 1991; Roberts et al., 2006). It ranges in thickness from 1.6 to 6.5 m.

Contrary to the underlying Salnova Formation, the Pleistocene Nahoon Formation is dominated by aeolianites and palaeosols, with evidence of hominid and associated vertebrate fossil trackways (e.g., hyena, birds; Figure 2.5; Roberts et al., 2006; Roberts, 2008), and limited evidence of marine fossils (Le Roux, 1989 his figs. 3-11; Claassen, 2014). The hominin footprint-bearing aeolianite in the Nahoon Formation was dated at 124 ± 4 ka by Jacobs and Roberts (2009). Considering that the underlying Salnova Formation is marine, it is likely that the Nahoon Formation was deposited during a period of regression (Hattingh, 2001; Le Roux, 1989). The Nahoon Formation is 6 to 50-m-thick.

Recording the last 6400 years of sedimentation, the unconsolidated Schelm Hoek Formation, was deposited during a phase of maximum transgression, which caused a 3 m rise in relative sea level (RSL) during the Holocene (Illenberger, 1992; Hattingh, 2001). It is made up of aeolian sands and soil horizons (Illenberger, 1992, his fig.2; Claassen, 2014). These unconsolidated dunes vary in height reaching up to 100 m in some places (Illenberger, 1992). The Nahoon and Schelm Hoek Formation dunes are reportedly significantly smaller relative to the dunes preserved in the Nanaga Formation (Hattingh, 2001).

3 Materials and methods

3.1 Introduction

This chapter reviews the methodology used to analyse data in this study, the strength, and limitations of different types of dataset, and the importance of integrating data to build sequence stratigraphic models (Figure 3.1). Geophysical (i.e., seismic and wireline) data are commonly used to complement geological (outcrop and core) data to provide a comprehensive subsurface evaluation.

Seismic data, which images up to thousands of meters of rocks in the subsurface are used to identify depositional systems, vertical and lateral trends in the strata, stratal terminations, tectonic setting and geometries of sedimentary basin (e.g., Catuneanu, 2006, p. 71). Before embarking on data interpretation, evaluating the limitations of the subsurface data with regards to acquisition and processing (i.e., multiple energy, imaging, etc.) are crucial.

In sequence stratigraphy, well data consisting of wireline logs are used for well-to-seismic ties (based on sonic and density logs) and well-to-well depositional trends correlation (GR, SP logs, etc.). The advantage of wireline logs is the more continuous vertical subsurface geological information registered down to thousands of metres depth, which facilitates the correlation of geological features at a regional scale. However, wireline information lacks the finer detail that outcrop data might provide, as it has a limited vertical resolution, on the scale of 10s of centimetres, at best.

While core data give one dimensional view around the wellbore, when outcrop data is not available, core data serves as the only truly reliable source of information on the subsurface geology. Although outcrops are the most direct way to study the geology of an area and provide excellent vertical resolution to rock successions, they are usually limited in their lateral dimension, which is generally in the orders of 100s meters even in the best quality outcrops. Moreover, if outcrop distribution is not frequent and at right angles, determining the shape of large geological features (e.g., main channel bodies) is difficult due to lack of three-dimensional control.

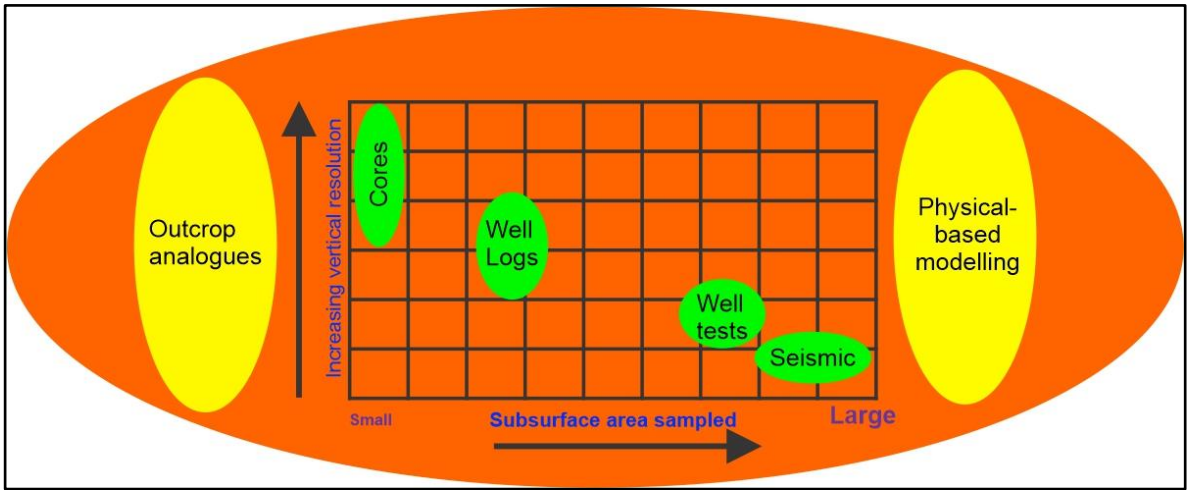

Figure 3.1 Chart showing the various subsurface data types that sample the reservoir volume plotted against the corresponding vertical resolution of the data type. Both outcrop analogue studies and physical-based modelling studies can help bridge the gaps between the different subsurface data types (modified after Keogh et al., 2007).

3.2 Seismic and wireline dataset

3.2.1 Algoa Basin

The dataset purchased from the Petroleum Agency of South Africa (PASA) for this study consists of fifteen boreholes, drilled between 1968 and 1987, of which, six are onshore and nine are offshore the Algoa Basin (Figure 3.2, Table 3.1). Although the density of the dataset in this basin is extensive, limited funding only allowed access to the dataset presented in Figure 3.2. Six of the studied boreholes had oil shows, eight had gas shows, and four were dry (Table 3.1). Primary borehole data used consist of gamma ray, spontaneous potential, photoelectric, density, sonic and neutron logs, and if available, core data (from borehole reports; Table 3.1). Seventy-seven 2D seismic reflection lines acquired between 1968 to 1989 and one 3D seismic volume acquired in 2001 by Petroleum Geo-Services (PGS), were also provided by PASA (Figure 3.2). This dataset ranges from poor to good quality, and ideally, would require reprocessing in order improve the seismic imaging, eliminate multiples, increase the vertical resolution, and minimise seismic misties between different vintages (these processes are beyond the scope and budget of this thesis). Some of the seismic lines are currently being reprocessed by New Age (African Global Energy) Ltd (current operators of the Algoa and Gamtoos License Blocks), however, this work is still proprietary and not available to this study (New Age Global Energy, 2018).

	Algoa Basin	
Data type	**Quantity**	**Years acquired**
Onshore boreholes	6	1968-1978
Offshore boreholes	9	1978-1987
Offshore seismic survey (2D)	71 lines	1976-1989
Onshore seismic survey (2D)	6 lines	1968-1977
Offshore seismic survey (3D)	424 km^2	2001

Figure 3.2 Inventory of the current dataset from the Algoa Basin licenced from the archives of the Petroleum Agency of South Africa (PASA). Base map data ©2020 Google, Maxar Technologies, AfriGIS (Pty) Ltd.

Table 3.1: Algoa Basin well dataset information (GR – Gamma ray; SP – Spontaneous potential; PEF – Photo electric; RHO – Density; NPHIE – Neutron logs)

Boreholes	Year	HC_status	GR	SP	PEF	RHO	DT	NPHI	Checkshot	Core
			API	Mv	Pe	g/m^3	us/ft	Unitless		
Ha-A1	1978	Oil and Gas shows								
Ha-B2	1985	Gas shows								
Ha-D1	1983	Gas shows								
Ha-F1	1985	Dry well								
Ha-G1	1984	Oil and gas shows								
Ha-H1	1985	Dry well								
Ha-I1	1990	Dry well								
Ha-J1	1986	Dry well								
Ha-K1	1987	Gas shows								
Ha-N1	1987	Dry well								

Offshore boreholes | Good quality | Moderate quality | Poor quality/absent

3.2.2 Gamtoos Basin

Comparable to the Algoa Basin, although the density of the dataset in this basin is extensive, due to limited funding, only the dataset presented in Figure 3.3 was accessible for this study. The Gamtoos Basin dataset was also provided by PASA, and comprises ten offshore wells, drilled between 1978 and 1998, accompanied by 2D seismic lines in the offshore regions acquired between 1975 and 1990 (Figure 3.3 and Table 3.2). Unlike in the Algoa Basin, no 3D seismic survey was acquired in the Gamtoos Basin, as a result, the dataset in this basin is generally of poor to moderate quality. GR, SP, RHO and sonic logs are generally available in all the wells, with moderate to good quality, while the PEF log is present in selective wells (Table 3.2).

	Gamtoos Basin	
Data type	**Quantity**	**Years acquired**
Onshore boreholes	NA	NA
Offshore boreholes	10	1978-1990
Offshore seismic survey (2D)	20 lines	1975-1987

Figure 3.3: Inventory of the current dataset from the Algoa licenced from the archives of the Petroleum Agency of South Africa (PASA). Base map data ©2020 Google, Maxar Technologies, AfriGIS (Pty) Ltd.

Table 3.2: Gamtoos Basin well dataset information (GR – Gamma ray; SP – Spontaneous potential; PEF – Photo electric; RHO – Density; NPHIE – Neutron logs)

Boreholes	Year	HC_status	GR	SP	PEF	RHO	DT	NPHI	Checkshot	Core
			API	Mv	Pe	g/m^3	us/ft	Unitless		
AL 1/69	1969	Oil shows								
CO 1/67	1968	Oil shows								
CO 3/71	1971	Dry								
KE 1/71	1971	Dry								
MV 1/78	1978	None								
SM 1/76	1976	None								
Hb-B1	1987	Oil and Gas shows								
Hb-C1	1978	Gas shows								
Hb-D1	1984	Gas shows								
Hb-G1	1987	Gas shows								
Hb-H1	1987	Oil and Gas shows								
Hb-H1i	1987	Oil and Gas shows								
Hb-I1	1987	Gas shows								
Hb-K1	1986	Oil shows								
Hb-P1	1987	Gas shows								

Onshore boreholes | Offshore boreholes | Good quality | Moderate quality | Poor quality/absent

During exploration activities in the basin, the Southern Oil Exploration Corporation (Pty.) Ltd. (previously known as "Soekor", presently PetroSA) focused their data gathering efforts in the syn-rift sequence, consequently, except for boreholes Ha-A1 and Hb-C1, wireline logs were mostly acquired in the syn-rift successions (pre-1At1). In the Gamtoos Basin, 2D seismic lines, which are generally moderate to poor quality, consist of six vintage data (HA75, HA78, HA82, HA85, HA87 and L75), with minimum grid spacing of 1.5 km and maximum grid spacing of 8.5 km. The disadvantage of different vintages is that, based on the contractors used, each contractor might have used different acquisition and processing parameters, which might result in different seismic character and in mis-ties (Figure 3.4). As an example, from Gamtoos Basin, the character differences and mis-tie between 1982 and 1985 seismic vintage is shown in Figure 3.4.

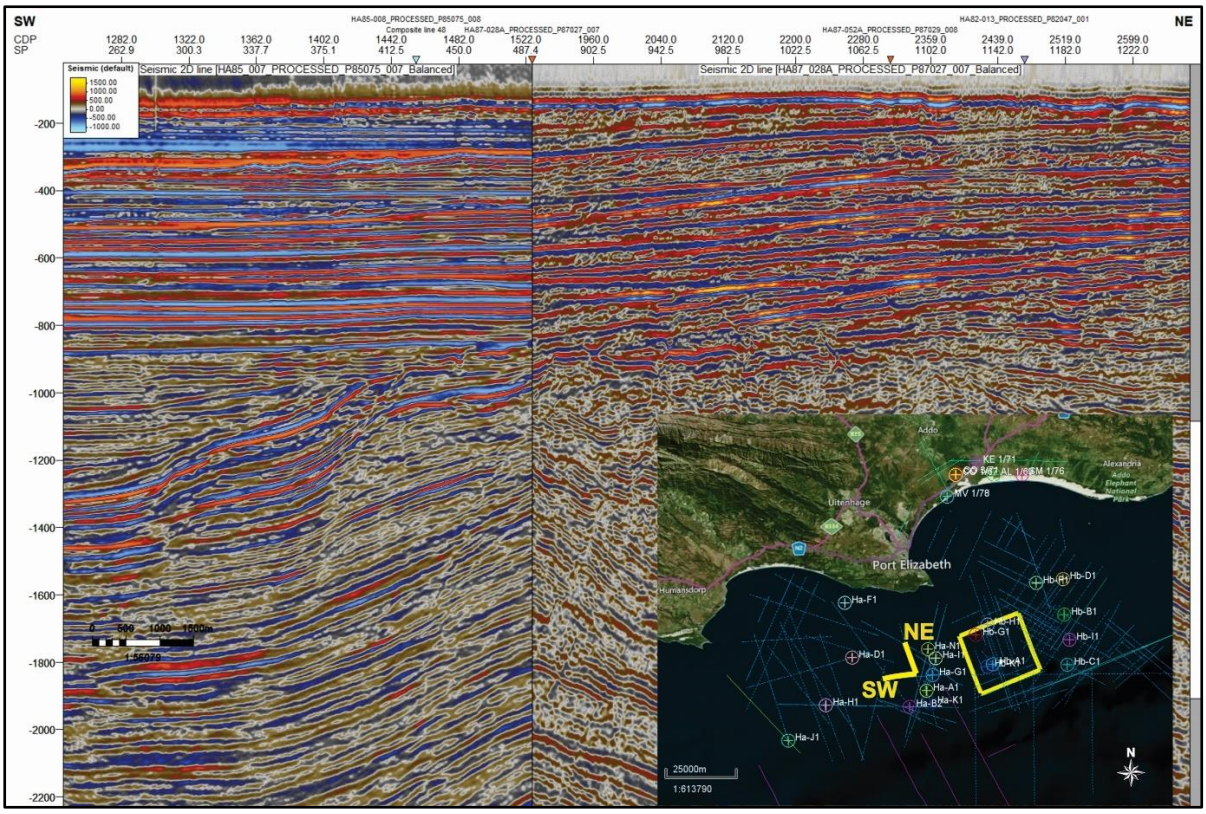

Figure 3.4: 2D reflection seismic lines showing mis-tie between 1982 and 1985 seismic vintage, the two lines show different frequencies, phase, amplitudes, etc. Base map data ©2020 Google, Maxar Technologies, AfriGIS (Pty) Ltd.

Mis-ties refer to a mismatch between 2D seismic lines at a point of intersection (Bishop and Nunns, 1994). Generally, mis-ties can be the result of using different receivers, sources, or recording instruments across different contractors/vintages (Bishop and Nunns, 1994), as well as differences in seismic processing. They both contribute to the seismic character being very different between varying vintages, which limit correlation across different vintages, reduce confidence in seismic picks, and create uncertainty in the derived subsurface maps (Bishop and Nunns, 1994). Mis-tie can be corrected over few seismic lines, however, in dense dataset, such corrections might require complex algorithm (Bishop and Nunns, 1994). In this study, mis-ties were corrected by shifting the line with the mis-tie by aligning with lines which have been tied to a borehole. Where the frequency was different (e.g., Figure 3.4), the higher frequency data was prioritised, and the line was aligned with the seismic line that was used for well-to-seismic-tie (i.e., HA87-042).

3.3 Seismic data

Reflection seismic data uses two-way time (TWT), measured in milliseconds (ms) to image subsurface events (e.g., Sheriff, 1977; Bacon et al., 2003, p. 2). This scale might differ from vertical depth due to vertical variations in wave propagation velocities, which might not coincide with the true distribution of the geology (Bacon et al., 2003, p. 2). Two-way-time represents the time it takes a seismic wave to reach a subsurface layer from a seismic source on surface (vibratory or explosive in onshore fields and impulsive in offshore fields) and return to the receiver on surface (electromechanical sensors - geophones in onshore fields, and hydrophones or nodes in offshore fields; Sheriff, 1977; Bacon et al., 2003, p. 2).

Reflection seismic data is acquired in three different forms. Firstly, one-dimensional (1D) seismic lines are generated, when multiple receivers, at uniform spacing interval are lowered down a borehole to known depths to listen to the waves emitted by the source at the surface; a process referred to as vertical seismic profile (VSP; Bacon et al., 2003, p. 17, 66). The VSP technique is one of the direct ways to relate geology and geophysics, because VSP data correlates seismic data in TWT, with the actual known borehole geology (Bacon et al., 2003, p. 17, 66). Borehole and seismic data can then be calibrated using the VSP's time-to-depth relationship, commonly known as checkshot, to match borehole data (formation tops) to seismic reflectors.

Secondly, two-dimensional (2D) seismic lines are generated when geophones are laid out in a single line to receive subsurface seismic waves. This type of data is primarily used by exploration companies for its affordability and ability to give a 2D cross-section of the subsurface. However, depending on the space between 2D seismic lines, this data might miss some crucial geological details in between seismic lines and alias faulting patterns. Geostatistical algorithms might assist to interpolate data between seismic lines, an advantage over more sparse correlations using only borehole data points, at the expense of less reliable interpolated information away from both borehole and seismic locations.

Thirdly, three-dimensional (3D) seismic volume is generated, when sound wave fronts generated by sources located on surface are recorded over wide receiver templates on surface, a process that provides a much broader subsurface image coverage compared to the single vertical depth image obtained from 2D seismic (Bacon et al., 2003, p. 17, 66). Although this is more expensive to acquire than 1D or 2D, it is the preferred dataset, mainly because it gives an interpreter a holistic 3D view of the subsurface. In addition, as the wavefield is 3D the processing workflow can more accurately reconstruct the subsurface image (Bacon et al., 2003, p. 17-26, 66-70). In this thesis, interpretation of

seismic reflectors (and their geometries) as well as wireline data was performed using Petrel E&P Software Platform of Schlumberger (Petrel) software, including TWT, depth and thickness maps to understand the depocenter and the potential source of sediments.

Seismic energy is recorded as sinusoidal, bandlimited waves made of peaks and troughs. In this regard, before any work is done on seismic data, it is critical that the interpreter identifies its phase (minimum or zero phase) and polarity, that is, understand what a peak and a trough represent in terms of geological contrasts in depth between soft and hard sediments (Bacon et al., 2003, p. 14 ,62; Sims and Bacon, 2014, p. 8). The polarity of the data depends on the processing contractor used (i.e., different seismic vintages might have different polarity), which was the case in both the Algoa and Gamtoos Basins. To correct for the different polarity, seismic vintages were phase rotated by 180^{o} to insure consistency in seismic picking in this study. Seismic polarity is typically presented after data processing in two ways; Society of Exploration Geophysicists (SEG) normal polarity, and SEG reversed polarity (Bacon et al., 2003, p. 14; Sims and Bacon, 2014, p. 9 their fig. 2.8). In SEG normal polarity, an increase in acoustic impedance (AI), which is the product of the density and the P-wave velocity of any rock is represented by a seismic peak (positive number), and a decrease in AI is represented by a seismic trough (negative number; Hampson and Galbraith, 1981; Bacon et al., 2003, p. 14; Sims and Bacon, 2014, p. 9 their fig. 2.8). In SEG reversed polarity, which is usually followed in the UK and Commonwealth countries, a peak represents a decreasing AI, and a trough represents an increasing AI (Hampson and Galbraith, 1981; Bacon et al., 2003, p. 14; Sims and Bacon, 2014, p. 9 their fig 2.8). In cases where the data processing report is not available, the polarity of the data can be determined by evaluating the response of the shallowest seismic reflectors, typically the seafloor in offshore data, which represents an increasing AI (Bacon et al., 2003, p. 14). In onshore data, a known point in depth where AI increases or decreases needs to be identified from wireline logs and correlated with seismic reflectors at the well location using a synthetic seismogram and varying the synthetic phase until the maximum correlation is reached (Hampson and Galbraith, 1981; Bacon et al., 2003, p. 58-59).

Subsurface images on seismic sections are a result of sound wave energy that is reflected, refracted, or diffracted back when they encounter subsurface strata of different rock properties (Sheriff, 1977; Bacon et al., 2003, p. 1). The contrasts in the subsurface where the sound waves get reflected are referred as reflectivities, which can be represented as the product of the velocity and density (or impedance) of the two adjacent subsurface layers at the interface where the contrast takes place (Sheriff, 1977; Sheriff and Geldart, 1995). Equation (1) shows the definition of impedance as the product of velocity and density. Most commonly, velocities and densities can be extracted from sonic and density logs recorded in wells (Sheriff, 1977). Using equation (2), the impedance definition is then

used to calculate the reflectivity (also known as reflection coefficient or RC), a unit-less measurement of the fraction of the number of seismic rays that are reflected back to the surface (Sheriff, 1977; Sheriff and Geldart, 1995).

$$\mathrm{Z} = \rho \mathrm{V} \tag{1}$$

$$\mathrm{RC} = \frac{\rho 2V2 \; - \rho 1V1}{\rho 2V2 + \; \rho 1V1} = \frac{Z2 - Z1}{Z2 \; + Z1} \tag{2}$$

Where RC: Reflection coefficient

V: Density ($\mathrm{g.\,cm^{-3}}$)

P1: Density ($\mathrm{g.\,cm^{-3}}$) of the upper strata

V1: Velocity ($\mathrm{m.\,s^{-1}}$) of the upper strata

P2: Density ($\mathrm{g.\,cm^{-3}}$) of the bottom strata

V2: Velocity ($\mathrm{m.\,s^{-1}}$) of the bottom strata

The reflection coefficient is then convolved with a seismic wavelet (a bandlimited representation of the seismic source signature) to produce a synthetic seismic trace (Figure 3.5) (Hampson and Galbraith, 1981; Bacon et al., 2003, p. 58-59). The wavelet is used to model the expected seismic response as a function of depth to compare against the actual seismic trace following a well (borehole)-to-seismic tie process (Bacon et al., 2003, p. 58-59). When tying borehole and seismic data using sonic and density logs, it is important to calibrate the sonic log with checkshot (a time to depth relationship recorded down the borehole) data to establish a time vs. depth relationship. Checkshot data uses similar acquisition processes as VSP, however unlike VSP, when checkshot data is acquired, a single geophone is lowered down the borehole to known depths (Bacon et al., 2003, p. 60). When the source emits the seismic energy, the geophone records the time it took for the waves to travel from surface to the known depth of the receiver (Sheriff, 1977; Bacon et al., 2003, p. 60). Such practice is repeated over multiple depths in order to create a time-depth curve (Bacon et al., 2003, p. 1). While VSP data generally provide a good well-to-seismic-tie, the disadvantage is that, unlike the conversional well-to-seismic-tie done using sonic and density log, VSP does not provide an interpreter with information regarding how reflectors behave based on density and velocity change of the lithology (Bacon et al., 2003, p. 71). Moreover, VSP provides additional data such as the 'Corridor stack', which is a multiple free seismic image (multiple refer to seismic energy reflected more than once between the source and receiver; Sherif, 1976; Sims and Bacon, 2014, p. 6 their fig 2.5).

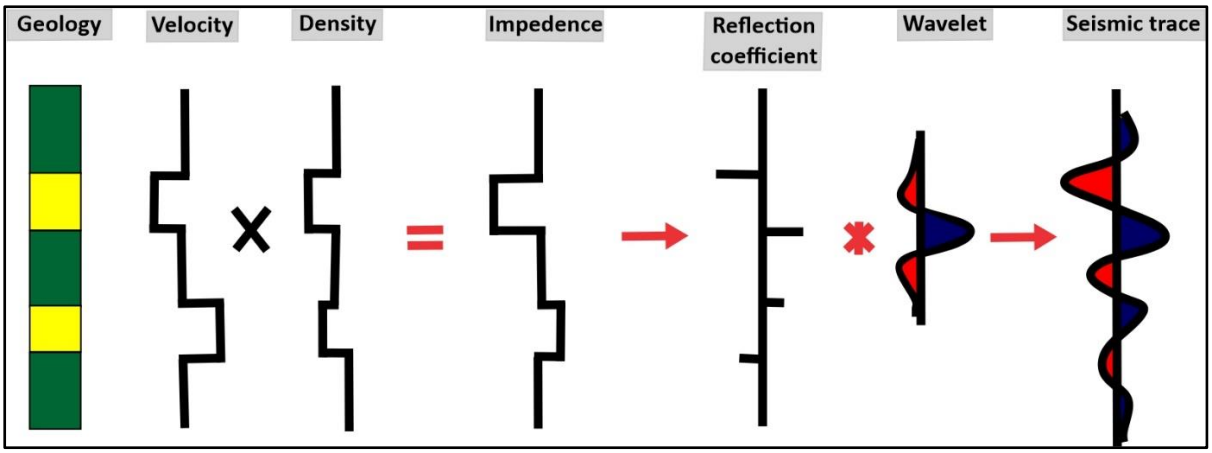

Figure 3.5: Acoustic structure of 5 rock layers showing steps in creating a synthetic seismic trace by convolving a seismic pulse wavelet with a reflection coefficient using the density and velocity of the subsurface lithology (modified from Bacon et al., 2003, p. 8 and AAPG, 2018).

When a time-depth relationship has been established, the reflection coefficient is then convolved with a wavelet to give a seismic trace (Figure 3.5; Bacon et al., 2003, p. 59). There are two types of wavelets typically used, a minimum phase wavelet and a zero-phase wavelet (Hampson and Galbraith, 1981; Bacon et al., 2003, p. 61; Sims and Bacon, 2014, p. 9 their fig. 2.8). The zero-phase wavelet, typically generated by controlled sources (e.g., seismic vibrators) is usually favoured over the minimum phase wavelet during well-to-seismic time and for interpretation (Hampson and Galbraith, 1981; Bacon et al., 2003, p. 61). This is because the zero-phase wavelet is symmetrical about reflection coefficients, with each reflection coefficient coincident at its maximum displacement (Hampson and Galbraith, 1981). The advantage of zero phase wavelet is that it eases the process of seismic interpretation following seismic reflectors coincident with reflectivities representative of lithological contrasts (Sheriff, 1977; Bacon et al., 2003, p. 61). Conversely, the minimum phase wavelet, typically generated by impulsive sources (e.g., explosives, air guns, weight drops) does not coincide with reflection coefficients at their maximum displacement due to its phase rotation; when seismic data exhibits such non-zero-phase effect, this wavelet is usually converted to zero phase wavelet during data processing (Bacon et al., 2003, p. 61).

The minimum thickness of geological features resolved on seismic data is limited by the vertical resolution of seismic data, which can be estimated using the velocity and frequency of the seismic data (Sheriff, 1977). Relative to the sub-centimetre scale vertical resolution of outcrop data or borehole cores, the vertical resolution of seismic data is limited by the frequency of the data (Figure 3.6; Keogh et al., 2007). Essentially, seismic sections show how fast seismic waves can move across different subsurface lithologies, therefore, a good understanding of the velocity, frequency and resolution of seismic data aids interpreters in building representative geological models. In successions dominated by clastic sediments and sedimentary rocks, velocities typically range from

2000 m/s for shallow strata, increasing to 4000 m/s in deeper, more compacted strata, while in successions dominated by non-clastic rocks (e.g., evaporites, carbonates), the velocity can range between 3500 m/s to 5000 m/s (Brown, 1999). As sediments are buried deeper, lithification, which is the process of compaction and cementation, increases the density of sedimentary rocks which in turn increases velocity (Sheriff, 1977; Brown, 1999). Moreover, because compaction increases with burial depth, velocity also increases with depth (Figure 3.6; Sheriff, 1977; Brown, 1999).

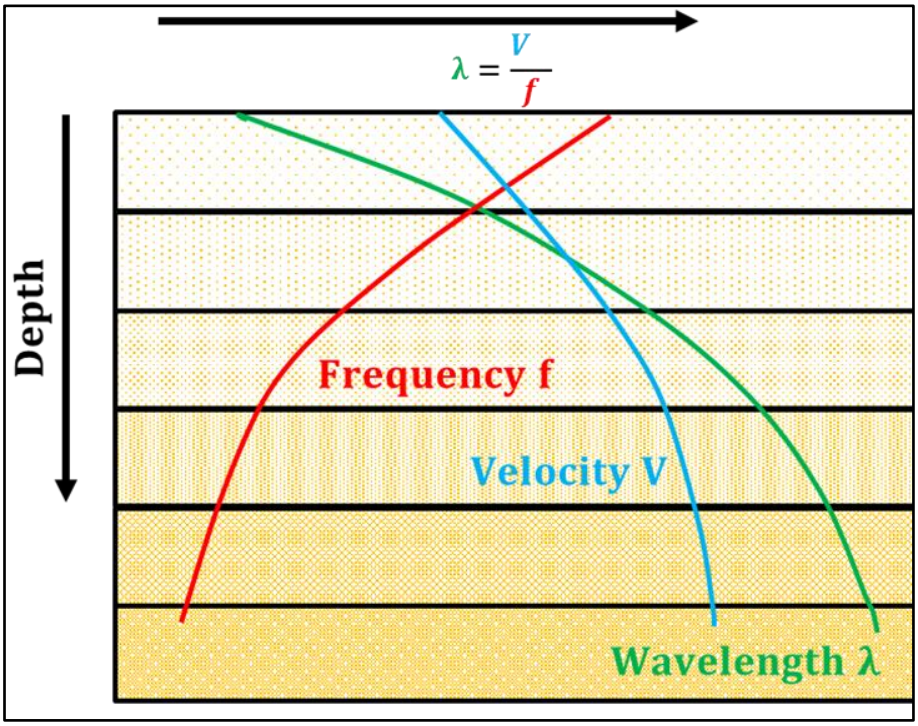

Figure 3.6 The relationship between frequency, velocity and wavelength as well as burial depth (modified from Brown, 1999).

Frequency, which defines the vertical resolution, decreases with increasing depth due to rapid attenuated of the signal from the source as it travels through strata (Figure 3.6; Brown, 1999; Bacon et al., 2003, p. 103). Generally, frequency range from 40-60 Hz at shallow depths (<1500 m) to 15-25 Hz for deeper strata (>2500 m; Brown, 1999; Bacon et al., 2003, p. 103). During data acquisition, both high and lower frequencies are released by the source, but relative to low frequencies, higher frequencies get more attenuated with depth (Brown, 1999). As a result, lower frequencies are better sampled in strata that are deeper buried, while higher frequency data can be recovered in shallower rock intervals, therefore giving finer details of the lithology that is closer to the surface (Brown, 1999). Depending on the contractor used to acquire and process the seismic data, the frequency of the data might be different across different seismic vintages (see Figure 3.4). Unfortunately, there is no quick fix to make sure the data is of the same frequency during interpretation, this can only be changed during acquisition and processing. Velocity and frequency of the data are then used to estimate the

wavelength of the data, a wave parameter representative of the resolution of the data, equation (3) and (4) (Brown, 1999).

Vertical resolution

The wavelength (λ) is calculated by y:

$$\lambda = \frac{V}{f} \tag{3}$$

The vertical seismic resolution is calculated by:

$$\frac{\lambda}{4} \tag{4}$$

λ = Wavelength (m)
f = Seismic frequency (Hz)
V = Seismic velocity (m/s)

Seismic resolution is the ability to differentiate two contrasting geological features from each other using seismic data (Sheriff, 1977). Seismic resolution can be separated into vertical (tuning thickness) and lateral (Fresnel zone) resolution (Sheriff, 1977). The vertical resolution is calculated by equation (4) and is concerned about the minimum vertical thickness (tuning thickness) at which seismic reflectors need to be resolved (Chopra et al., 2006). Vertical resolution is determined by the frequency of the signal, the bandwidth of the seismic data, the internal velocity of strata of interest and the acoustic impedance between two layers (Sheriff, 1977; Emery and Myers, 1996). Any feature that is less that the vertical resolution calculated by equation (4) cannot be fully resolved on the seismic data. The actual vertical resolution is very sensitive to the signal to noise ratio, as a result, vertical resolution can be reduced by the presence of noise in the data (Long, 2003).

Horizontal resolution on the other hand is the minimum distance required to resolve a geological feature (e.g., discontinuity caused by a fault, a lateral change in structural dip) laterally on a seismic data (Brown, 1999; Chopra et al., 2006; Veeken, 2006). Horizontal resolution is given by the Fresnel zone (a minimum distance required to resolve an event within 1/4 of a seismic wavelength λ). In this regard, geological features smaller than the Fresnel zone cannot be distinguishable in a seismic section (Hubral et al., 1993). The Fresnel zone increases with depth, as velocity increases and frequency decreases (Hubral et al., 1993; Brown, 1999; Veeken, 2006).

Because seismic data are fundamental in sequence stratigraphic studies, their limitations are worth noting (Sheriff, 1977; Hampson and Galbraith, 1981; Brown, 1999; Bacon et al., 2003, p.3; Catuneanu, 2006, p.2-3):

1) Seismic data is vertically measured in travel time and not depth, therefore various depth conversions (velocity models) might have to be tested to best convert interpreted seismic horizons from time to depth.
2) Geological features are not imaged in the correct lateral location; therefore, data need to be migrated to reposition those features to the right location.
3) Seismic reflection occurs due to changes in acoustic impedance, if there is no contrast in such rock properties, stratigraphic change cannot be observed.
4) At best, the highest resolution you can obtained from seismic data is 5 metres, and it decreases with increasing depth, such that it is easier to interpret shallow events than it is for deeper strata.

3.4 Wireline logs

Wireline logs are geophysical tools that measure vertical changes in rock properties in boreholes and amongst their many uses, they are also used to correlate different lithologies in the subsurface (Catuneanu, 2006, p. 71). Because vertical changes in rock properties can be equated to vertical grain size changes in clastic rocks, wireline logs are important tools in determining vertical stacking patterns (vertical trends in grain size changes) which in turn can help decipher changes in depositional conditions and environments during the evolution of the basin (Catuneanu, 2006, p. 71). In sequence stratigraphy, the commonly used logs are: gamma ray (GR), spontaneous potential (SP) and photo electric factor (PEF) borehole-to-borehole lithological correlation, while the sonic and density logs are used for well-to-seismic-tie process. However, because wireline logs measure rock property changes with depth, the data derived from them is one-dimensional, giving information up to a few centimetres away from the borehole. This low lateral resolution limits the extrapolation of the data for the entire stratigraphic unit (i.e., wireline logs are not fully representative of the entire formation; Bacon et al., 2003, p. 58). Furthermore, during drilling, a permeable formation can be invaded by drilling fluids, affecting some wireline log readings (Bacon et al., 2003, p. 589). It is also important to highlight that lithology logs (i.e., GR, PEF and SP) do not infer geological environments, these logs need to be used in conjunction with other dataset (i.e., biostratigraphy, petrology, etc.) in order to give a fair geological model. This is because wireline logs do not measure grain size directly, they measure the matrix (i.e., porosity and permeability) of a rock (Schlumberger Wireline and Testing, 1989).

3.4.1 Gamma ray (GR) log

One of the most commonly used wireline logs is the GR logs, which is practical for differentiating between fine-grained, clay-rich rocks (i.e., argillites: claystones, siltstones/shale) and clay-free arenaceous rock types (e.g., "clean" sands, arenites, clast-supported, well-sorted conglomerates). Relative to arenites, fine-grained rocks (essentially mudstones) usually contain high amounts of radioactive minerals [potassium (K40), uranium (U238) and thorium (Th238)]. The GR tool uses the scintillation detector inside the gamma ray tool to record a count of incoming gamma rays that are generated in the lithology during radioactive decay (Figure 3.7). The raw data, in counts per second, are converted to American Petroleum Institute (API) units by a calibration based on two standard lithologies of "high" and "low" GR. Gamma ray logs are customarily scaled in API units, typically over a range of 0-150 API; however, the scale is not fixed and might change depending on the tool and contractor used to acquire the logs. It is important to calibrate all GR logs to the same scale during correlation for consistency. In areas where there are high percentage minerals rich in Th, U and K (e.g., zircon), the tool records higher API values. The GR curve is usually assumed to vary linearly with the proportion of clay content (aka 'shale' - V_{sh}) as expressed in equation (5). The values of GR_{min} and GR_{max} are usually picked over a given interval by direct observation of the log or from histograms. The simplest possible lithological interpretation using the gamma ray is to classify rock as being either 'clean' sand or 'shale' in other words sandy or clayey clastic rocks. A cut-off line, referred to as the "shale line", is used to define the limit between shales and sands. If a GR value falls on the left side of the shale line, it is be classified as either clean sands, evaporites or carbonates, whereas a GR value that falls on the right side represents either 'dirty' sands, siltstones, shales or clays (Merkel, 1979; Schlumberger Wireline and Testing, 1989).

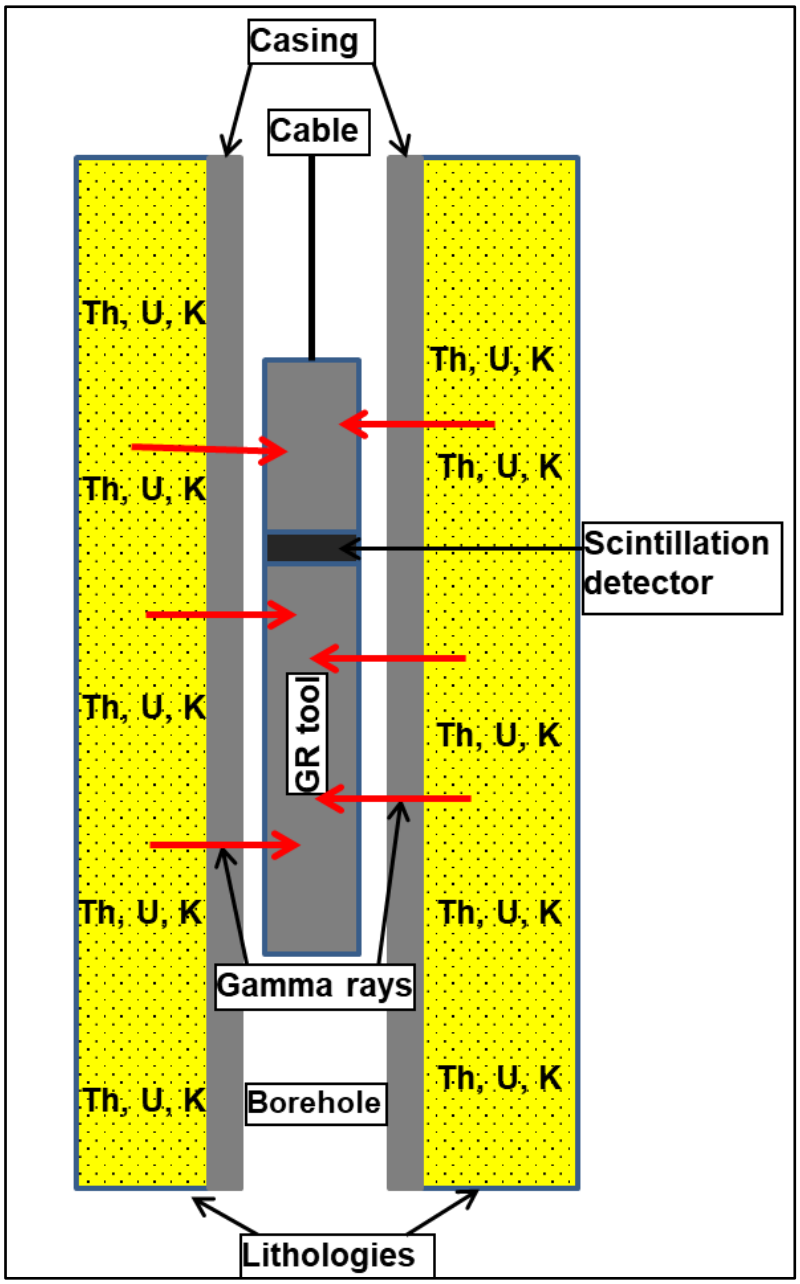

Figure 3.7: Schematic borehole cross-section showing how the gamma ray tools work (modified from Schlumberger Wireline and Testing, 1989).

$$\mathrm{V}shale(\%) = \frac{\mathrm{GRlog} - \mathrm{GRmin}}{\mathrm{GRmax} - \mathrm{GRmin}} \quad (5)$$

Where GR_{log}: Average gamma ray response in the lithology of interest

GR_{min}: Lowest gamma ray response in the lithology of interest

GR_{max}: Highest gamma ray response in the lithology of interest

3.4.2 Spontaneous potential (SP) log

In conjunction with or in the absence of GR logs, the spontaneous potential (SP) log is also commonly used for borehole-to-borehole lithological correlation. The SP log uses millivolts (mV) to measure the electric potential difference between movable electrodes in the borehole and a fixed electrode on the surface (Figure 3.8). Depending on the relative salinity of the formation water and mud filtrate, the SP deflects either to the right (positive readings) or to the left (negative readings; Figure 3.8). Commonly, the mud filtrate is less saline than the formation water, and thus both GR and SP logs give a similar response to changes in lithology. Therefore, deflection to the right on the SP log is associated with shales and clay, and a deflection to the left is associated with clean sandstones, carbonates or evaporites (Figure 3.8; Merkel, 1979; Schlumberger Wireline and Testing, 1989).

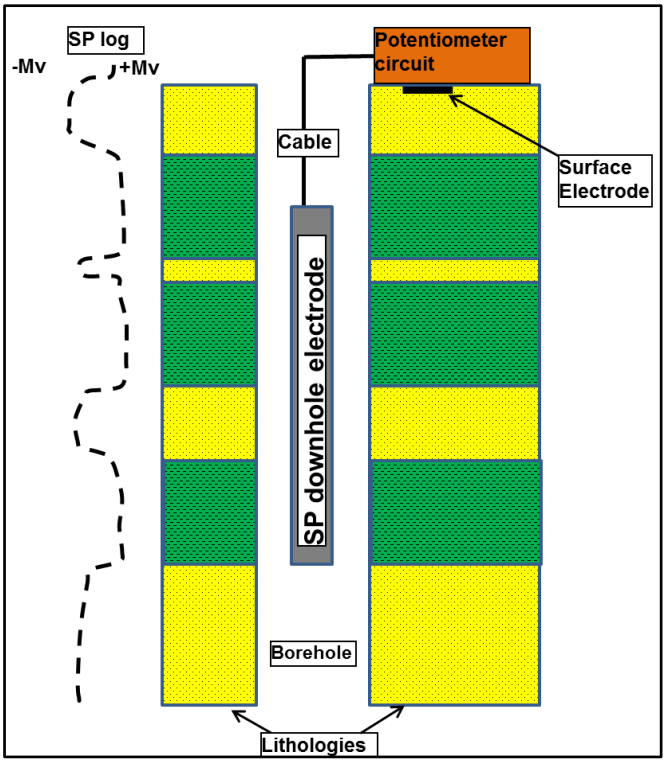

Figure 3.8: Schematic borehole cross-section showing how the SP tools work (modified from Schlumberger Wireline and Testing, 1989).

As mentioned above, GR and/or SP logs are used to infer vertical grain size trends (Figure 3.9), which may coarsen or fine upwards, or show no trend but rather frequent fluctuations (e.g., serrated logs; Emery and Myers, 1996; Kendall, 2003). The limitation of these trends is that they could occur in multiple geological settings, e.g., a coarsening upwards trend can result from a crevasse splay, a delta front, river mouth bar, etc (Figure 3.9). While a fining upwards trend could be a result of a fluvial point bar, transgressive shelf, etc (Figure 3.9). The non-uniqueness of these trends makes it challenging to

infer geological environments with confidence if wireline logs are not used in conjunction with other dataset.

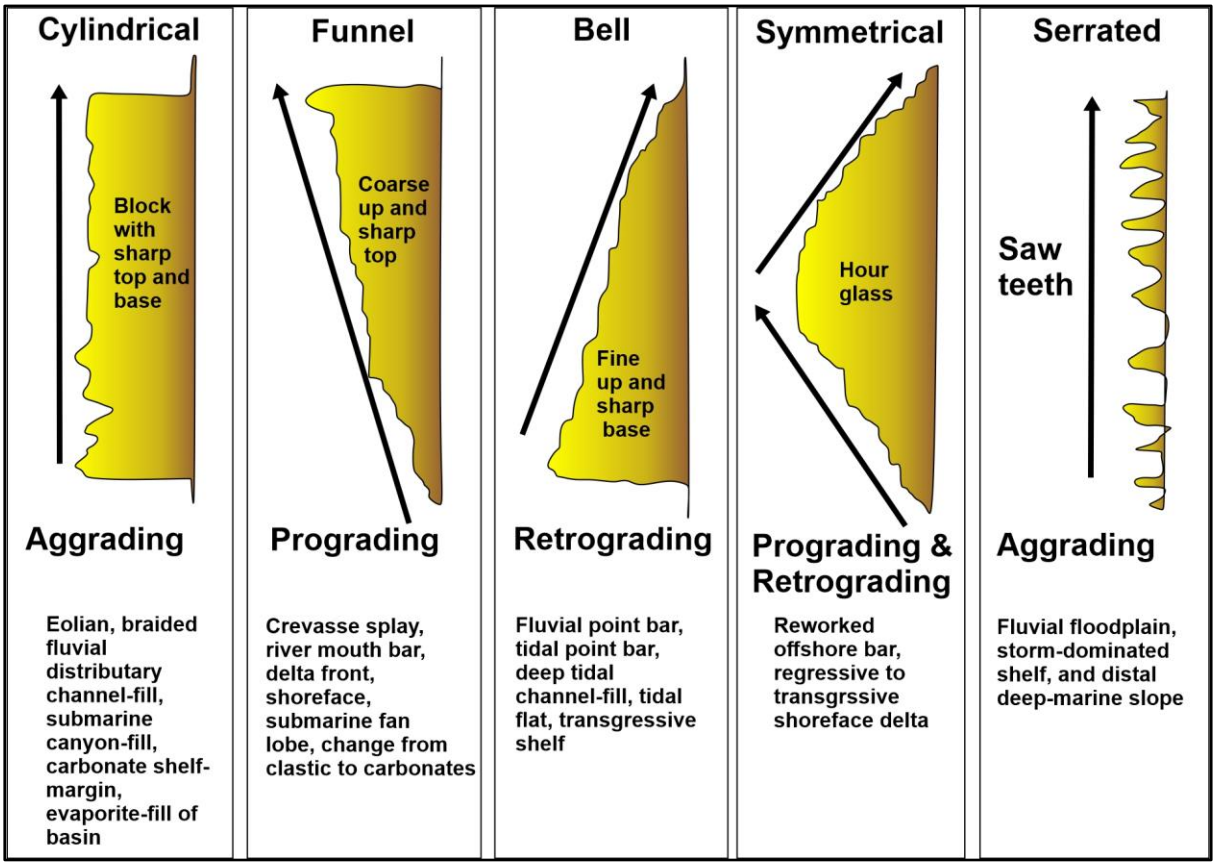

Figure 3.9: GR response to grain size variation in lithology. These responses can be used to infer geological environments in conjunction with another dataset. E.g., a cylindrical evenly distributed grain size trend with a sharp top and base indicate aggrading stacking pattern, while an increasing grain size funnel shaped trend with a sharp top indicates progradation (modified from Cant, 1992; Emery and Myers, 1996).

3.4.3 Photoelectric factor (PEF) log

The photoelectric factor (PEF) log can also be used to discriminate lithology. This log types measures the photoelectric absorption (Pe, Barns/electron), which is a measure of the average atomic number of the formation. Fluids generally have a low atomic number, and consequently very low Pe, meaning, in formations, PEF measures the rock matrix properties (i.e., porosity). The advantage of the PEF log is that in areas where the GR and Sp logs are unable to differentiate between sandstone and carbonates, the PEF log can make this distinction because sandstones, being more porous, tends to have low Pe readings, while dolomites, carbonates, clays and iron bearing rocks, being less porous, tends to have high Pe reading values. Because barite ($BaSO_4$), often used as a weighting agent during the drilling process, has a very high Pe, it can mask the natural Pe signal of the drilled succession, and

thus care needs to be taken in utilizing PEF logs from boreholes that are drilled using barite-rich drilling substances (Doveton, 1994).

3.4.4 Sonic (DT) log

Sonic and density logs can have multiple uses for subsurface evaluation, in seismic interpretation, one of their primary uses is linking boreholes to seismic profiles (i.e., well-to-seismic-tie). Sonic logs are used to estimate interval velocities, measuring the subsurface acoustic slowness (Δt), or the time that is taken by an acoustic pulse to travel through subsurface rocks from the transmitter to the receiver (Figure 3.10). The recorded acoustic slowness is inversely proportional to the P-wave velocity (1/P-wave velocity) and is measured in microseconds/foot (µs/ft). In clastic sedimentary successions, the value of Δt decreases with the degree of compaction of sediments, and hence also decreases with depth, mainly because deeper sediments are more compacted and less porous, whereas in shallow, less compacted sediments, the value of Δt will increase (Merkel, 1979; Schlumberger Wireline and Testing, 1989; Bacon et al., 2003, p.61).

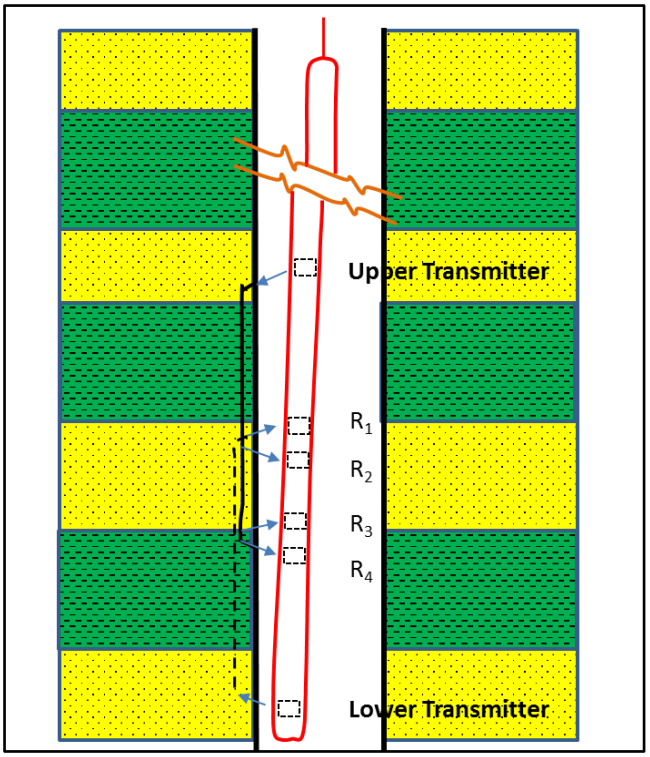

Figure 3.10: Schematic illustration of the sonic log tool (modified from Schlumberger Wireline and Testing, 1989).

3.4.5 Density (RHO) log

The density log measures the attenuation of gamma rays due to an effect called “Compton scattering”, where gamma rays emitted by the logging tool into the intersected rocks are absorbed by the rock where they collide with electrons within the rock itself (Figure 3.11) and thus the density log measures electron density within the rock. Conveniently, the ratio of bulk density (mass/unit volume) to electron density is roughly constant for most sedimentary rocks and pore fluids (except gas). The output of the density tool is therefore scaled in g/cc. The combination of density and sonic log responses at a given interval defines the acoustic impedance of the rock (Figure 3.5). The acoustic impedance is then used in well-to-seismic tie, where synthetic wavelets can be extracted to tie the borehole information with the seismic data (Figure 3.5; Merkel, 1979; Schlumberger Wireline and Testing, 1989; Bacon et al., 2003, p.61).

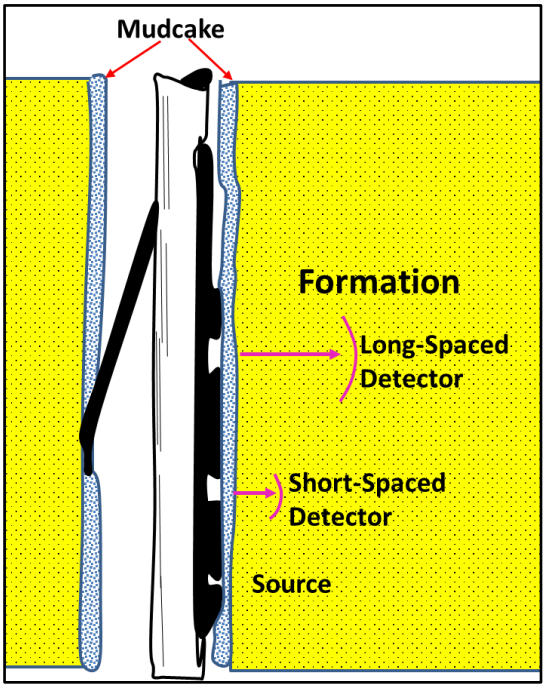

Figure 3.11: Schematic section of the density log to (modified from Schlumberger Wireline and Testing, 1989).

3.5 Well-to-seismic tie

3.5.1 Algoa Basin

The process of well-to-seismic tie was performed to relate the geology observed in borehole data, to seismic reflectors, which are recorded in TWT (see section 3.3). A synthetic seismic trace was generated by convolving a statistical zero phase wavelet (with a dominant frequency of 30Hz) with the reflection coefficient log derived using sonic and density logs from borehole Hb-A1 (Figure 3.12).

Checkshot data acquired made it possible to create a time-depth relationship, making it less challenging to pick sequence boundaries (1At1, 13At1, 15At1 and 22At1; Figures 2.1 and 3.12) on the 3D seismic volume in the Port Elizabeth Trough. Without stretching and squeezing the synthetic, a correlation of 71% was achieved in the well-to-seismic tie process using HB20013D seismic volume and the borehole HB-A1 (Figure 3.12). In this 3D seismic vintage, a decrease in acoustic impedance, which is a trough represents hard events (reverse SEG polarity). This well-to-seismic-tie was used to correlate seismic reflectors and formation welltops in the Port Elizabeth sub-basin, which was extended to other sub-basins, where possible.

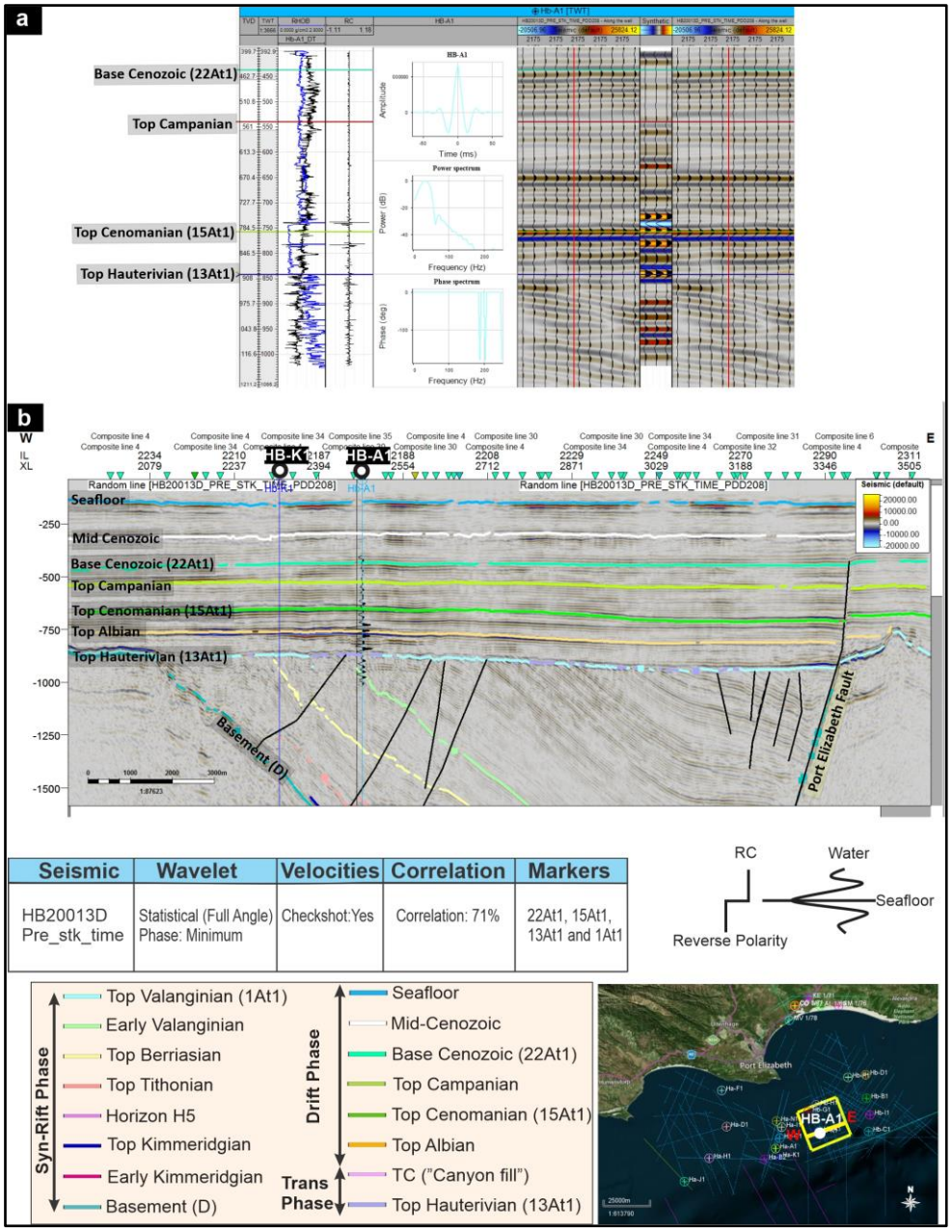

Figure 3.12: a Sonic long convolved with the density log to create a reflection coefficient. The wavelet is statistical with a 30 Hz dominant frequency. **b** Seismic-well-tie applied to HB20013D and borehole Hb-A1. With this well-seismic-tie, a maximum correlation of 71% was achieved. Base map data ©2020 Google, Maxar Technologies, AfriGIS (Pty) Ltd.

3.5.2 Gamtoos Basin

Well-seismic-tie was derived using HA-B2 borehole and HA87-042 seismic line (Figure 3.13), which was then correlated across the basin, as far as data quality permitted. Similar to the Algoa Basin, a statistical wavelet was extracted, rather than using the default Ricker Wavelet. This is because statistical wavelets are derived from the actual data, while Ricker wavelets are from Petrel E&P Software Platform default setting. Wavelet extraction on HA87-042 seismic line shows zero phase wavelet, with a central frequency of 35 Hz (Figure 3.13a). The product of density and sonic logs was convolved with the extracted statistical zero phase wavelet extracted in order to produce a synthetic wavelet, which was tied to the seismic data (Figure 3.13a, b). Due to the poor seismic data quality, maximum correlation of 50% was achieved, with a bulk shift of 20ms, without stretching and squeezing the synthetic. Furthermore, the anomalous low P-wave and high-density readings at depths 2376-4003 m, 2582-2669 m and 3648-3754 m in HA-B2 borehole are due to formation washouts, affecting the reflection coefficient and synthetic trace. Without this washout zone, the well-to-seismic tie correlation would have been higher.

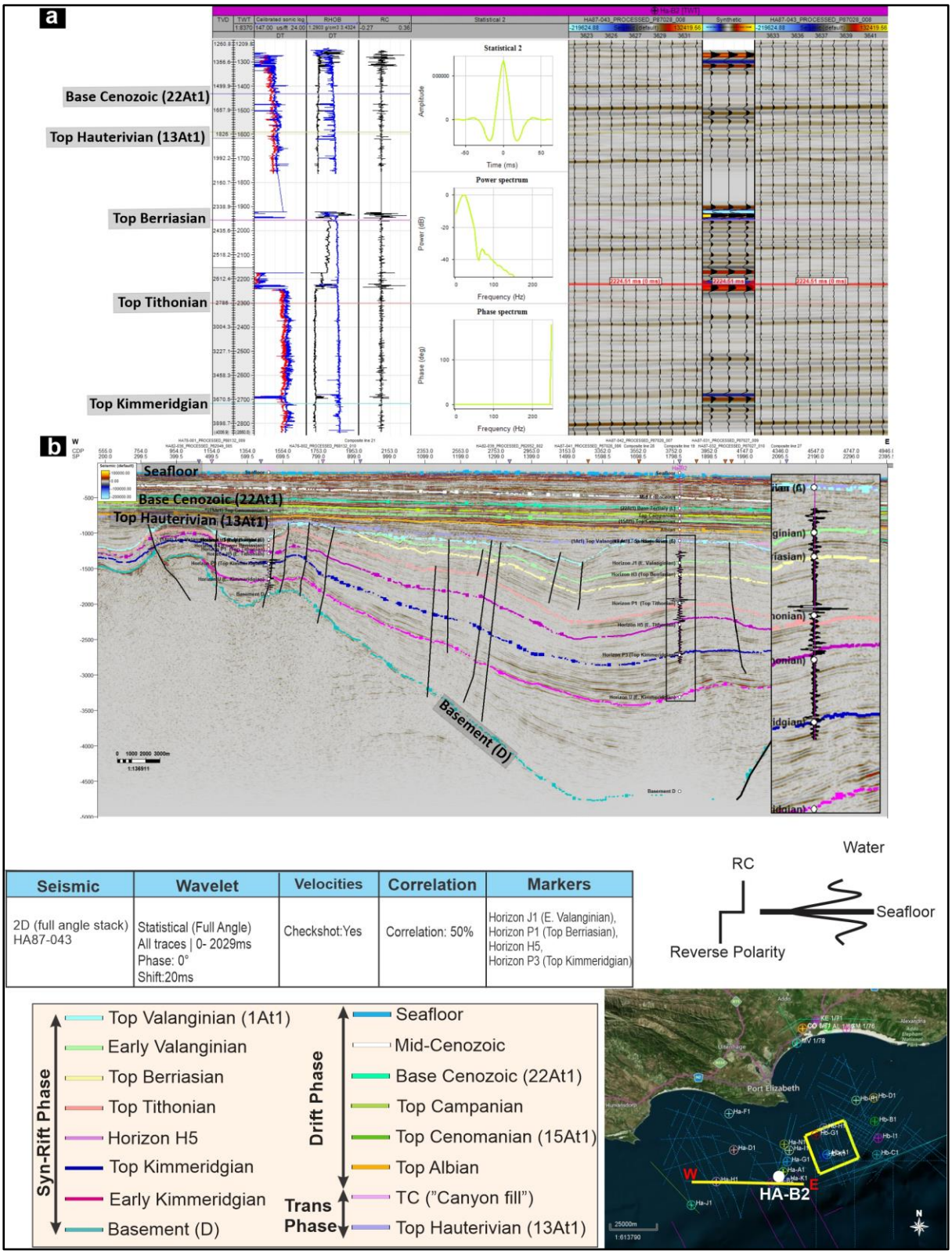

Figure 3.13: a Sonic long convolved with the density log to create a reflection coefficient. The wavelet is statistical with a 30 Hz dominant frequency. **b** Seismic-well-tie applied to HA-B2 borehole and HA87-042 seismic line. With this well-to-seismic tie, a maximum correlation of 50% was achieved. Base map data ©2020 Google, Maxar Technologies, AfriGIS (Pty) Ltd.

3.6 Depth conversion (velocity modelling)

3.6.1 Algoa Basin

Two-way-time (TWT) maps were produced by gridding (50X50m grid spacing) interpreted seismic horizons in Petrel E&P Software Platform, using the convergent interpolation gridding algorithm. The TWT maps were then depths converted, and thickness (isopach) maps were generated to understand the basin fill.

Several depth conversion methods (V0k, layered cake, etc.) were tested, and quality checked against the welltops. In the end, the V0k method was the preferred method for depth converting the TWT maps, because this method produced depth maps that ties to borehole data better, relative to the other methods. This is because of the reasonable complex geology of the Algoa Basin requires a complex velocity model (such as the V0K method) to build fairly accurate depth maps. The V0K method (Figure 3.14) plots average velocities against mid-point depth of an interval and uses a gradient to estimate the velocity (V0) at Z (0). The V0K method is a compaction method, assuming a velocity increase with depth (Dupre et al., 2007). Because we do not expect any significant carbonates, evaporites or over pressured sediments in the study area, velocity is expected to increase linearly with increasing depth (i.e., normal compaction trend). The gradient K was then estimated by extrapolating the correlation curve from the datum to the basement to show how the velocity varies with depth. This relationship is expressed by equations (6) to (9) below (Dupre et al., 2007).

$$\mathrm{V(z)} = \mathrm{Vo} + \mathrm{kz} \tag{6}$$

Z: Depth (m)

V(z): interval velocity ($m.s^{-1}$)

Vo: Initial velocity ($m.s^{-1}$)

K: Rate of change in velocity with increasing depth (s^{-1})

$$V(t) = Vo.e^{kt} \tag{7}$$

t: One-way travel time (s)

$$z = \frac{Vo\ (e^{kt} - 1)}{k} \tag{8}$$

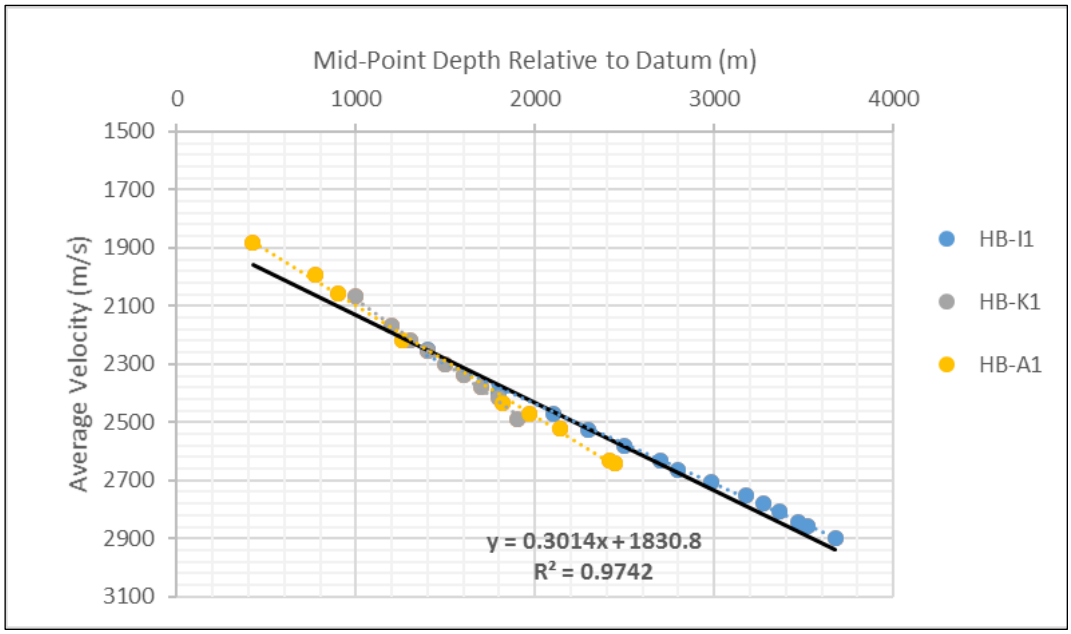

Figure 3.14: Interval Velocity vs Mid-Point Depth. Sediments in the Algoa Basin show an increase of velocity with depth, without any velocity inversion. V0: 1830 m/s, k:0.3014. Data points were based from borehole HB-I1, HB-K1 and HB-A1.

3.6.2 Gamtoos Basin

Like in the Algoa Basin, two-way-time (TWT) maps were produced by gridding (50X50m spacing) interpreted seismic horizons in Petrel E&P Software Platform, using the convergent interpolation gridding algorithm. The TWT maps were then depths converted, and thickness maps were generated to understand the provenance of sediments during basin fill.

Unlike the Algoa Basin, the V0k method did not yield favourable maps in the Gamtoos Basin, the average velocity method was used instead. This is because the average velocity methods yielded maps, which ties better to the welltops. Although the average velocity method is one the simplest of depth conversions methods, it still yielded favourable results due to the less complicated geology in the Gamtoos Basin. Depth maps were produced as a product of gridded average velocities of a specific horizon derived from checkshot data at selected boreholes, and gridded TWT maps of that horizon (Figure 3.15 and equation (9)).

$$Depth\ (m)\ = \frac{(Velocity\ (m/s)\ X\ Time\ (s)}{2} \qquad (9)$$

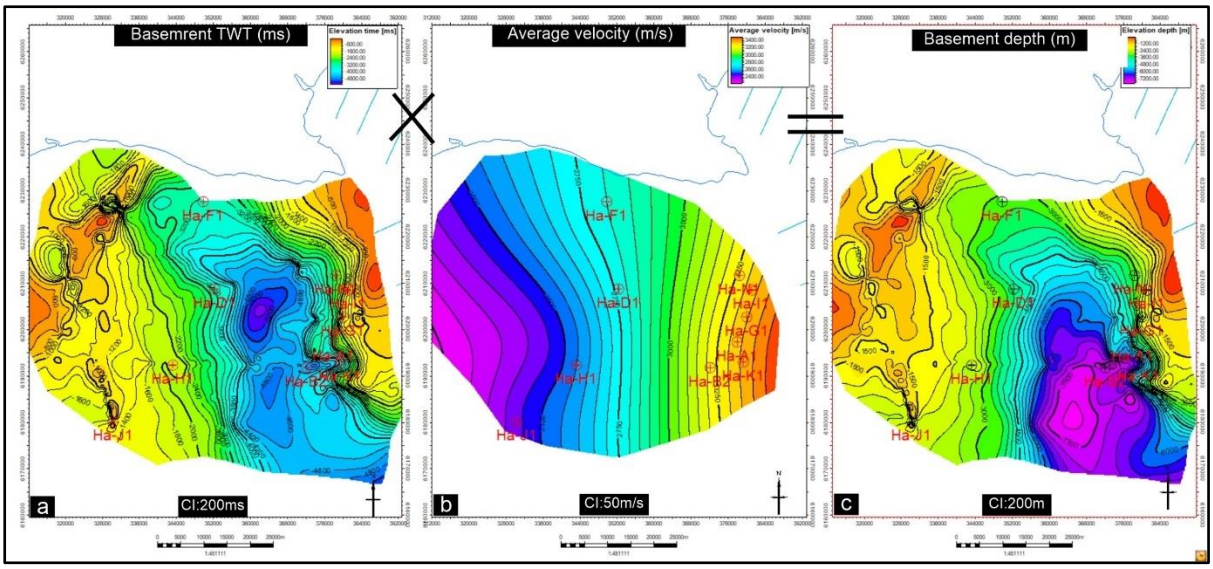

Figure 3.15: Gridded TWT Basement map multiplied by average velocity from checkshot data to produce a depth maps in the Gamtoos Basin. This process was repeated for all surfaces in the Gamtoos Basin.

3.7 Outcrop Data

Ideally, field data from large scale outcrop is preferred to incorporate into depositional models, however, these outcrops need to be laterally wide enough to provide robust, high resolution input data. Such large-scale outcrop is very rare globally. As a result, small-scale (10s to 100s metres) outcrop studies are usually carried out and field data is extrapolated to the subsurface. Small-scale outcrop data is usually complemented with either core or seismic data to give a comprehensive 3D view of the basin fill. Because recent field studies in the Algoa and Gamtoos Basins were published recently by Muir et al. (2015, 2017a, b, 2020), this public information was integrated with seismic and well data in this study.

3.8 Core data

Core data is the most useful set of subsurface datasets and it is key to relate geophysical properties obtained in other subsurface methods (Figure 3.1) to the actual rock successions that build be basin fill. Cores are typically used to interpret lithology, facies changes, sedimentary structures, paleocurrent directions, and nature of stratigraphic contacts (Catuneanu, 2006, p. 71). Core data however is also one of the most expensive datasets acquired during any basin study, and as such, it is not routinely acquired. When available, this dataset is usually proprietary and only released into the public domain after the contract petroleum companies signed with the government has expired. Moreover, core data is susceptible to damage during transportation and storage if not handled well,

rendering the core data inadequate for interpretations. In this study, we did not carry out core interpretations, however mudlog and core description recorded in end of well reports (supplied by Petroleum Agency SA) were used for lithological descriptions when available.

3.9 Workflow used

The workflow in basin analysis is a set of guidelines (not strict rules) that can be used from data loading into the data analysis software (eg., Petrel E&P Software Platform), to interpretations, to building gross depositional environments (GDE) models. Ideally, the integration of outcrop, core, wireline and seismic data should be performed, in order give comprehensive interpretations. The workflow in this study followed the steps listed below (Figure 3.16):

- Import wireline logs and seismic data (typically in SEGY, ASCII or LAS format) into an interpretation software (in our case, Petrel).
- Quality check (QC) seismic and wireline data for processing and acquisition artefacts. If available, also QC core and outcrop data for consistency and any damage resulting from transportation or storage (in case of cores).
- If formation tops are not provided, use biostratigraphy or petrological studies from core and/or outcrop to identify major sequence boundaries on wireline data.
- Perform seismic-to-well-tie process.
- When calibration is achieved, pick major sequence boundaries, faults and identify stratal terminations on seismic data.
- Identify depositional trends in wireline logs and correlate boreholes.
- Use depositional trends and stratal terminations infer local shoreline trajectories.
- Understand the mechanisms (autocyclic and/or allocyclic) responsible for seismic reflector geometries and wireline trends.
- Interpret how accommodation space changed based on local tectonics and relative sea level (RSL) change.
- Build GDE models based on observations from dataset, without inference of stratigraphic sequence model.
- Compare the GDE model with a modern day/field analogue.
- Identify system tracts based on depositional trends, and stratal geometries.
- Compare sequence boundaries and geometries observed in dataset, to stratigraphic boundaries and geometries defined in different sequence stratigraphic models.
- If the models do not fit the data, propose an alternative explanation of the data.

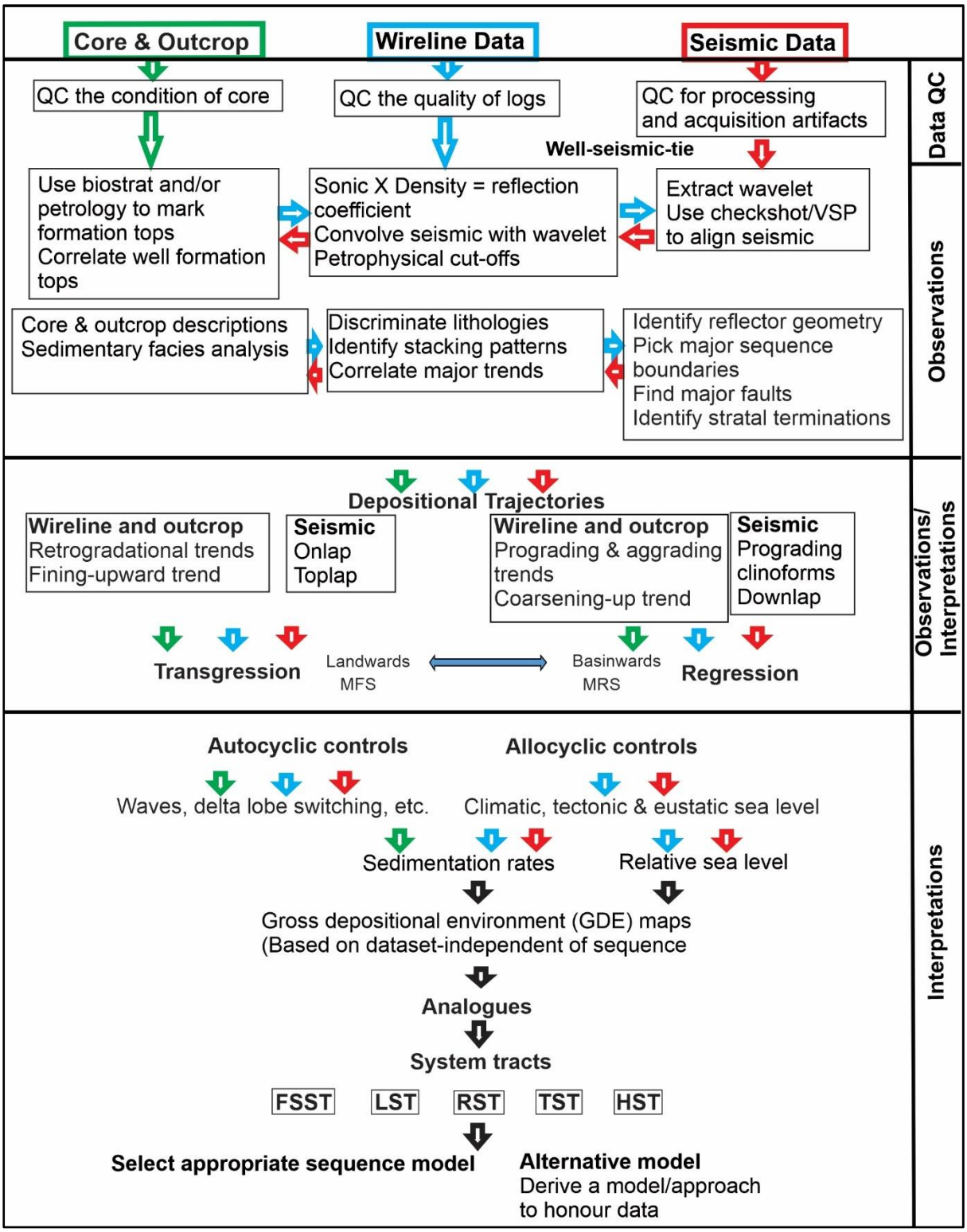

Figure 3.16: Proposed workflow for sequence stratigraphic interpretations and building depositional models. Abbreviations: LST—lowstand systems tract; TST—transgressive systems tract; HST—highstand systems tract; FSST—falling-stage systems tract; RST—regressive systems tract (Workflow inspired by Neal et al., 1993; Catuneanu, 2006, p. 6; Miall and Strasser, 2018; Neal et al., 2016; Burgess et al., 2016 and others).

3.10 Summary

To fully understand the geological evolution of depositional settings in a basin, wide ranging datasets (Catuneanu, 2006, p. 71 his fig. 2.70) must be evaluated and integrated, independent of any sequence stratigraphic model, using the dataset available as a guide to evaluate basin fill. However, wide-ranging datasets are rarely available for any given basin. This is not only because large outcrops are rare in most basin but also because acquiring such complementary seismic, core and borehole data is expensive, usually proprietary to petroleum companies, and off-limits for academic studies. Often, by the time proprietary datasets become available in the public domain, they turn out to be either poorly curated or of bad quality due to poor or antiqued acquisition and processing methods. Using the proposed workflow shown in section 3.9, this study aims to integrate different vintage datasets to achieve a comprehensive and modern re-evaluation of the evolution of the Algoa and Gamtoos Basins.

4 Sequence stratigraphy: concepts, terminology, and models

4.1 Introduction

The application of sequence stratigraphy in identifying hydrocarbon traps in frontier basins has been successful globally (e.g., ExxonMobil Liza discover offshore Guyana; Platon, 2017; Feder, 2019) and to some extent in southern Africa too (e.g., the Brulpadda and Luiperd discoveries in the Outeniqua Basin; Africa Energy Corp, 2020). However, from economic geology view-point, a solid knowledge of the geological history is important not only for exploiting hydrocarbons while transitioning to alternative energy resources but also for siting deep geological mediums to mitigate the negative impact of anthropogenic climate change (e.g., CO2 storage, deep burial of hazardous waste; e.g., Hong et al., 2015). This is because sequence stratigraphy can assist in predicting facies distribution by understanding how facies change in time and space beyond data control (Neal et al., 1993; Catuneanu, 2006, p.1; Catuneanu et al., 2011; Hampson, 2016). Sequence stratigraphy is concerned with the cyclicity of sedimentation in basins, regardless of scale (i.e., from bedform migration to basin-wide depositional system; Miall, 2014; 2016; Catuneanu, 2019a, b). Sequence stratigraphy can thus be defined as a stratigraphic method, which subdivide stratigraphic succession into a coeval rock bodies (systems tracts) using key geological surfaces by integrating geophysical (e.g., seismic, borehole data) and outcrop data define sequence boundaries (Posamentier et al., 1988; Posamentier and Vail, 1988; Van Wagoner et al., 1990; Neal et al., 1993; Boggs, 2006, p. 435; Keogh et al., 2007, their fig. 2; Catuneanu, 2006, p. 4, 2019a). A 'sequence' in sequence stratigraphy is defined as genetically related successions, which are bound by stratigraphic surfaces (Catuneanu, 2019a, b; Catuneanu and Zecchin, 2020). This definition moves away from the idea that only: 1) subaerial unconformities (SU) can be used as sequence boundaries, and 2) conformable successions can occur within a sequence (Catuneanu, 2019a; Catuneanu and Zecchin, 2020). It has been repeatedly shown that stratigraphic boundaries should not only be limited to SUs, but to surfaces that mark a full cycle of genetically related sequences (Catuneanu, 2006, 2019a, 2019b; Neal et al., 2016; Ridente, 2016). Catuneanu (2019a, b) argues that sequence stratigraphic surfaces and units can form at any scale, driven by both allocyclic and autocyclic mechanism. The only limitation to observing these surfaces and units is the resolution of the data, which varies from 10^{-6} Ma scale for bedform migration to 10^{2} Ma scale in depositional systems (e.g., Miall, 2014; Catuneanu, 2019a, b; Catuneanu and Zecchin, 2020). Therefore, understanding of shoreline trajectories, vertical stacking patterns, geometry of stratal terminations and

mapping of facies change contributes defining the building blocks of a sequence stratigraphic framework, which comprise the sequences and their subcomponents (i.e., the system tracts; Neal et al., 2016). Unsurprisingly, the best depositional models are those that integrate different type of datasets (core, outcrop, wireline, seismic surveys, etc.) to give a more complete evaluation of the rock record (Neal and Abreu, 2009; Catuneanu et al., 2011). This chapter is a high-level overview of the key concepts, terminology and accepted models used in sequence stratigraphy of clastic depositional environments.

4.2 Sea level change

Sea level is defined as being either eustatic (global) or relative (local; Mitchum et al., 1977; Emery and Myers, 1996; Catuneanu, 2006, p. 5). Eustatic sea level is the vertical distance between the centre of the earth and the water surface (Catuneanu, 2006, p. 84), while relative sea level (RSL) is defined as the vertical distance between a local basinal datum and the water surface and is a function of local tectonics and global sea level (Catuneanu, 2006, p. 86, p. 83 his Fig. 3.14). Coupled with changes in sedimentation, RSL change (accommodation space) influences shoreline trajectories, and result in either transgression, regression, degradation or aggradation in nearshore settings (Posamentier et al., 1988; Galloway, 1989; Catuneanu, 2006, p. 77).

For predicting shoreline trajectories along different continental margins, the early sequence stratigraphic schools of thought (i.e., Posamentier et al., 1988; Posamentier and Vail, 1988) assumed a worldwide synchronicity of the sea level changes as summarized by Haq et al. (1987) in their 'global sea level chart'. Cautions against the practice of using this chart to predict local sea level changes has been frequently made (Miall, 1992, 2009; Muto et al., 2016; Neal et al., 2016). This is because, even if depositional basins are within the same depositional region (e.g., along the same passive continental margin or within the same rift basin system), the effects of local processes (e.g., especially local tectonics, local variations in sediment input, but also autocyclic processes inherent in depositional systems) can overwrite global sea level changes (Miall, 1992, 2009; Muto et al., 2016; Neal et al., 2016).

4.3 Allocyclic and autocyclic controls

Allocyclic control refers to processes or stratigraphic features within a depositional system occurring due to external forcing mechanisms (i.e., changes in the local or global climate, local or global tectonics, eustatic sea level; Einsele et al., 1991; Muto et al., 2016). Autocyclic control refers to stratigraphic features within a depositional system that formed due to intra-basinal mechanisms that are usually laterally limited within basins (i.e., wave action, delta lobes switching, channel avulsion, local but large-scale slumps, etc.; Shanmugam, 1988; Einsele et al., 1991; Muto et al., 2016; Catuneanu, 2006, 2019a). These two mechanisms are always at play simultaneously in any basin (Muto et al., 2016; Catuneanu and Zecchin, 2016, 2020; Ridente et al., 2016), and untangling their impact on the rock record has been the quest not only of sequence stratigraphers, but generations of geologists (e.g., Shanley and McCabe, 1994; Allen et al., 2002).

4.4 Stratal terminations

Stratal terminations are stratigraphic geometries that form when strata terminate against a bounding surface, indicating either a missing or condensed stratigraphic unit (Mitchum, 1977; Christie-Blick, 1991; Catuneanu, 2006, p. 69, 106; Neal et al., 2016). The association of stratal terminations with specific depositional trends allows inferences on the shoreline trajectories in the basin (Catuneanu, 2006, p. 106). However, the non-uniqueness of stratal terminations geometry makes it challenging to use them for identifying depositional environments (Catuneanu and Zechani, 2016). The most common stratal terminations are: (a) truncation, (b) onlap, (c) downlap, (d) offlap and (e) toplap (Christie-Blick, 1991; Catuneanu, 2006, p. 106 his fig 4.1; Catuneanu, 2019a his fig. 18).

4.5 Stratigraphic surfaces and sequence models

There are currently six conventional sequence stratigraphic models grouped into depositional, genetic and T-R sequence stratigraphic models (Figure 4.1). These sequence models use different bounding surfaces to define a stratigraphic framework within which the most fundamental unit is the ‘sequence’ (see section 4.1). The most commonly used stratigraphic surfaces (Catuneanu, 2019b his fig. 7) are highlighted in Figure 4.1 and are: subaerial unconformities (SU), basal surface of forced regression (BSFR), maximum regressive surface (MRS), maximum flooding surface (MFS), transgressive ravinement surface

(TRS), and correlative conformities (CC). Detailed definitions and descriptions of these surfaces can be found in the relevant literature (e.g., Mitchum et al., 1977; Posamentier et al., 1988; Galloway, 1989; Hunt and Tucker, 1992, 1995; Plint and Nummedal, 2000; Catuneanu, 2002, 2006, p.123; Embry et al., 2007).

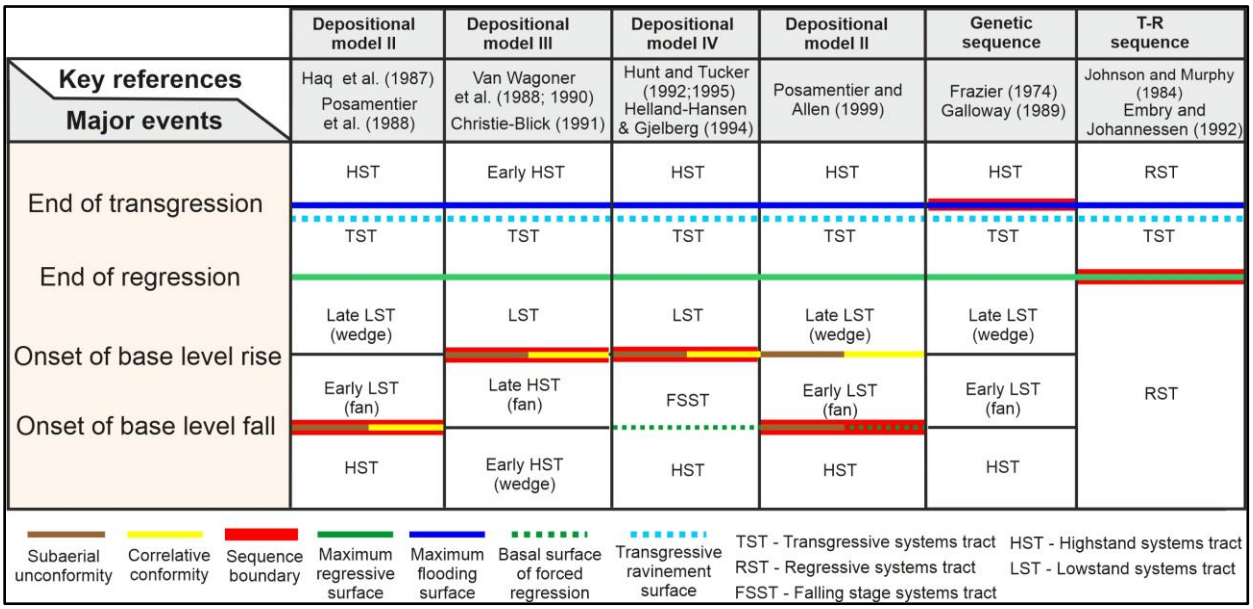

Figure 4.1: Stratigraphic models and their associated system tracts and sequence boundaries placement. Depositional sequence II, places sequence boundary at the onset of base level fall; depositional sequence model III&IV both places the sequence boundary at the end of base level fall; depositional sequence IV places the sequence boundary between the FSST and LST deposits. The genetic sequence stratigraphic model places the sequence boundary at the end of transgression. The T-R sequence model places the sequence boundary at the end of regression. Abbreviations: LST—lowstand systems tract; TST—transgressive systems tract; HST—highstand systems tract; FSST—falling-stage systems tract; RST—regressive systems tract; T–R— transgressive-regressive (modified from Catuneanu, 2002; Catuneanu, 2019b).

The main difference between these stratigraphic models is that depositional sequence models use subaerial unconformities as sequence boundaries, while the genetic and T-R sequence stratigraphic models use shoreline trajectories (MFS and MRS) to define a sequence boundary (Embry et al., 2007; Catuneanu et al., 2011). It has been repeatedly argued that bounding surfaces should not only be limited to SU, but to surfaces that mark a full cycle of genetically related successions (e.g., Catuneanu, 2006, 2019a, 2019b, 2020; Neal et al., 2016; Ridente, 2016; Catuneanu and Zecchin, 2020). This is because stratigraphic units that make up one sequence can form at various scales, making the principles of sequence stratigraphy independent of scale (Catuneanu, 2020). Consequently, depending on the resolution of the data and the scale of investigation, a full cycle of genetically related succession can be bound by flooding surfaces (Catuneanu, 2006, p. 239, 2019a, 2020; Neal et al., 2016; Ridente, 2016; Catuneanu and Zecchin, 2020). Although numerical modelling in sequence stratigraphy (Neal et al., 2016;

Muto et al., 2016) has been used to simulate stratigraphic surfaces, Catuneanu and Zecchin (2016) argues that numerical modelling can generate multitude sequence stratigraphic scenarios, some of which might not be representative of real geological events. For this reason, experimental sequence stratigraphy is not yet able to compete with models based on robust integrated datasets of high vertical and horizontal resolution, however this approach can complement limited datasets especially in frontier basins, where baseline stratigraphic frameworks are in constant need of refinement as more data becomes available (Catuneanu and Zecchin, 2016).

4.6 System tracts

Irrespective of where the sequence bounding surfaces are positioned within a succession of rocks (i.e., notwithstanding the sequence model used), the building blocks of any sequence are the system tracts. Depositional sequence models II&III together with the genetic sequence stratigraphic model recognise three types of system tracts (LST, TST and HST), depositional sequence model IV recognises four system tracts (FSST, LST, TST and HST), and the T-R sequence model works with only two system tracts (RST and TST). These system tracts are explained in this section.

4.6.1 Falling stage system tract (FSST)

The FSST, which is unique to depositional sequence IV, occurs only during forced regression (Hunt and Tucker, 1992, 1995; Helland-Hansen and Gjelberg, 1994; Plint and Nummedal, 2000; Catuneanu, 2006, p. 178), before the RSL reaches its lowest point (Hunt and Tucker, 1992, 1995; Plint and Nummedal, 2000). In marine setting, the FSST is bounded at the base by regressive surface of marine erosion and basal surface of forced regression, with the correlative conformity bounding at the top (Hunt and Tucker, 1992; Helland-Hansen and Gjelberg, 1994, 1995; Catuneanu, 2006, p.179). FSST deposits have an overall upward coarsening gamma ray signature in coastal and shallow marine successions (Neal et al., 1993). During FSST formation, the resulting subaerial erosion generates truncational (offlap) stratal termination over the top of previously deposited nearshore deposits, while downlapping surfaces form in shallow marine settings due to equilibrium graded profile (Catuneanu, 2002, 2006). FSST can also be characterized by significant slope fans, slumps and basin floor fans, which result from gravity flows that are generated due to the instability of the shelf region (Hunt and Tucker, 1992; Helland-Hansen and Gjelberg, 1994; Plint and Nummedal, 2000; Catuneanu, 2002). Generally, in the early stage of FSST low sand-to-shale ratio basin

floor fans are generated that are thus mud-dominated, whereas in the late phase of FSST formation, sand content can increase leading to the development of sand-dominated basin floor fans (Catuneanu, 2006, p. 186 his figs 5.26 and 5.27). However, Hunt and Tucker (1992) cautions that the slope wedge and the basins floor fans might not always occur simultaneously during the FSST, as one might be present without the other. Moreover, when the duration of base level fall is too short or there is a very fast base level rise, this system tract might not be deposited at all (Hunt and Tucker, 1992).

4.6.2 Lowstand system tract (LST)

The definition of this system tract differs considerably across the different schools of thought. The top bounding surface is generally accepted to be the transgressive surface (or MRS; Posamentier et al., 1988; Van Wagoner et al., 1988; Galloway, 1989; Hunt and Tucker, 1992; Posamentier and Allen, 1999; Helland-Hansen and Gjelberg, 1994; Plint and Nummedal, 2000; Catuneanu et al., 2011). Depositional sequence II and genetic sequence stratigraphic models defines the LST as the lowest system tract, bound at the base by the correlative conformity in distal marine, and subaerial unconformity in shallow marine environments, respectively. According to Posamentier et al. (1988) as well as Posamentier and Allen (1999), LST represents sediments deposited during an RSL fall and early rise, separating it into LST fan and LST wedge, respectively. In depositional sequence models III & IV, the LST forms when sea level is at its lowest, during the early stages of RSL rise, when the rate of RSL rise is outpaced by sedimentation (Hunt and Tucker, 1992; Van Wagoner et al., 1988; Boggs, 2006; Catuneanu, 2006, p. 197). The difference is that, in depositional sequence model IV, the correlative conformity forms at the end of base level fall and not at the start of base level fall (Hunt and Tucker, 1992; Catuneanu, 2002). LST deposits are identifiable on gamma ray logs by their coarsening-upward signatures in shallow marine settings, and fining-upward successions in the nonmarine settings (Neal et al., 1993). In seismic profiles, LST wedge sediments often show toplapping stratal terminations (with onlaps on the sequence boundary), and form aggrading alluvial and coastal plain, as well as prograding marine (e.g., offshore marine to sub-marine fan) deposits, respectively (Catuneanu, 2002, 2006; Catuneanu et al., 2011). In deep water setting, the LST (*sensu* Hunt and Tucker, 1992;1995) is associated with low density (low sand-to-shale ratio) turbidites, entrenched channels and frontal slays (Catuneanu, 2006, p. 198 his fig. 5.44).

4.6.3 Transgressive system tract (TST)

The definition of the TST is consistent across the different schools of thought in that, the TST forms when the rate of RSL rise outpaces sedimentation rates along the shoreline, resulting in a landward shift of the shoreline (Van Wagoner et al., 1988; Posamentier et al., 1988; Galloway 1989; Hunt and Tucker, 1992; Embry and Johannessen, 1992; Embry, 1993, 1995; Catuneanu, 2006, p. 205; Catuneanu et al., 2011). The transgressive system tract is defined (e.g., Posamentier et al.,1988; Hunt and Tucker, 1992; Embry, 1993, 1995; Posamentier and Allen, 1999; Catuneanu, 2002) as the system tract bounded by the transgressive surface and the maximum flooding surface at the base and top, respectively. In both marine and non-marine sections, TST deposits are identifiable by a fining-upward gamma ray signature and onlapping stratal terminations in shallow (and some deep) marine settings. Near the shoreline, the newly generated 'healing phase' sediments, which can contain the transgressive lag, onlap on the wave ravinement surface (Neal et al., 1993; Catuneanu, 2006, p.205).

4.6.4 Highstand system tract (HST)

The HST is also consistently used across different schools of thought and is defined as a system tract that forms during normal regression when sedimentation rate outpaces the late stage (decelerating) RSL rise (Hunt and Tucker, 1992; Embry and Johannessen, 1992; Posamentier and Allen, 1999; Catuneanu, 2006; Catuneanu et al., 2011). The HST is bound at the base by an MFS, and at the top, by either a subaerial unconformity in fluvial environment, BSFR in coastal and deep-water environment, and RSME in shallow marine environment (Hunt and Tucker, 1992; Catuneanu, 2002, 2006). In marine successions, the gamma ray signature of the HST is coarsening-upwards in marine, and fining-upwards in non-marine strata (Neal et al., 1993). Aggradation mostly in nearshore and non-marine as well as progradation in marine sediments are common in HST, due to high sediment influx, which, coupled with the slow RSL rise, ultimately result in a normal regressive shoreline (Neal et al., 1993; Catuneanu, 2006, p. 172).

4.6.5 Regressive systems tract (RST)

This system tract is unique to the T-R sequence model (e.g., Embry and Johannessen, 1992; Embry, 1993, 1995), representing all sediments deposited during shoreline regression, including those that are deposited during HST, FSST and LST (Catuneanu, 2002, 2006). In both marine and non-marine settings, the RST is bounded at the base by the MFS, while the top bounding surface is a subaerial unconformity or

the MRS in non-marine and marine settings, respectively (Embry, 1995; Catuneanu, 2002). This system tract shows a coarsening-upward trend in marine settings (Embry, 1995; Catuneanu, 2002). If the shallow deposits that form in the early stages of sea level rise (i.e., LST in other nomenclature) are not completely removed by the transgressive ravinement surface, the MRS ends up amalgamating with the subaerial unconformity (Catuneanu, 2002). Using the T-R sequence model is highly appropriate in areas where the resolution of subsurface data does not permit the separation of deposits that form in forced regression (i.e., base level fall) from those that are generated during early and late sea level rises (i.e., the normal regressive, upward-coarsening and mostly, but not only prograding strata).

4.7 Hierarchy in sequence stratigraphy

There are two approaches used for grouping sequences into hierarchy. The first one is that of Vail et al. (1977), which relies on eustatic controls that are driven by a combination of orbital mechanisms (i.e., climate change) and tectonics. The limitation of this frequency-based approach is that it ignores the powerful and often intertwined effect of local tectonics and climate on the generation of sediment supply and accommodation space. Because the cyclicity of sequences in this method is assumed to be eustasy driven (i.e., global events), it implies that sequences of different hierarchies are globally synchronised and thus can be correlated (Miall, 1992, 2009; Catuneanu 2006, p. 329). Furthermore, the pitfall of this approach is that, to justify hierarchy order, the approximate duration preserved in rock record must be known (Catuneanu 2006, p. 329). The second approach categorizes sequences into hierarchies by using the magnitude the relative sea level change on creating boundary surfaces, independent of the duration of the cycles (i.e., the cycles are short or long or anything in between). In this approach, explained further in the work of Catuneanu (e.g., 2006, p. 328, 2019a, 2020) the attributes of a sequence boundary is different during a relative sea level change of 10 vs 200 m, regardless of the length of the time during which the RSL changes (i.e., slow or fast RSL change; Embry, 2009a, p. 60). In other words, relative to the duration/rate, the magnitude of RSL changes are argued to have a more prominent effect on the rock record.

When there are numerous and closely spaced sequence stratigraphic surfaces within a succession (which occurs when the cyclicity is frequent and thus not easily detectable by standard, commonly used subsurface methods which normally lack high resolution), regardless of the scale of magnitude, theoretically any of those surfaces can be used as sequence boundaries (Embry, 2009a, p.59; Catuneanu,

2006, p. 327, 2019a). However, such practice would result in multiple subdivisions of sequences, and a good approach around the problem is by grouping them into hierarchies of first, second, third, fourth and fifth order-scale magnitude events and surfaces that result from them (Embry, 2009a, p. 59; Catuneanu, 2019a). Generally, the first, second and third order-scale events are referred to as low-order, while fourth, fifth, etc., events are referred to as high-order events (i.e., high- vs low-rank events, *sensu* Catuneanu, 2006, 2019a,b, 2020). When a higher order (high frequency, low magnitude) event is superimposed on a low order (low frequency, high magnitude) event, the high order event does not change the importance of the low order event (Catuneanu 2006, p. 328, 2019a his fig.15, 2019b; Catuneanu and Zecchin, 2020). Moreover, it is possible to have high-order progradation within a low-order transgressive succession, and vice versa (Catuneanu, 2019a). Historically, sequence stratigraphy was limited to low-order events (Miall 2013; 2016), however as discussed, high-order events have the potential to form part of sequence stratigraphic framework (see discussion in Catuneanu, 2019a, 2020; Catuneanu and Zecchin 2020). As such, because of the potential to form stratigraphic surfaces at any scale, Catuneanu (2019a) cautions that, nomenclature and methodology in sequence stratigraphy should be independent of scale.

4.8 Summary

Although there are several valid sequence stratigraphic models, interpreters should first interrogate the applicability of the current models to a given dataset, because these models were tested independently, on different datasets and in different basin margins and have been modified through time (Catuneanu, 2002, 2006, p.7). Therefore, a one-size-fit all approach in using models for building sequence stratigraphic frameworks is as problematic as using rigidly facies models to determine the depositional environment of sedimentary rocks (see discussion in Walker, 1990, 2006).

Facies distribution in areas with lean direct observational data can be predicated if interpretations used for building depositional models are consistent with rigorous and unbiased observations from data-reach regions of study areas. Instead of using stratal geometry to interpret and infer sea level changes, stratal terminations should be described based on how sediments fill the accommodation space (i.e., progradation, aggradation, degradation; Neal and Abreu, 2009; Hampson et al., 2016). However, the non-uniqueness (generic-nature) of certain stratal terminations means that those geometry cannot be used without other corroborating observations to identify a system tract (i.e., using downlaps to infer FSST is problematic as downlaps can form due to both normal and forced regression – Catuneanu, 2006, p. 107),

because stratal terminations can result from multiple mechanisms that drive sedimentation (Catuneanu and Zecchin, 2016).

The importance of understanding the main driving mechanisms (i.e., allo- vs autocyclic) for any stratigraphic work cannot be overstated (e.g., Miall, 2009; Muto et al., 2016; Neal et al., 2016), however, as several authors pointed out (e.g., Catuneanu and Zecchin, 2016, 2020; Ridente et al., 2016), it is not always obvious how to untangle the compounded effect of the main factors responsible for stratal terminations. Finally, it has been repeatedly proposed that sequence boundaries should not be limited to unconformities, but to surfaces that can be correlated across the basin to mark the beginning and end of a full cycle of relative sea level changes (i.e., delineate full sequences; e.g., Catuneanu, 2006, p. 239, 2019a, 2020; Neal et al., 2016; Ridente, 2016).

5 The Algoa Basin

5.1 Introduction

Although a working petroleum system was proven in the Mesozoic Algoa Basin of South Africa (Figure 1.1), data acquired to-date yielded limited exploration success unlike in the neighbouring Bredasdorp Basin (e.g., Malan, 1993; McMillan et al., 1997; Mudaly et al., 2009). Possibly due to the absence of economic incentive, a detailed sequence stratigraphic framework is lacking for the Algoa Basin, and this limit, especially in the offshore regions, the understanding of the: a) sedimentary facies distribution, b) basin development history and c) nature of the petroleum systems (Muir et al., 2020). Herein, a sequence stratigraphic framework for the Mid-Mesozoic to Holocene is presented in the Algoa Basin based on the integration of a subset of the available vintage data (seismic, wireline and some outcrop data).

Hydrocarbon exploration in the Mesozoic Algoa Basin commenced during late 1960s with the onshore and offshore drilling of 31 wells and acquiring of ~5 000 km of offshore 2D seismic lines by Soekor E&P (Pty.) Ltd. (Figure 1.1; McMillan et al., 1997; Broad et al., 2012). Moreover, 3D seismic data was acquired in the offshore Algoa Basin by the Petroleum Geo-Services (PGS) and New Age Global Energy in 2001 and 2010, respectively (Petroleum Agency SA, 2020; New Age Global Energy, 2018). In spite of the relatively poor data quality from this region, previous studies have shown that the architecture of the Algoa Basin and deposition within it during the syn-rift phase were primarily controlled by the structural nature of the bounding faults, which follow the structural grain of the underlying Palaeozoic Cape Supergroup (Figures 1.1 and 2.1; Broad, 1990; Malan et al., 1990; Bate and Malan, 1992; Ben-Avraham, 1993, 1997; McMillan et al., 1997). These bounding faults subdivide the Algoa Basin into three structurally complex sub-basins namely: Sundays River, Port Elizabeth and Uitenhage Troughs (Figures 1.1 and 2.1; Broad, 1990; Malan et al., 1990; McMillan et al., 1997). In the post-rift phase, the generation of the accommodation space was primarily driven by thermal subsidence (Broad, 1990; Malan et al., 1990; McMillan et al., 1997; Baby et al., 2018).

5.2 Results

In this study, major stratigraphic units were defined based on changes in vertical grain-size distribution in the borehole data (including borehole reports), changes in reflection seismic facies, stratal geometries in the seismic data as well as regional geological consensus (e.g., Dingle et al., 1983; Malan et al., 1990, 1997; Brown et al., 1995; Broad et al., 2012; Muir et al., 2017a, b; Muir et al., 2020). In harmony with many other previous studies [including biostratigraphic analysis (i.e., McMillan and McMillan, 1976; Du Toit, 1990; McMillan, 2010)], the main sequence boundaries identified are: Basement D, Top Valanginian (1At1/6At1), Top Hauterivian (13At1), Top Albian (15At1), Top Campanian, Base Cenozoic (22At1), Mid-Cenozoic and Seafloor (Figure 2.1; Malan et al., 1990; Malan, 1993; Brown et al., 1995; McMillan et al., 1997; PASA, 2012). Between them, the stratigraphic units were deposited from the Jurassic syn-rift to Holocene drift-sag tectonic phases (McMillan et al., 1997). Minor sequence boundaries identified in the syn-rift sequence are the flooding surfaces (Vail et al., 1991; Embry et al., 2007; Catuneanu, 2019a, b), and include the following: P3 (Top Kimmeridgian), H5 (Top Tithonian), P1 (Top Berriasian), and J1 (Early Valanginian). Arbitrarily selected SW-NE and NW-SE cross-sections (Figures 4.4 and 4.5) show the major sequences identified in this study. Unless otherwise stated, the vertical distance of the seismic data is in two-way time (TWT) expressed in milliseconds (ms) and the horizontal distance is showed by a scale bar in metres. In this chapter, the standard terminology for stratal terminations (onlaps, truncation, etc.) is used to show the nature (geometries) of seismic reflectors and not to infer system tracts or relative sea level changes.

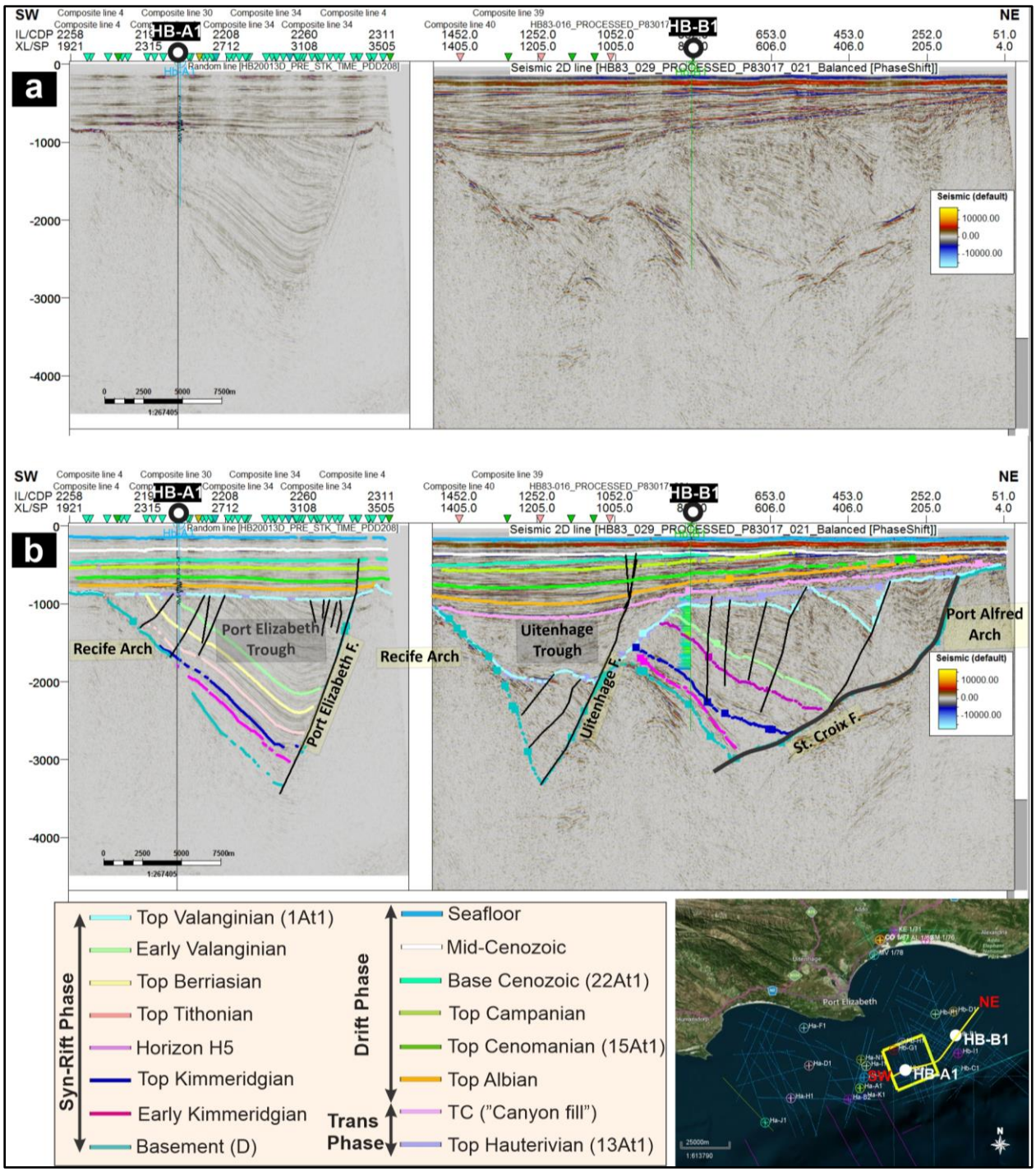

Figure 5.1: Strike oriented semi regional Algoa Basin seismic section. **a** Uninterpreted NW-SE section across the Algoa Basin. **b** Interpreted NW-SE section across the Algoa Basin. Base map data ©2020 Google, Maxar Technologies, AfriGIS (Pty) Ltd.

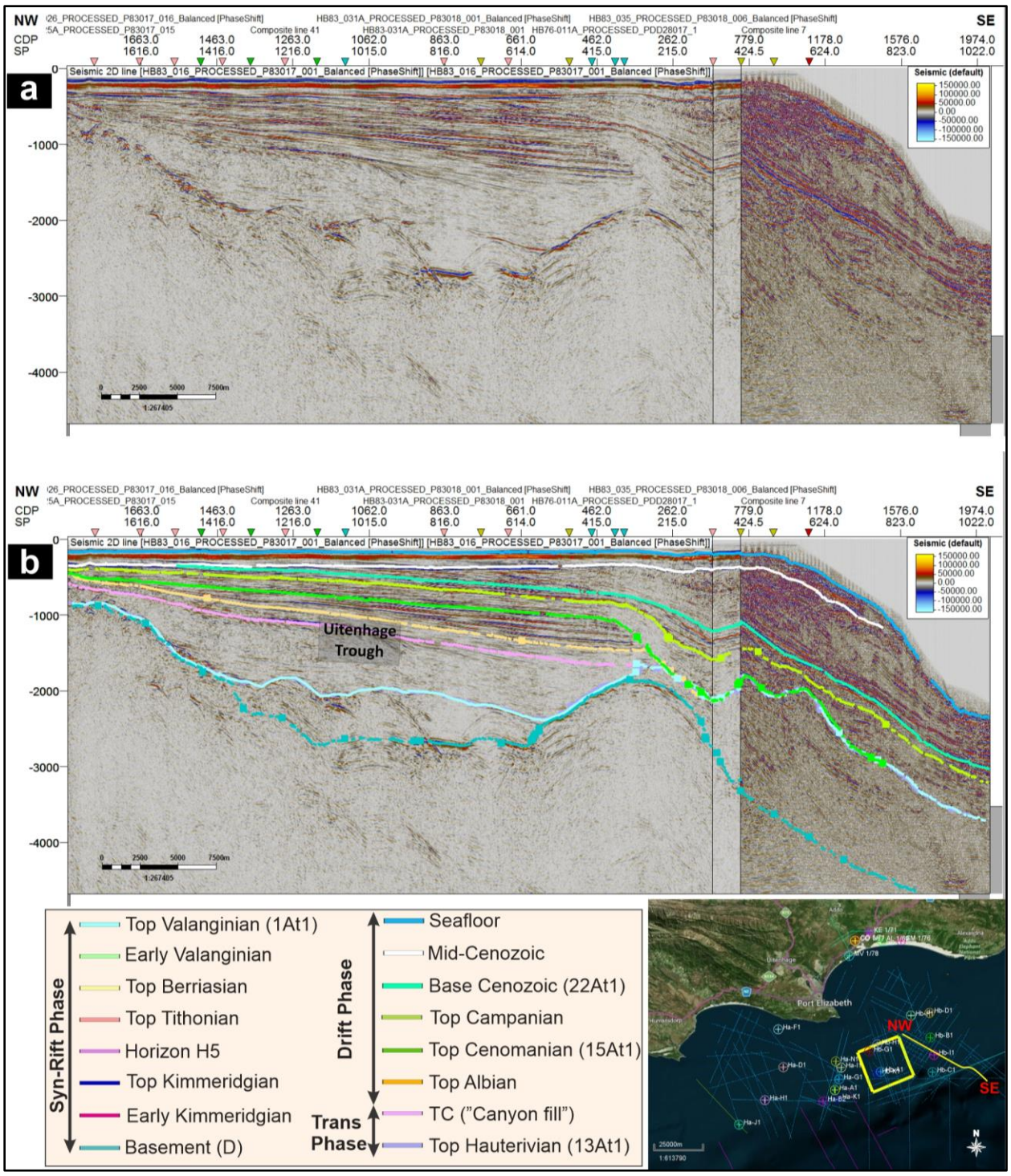

Figure 5.2: Dip orientated semi regional Algoa Basin seismic section. **a** Uninterpreted NW-SE section across the Algoa Basin. **b** Interpreted NW-SE section across the Algoa Basin. Base map data ©2020 Google, Maxar Technologies, AfriGIS (Pty) Ltd.

5.2.1 Borehole correlations

5.2.1.1 Basement (pre-Aalenian) to upper Kimmeridgian

With only two boreholes 30 km apart intersecting this succession, considerable amount of section remains unexplored (McMillan et al., 1997). Moreover, the boreholes (Figure 5.3) do not represent the entire Basement to Top Kimmeridgian succession, because only ~400 m and ~85 m of rocks were logged in the boreholes HB-P1 and HB-C1, respectively (Figure 5.3). In the southern borehole HB-C1, the low GR values, ranging from 44 to 151 American Petroleum Institute (API), become less connected and are detected over the ~85-m-thick unit with low sand-to-shale ratio (Figure 5.3). In the northern borehole HB-P1, high GR values dominate, detecting over the 400-m-thick succession with high sand-to-shale ratio (Figure 5.3). The GR signatures and the relative position of the two boreholes suggest that the intersected sediments formed in two different environments: likely a high-energy fluvial/alluvial setting and a low-energy marine setting within boreholes HB-P1 and HB-C1, respectively. However, the non-uniqueness of these trends makes it challenging to infer geological environments in the absence of other complementary data (see Figure 3.9). A more intergraded approach is presented in Chapter 7.

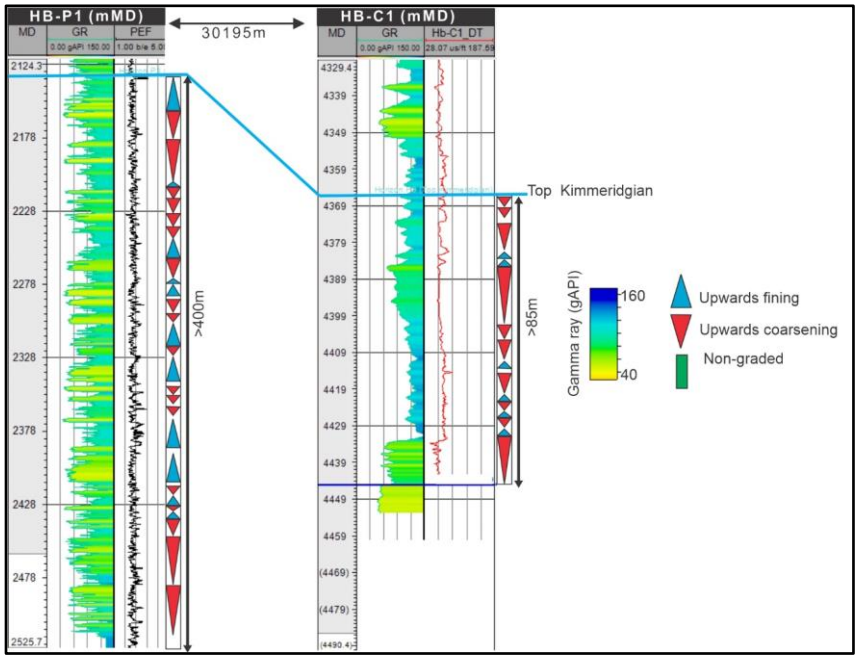

Figure 5.3: Basement D to upper Kimmeridgian wireline correlation based on boreholes Hb-P1 and Hb-C1 (for boreholes location, see Figure 3.2) in the Uitenhage Trough.

5.2.1.2 Post-Kimmeridgian to upper Tithonian

The Tithonian succession is also challenging to correlate across the basin, because it was only intersected in boreholes HB-D1, HB-B1 and HB-C1 located in the Uitenhage Trough. Borehole HB-D1 is dominated by a ~650-m-thick, fining-upward succession with mostly low GR signatures that occasionally alternate with high GR signatures (45 to 90 API; Figure 5.4). Borehole HB-B1 intersected a ~914-m-thick, overall coarsening-upward succession that also contains alternating fining-upward and coarsening units that are 5- to 50-m-thick (35 to 82 API; Figure 5.4). A ~995-m-thick succession with an overall coarsening-upward grain-size trend was intersected in borehole HB-C1 (40 to 140 API; Figure 5.4). Borehole HB-D1 is dominated by silty facies with some sand interbeds, and the predominant fining-upward trends in this borehole suggest a fluvial setting, most likely floodplains with multi-phase channel incisions. Both boreholes HA-B1 and HA-C1 are dominated by coarsening-upward trends, in contrast to HA-D1, which is dominated by fining-upward trends, suggesting fluvial dominated floodplain setting. The overall coarsening-upward trends observed in both HB-B1 and HB-C1 suggest a change from relatively low-energy setting (likely shallow marine), further from sediment source to a higher energy setting (probably nearshore), closer to sediment source.

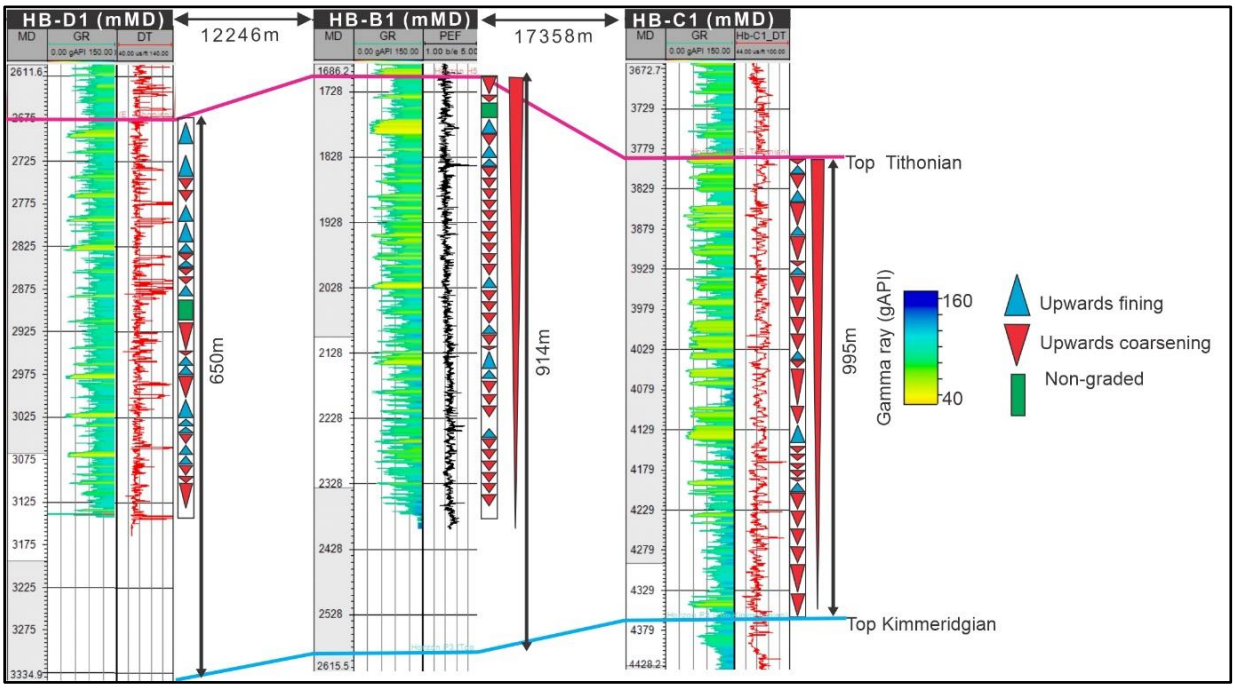

Figure 5.4: Post-Kimmeridgian to upper Tithonian N-S wireline correlation based on boreholes HB-D1, HB-B1 and HB-C1 in the Algoa Basin. The boreholes show an increase of low GR signatures towards the S (for boreholes location, see Figure 3.2).

5.2.1.3 Post-Tithonian to upper Berriasian

This interval is only intersected in borehole HB-C1 located in the Uitenhage Trough, and attains a maximum thickness of ~800 m (Figure 5.5). GR log shows isolated coarsening-upward trends (~5 to 65-m-thick) separated by low GR signatures (45 to 136 API). In the Uitenhage Trough, this interval is laterally restricted due to basement subcrops and thus pinches out towards borehole HB-B1. Dominated by coarsening-upward sands with interbeds of silty to shaly facies, the Berriasian succession suggests a possible shallow marine setting (shoreface/mouth bar), located near a sediment source.

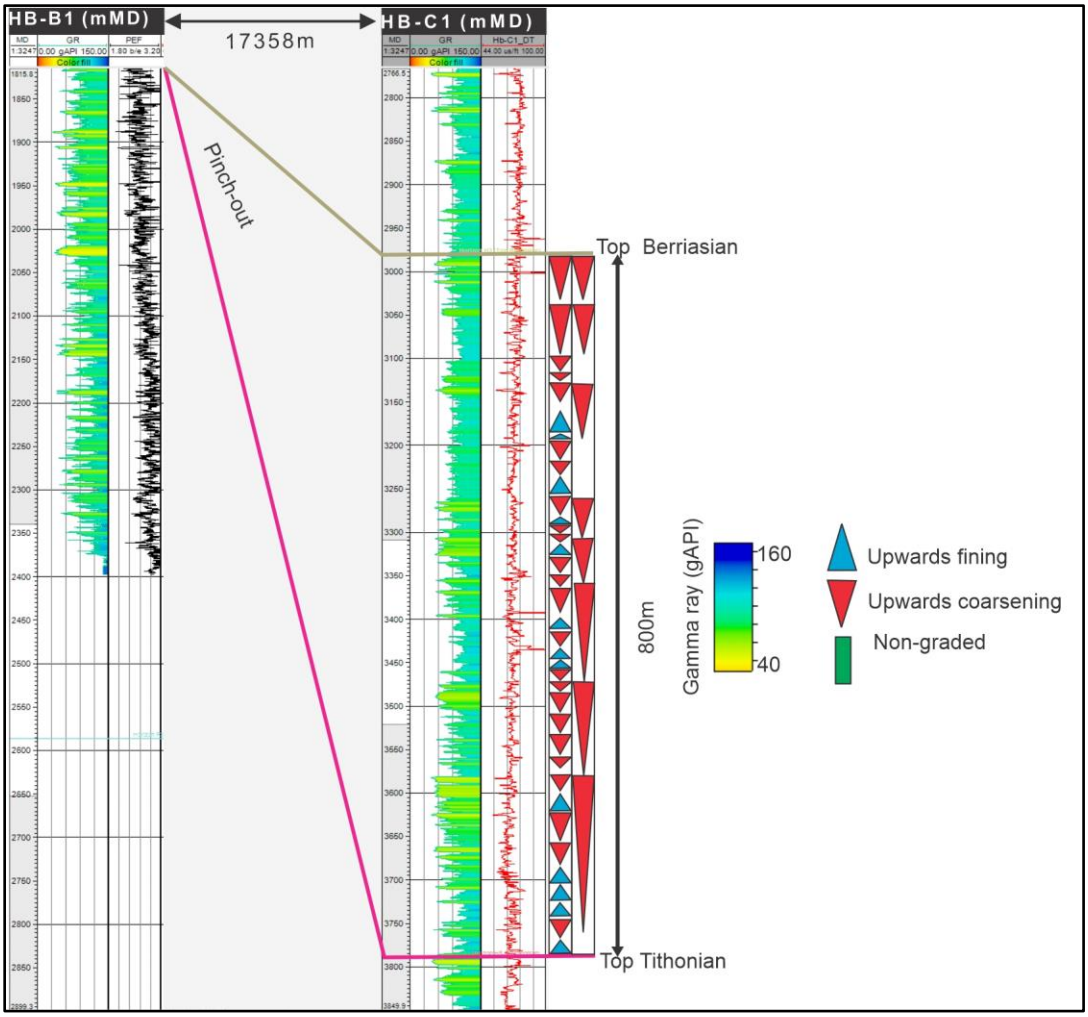

Figure 5.5: Post-Tithonian to upper Berriasian wireline correlation based on boreholes HB-B1 and HB-C1 in the Uitenhage Trough. This interval pinches out towards borehole HB-B1 (for boreholes location, see Figure 3.2).

5.2.1.4 Post-Berriasian to upper Valanginian

Borehole HB-B1 intersected ~320-m-thick Berriasian to Early Valanginian succession, consisting of alternating fining-upward and coarsening trends with a high sand-to-shale ratio (GR: 35-82 API; Figure 5.6). Borehole HB-C1, located 18 km south of borehole HB-B1, intersected very isolated coarsening-upward sandy and silty facies (GR: 40-140 API) in the lower half of the succession (Figure 5.6). However, the upper part of borehole HB-C1 is dominated by a ~310-m-thick, shaley succession with few sandy interbeds (GR: 70-140 API; Figure 5.6).

The dominant stacked fining-upward sandy facies in borehole HB-B1 suggest a high-energy process (high energy setting usually reads low GR signatures and vice versa) within with river/stream channels that were cut into the floodplain sediments in fluvial setting. Borehole HB-C1 shows a change from relatively high-energy (possibly nearshore/transitional) setting to relatively low-energy setting, indicating either sediment shut-off or switching of the mouth bar in the shallow marine setting.

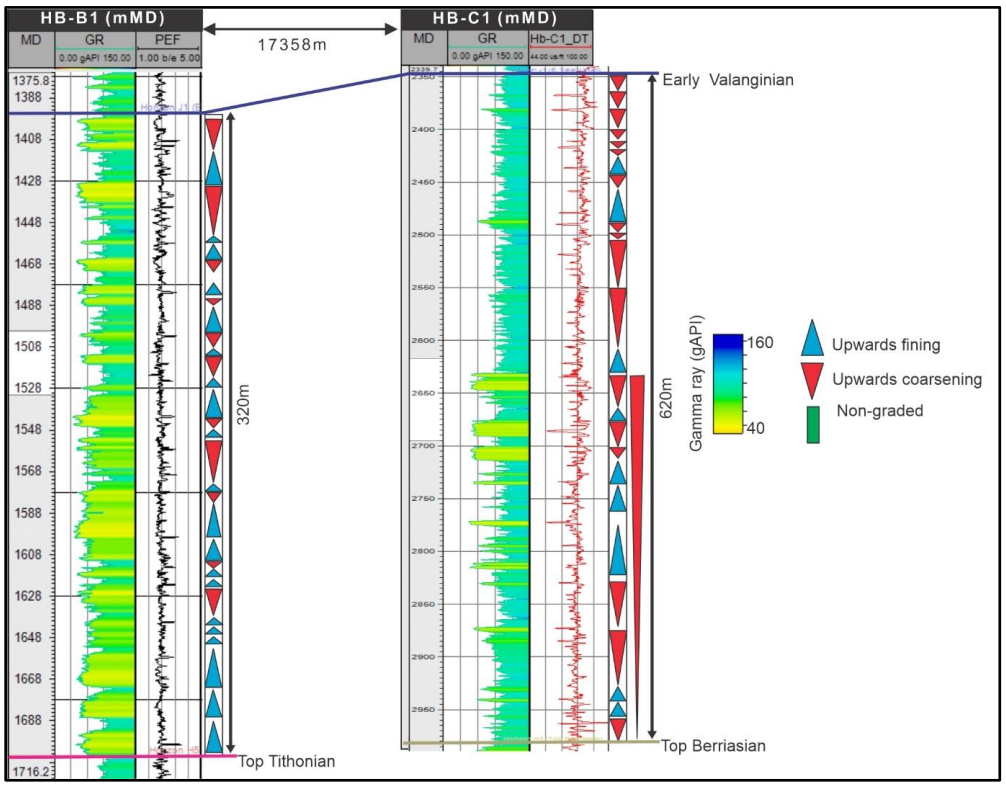

Figure 5.6: Post-Tithonian/Berriasian to lower Valanginian N-S wireline correlation based on boreholes HB-B1 and HB-C1 in the Algoa Basin. Borehole HB-B1 suggest a floodplain setting with channels, while borehole HB-C1 suggest a shallow marine setting (for boreholes location, see Figure 3.2).

Wireline data from the upper Valanginian succession in the Uitenhage Trough show a series of 190-m-thick, alternating low and high GR signatures (GR: 51-129 API) with upwards-coarsening and fining trends (~2 to 30-m-thick) in borehole HB-B1 (Figure 5.7). Borehole HB-I1, contains a > 800 m-thick succession that is dominated by low to high GR readings (GR: 52-145 API; Figure 5.7) with and alternating coarsening-upward and fining trends. Mudlog reports describe this interval in borehole HB-I1 as sandstone with siltstone interbeds. In the distal borehole HB-C1, the same interval shows an upwards-coarsening trend in a ~50-m-thick succession with relatively low GR signature (GR: 50-104 API). GR signatures in borehole HB-B1 suggest a long-lived fluvial setting, with channels and floodplains. In borehole HB-I1, the succession is more complete and shows a change from high-energy, sand-dominated to low-energy, shale/clay-dominated facies. This well-defined overall upwards-fining succession in these likely Sundays River Formation which is correlated to the late Valanginian to Hauterivian transgression known from previous studies (McLachlan and McMillan, 1976; Dingle et al., 1983; Malan, 1993; McMillan et al., 1997; Muir, 2019; Muir et al., 2020). The thickness variation across the three boreholes (Figure 5.7) suggest that erosion partly or completely removed the sediments in boreholes HB-B1 and HB-C1. The erosional remnant of this succession in borehole HB-C1 is an upward coarsening sandy unit, which suggest a high-energy, probably shallow marine (transitional) setting that was situated close to a sediment source.

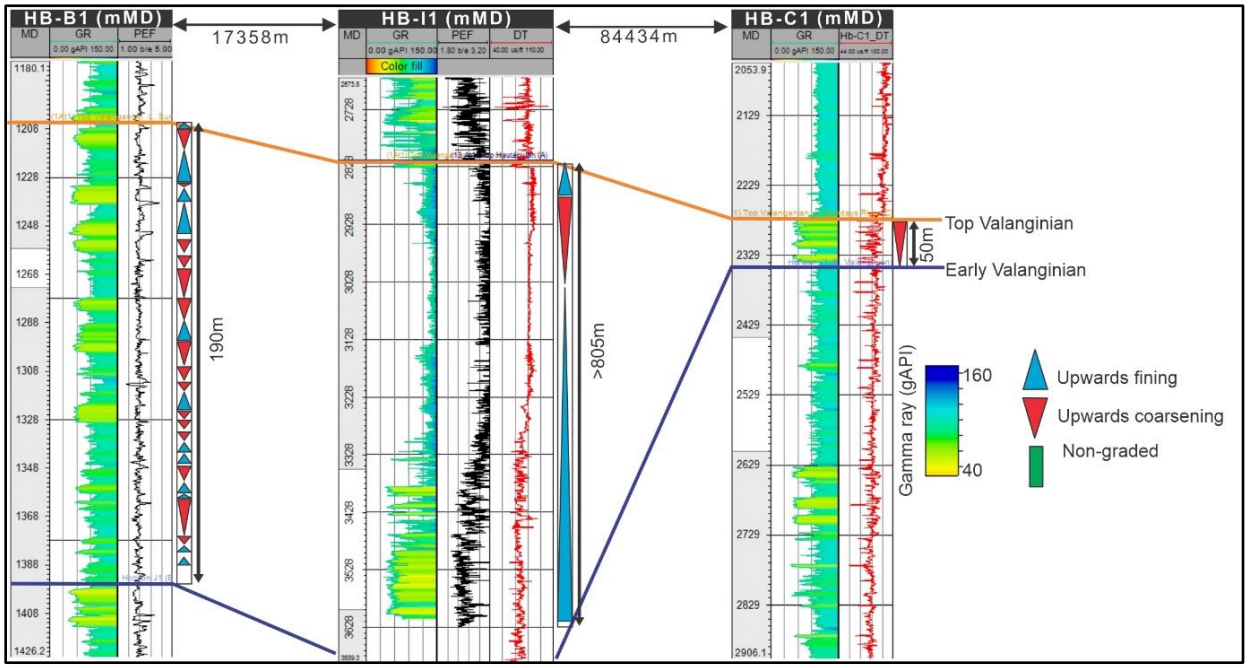

Figure 5.7: Lower Valanginian to upper Valanginian N-S wireline correlation based on boreholes HB-B1, HB-I1, and HB-C1 in the Algoa Basin (for boreholes location, see Figure 3.2).

5.2.1.5 Post-Valanginian to upper Hauterivian

Preserved in a total thickness of 120 m in borehole HB-B1, the GR signatures for the Hauterivian succession shows a change from predominantly upwards-coarsening at the base (~75-m-thick, GR: 45-110 API) to upwards-fining at the top (~45-m-thick, GR: 54-125 API; Figure 5.8). There is a clear change from a predominately coarsening-upward setting in the early Hauterivian to a predominately fining-upward setting in the late Hauterivian. The coarsening-upward trend at the base suggests a possible shoreface/deltaic shallow marine setting. While the change in GR signature in the upper succession suggest possible reactivation of the fluvial system, which may have coincided with the uplift of the shelf during the late Hauterivian (McLachlan and McMillan, 1976; Dingle et al., 1983; Malan, 1993; Brown et al., 1995; Thompson, 1999; Paton and Underhill, 2004).

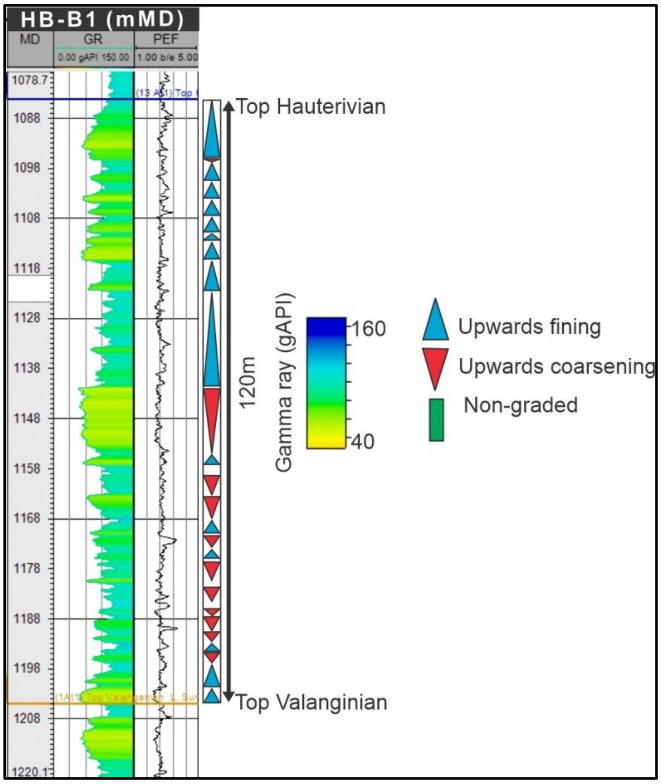

Figure 5.8: Post-Valanginian to upper Hauterivian succession GR and PEF logs suggesting a fluvial system in the upper Hauterivian (for borehole location, see Figure 3.2).

5.2.1.6 Post-Hauterivian to “Canyon fill” (lower Albian)

Borehole HB-H1 in the Port Elizabeth Trough is dominated by a ~65-m-thick sandy unit (GR: 28 -62 API) with an overall cylindrical-shaped GR signature (Figure 5.9). Although the Uitenhage Trough is dominated by fine-grained sediments (i.e., 200-m- and 1420-m-thick in boreholes HB-B1 and HB-I1, respectively), there are some isolated, thin (>5-m-thick), upwards-coarsening sandstones in this interval. Mudlog report describe the base of this interval HB-I1 being sandstone, siltstone with abundant coal streaks at the base (38 to 100 API) and interbeds of claystone, and siltstone with minor sandstone development over the succession (95 to 125 API). The more S borehole HB-C1 is intersected a ~470-m-thick, fine-grained unit (GR: 83-116 API) that lacks sandy interbeds (Figure 5.9). The more N borehole HB-H1 is dominated by overall box-shaped sandy facies on the GR log. This trend, which is intersected closer to the head of the Algoa Canyon (see Figure 1.1 for the geometry of the Algoa Canyon) could indicate the sediment fill of an incised canyon. Whereas boreholes HB-B1, HB-I1 and HB-C1 are dominated by low-energy, silty to shaly facies with very limited sand input. However, the lower “Canyon fill” sediments in borehole HB-I1 show fining-upward trends, indicating a potential landwards shift of the shoreline in the early Albian. While the coal streaks described in the mudlog report shows a transitional setting (coastal wetlands/ delta plain).

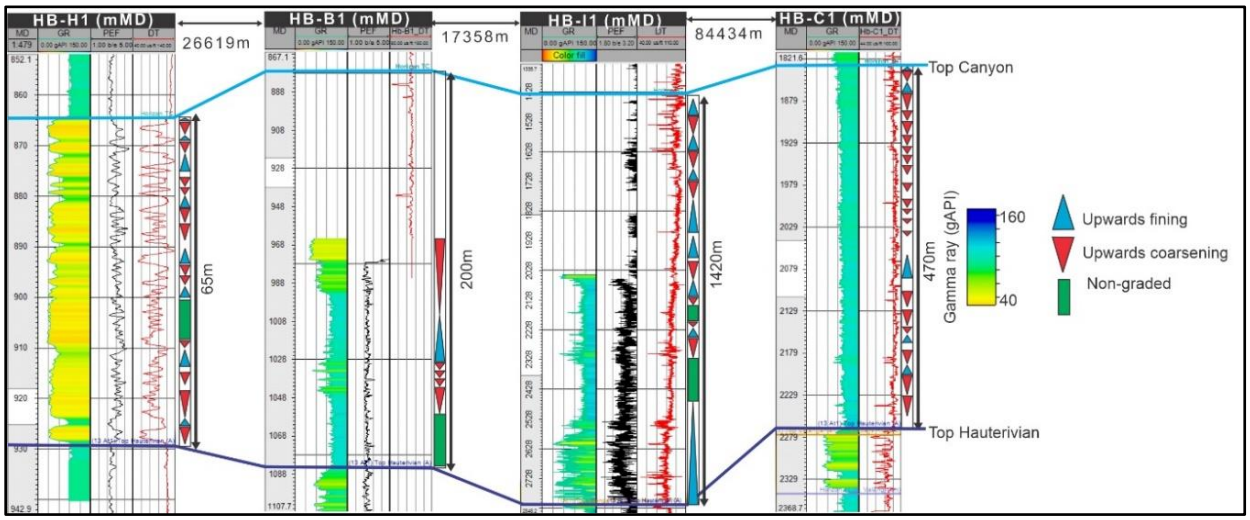

Figure 5.9: Algoa Basin post-Hauterivian to “Canyon fill” wireline correlation based on boreholes HB-H1, HB-B1, HB-I1 and HB-C1 (for boreholes location, see Figure 3.2).

5.2.1.7 Post-Hauterivian/"Canyon fill" to upper Albian

From the borehole data that was accessible for this study, only borehole HB-C1 has gamma ray log in the post-rift section. For the Albian succession, a coarsening-upward overall trend is recorded (380-m-thick, 37 to 138 API) with shales and clay facies at the base and low GR sandy facies towards the top of the unit (Figure 5.10). In borehole HB-I1, located ~8 km N of borehole HB-C1, this succession is only recorded with a DT log that shows a ~250-m-thick, overall coarsening upwards trend (Figure 5.10). The facies in the two boreholes reveal a potential shoreface setting with a possible delta supplying sandy sediments into the shallow shelf. The fining upwards silty to shaly facies at the base indicate a possible landwards shift of the shoreline, overlain by increased sedimentation rates in the late Albian, which may have resulted in the regression of the shoreline.

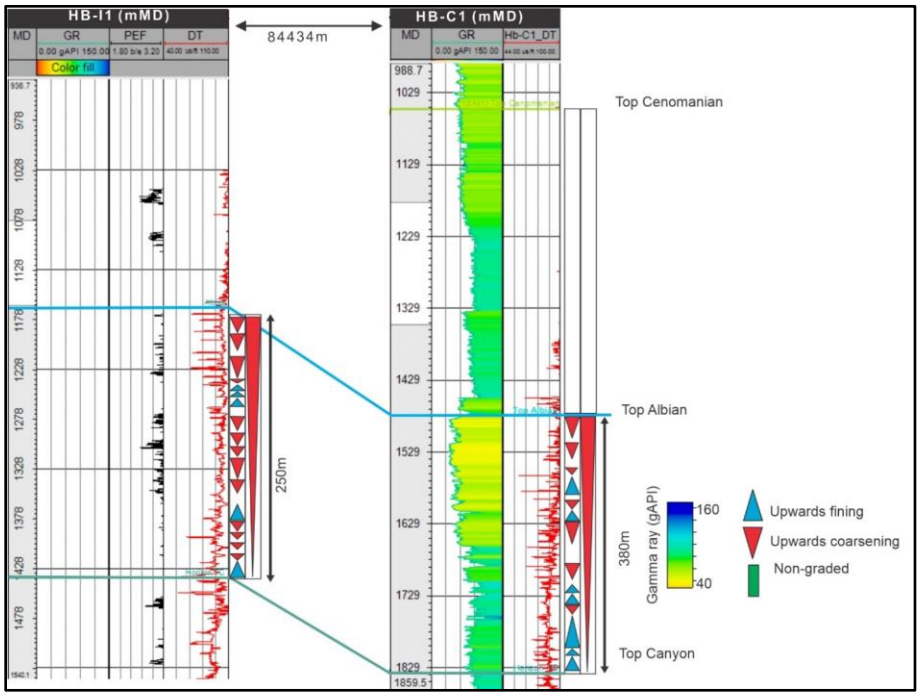

Figure 5.10: Post-"Canyon fill" to upper Albian succession in the wireline log of borehole HB-C1. The interval shows an overall coarsening-upward trend in a shoreface setting (for boreholes location, see Figure 3.2).

5.2.1.8 Post-Albian to Upper Cenomanian

The Cenomanian succession is ~440-m-thick, overall coarsens upwards and contains two upwards-coarsening units in borehole HB-C1 with the lower one being dominated by high GR readings between 63-85 API, while the upper one being dominated by relatively low GR signatures of 56-72 API (Figure 5.11). The shaly facies that overlie the coarsening-upward, very fine-grained sand-silty facies in the lower Cenomanian was probably due to a shut-off or switching of the sediment source. Moreover, this may also suggest lower sedimentation rates in the early Cenomanian compared to the late Cenomanian when the sedimentation rate increased and sediment supply to the shelf was reactivated. This may have resulted in the regression of the shoreline.

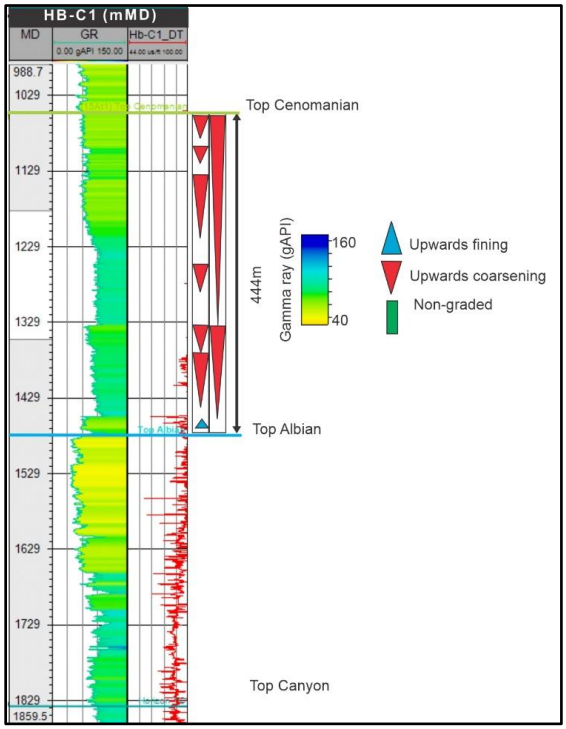

Figure 5.11: Post-Albian to upper Cenomanian succession in the wireline log of borehole HB-C1 that is dominated by coarsening-upward units (for borehole location, see Figure 3.2).

5.2.1.9 Post-Cenomanian to Upper Campanian

Unlike underlying Cenomanian succession, the Campanian consists mostly of relatively low GR signatures with very few high GR signatures (Figure 5.12). A subtle overall fining-upward trend (~260-m-thick, 48 to 72 API), made up of a lower non-graded unit and an upper unit comprising of small, coarsening-upward

and fining, mostly sandy facies may suggest: a) high sedimentation rates on the shelf (due to a likely delta in close proximity), b) increase accommodation space, and c) a slight landwards shift of the shoreline.

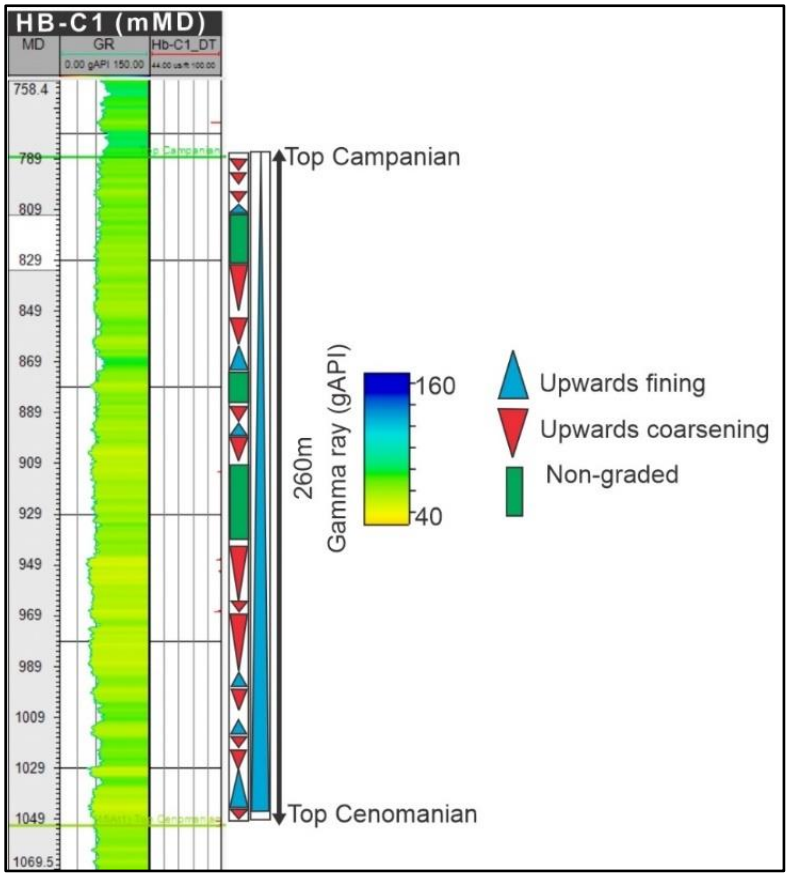

Figure 5.12: Post-Cenomanian to upper Campanian succession intersected by borehole HB-C1. This subtle fining-upward interval is interpreted to have formed during a transgressive shoreline (for borehole location, see Figure 3.2).

5.2.1.10 Post-Campanian to Lower Cenozoic

Contrary to the underlying Campanian, the uppermost Cretaceous succession, which is an ~80-m-thick unit in borehole HB-C1 in the Algoa Basin, shows relatively high GR readings of 58-97 API with an overall fining-upward trend (Figure 5.13). The base of the succession is made up of coarsening-upward sands, which are overlain by fining-upward shales with very low net sand-to-shale ratio. This interval shows a clear fining-upward trend and suggests a transgressive shoreline during the latest Cretaceous. This also suggests a shut-off (drowning) of the sandy sediment source (fluvial), probably due to drowning of the source as the shoreline advanced landwards. Although a fining-upward trend can also suggest fluvial/tidal point bar, deep tidal channel fill, or tidal flats, as pointed out before, inferring geological environments

requires the integration of other datasets due to the non-uniqueness of wireline trends (see Figure 3.9). However, the Lower Cenozoic is described as glauconitic dominated claystone succession (McMillan et al., 1997), which suggest a marine setting, and thus a shoreface setting can be inferred.

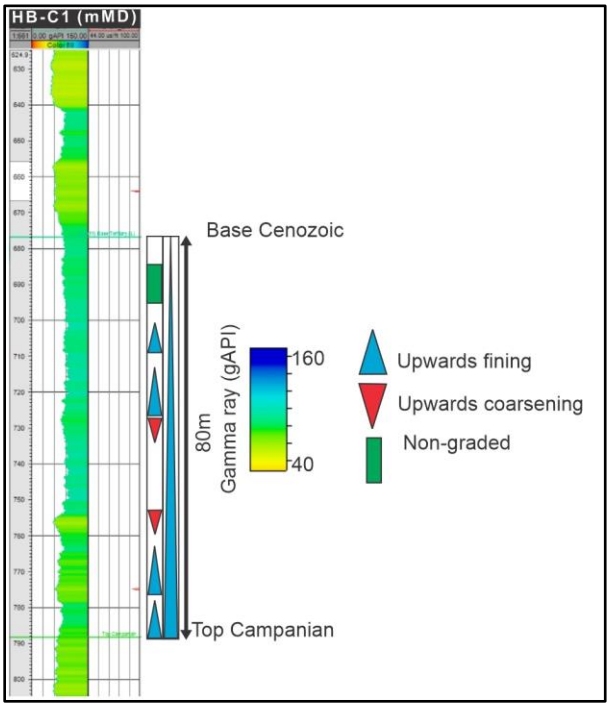

Figure 5.13: Upper Campanian to Lower Cenozoic succession intersected by borehole HB-C1. This interval shows an overall fining upwards succession (for borehole location, see Figure 3.2).

5.2.1.11 Lower to Middle Cenozoic

Borehole HB-C1 contains a ~356-m-thick, overall upwards-coarsening unit with GR readings of 38-93 API (Figure 5.14). The base of the succession shows a coarsening-upward (~40-m-thick), shaly to very fine sandy facies (~20-m-thick), which is overlain first by fining-upward shales, and then by coarsening-upward silty to sandy facies (~290-m-thick; Figure 5.14). The coarsening-upward sands at the base of the succession suggest reactivation of the sediment source and increased transport of sandy sediments into the shelf after the Late Cretaceous drowning of coastal fluvial systems. However, the overlying fining upwards shaly facies suggest deepening of the nearshore setting during a likely sudden transgression. The coarsening-upward silty to sandy facies atop of the shaly facies indicates increased sedimentation (or decreasing rates of transgression) in the shelf and a likely normal regressive shoreline.

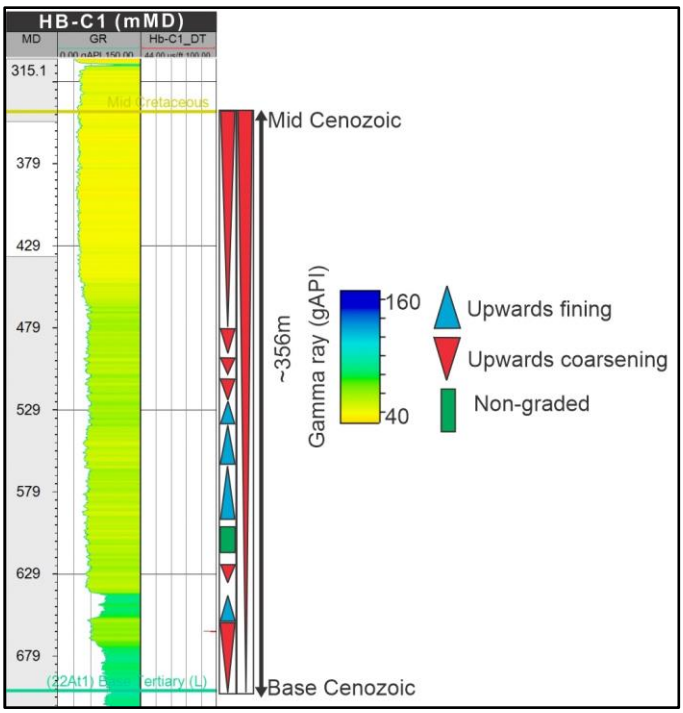

Figure 5.14: Lower to Upper Cenozoic succession intersected by borehole HB-C1, indicating a regressive shoreline (for borehole location, see Figure 3.2).

5.2.1.12 Upper Cenozoic

Borehole HB-C1 intersected a ~170-m-thick (25 to 115 API) Upper Cenozoic succession, which is dominated by fining-upward sandy units at the base, fining-upward shaly units in the middle and both fining-upward and coarsening sandy facies towards the top (Figure 5.15). Moreover, two large-scale trends are identified in this succession: 1) a lower, fining-upward succession that indicates a period when the rate of transgression was higher than the rate of sedimentation, despite the high sedimentation on the shelf; 2) an upper, coarsening-upward succession that indicates increased sedimentation rates and decelerated transgression rates. These two major trends are separated by high GR shaly facies, probably deposited when the shoreline was in its most landward position before the onset of normal regression indicated by in the upper, coarsening-upward succession.

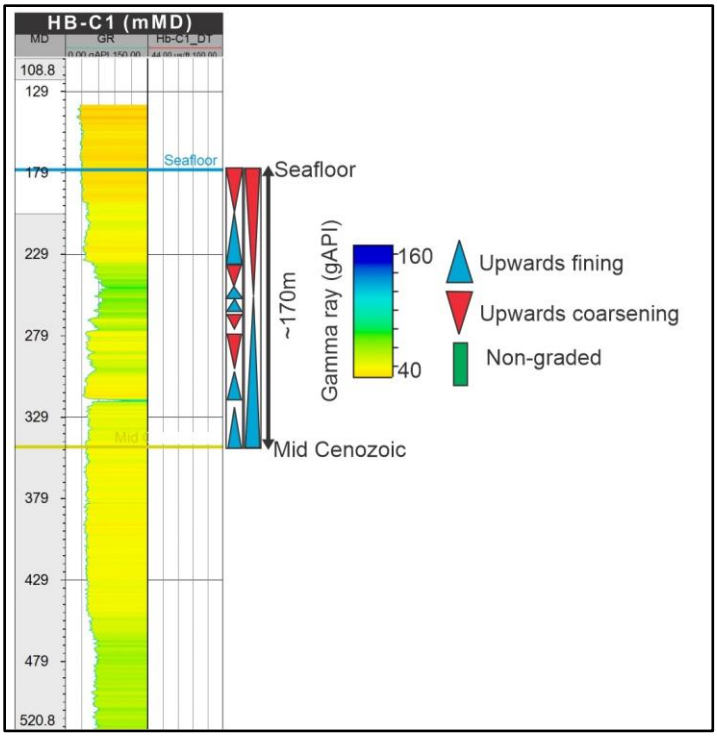

Figure 5.15: Upper Cenozoic succession intersected by borehole HB-C1, showing a change from high transgression rates to high sedimentation rates (for borehole location, see Figure 3.2).

5.2.2 Surface and thickness map

5.2.2.1 Pre-Aalenian to upper Valanginian

The interval from the pre-Aalenian Basement to the Holocene attains a maximum thickness of ~7000 m with the depocenter showing a NW-SE striking trend (Figure 5.16a). Correlating the Top Kimmeridgian reflector is challenging due to the structural complexity of the Algoa Basin and insufficient borehole data. The resultant maps are localised to parts of the depocenter where mapping was possible, and therefore carry a high level of uncertainty, which needs to be considered during interpretations. Based on the available data however, the depocenter of the succession between the Basement to Top Kimmeridgian reflectors is in the Uitenhage Trough, attaining maximum thickness of 3000 m with a NW-SE striking trend (Figure 5.16b). Overlying the Kimmeridgian is the Tithonian succession, which was only possible to map in the Port Elizabeth Trough. The Tithonian succession seems to attain a maximum thickness of 1800 m towards the SE, while the Berriasian succession is ~1200-m-thick (Figure 5.16c). Although the depocenter is not well defined, the Berriasian seems to thicken towards the NW. The lower Valanginian succession, which overlies the Top Berriasian reflector and attains a maximum thickness of ~2600 m (Figure 5.16d),

can be mapped in the Port Elizabeth Trough, and in some parts of the Uitenhage Trough. The upper Valanginian succession attains a maximum thickness of 2000 m towards the E (Figure 5.16e) in the Port Elizabeth Trough, and a maximum thickness of 3000 m in the Uitenhage Trough (Figure 5.16e). The Top Valanginian reflector (1At1) is laterally extensive in the basin and extends to the W into the Gamtoos Basin (see next chapter).

Because the syn-rift succession is severely eroded in the Algoa Basin, especially in the Uitenhage Trough, accurately determining the true orientation of the depocenters is not possible. However, the overall depocenter (from Basement D to Holocene; Figure 5.16a) shows a preferred NW-SE striking trend, which follows the orientation of syn-rift faults (which inherently follow the Cape Supergroup lineaments).

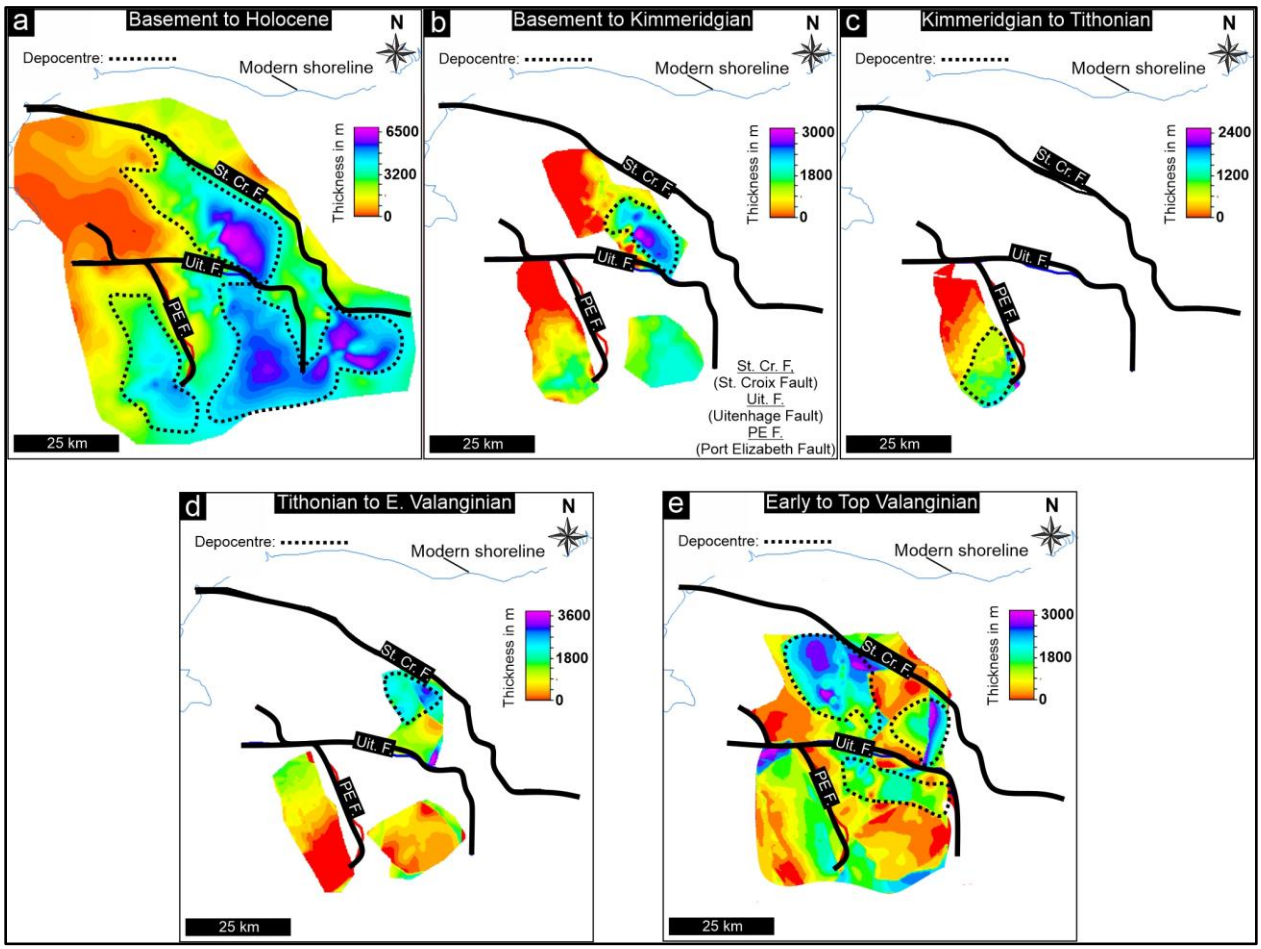

Figure 5.16: a Thickness map from the Basement to Holocene, highlighting the main depocenters during basin infill. **b** Pre-Aalenian to Kimmeridgian thickness map, showing a NW-SE striking depocenter in the Uitenhage Trough. **c-e** NW-SE striking depocenter in the Algoa Basins from the Tithonian to upper Valanginian.

5.2.2.2 Post-Hauterivian to "Canyon fill" (lower Albian)

Overlying the 1At1 reflector is the post-rift Hauterivian succession, which is truncated by the 13At1 (Top Hauterivian) reflector, which ultimately forms the Algoa Canyon. Although the 13At1 reflector is mappable across the basin, in most places, this reflector truncates the syn-rift succession, as a result, the 1At1 and 13At1 reflectors are amalgamated in some parts of the basin. This reflector amalgamation results in the topography of these two reflectors being very similar and irregular. Where their separation is possible, as shown in the isopach map (Figure 5.17a), a succession bounded by these reflectors forms small, spatially discontinuous mini-depocenters on the E and W flanks of the basin with an average thickness on of 200 m (Figure 5.17a). Overlying the Top Hauterivian reflector (13At) is the "Canyon fill" succession, which is mostly localized in the Uitenhage Trough, has a NNW-SSE strike and a thickness reaching 1400 m (Figure 5.17b). Although borehole HB-H1 intersected Top Canyon sediments, mapping this unit in the Port-Elizabeth Trough is challenging, because the unit seems to be localised around the borehole (note that due to the poor data quality Figure 5.17b does not show this section in the Port Elizabeth Trough).

The transitional phase depocenters, which are orientated mostly towards the N are less dependent on the syn-rift fault orientation and are mainly driven by the incised topography formed during the late Hauterivian to early Aptian uplift and subsequent erosion (Figure 5.17b).

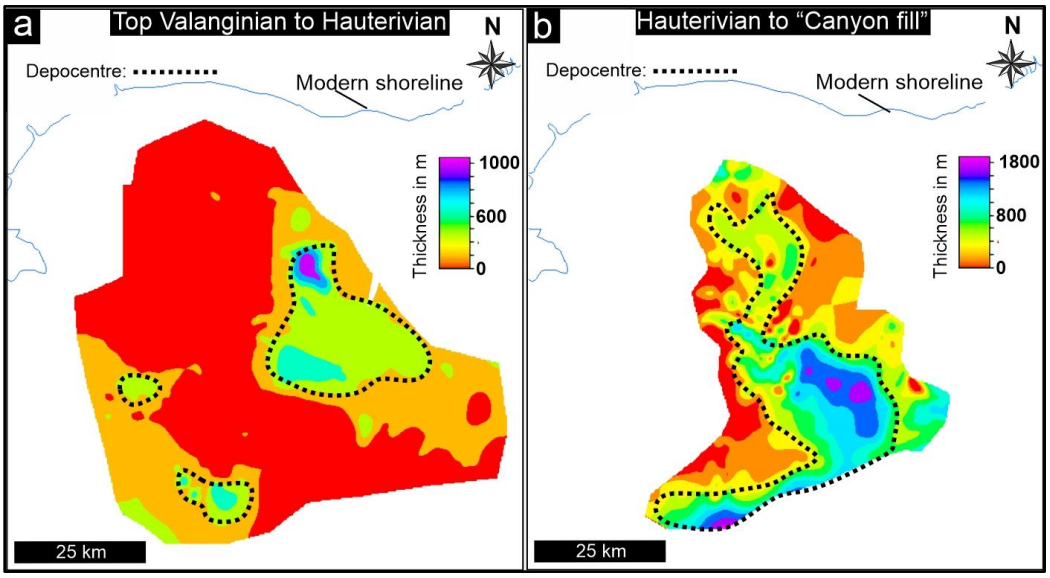

Figure 5.17: a-b Transitional phase thickness maps representing sediments deposited in the Algoa Basin from the Hauterivian to early Albian period.

5.2.2.3 Post-Albian to Holocene

The Albian depocenter, which strikes N-S, is mainly centred in the Uitenhage Trough, and attains a maximum thickness of 800 m (Figure 5.18a). The Cenomanian succession, which overlies the Top Albian reflector has a NE-SW striking depocenter and attains a maximum thickness of 2100 m towards the S (Figure 5.18b). Overlying the Top Cenomanian (15At1) unconformity is the Campanian succession with a depocenter showing a NE-SW trend and maximum thickness of ~2100 m towards the SE (Figure 5.18c). The Campanian reflector is overlain by the Upper Cretaceous succession, which shows uniform thickness on the shelf, averaging at ~300 m (Figure 5.18d). The NE-SW striking depocenter for this succession attains a maximum thickness of ~600 m and is located towards the SW (Figure 5.18d). The Base Cenozoic reflector, which marks the end of the Cretaceous, is overlain by the Lower to Upper Cenozoic succession with the depocenter showing a NE-SW trend towards the SE part of the basin, where it attains a maximum thickness of ~1500 m (Figure 5.18e). The Upper Cenozoic interval generally shows uniform thickness of ~150 m on the shelf with localized thicknesses of up to 500 m (Figure 5.18f).

Unlike the underlying syn-rift and transitional phase depocenters with NW-SE and N-S striking trends, respectively, the drifting phase shows a preferred NE-SW striking depocenter mainly located towards the shelf edge/slope. The location of the depocenter suggest increased accommodation space towards the shelf edge/slope setting relative to the shelf. This could be related to the multiple phases of erosion on the shelf (during the generation of the 13At1, 15At1 and Mid-Cenozoic unconformities), which resulted in minor/non-deposition on the shelf and an increased basinward (offshore) deposition.

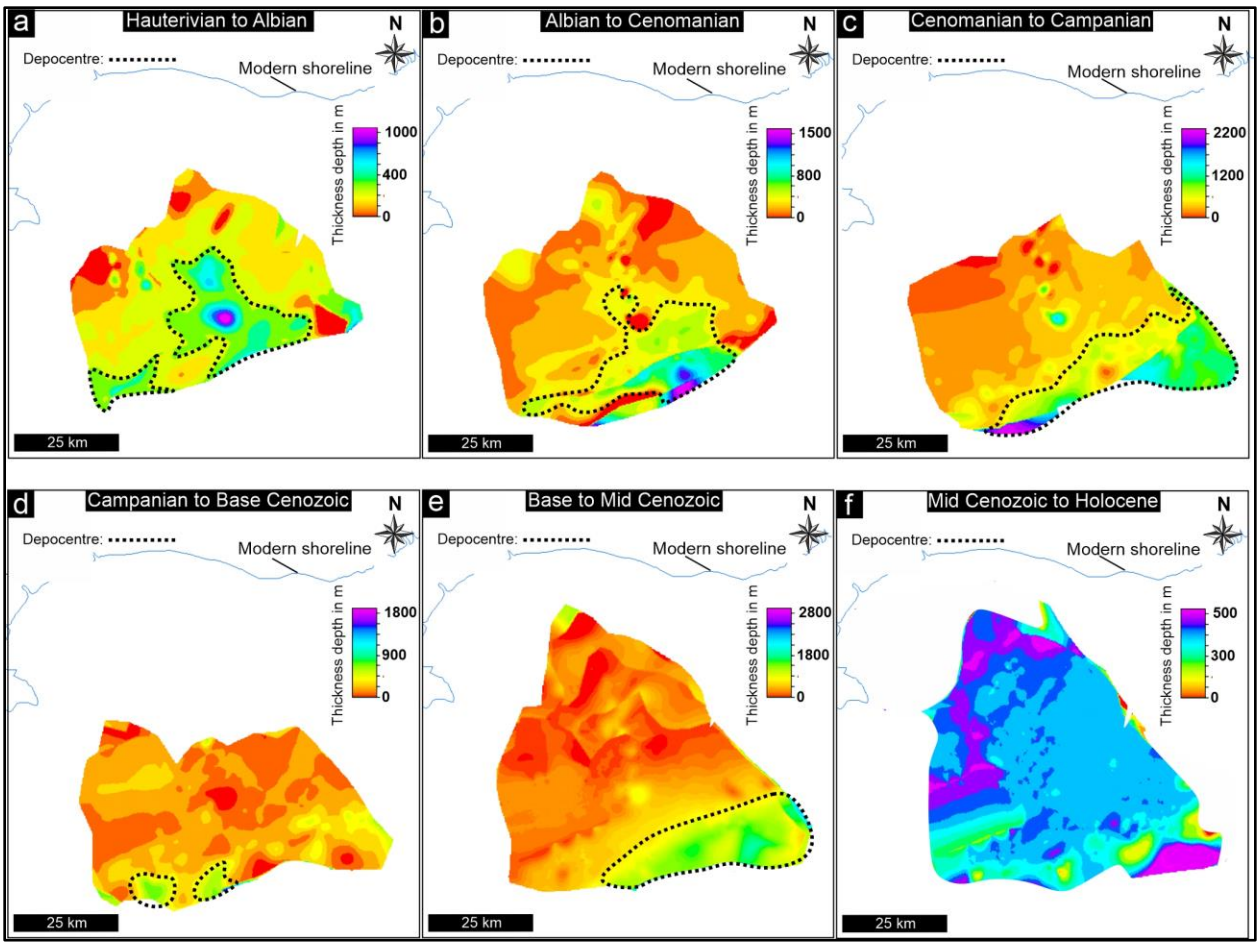

Figure 5.18: a-f Drift phase thickness maps representing sediments deposited in the Algoa Basin from the late Albian to Holocene period. Drift-phase depocenters are located mainly towards the shelf edge.

5.2.3 Seismic interpretation

5.2.3.1 Basement D (pre-Aalenian) to upper Kimmeridgian

This pre-Tithonian succession (ranging in age from pre-Aalenian to Kimmeridgian), onlaps onto the Basement D reflector, and generally contains dimmer seismic reflectors than the overburden and the underlying older successions (Figure 5.19A-A'). The internal reflector geometries are commonly discontinuous and chaotic. This unit also forms a wedge that pinches out towards the N-W and increases in thickness towards the E, where the faults are located (Figure 5.19C-C'). In the Algoa Basin, especially in the Uitenhage Through (Figure 5.19 E-E', F-F', G-G') this unit is mostly eroded, and this makes it challenging to confidently correlate it across the basin. The wedging geometry, which increases in thickness towards the faults, indicate accommodation space influenced by the movement of faults from the pre-Aalenian to

Late Jurassic. Onlapping stratal geometries on the Basement D reflector shows the topographical influence of the basement on deposition and accommodation space creation.

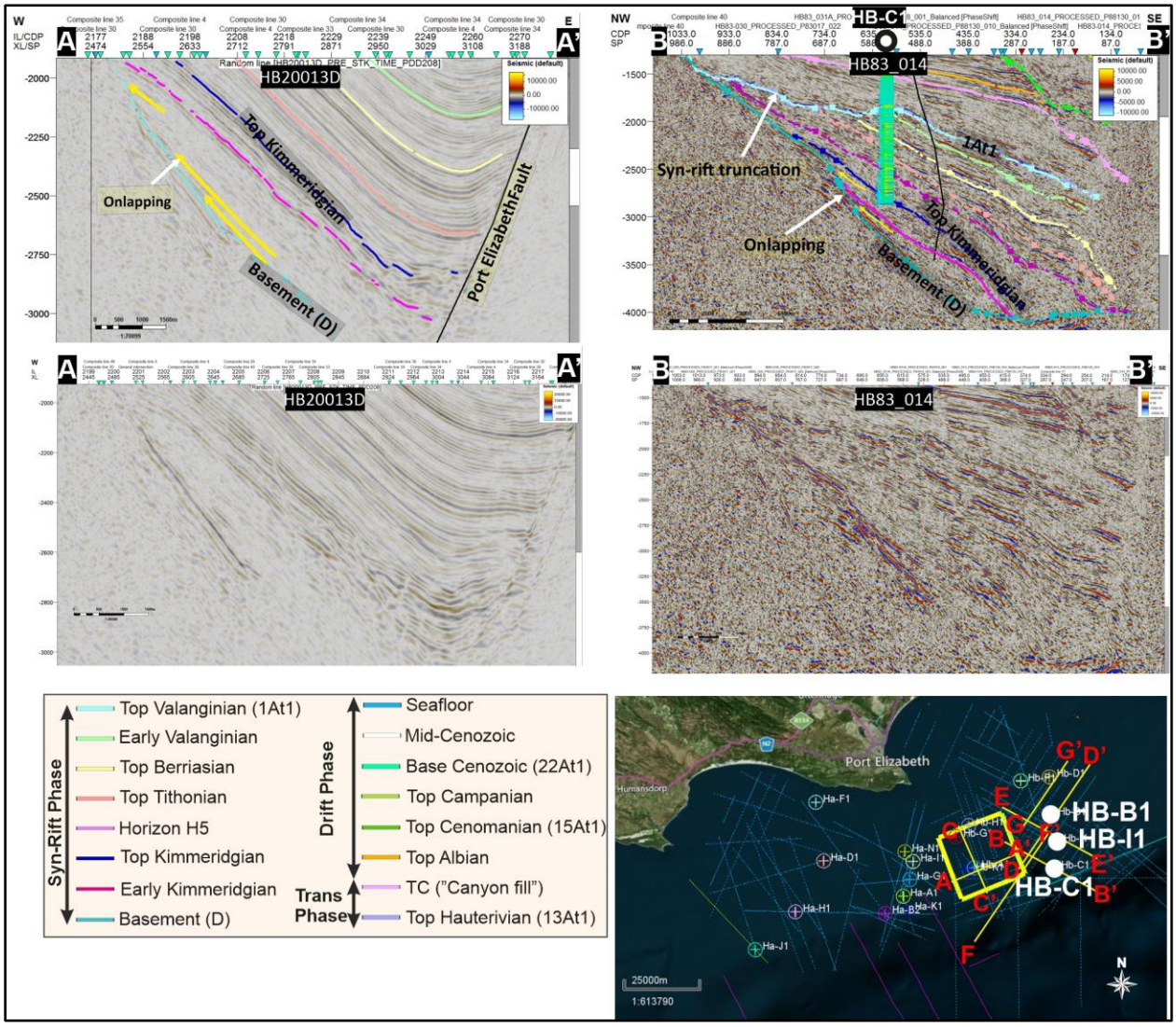

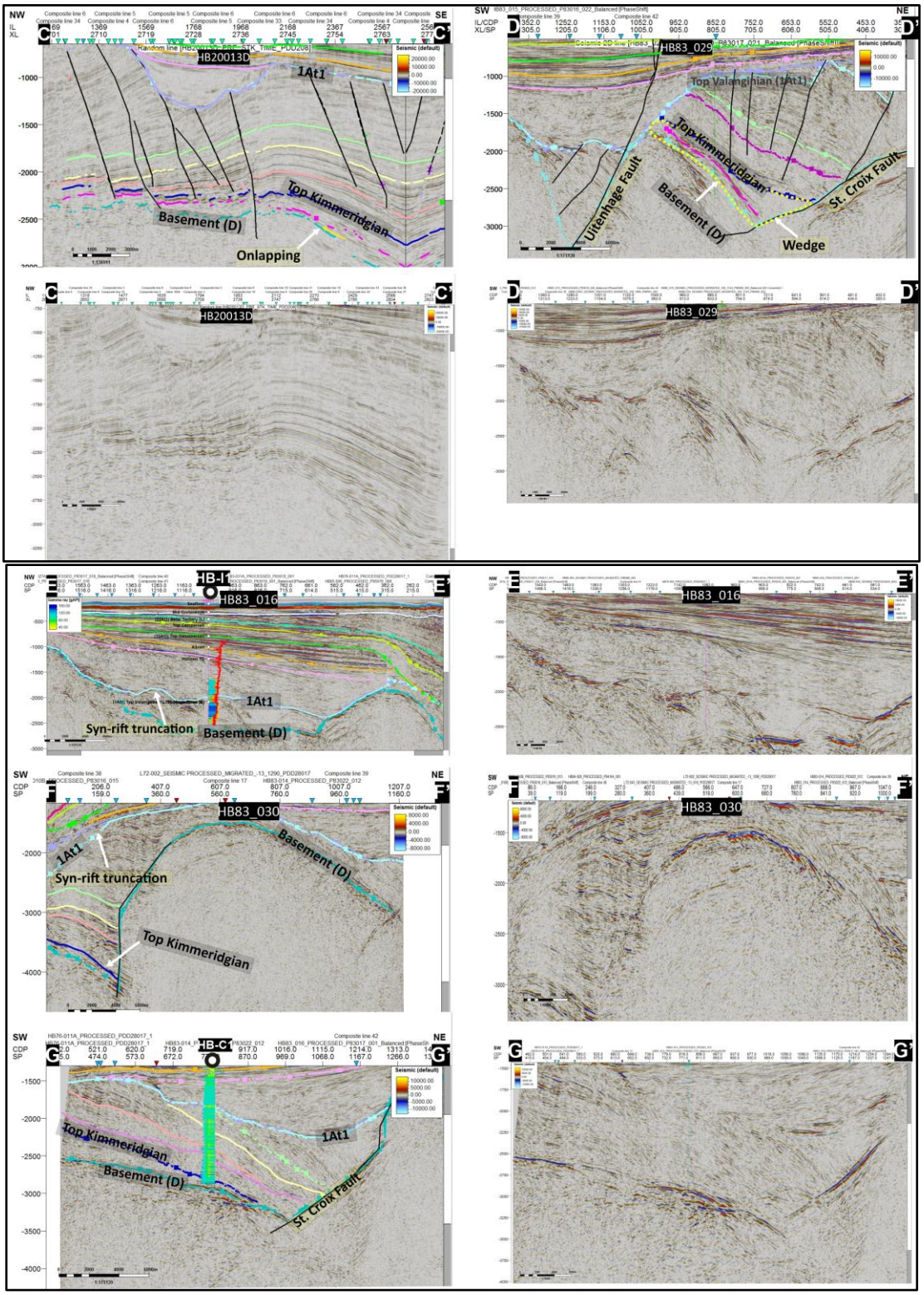

Figure 5.19: A-A' Kimmeridgian reflectors onlap on the Basement. **B-B'** The Kimmeridgian pinches out towards the N-NW and onlaps on the Basement in the Port Elizabeth Trough. **C-C'** The Kimmeridgian pinches towards the N-NW and onlaps on the Basement in the Uitenhage Trough. **D-D'** Truncation by the 1At1 reflector and increase in thickness towards the St. Croix fault. **E-E', F-F', G-G'** Severely truncated syn-rift sequence in the Uitenhage Trough. Base map data ©2020 Google, Maxar Technologies, AfriGIS (Pty) Ltd.

5.2.3.2 Post-Kimmeridgian to upper Tithonian

The Top Tithonian reflector is mappable in the Port Elizabeth Trough. Here, the Top Kimmeridgian to Tithonian reflectors are discontinuous, faulted and parallel along the NW-SE cross section (Figure 5.20). This succession forms a folded wedge, which pinches towards the NW, and thickens towards the Port Elizabeth Fault (Figure 5.20A-A'). From W to E, the top of this unit is marked by truncation along the 1At1 reflector (Figure 5.20B-B'). Considerable amount of succession is missing in the Uitenhage Trough, where it is truncated by the 1At1 and the Top Hauterivian surfaces. Thus, both mapping and correlating this succession across the basin is challenging (see Figure 5.19). The wedge-like geometry suggests that sedimentation in the Port Elizabeth Trough was mainly towards the E, with accommodation space influenced by movement along the Port Elizabeth Fault during the deposition of the unit. This wedge geometry, present in the underlying succession as well, suggests that the fault movement occurred at least in the Aalenian (or earlier).

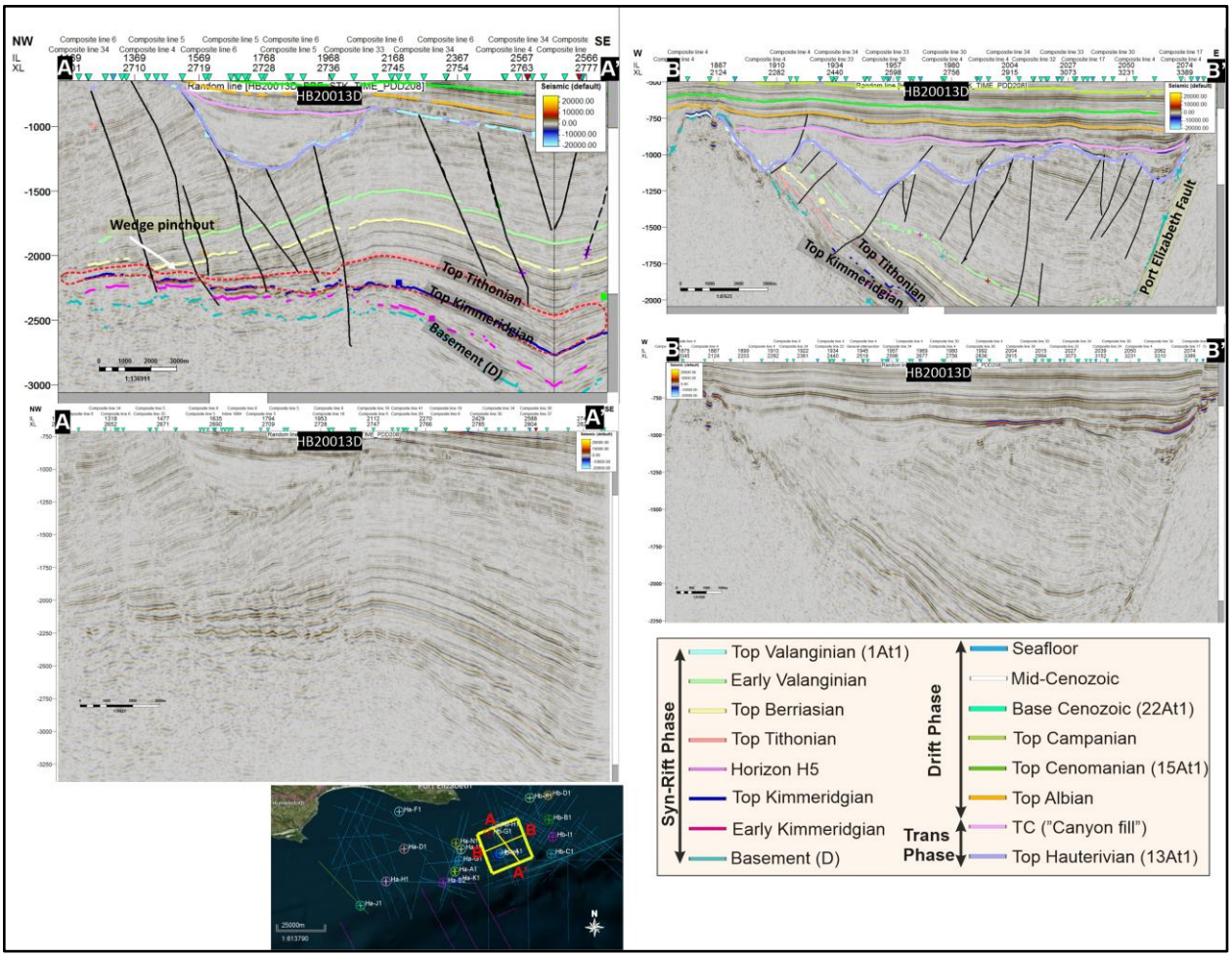

Figure 5.20 A-A' Post-Kimmeridgian to upper Tithonian succession, showing a wedge-like geometry, and thinning towards the N-NW. **B-B'** Towards the east, the Tithonian is truncated by the 1At1 reflector. Base map data ©2020 Google, Maxar Technologies, AfriGIS (Pty) Ltd.

5.2.3.3 Post-Tithonian to upper Berriasian

The Top Berriasian is generally poorly mappable in the Algoa Basin, although it is reasonable well detected in the Port Elizabeth Trough, and in the southern part of the Uitenhage Trough (see Figure 5.19). The Berriasian appears to be faulted and shows downlapping stratal terminations against the Top Tithonian reflector (Figure 5.21a). Comparable with the underlying succession, the Berriasian also forms a wedge, pinching out towards the N-W with increasing thickness towards SE (Figure 5.21a). There is also evidence of high-energy reflectors (i.e., brighter, stronger seismic reflectivity) that downlap on the Top Tithonian reflector and appear to be localised in the flanks of the wedge (Figure 5.21a). In the W-E direction, these reflectors are parallel, continuous, and terminate against the 1At1/13At1 reflector at an acute angle (Figure 5.21b). Again, the wedge-like geometry suggest that sedimentation was mostly towards the E,

with accommodation space being generated by movement along the Port Elizabeth Fault. Moreover, the downlapping bright reflectors could be indicative of a changing lithology (possibly sands reworked from the basement subcrops). The geometry of these downlapping strata near the antiform suggest that the Berriasian succession predates the folding event in the Port Elizabeth Trough (as seen in Figure 5.21A-A'). If the folding was older, onlapping stratal terminations would have been observed on either side of the antiform.

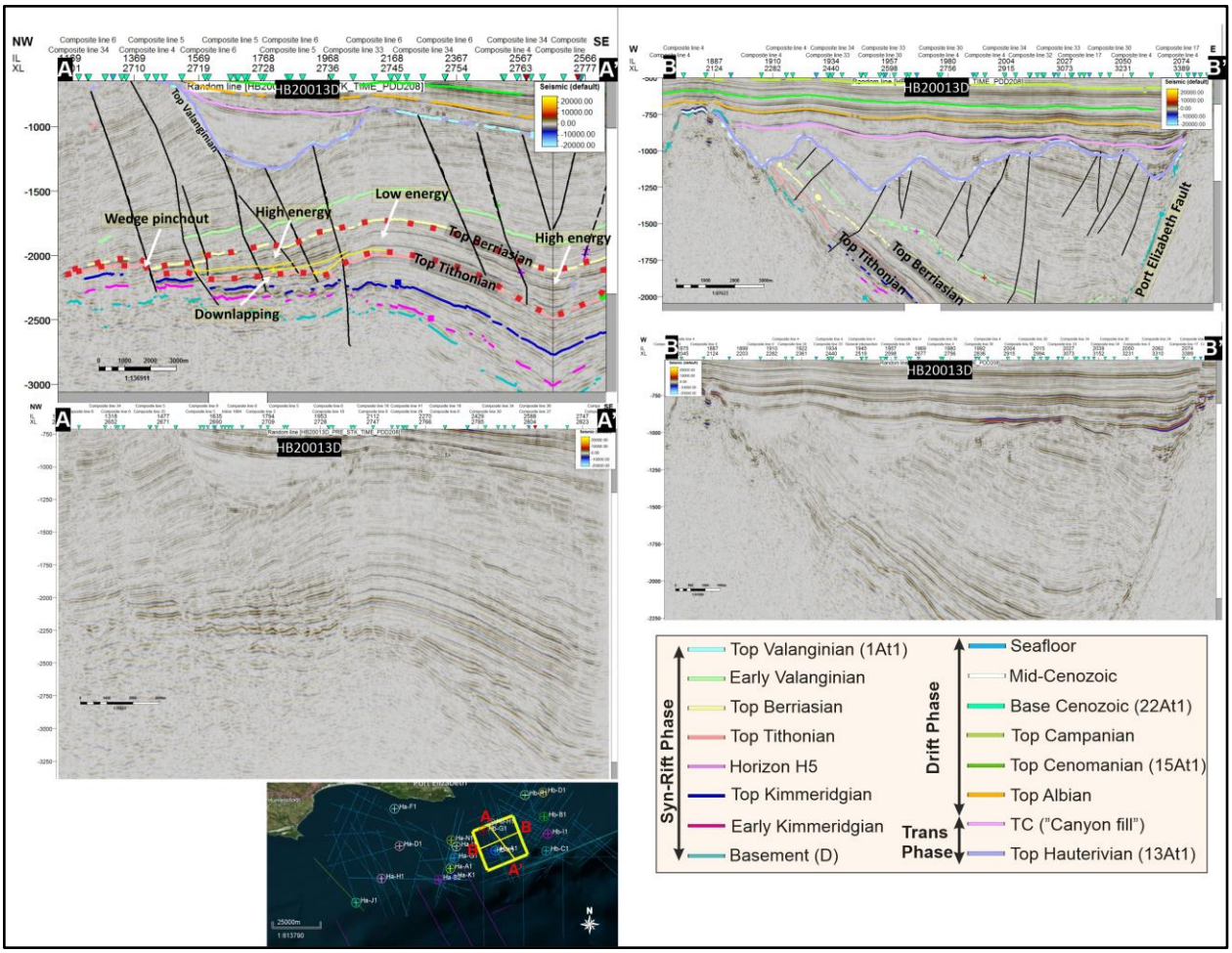

Figure 5.21: A-A' Post-Tithonian to upper Berriasian succession, showing a folded wedge geometry, and thinning towards the N-NW. **B-B'** Truncation of the Berriasian succession by the 1At1 reflector towards the east. Base map data ©2020 Google, Maxar Technologies, AfriGIS (Pty) Ltd.

5.2.3.4 Post-Berriasian to upper Valanginian

In the Port Elizabeth Trough, these reflectors are parallel and semi-continuous in the in the NW-SE direction (Figure 5.22A-A'). Unlike the underlying successions, the wedge-like geometry in the Port Elizabeth Trough is less defined in the W-E direction, and the succession appears to be severely faulted (Figure 5.22B-B'). Although the lower Valanginian can be picked on some few seismic lines in the Uitenhage Trough, it is generally highly truncated by younger reflectors (Figure 5.22B-B'). Overall, this succession shows lower energy, dimmer reflectors compared to the surrounding brighter, higher energy reflectors. The disappearance of the wedge-like geometry and the parallel, continuous and homogenous reflectors in this interval could indicate a period of relative tectonic quiescence in the Port Elizabeth Trough, when the rates of accommodation space generation and sediment supply were in balance. Generally, a wedging geometry is typical during syn-rift deposition (see Holz et al., 2017 their fig. 2), therefore the lack of this wedging either suggest low tectonic activity or high rates of sedimentation that outpaced subsidence rates.

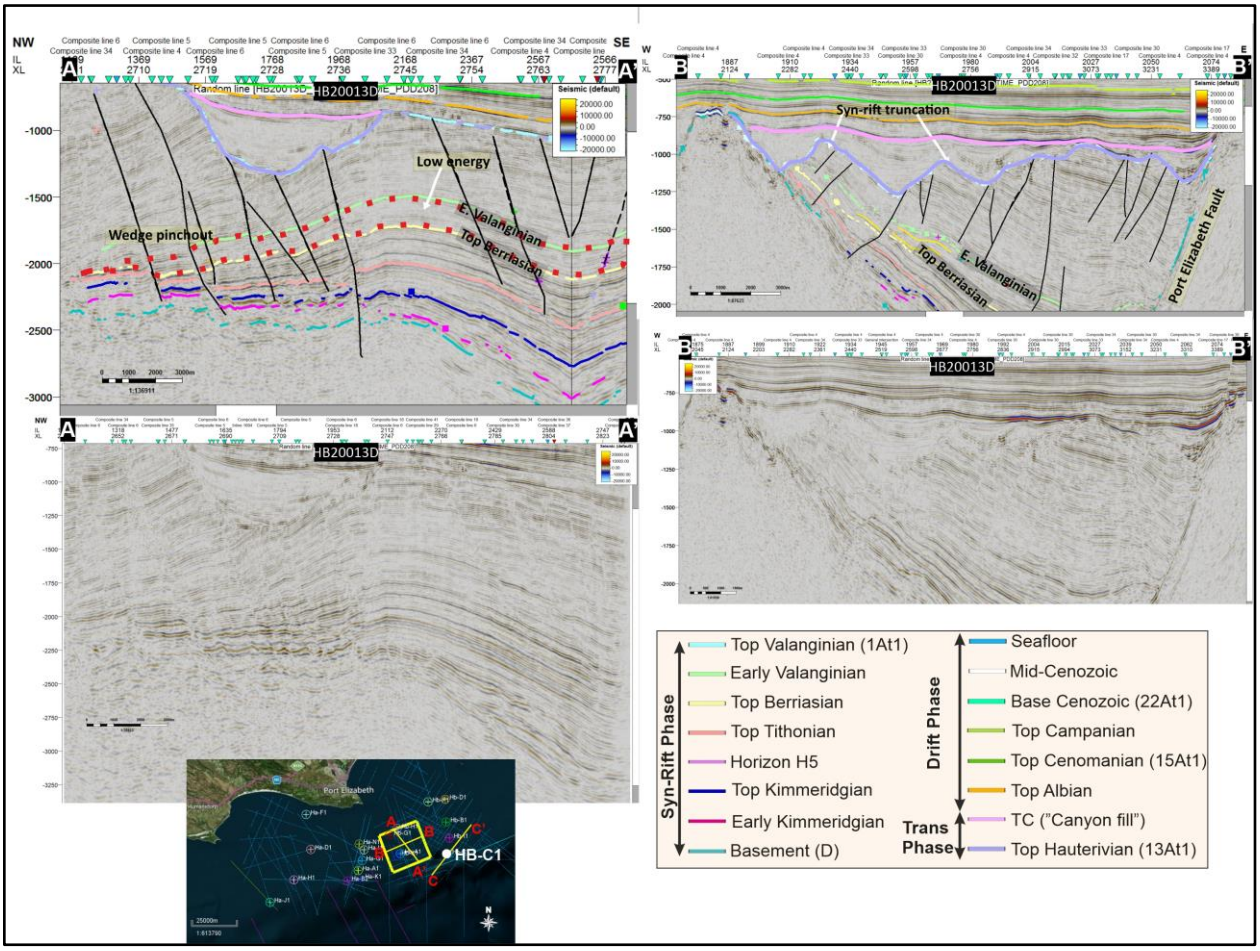

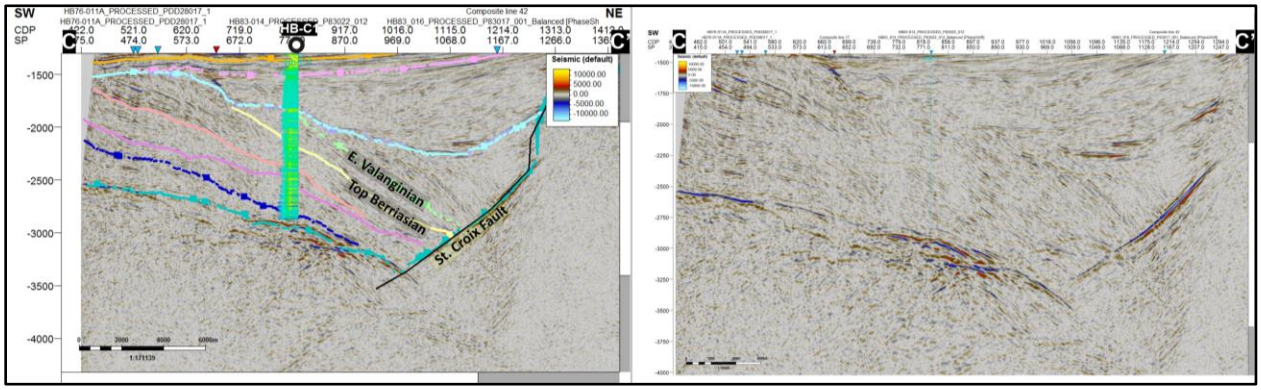

Figure 5.22: The tabular geometry of the lower Valanginian that overlies the Top Berriasian surface. Base map data ©2020 Google, Maxar Technologies, AfriGIS (Pty) Ltd.

The upper Valanginian succession, bounded by the Early Valanginian to Top Valanginian (1At1) surfaces, is also severely eroded and marks the last succession deposited during the syn-rift period (McMillan et al., 1997). Although the succession can be up to 3000-m-thick, it lacks distinct seismic features in the current dataset and thus its internal stratal geometries remain unknown (Figure 5.22B-B and Figure 5.23A-A'). Near the Port Elizabeth Fault, these Valanginian reflectors show chaotic character with some lateral continuity, whereas near the Uitenhage Trough Fault, this succession appears to be folded at the top (Figure 5.23). The thickness and the homogenous stratal geometries in the upper Valanginian succession suggest a period of high rates of both accommodation space generation and sediment supply. The Top Valanginian forms an angular unconformity with the underlying succession, which shows a change from syn-rift to transitional phase tectonic conditions. The folded geometry does not affect the overlying succession suggesting an early to late Valanginian tectonic inversion (probably from extension to compression; See Thomson, 1999).

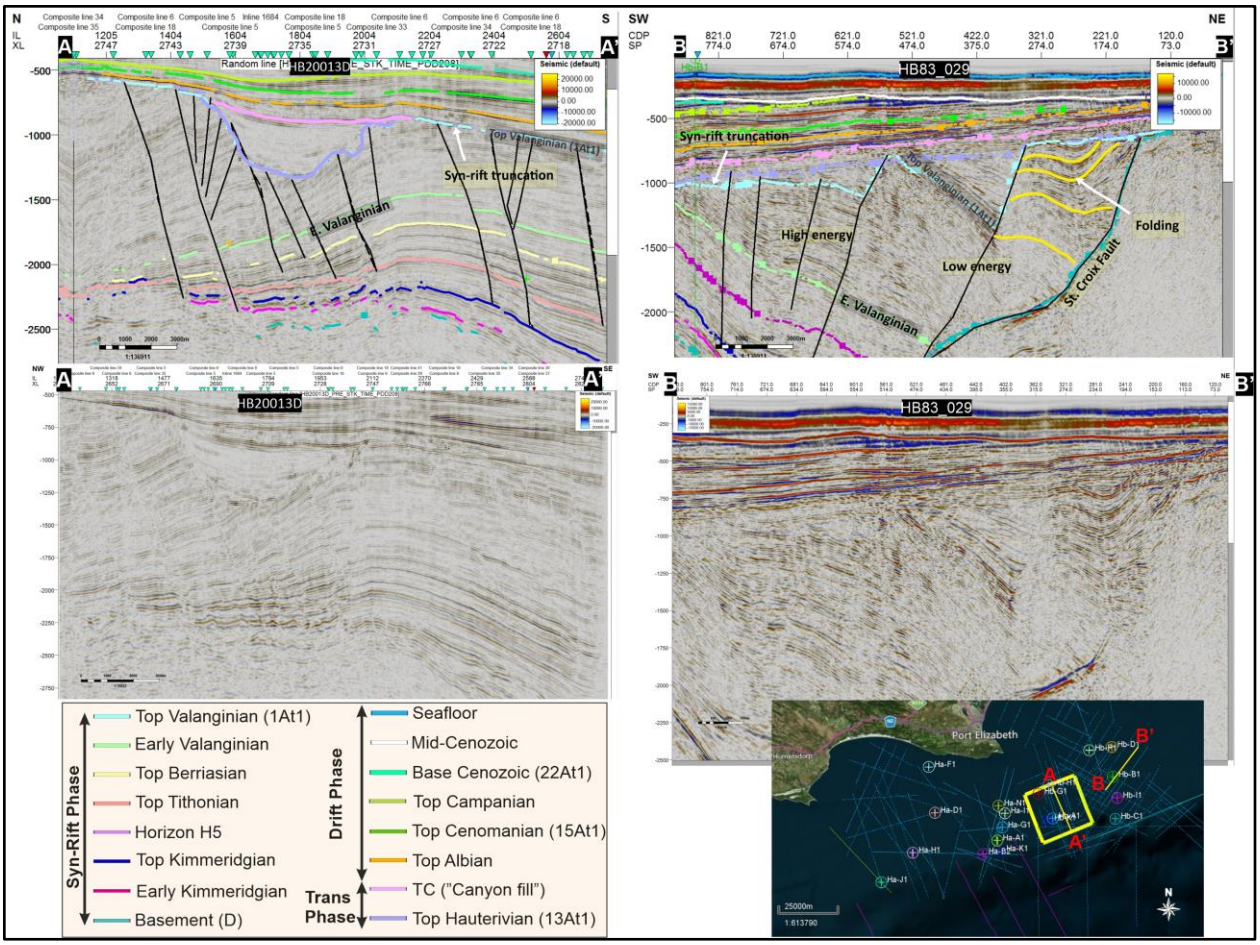

Figure 5.23: A-A' The upper Valanginian succession is truncated by the Top Valanginian (1At1) reflector. **B-B'** The upper Valanginian is folded towards the St. Croix Fault. Base map data ©2020 Google, Maxar Technologies, AfriGIS (Pty) Ltd.

5.2.3.5 Post-Valanginian to upper Hauterivian

In areas where the Hauterivian succession is preserved, the reflectors are parallel, semi-discontinuous, and dimmer than the surrounding reflectors (Figure 5.24A-A').The Hauterivian is also less faulted than the underlying syn-rift succession (Figure 5.24). The Top Hauterivian reflector is strongly erosional and truncates the syn-rift succession (Figures 5.19, 5.22 and 5.24). In mostt of the basin, the Top Hauterivian reflector (13At1) truncates into the syn-rift succession, as a result, the Hauterivian succession is only partially preserved (Figure 5.22B-B). The rare faulting through this succession suggest that the influence of syn-rift extensional faults was diminishing during deposition.

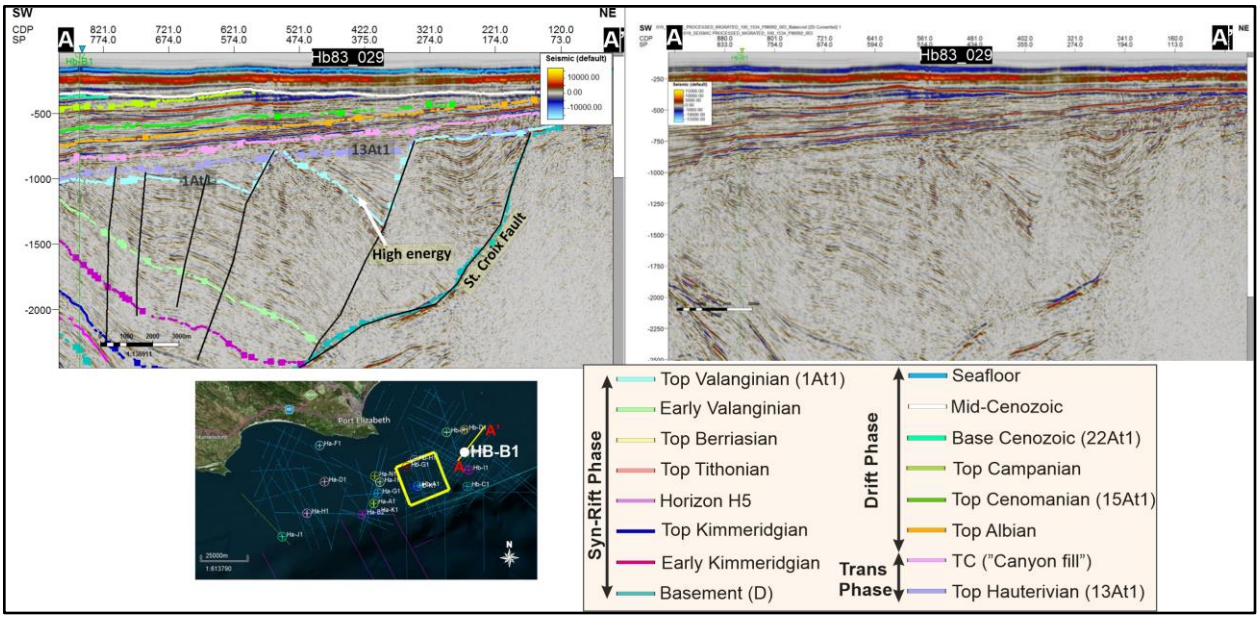

Figure 5.24: A-A' Faulting in the Hauterivian succession in the Uitenhage Trough. Base map data ©2020 Google, Maxar Technologies, AfriGIS (Pty) Ltd.

5.2.3.6 Post-Hauterivian to "Canyon fill" (lower Albian)

This interval can be separated into upper and lower "Canyon fill" succession based on the stratal geometries. The lower part of this succession shows semi-continuous, horizontal reflectors onlapping on the 1At1reflector (Figure 5.24A-A'). These are succeeded by erosional truncation and fill features, as well as overall southward (i.e., S, SE, SW) prograding clinoforms (Figure 5.25). The change in seismic character from semi-continuous onlapping stratal geometries to erosional truncation and then prograding clinoforms can be used to infer a change from low-energy marine to possibly high-energy fluvial and then shallow marine/shoreface (deltaic?) setting. The incised geometries, which cut into each other, show multiple phases of channel incisions. The prograding clinoforms, which are limited to the upper succession suggests a sediment source located overall in the N (i.e., N, NW, NE).

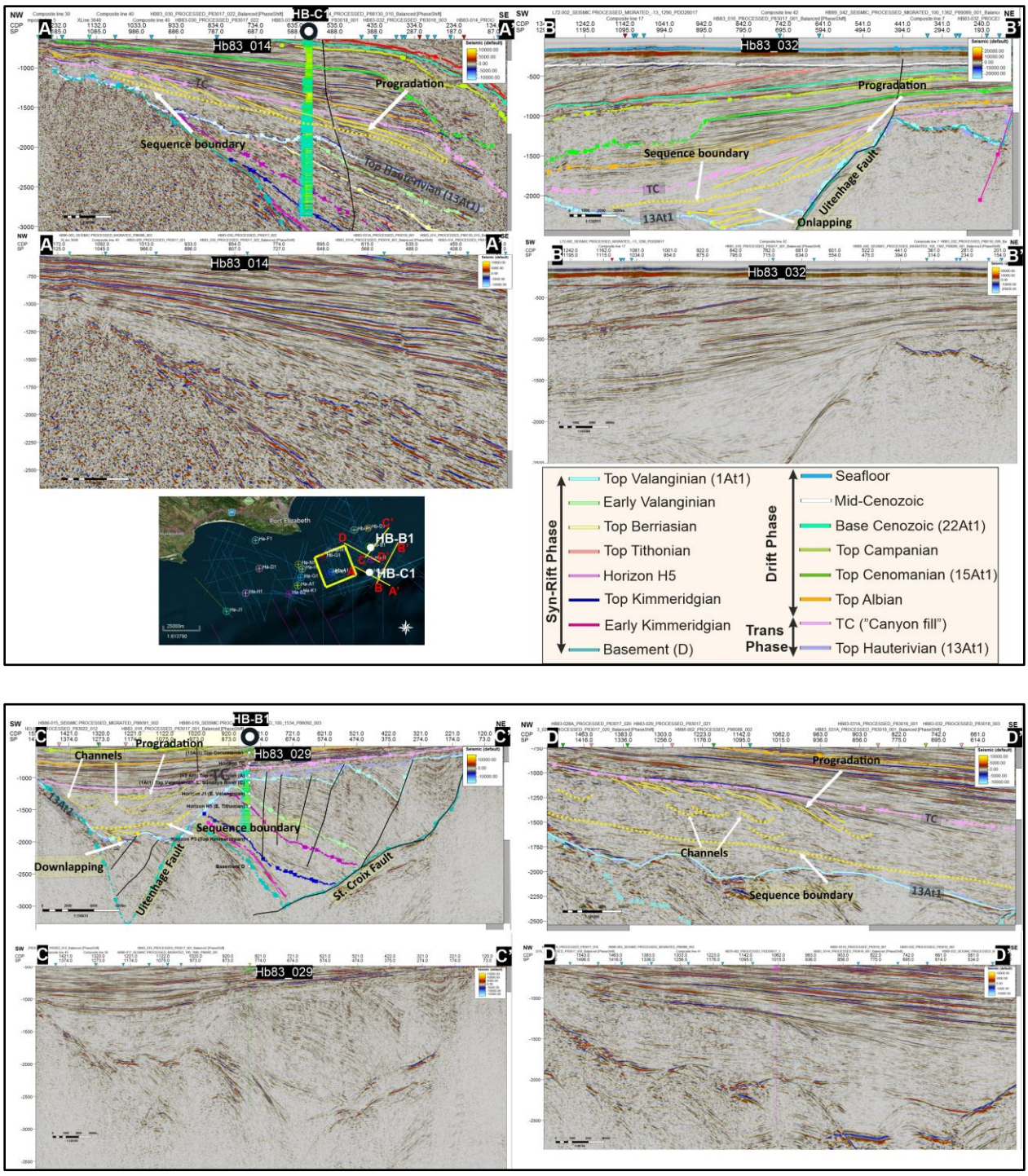

Figure 5.25: The post-Hauterivian to "Canyon fill" interval. These Canyon fill reflectors show prograding clinoforms at the top of the succession, and onlapping on the Top Hauterivian (13At1) reflector at the base. Base map data ©2020 Google, Maxar Technologies, AfriGIS (Pty) Ltd.

5.2.3.7 Post-Hauterivian/“Canyon fill” to upper Albian

The Top Canyon/Hauterivian to Top Albian succession shows reflectors that are parallel, continuous, brighter than those in the underlying succession (Figure 5.26). This interval is dominated by another set of clinoforms prograding from the N and NW, which terminate in the up-dip setting, suggesting toplap stratal geometries (Figure 5.26C-C). In the Port Elizabeth Trough, this succession shows a wedge geometry, which thins towards the W, and increases in thickness towards the Port Elizabeth Fault (Figure 5.26b). There is also evidence of onlapping geometries, however, these onlaps are more evident along the strike line (Figure 5.26a). The Albian succession also appears to be truncated by the overlying Top Cenomanian reflector, especially towards the shelf edge/slope (Figure 5.26d).

The progradation from the N and NW and an up-dip truncation (i.e., toplap) indicate the depositional limit of the Albian succession in the middle shelf. The Albian succession also appears to increase in thickness over the “Canyon fill” sediments, and this increase in accommodation space was probably due to differential compaction over the Algoa Canyon, where the older, syn-rift succession was thin or eroded. In the Port Elizabeth Trough, where the Algoa Canyon is laterally limited, the Albian succession increases in thickness towards the Port Elizabeth Fault, suggesting reactivation of the fault.

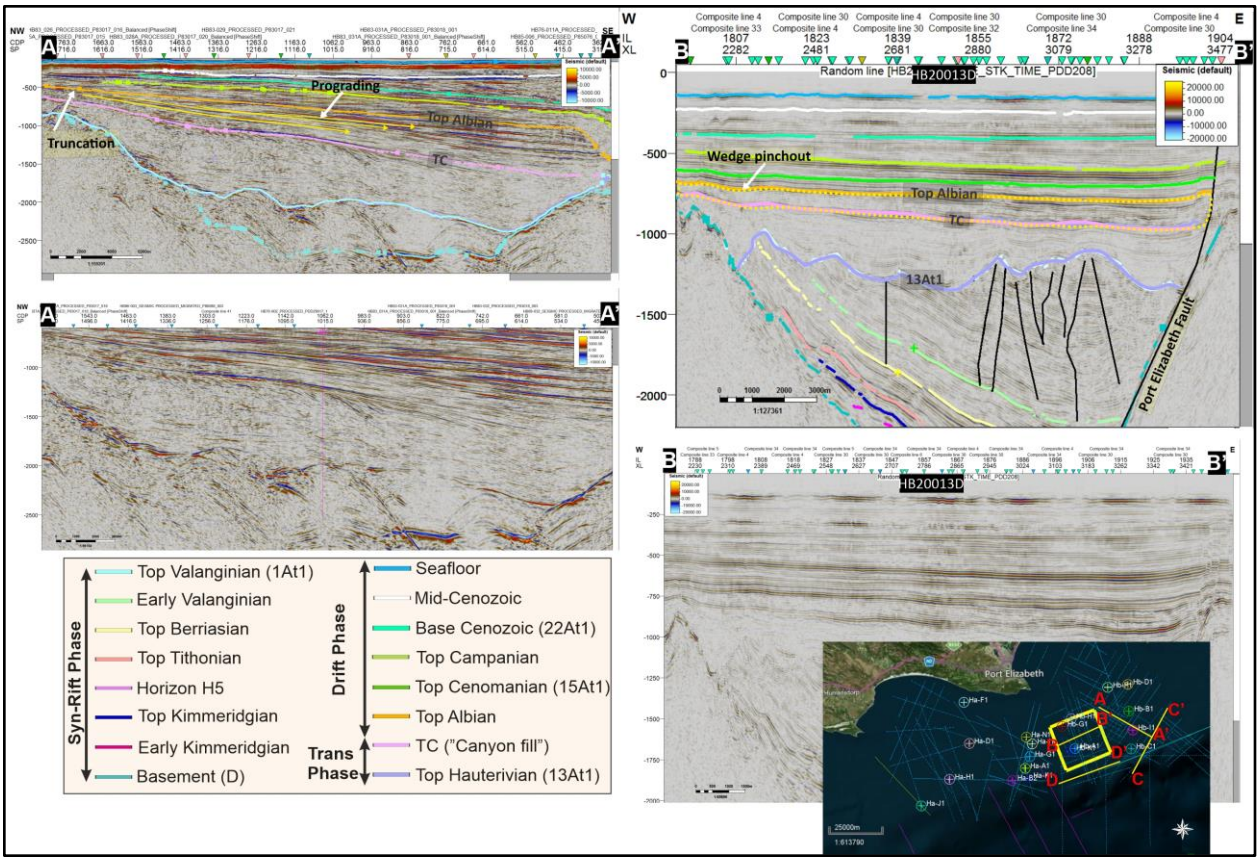

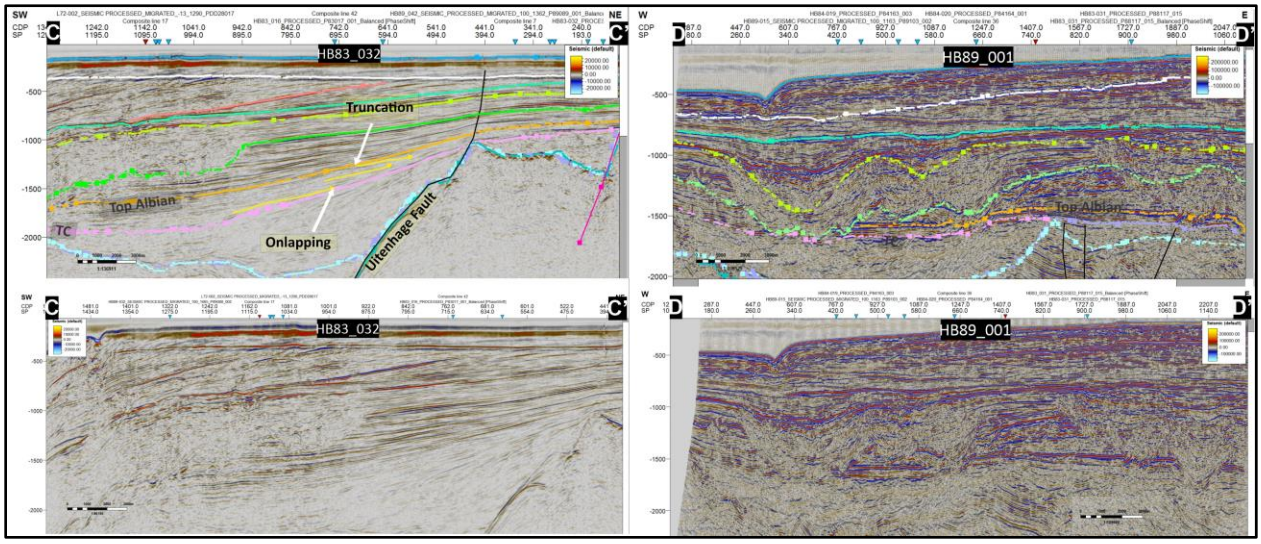

Figure 5.26: Seismic features in the Albian succession bounded by Top Canyon/Top Hauterivian and Top Albian surfaces. **A-A'** Prograding clinoforms from the NW. **B-B'** Westwards thinning in the Port Elizabeth Trough. **c** Thickening of the Albian succession possibly due to differential compaction along the Algoa Canyon. **C-C'** Truncation by overlying succession along the shelf edge. Base map data ©2020 Google, Maxar Technologies, AfriGIS (Pty) Ltd.

5.2.3.8 Post-Albian to upper Cenomanian

Cenomanian succession conformably overlies the Top Albian reflector with continuous and brighter reflectors than those in the underlying succession (Figure 5.27). The basal reflectors onlaps on the Top Albian reflector, and are overlain by S-SE-ward prograding clinoforms (Figure 5.27A-A'). This succession also thins towards the N-NW and shows an up-dip truncation (Figure 5.27A-A', B-B'). The Cenomanian succession is truncated by the 15At1 (Top Cenomanian) reflector, which also truncates the Albian succession, and in some places even the syn-rift succession (Figure 5.27c-e). This truncation is more evident towards the middle to outer shelf, while the inner shelf shows toplap geometries (Figure 5.27A-A'). The truncation is very irregular and more evident in the shelf break (Figure 5.27D-D').

The basal onlapping stratal geometries shows an increase in accommodation space in the early Cenomanian. The newly created accommodation space was filled with prograding sediments, which probably resulted from normal regression. The toplap geometries observed in the proximal setting, probably shows the up-dip depositional limit of the Cenomanian succession in the inner to middle shelf setting. However, in the mid-outer shelf, the Cenomanian succession seem to be highly eroded.

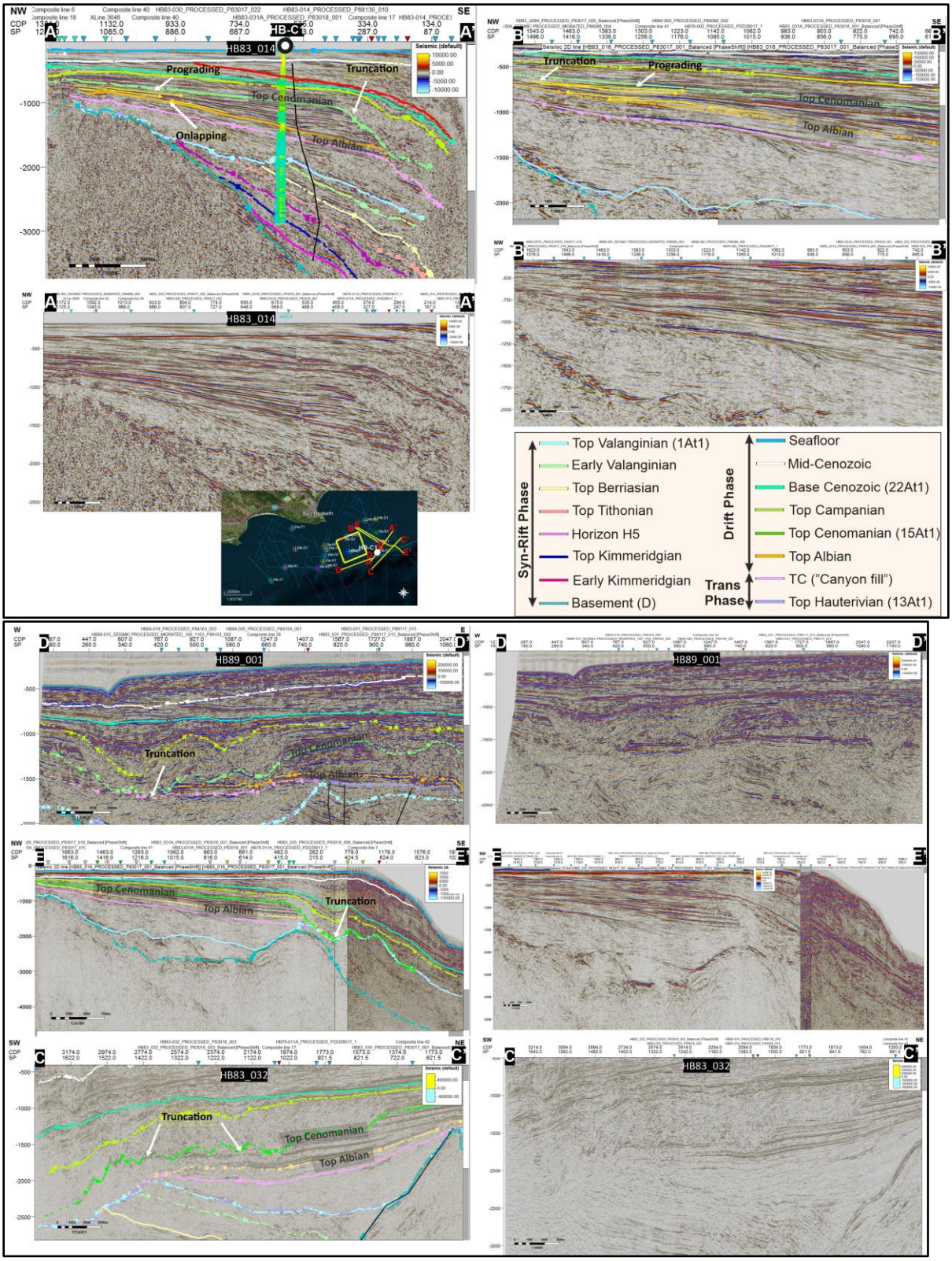

Figure 5.27: Seismic features in the Cenomanian succession bound by the Top Albian to Top Cenomanian reflectors. **A-A', B-B'** Basal onlapping onto the Top Albian reflector. **C-C', D-D', E-E'** Mid-inner shelf erosion by the Top Cenomanian (15At1) reflector. Base map data ©2020 Google, Maxar Technologies, AfriGIS (Pty) Ltd.

5.2.3.9 Post-Cenomanian to upper Campanian

On the shelf, the Campanian succession, which overlies the 15At1 unconformity generally shows bright, parallel, and laterally continuous reflectors (Figure 5.28). This interval forms a wedge, which shows drastic thinning towards the N (i.e., inner shelf; Figure 5.28b). This succession also shows clinoforms prograding from the NW-NE, downlapping on the Top Cenomanian reflector with incised stratal geometries observed in the upper part of the succession in the middle to outer shelf (Figure 5.28a). However, in the shelf edge/slope setting, this succession shows sub-parallel, semi-continuous stratal geometries onlapping onto the Top Cenomanian reflector (Figure 5.28A-A', B-B', C-C').

The shelf edge/slope stratal geometries suggest basinwards deposition, probably during a period when the shoreline was situated towards the shelf edge, before subsequently moving landwards. The landwards shift of the shoreline generated accommodation space for sediments, which then accumulated on the shelf and formed prograding clinoforms. The thinning of this succession in the middle shelf indicates that the Campanian shoreline was mostly situated in the middle shelf and did not reach the landward position of the previous shoreline before the early Late Cretaceous regression. Evidence for subaerial erosion on the shelf is lacking, and the erosional geometries observed in the slope are probably due to slope processes such as contourites or mass movements (Hernández-Molina et al., 2008).

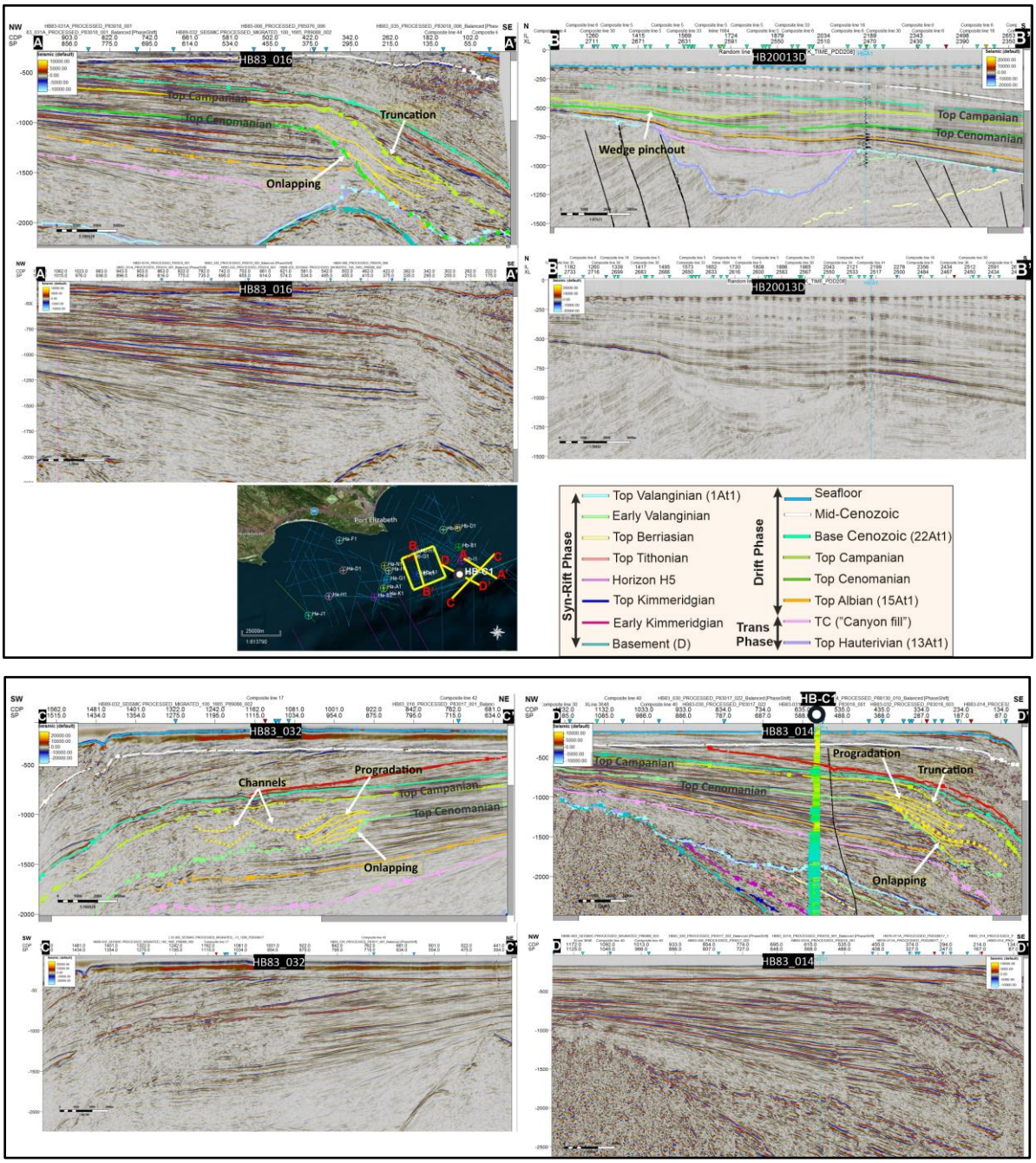

Figure 5.28: Seismic features in the Campanian succession bound by the Top Cenomanian (15At1) reflector at the base and Top Campanian reflector at the top. **A-A'** The lower Campanian predominately onlaps onto the 15At1 reflector on the slope. **B-B'** the Campanian succession wedging out towards the N. **C-C'** Onlapping stratal geometries overlain by progrades and subsequence truncational cuts. **D-D'** Basal onlap of the Campanian succession overlain by progrades towards the shelf edge. Base map data ©2020 Google, Maxar Technologies, AfriGIS (Pty) Ltd.

5.2.3.10 Post-Campanian to Lower Cenozoic

In the slope setting, where this succession is thicker, reflectors onlap on the Top Campanian reflector, showing dim and chaotic reflectors (Figure 5.29). Although this interval is generally thin in the middle to outer shelf setting, there is an increase in thickness (towards the inner shelf) over the Upper Cretaceous wedge with the basal reflectors showing lower energy (dimmer), discontinuous and chaotic character (Figure 5.29b). The upper succession shows bright (higher energy), parallel, horizontal, and continuous reflectors, which are consistent throughout the shelf. This succession is generally thin in the middle to outer shelf with occasional clinoforms prograding from the N-NW.

This relatively thick succession occupies the accommodation space in the inner shelf, resulting from the shoreline advancing landwards (i.e., accommodation space creation outpaced sedimentation) during the Late Cretaceous. It is likely that in the latest Cretaceous the shoreline moved past the location of the Campanian shoreline to reach the inner shelf setting. There is no evidence to suggest any subaerial exposure of the shelf during the latest Cretaceous.

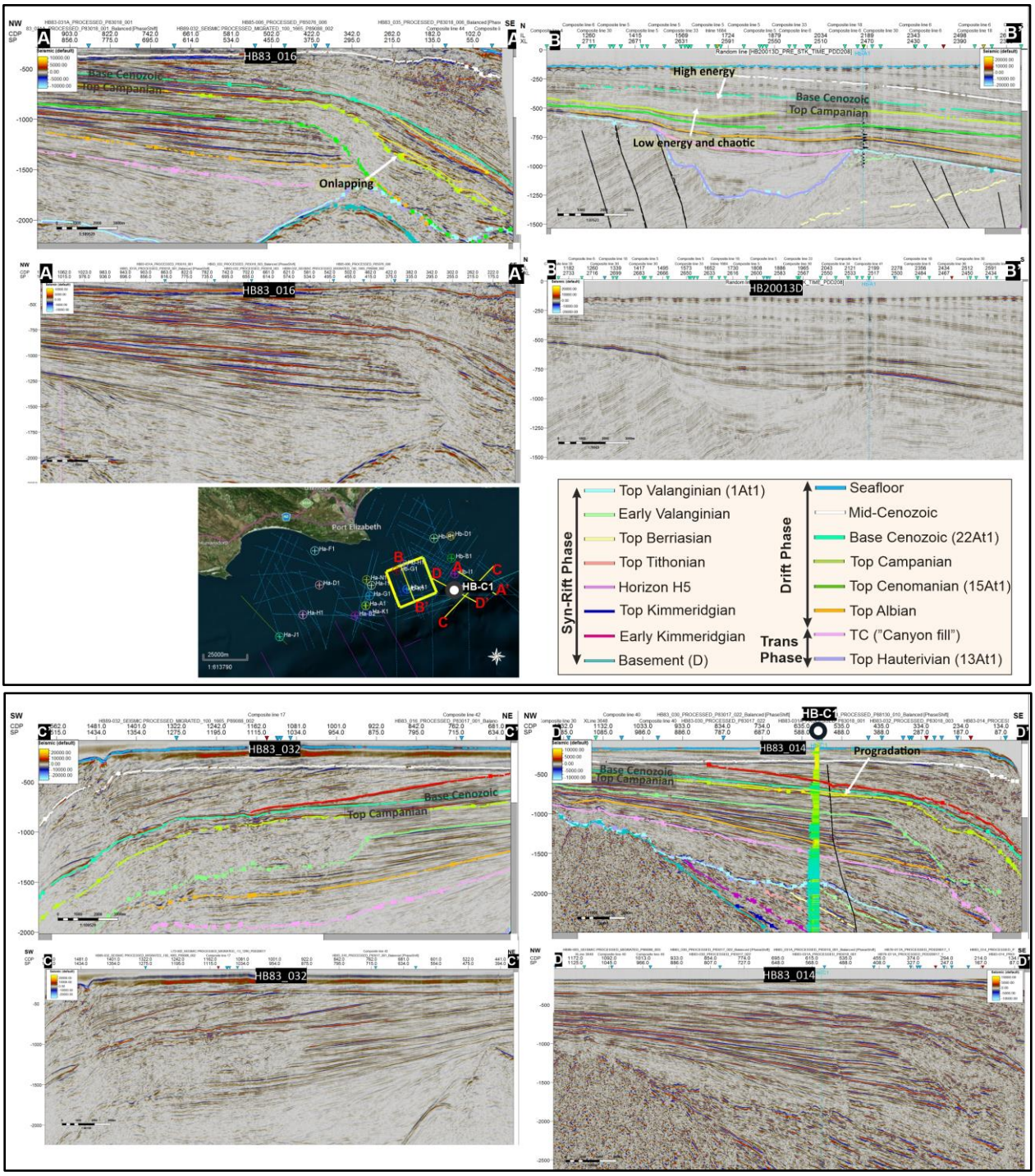

Figure 5.29: Seismic features of the succession bound by the Top Campanian and Base Cenozoic reflectors. **A-A'** Upper Cretaceous succession onlapping on the Top Campanian reflector. **B-B'** Thicker upper Cretaceous succession towards the N. **C-C'** Parallel and continuous reflectors of the upper Cretaceous along the shelf. **D-D'** Subtle progrades along the dip line.. Base map data ©2020 Google, Maxar Technologies, AfriGIS (Pty) Ltd.

5.2.3.11 Lower to Middle Cenozoic

The Base to Mid-Cenozoic reflectors are semi-continuous and show a dimming character compared to the underlying post-rift succession (Figure 5.30). Along a NW-SE section, these reflectors downlap onto the Base Cenozoic reflector on the shelf, and prograde from the N to S in the shelf edge/slope setting (Figure 5.30). The Mid-Cenozoic reflector truncates the underlying, older post-rift succession at an acute angle, especially in the N (Figure 5.30). This truncation is also notable towards the shelf edge/slope (Figure 5.30).

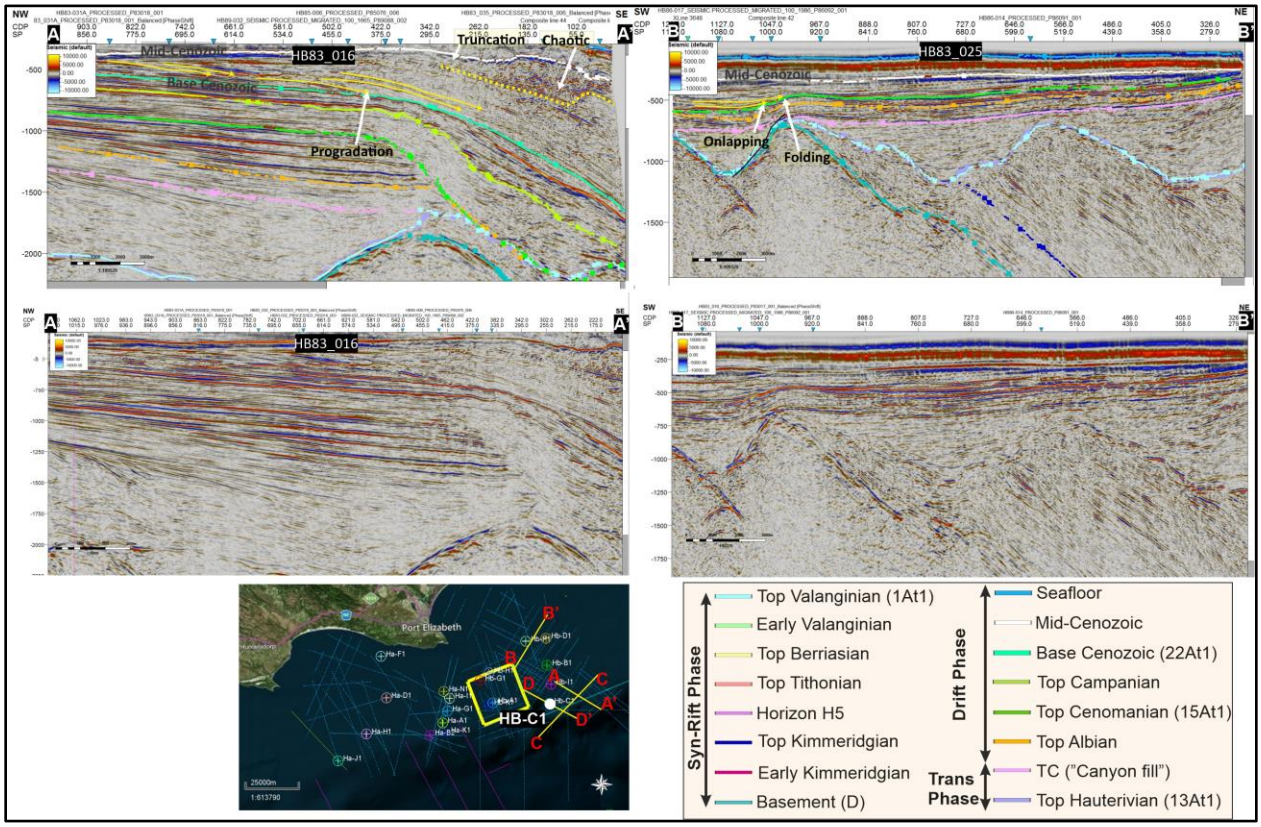

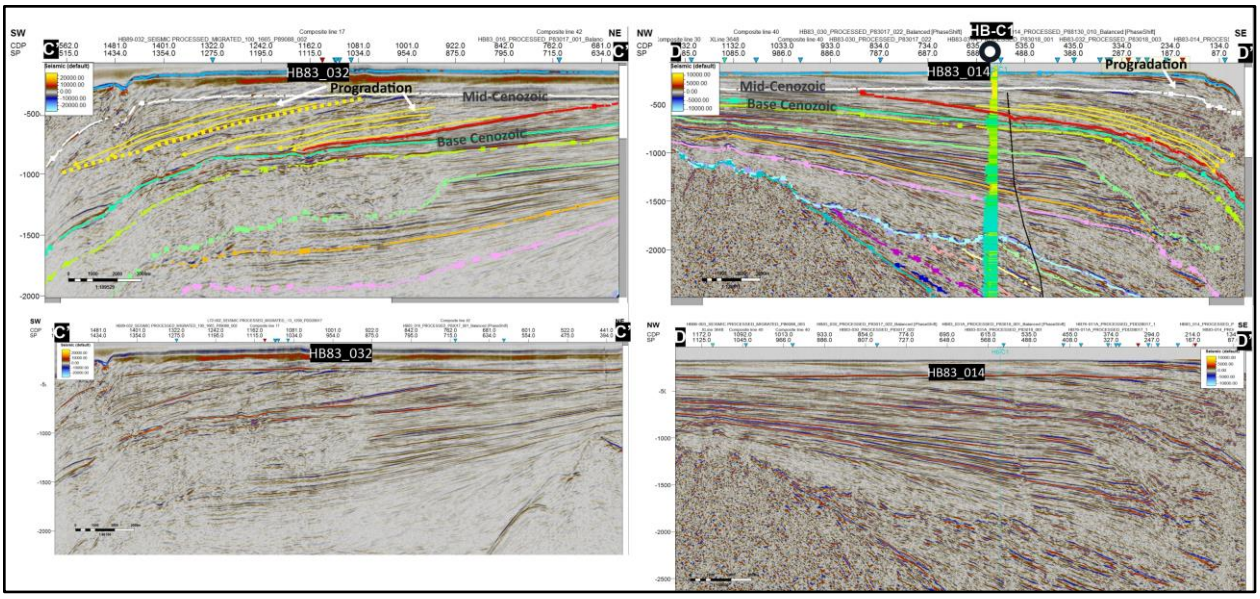

Figure 5.30: Seismic features of Lower Cenozoic succession are dominated by prograding clinoforms. Base map data ©2020 Google, Maxar Technologies, AfriGIS (Pty) Ltd.

5.2.3.12 Upper Cenozoic

This succession is very thin in the Algoa Basin, and although stratal terminations are not observed in the shelf succession, southward prograding clinoforms are present in the slope region (Figure 5.30).

6 The Gamtoos Basin

6.1 Introduction

The Gamtoos Basin, which also form part of the Outeniqua Basin, is a ~5038 km^2 half graben that is bound to the W by the St Francis Arch and to the E by the Recife Arch (Figure 1.1; Broad, 1990; Malan, 1993; McMillan et al., 1997; Paton and Underhill, 2004; Broad et al., 2012; Davids et al., 2017). Contrary to the structurally complex Algoa Basin, the Gamtoos Basin has a single depocenter associated one main fault (Figures 1.1 and 2.1; Broad, 1990; McMillan et al., 1997; Paton and Underhill, 2004). On par with the Algoa Basin, without economic incentives to-date, modern sequence stratigraphic studies in the Gamtoos Basin have not been undertaken (McMillan et al., 1997; Broad et al., 2012). This chapter has a similar structure to chapter 0, and therefore it deals with the: a) sedimentary facies distribution, and b) basin development history, from the Mid-Mesozoic to Holocene.

6.2 Results

Similar to the Algoa Basin, the second-order (Vail et al., 1991; Embry et al., 2007; Catuneanu, 2019a, b) sequence boundaries identified are: Basement D, Top Valanginian (1At1/6At1), Top Hauterivian (13At1), Top Albian (15At1), Top Campanian, Base Cenozoic (22At1), Mid-Cenozoic and Seafloor (Figures 2.1, 6.1 and 6.2; Brown et al., 1995; McMillan et al., 1997; PASA, 2012). Minor sequence boundaries identified in the syn-rift sequence are the third-and fourth-order flooding surfaces (Vail et al., 1991; Embry et al., 2007; Catuneanu, 2019a, b), and include the following: P3 (Top Kimmeridgian), H5 (Top Tithonian), P1 (Top Berriasian), and J1 (Early Valanginian; Figures 6.1 and 6.2).

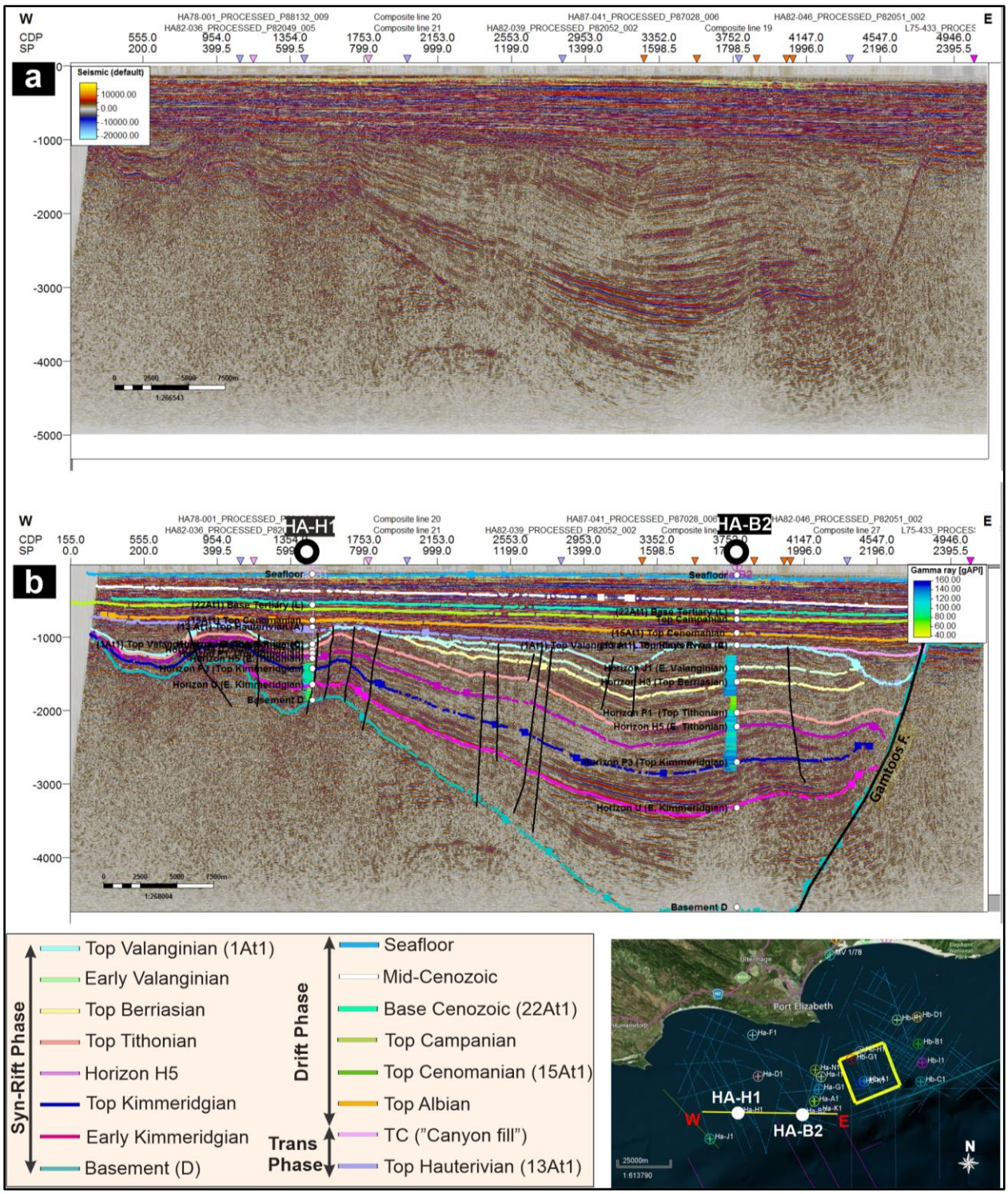

Figure 6.1: Strike oriented semi regional Gamtoos Basin seismic section. **a** Uninterpreted W-E section across the Gamtoos Basin. **b** Interpreted W-E section across the Gamtoos Basin. Base map data ©2020 Google, Maxar Technologies, AfriGIS (Pty) Ltd.

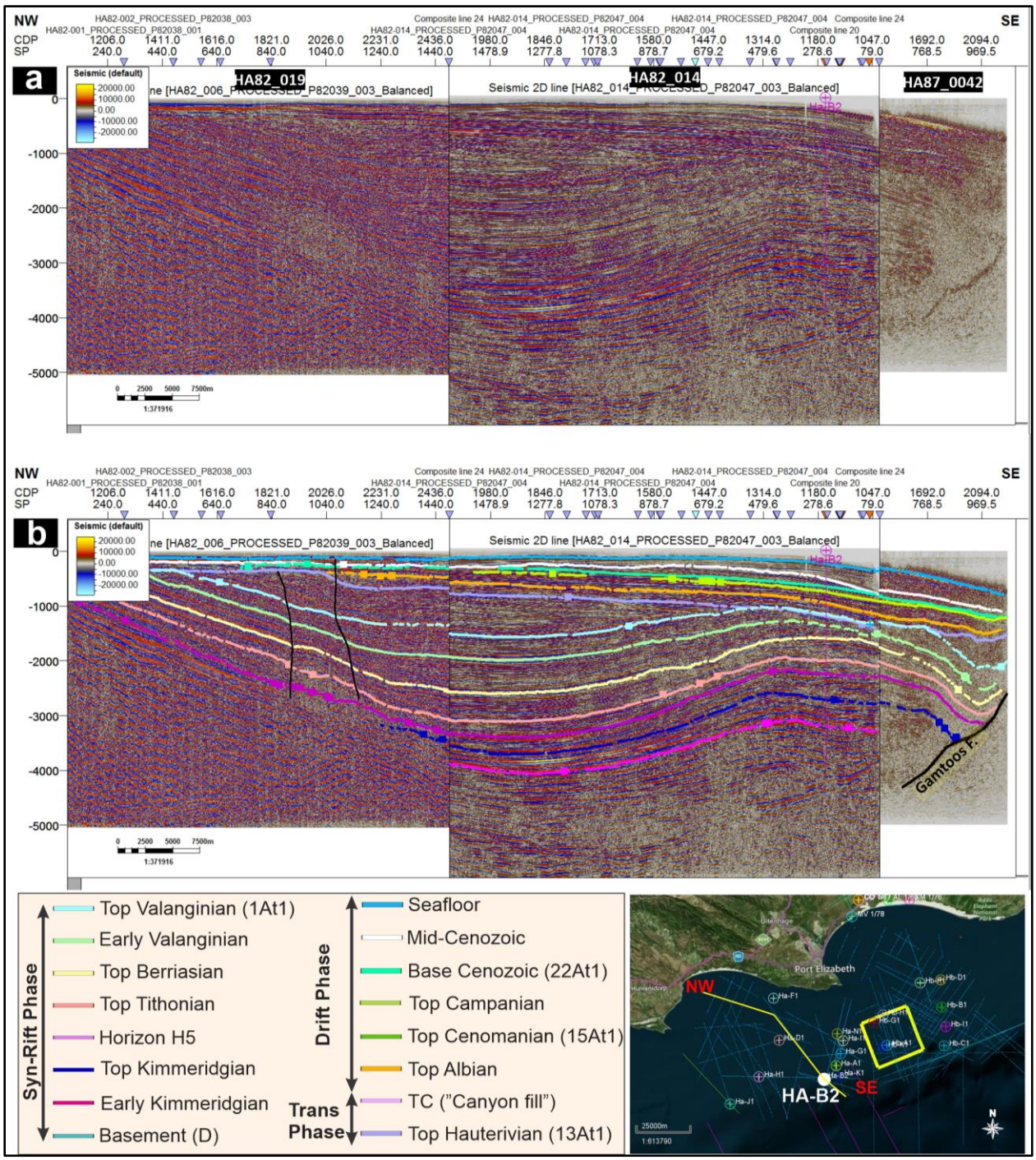

Figure 6.2 Dip orientated semi regional Gamtoos Basin seismic section. **a** Uninterpreted NW-SE section across the Gamtoos Basin. **b** Interpreted NW-SE section across the Gamtoos Basin. Base map data ©2020 Google, Maxar Technologies, AfriGIS (Pty) Ltd.

6.2.1 Borehole correlations

6.2.1.1 Pre-Aalenian to upper Kimmeridgian

This interval was intersected by four boreholes (Figure 6.3): boreholes HA-J1 and HA-H1 in the W (drilled into the Palaeozoic basement) and boreholes HA-B2 and HA-K1 towards the E (only intersect the upper part of this unit). Borehole HA-J1 in the far W intersected fining-upward silty facies at the base (GR: 60–90 API), which is overlain by units with very high GR signatures (ranging from 90 to > 150 API), which are then overlain by a s fining-upward very fine-grained sandy to silty succession (GR: 32–76 API; Figure 6.3). This Lower to Middle Jurassic succession is thin and pinches towards borehole HA-J1, in which the Kimmeridgian succession was intersected (~130-m-thick; GR: 45 –>150 API; Figure 6.3). In the centre of the Gamtoos Basin, borehole HA-H1 is dominated by a > 700-m-thick, fining-upward unit (GR: 30-112 API; Figure 6.3). Within this unit, the lower portion shows a high net sand-to-shale ratio, while the upper portion shows silty and claystones facies. Near the Gamtoos Fault, borehole HA-B2 intersected a > 265-m-thick succession of shales and clays that contain some isolated coarsening-upward sandy facies (GR: 42-145 API). Borehole HA-K1, which is closer to the Recife Basement High, contains a > 1720-m-thick succession of predominantly coarsening-upward units (GR: 36–120 API; Figure 6.3).

There is significant lateral lithological heterogeneity in the Gamtoos Basin wireline data, with logs showing varying inferred grain-size and facies trends across the basin. The base of borehole HA-J1 is dominated by low-energy setting clays and shaly facies at the base, which are then overlain by fining-upward fluvial deposits (in the floodplains). Borehole HA-H1 intersected silty to sandy facies at the base, which overlain by silty to shaly facies at the top of the sequence, indicating a possible transgressive shoreline, from floodplain setting to shallow marine. Borehole HA-B2 is dominated by low-energy facies, with some sand interbeds, probably indicating a distal marine setting. The primarily coarsening-upward very fine-grained sand and silty facies in borehole HA-K1 suggest a likely shallow marine setting (e.g., river mouth bar, delta plain, shoreface).

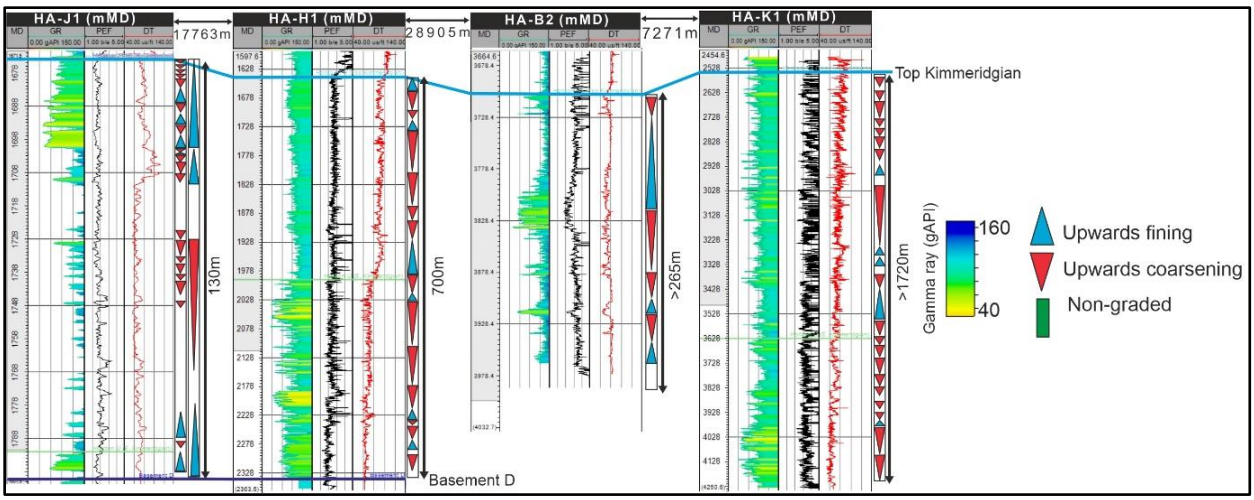

Figure 6.3: Pre-Aalenian to upper Kimmeridgian wireline correlation-based on boreholes HA-J1, HA-H1, HA-B2 and HA-K1 in the Gamtoos Basin (for boreholes location, see Figure 3.3).

6.2.1.2 Post-Kimmeridgian to upper Tithonian

This interval, which was intersected in boreholes HA-D1, HA-B2 and HA-G2, is dominated by coarsening-upward trends, with isolated fining-upwards trends (Figure 6.4). Borehole HA-D1 intersected a 1288-m-thick succession with overall high GR signatures (GR: 110 to 145 API) and a few o low GR readings (GR: 32 to 56 API; Figure 6.4). Borehole HA-B2 contains a >3240-m-thick succession of mainly coarsening-upward units (GR: 55 to 140 API; Figure 6.4) of siltstone with minor claystone, thin fine- to medium-grained sandstone (at depth 2928 m). Borehole HA-G1 intersected a 725-m-thick, silty coarsening-upward successions (GR: 45 to 122 API; Figure 6.4).

Borehole HA-D1 is dominated by low-energy setting (likely marine) shales and clays, with isolated sandstone interbeds. The occasional sandy facies in this HA-D1 were probably deposited as turbidites or basin floor fans. Both boreholes HA-B2 and HA-G2 are dominated by very fine-grained sands to silty facies that likely deposited in a marine setting, with borehole HA-G1 traversing slightly shallow marine deposits, while borehole HA-B2 intersected deeper marine setting units.

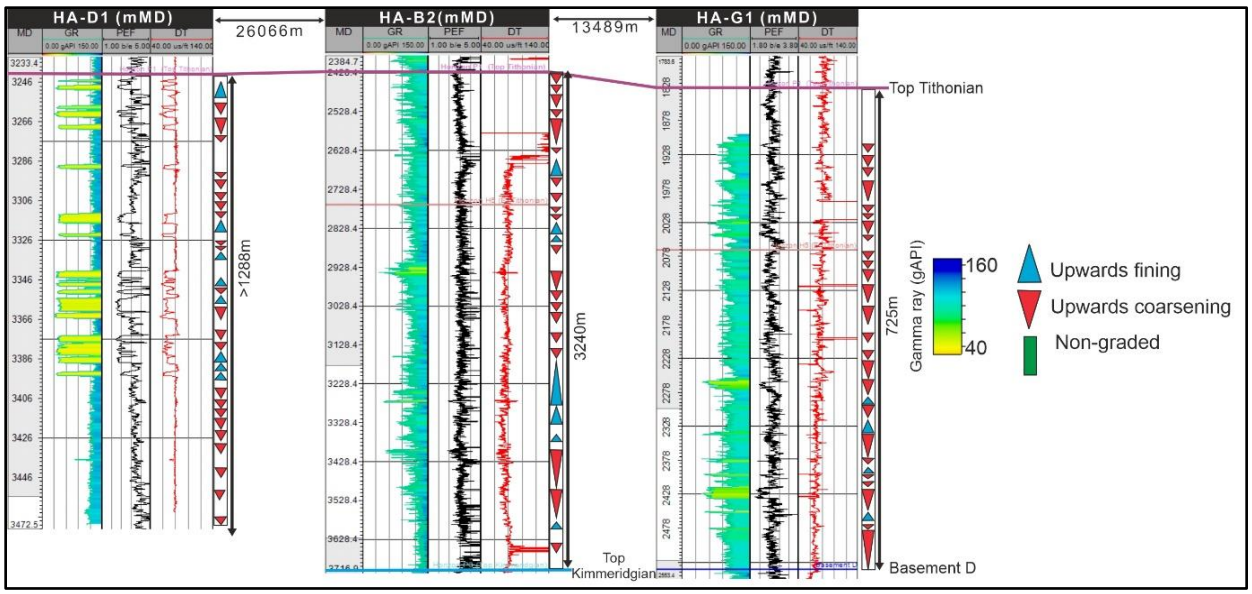

Figure 6.4: Post-Kimmeridgian/Basement D to upper Tithonian W-E wireline correlation based on boreholes HA-D1, HA-B2 and HA-G1 in the Gamtoos Basin (for boreholes location, see Figure 3.3).

6.2.1.3 Post-Tithonian to upper Berriasian

The more proximal borehole HA-F1 shows an overall coarsening-upward trend (GR: 30 to 96 API; >570-m-thick; Figure 6.5) made up of cycles of smaller, coarsening-upward units with isolated fining-upward trends. Borehole HA-D1 is dominated by silty and clays facies (GR: 88-120 API; Figure 6.5) with very low sand-to-shale ratio. The base of the succession intersected a coarsening-upward unit, followed by an fining-upward, overlaid by nongraded units. In borehole HA-B2, this succession has been invaded by drilling fluids, resulting in acquisition artefacts at depths 2376-4003 m, 2582-2669 m and 3648-3754 m, however, part of the borehole that was successfully logged and the mudlog report describes alternating claystone and siltstone with occasional limestone (GR: 95-140 API; Figure 6.5; Winters, 1985). In borehole HA-G1, GR log is not available for this interval, however, sonic (DT) and photoelectric (Pe) logs traverse a ~390-m-thick succession with alternating coarsening-upward and fining-upward trends (85 to 111 ms/ft; 2.37 to 3 b/e; Figure 6.5).

The more proximal borehole HA-F1 shows reoccurring coarsening-upward units with low GR values, indicating a high-sand-to-shale ratio, probably shoreface deltaic or mouth bar setting. Gamma ray values increases towards the south, indicating deepening, low-energy environment. Furthermore, the limestone described in the mudlog of borehole HA-B2 suggest a shallow marine environment.

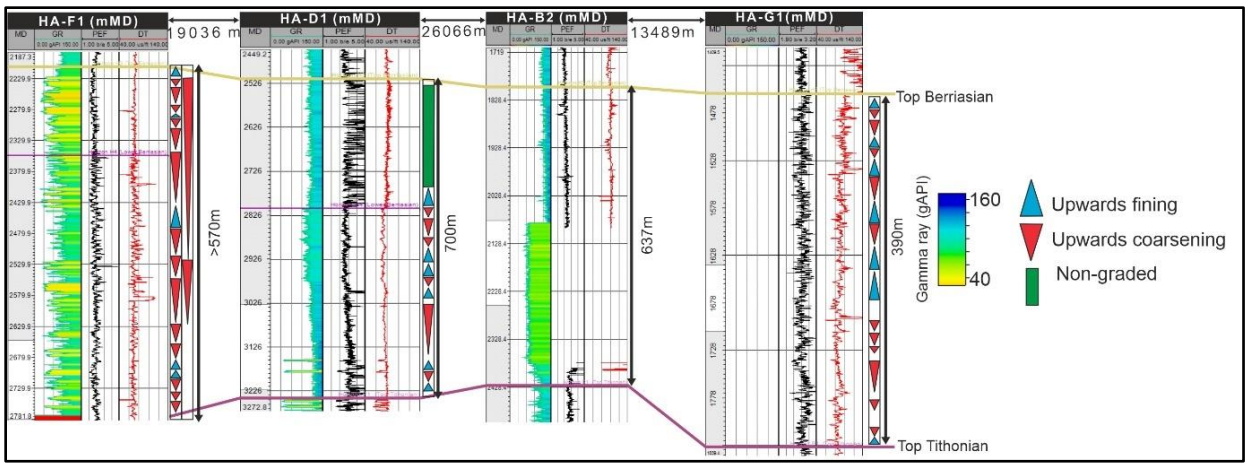

Figure 6.5: Post-Tithonian to upper Berriasian wireline correlation based on boreholes HA-F1, HA-D1, HA-B2 and HA-G1 in the Gamtoos Basin (for boreholes location, see Figure 3.3).

6.2.1.4 Post-Berriasian to Upper Valanginian

This interval is fully logged in boreholes HA-I1 and HA-B2, while only partially logged in boreholes HA-G1 and HA-A1 (Figure 6.6). In borehole HA-I1, a ~570-m-thick succession was intersected, consisting of aggrading and coarsening upwards GR readings (GR: 15 to 105 API; Figure 6.6). Borehole HA-A1 is dominated by fining-upward and coarsening trends (GR: 67 to 112 API), with 1276 to 1288 m interval described in the mudlog as porous, very fine-grained and calcareous sandstone (Figure 6.6). Borehole HA-B2 intersected a ~272-m-thick succession with coarsening-upward trends in shaly and silty facies (GR: 107 to 128 API).

The primarily coarsening-upward very fine-grained to silty facies in boreholes HA-I1 and HA-G1 suggests either mouth bars, deltas or shoreface deposits in a shallow marine setting. Borehole HA-A1 shows fining-upward silty sands changing to a coarsening upwards very fine-grained sand, suggesting increasing sedimentation rates and a change from a transgressive to a regressive shoreline. Borehole HA-B2 shows very low sand-to-shale ratio, which could indicate marine (likely deep marine) deposits, where sand input is low.

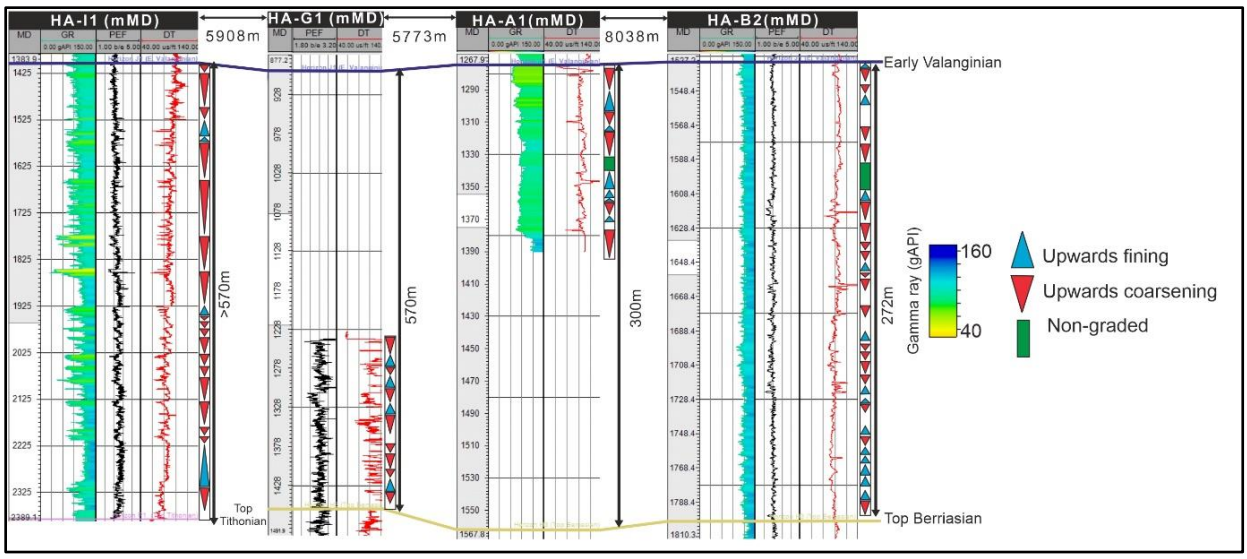

Figure 6.6: Post-Tithonian/Berriasian to lower Valanginian N-S wireline correlation based on boreholes HA-I1, HA-G1, Ha-A1 and Ha-B2 in the Gamtoos Basin (for boreholes location, see Figure 3.3).

Borehole HA-J1 is dominated by a ~330-m-thick clay- and shale-rich unit that is sand free (GR: 107-142 API), while borehole HA-D1 is dominated by a ~500-m-thick, aggrading sandy and silty unit (GR: 30-95 API; Figure 6.7). Moreover, the uppermost 50 m in borehole HA-D1 intersected two cycles of coarsening-upward clean sands (GR: 20-45 API) separated by a flooding surface. Borehole HA-B2 is dominated by a ~375-m-thick unit of clean shales/clays (GR: 45-120 API) without any sand content. Alternating, upwards-fining and coarsening silty sands dominate in boreholes HA-G1 and HA-I1 over a thickness of 240 and 657 m and with GR values of 69-104 and 50-125 API, respectively (Figure 6.7).

Borehole data from the upper Valanginian succession is dominated by fine-grained sediments typical in low-energy settings, with some coarsening-upward sands observed in boreholes HA-D1 and HA-I1. These coarsening-upward sands could represent shallow marine shoreface sands. Generally, borehole data suggests a shallow to deep marine setting during the late Valanginian, with very low sand-to-shale ratio.

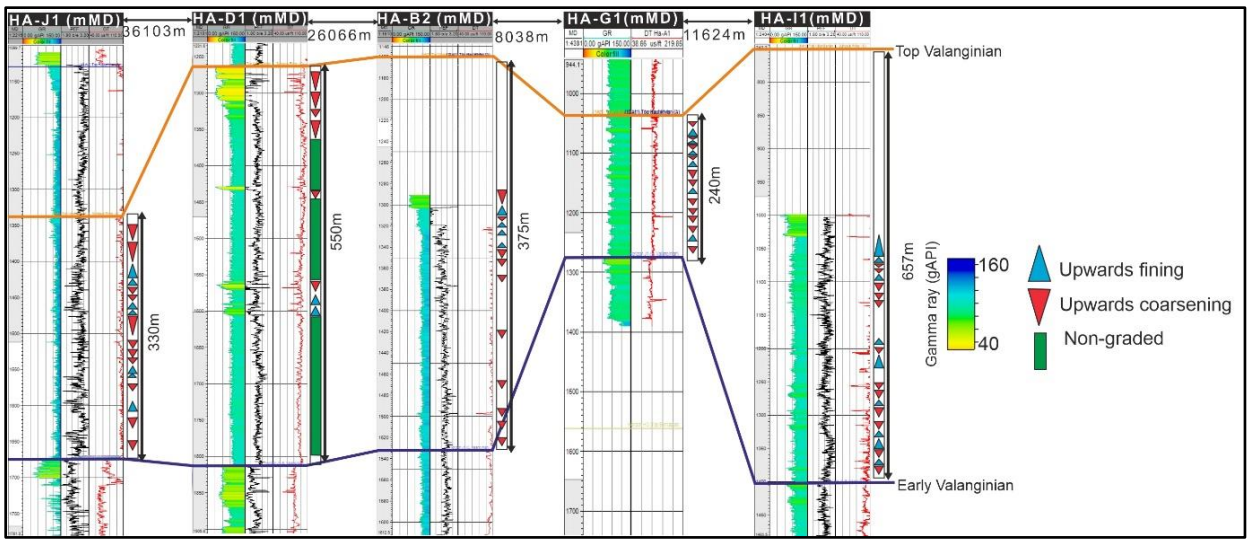

Figure 6.7: Lower to upper Valanginian W-E wireline correlation based on boreholes HA-J1, HA-D1, HA-B2 and HA-I1 in the Gamtoos Basin (for boreholes location, see Figure 3.3).

6.2.1.5 Post-Valanginian to upper Hauterivian

The Hauterivian succession is captured in boreholes HA-J1 (~208 m-thick, GR: 92 -143 API) and HA-D1 (~600-m-thick, GR: 35-105 API), which intersected a predominantly silty to shaly succession that shows coarsening-upward trend (Figure 6.8). In borehole HA-J1, this succession shows low-energy facies that lacks sandy interbeds and thus was probably deposited when the basin was still experiencing marine condition during the early Hauterivian before the late Hauterivian/Aptian uplift and erosion (Figure 6.8). Borehole HA-D1 also shows low-energy facies (likely shallow marine) dominated by alternating coarsening- and fining-upwards units, which suggest frequent transgressions and regression of the shoreline during this interval.

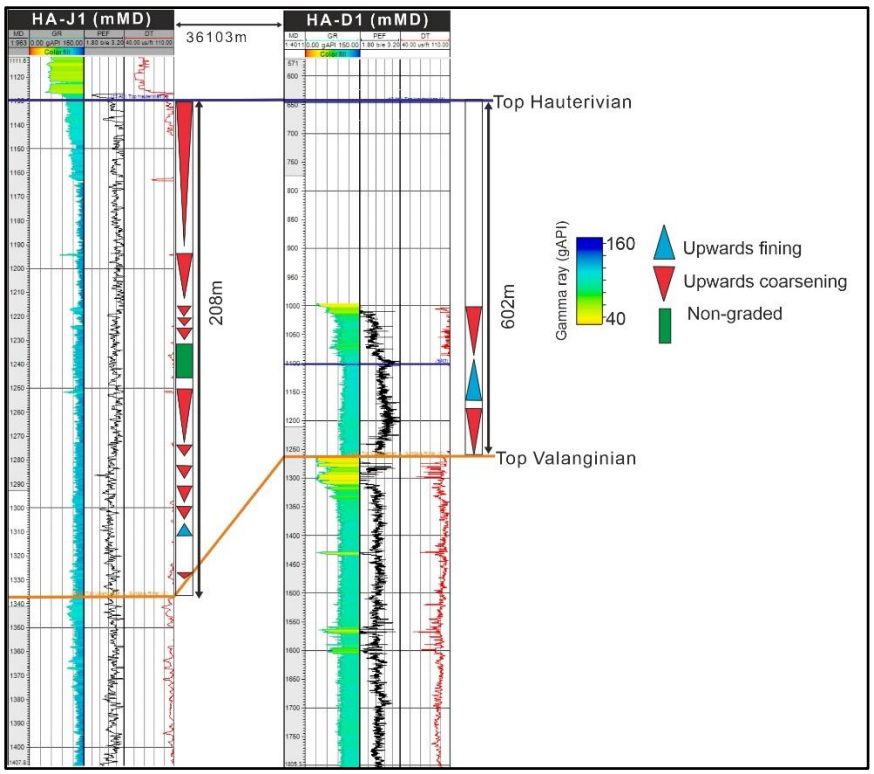

Figure 6.8: Post-Valanginian to upper Hauterivian succession intersected by boreholes HA-J1 and HA-D1, suggesting a low-energy marine setting (for boreholes location, see Figure 3.3).

6.2.1.6 Post-Hauterivian to Holocene

Wireline data for the successions between the Top Hauterivian to Holocene reflectors is only available in borehole HA-A1 (Figure 6.9a-f), which has no archived core or cuttings. This interval marks a period when the basin underwent a change in tectonics from transitional to drift phase, and when fully marine conditions became dominant (Malan et al., 1990; Bate and Malan, 1992; McMillan et al., 1997; Paton and Underhill, 2004). The general trend from the Hauterivian to the Holocene seafloor is a decrease in GR readings (Figure 6.9a-f), and an overall coarsening-upward trend from the post-Hauterivian to Holocene, indicating increased sedimentation rates on the Gamtoos Basin shelf. The limited observations that could be recorded for this interval are summarised in Table 6.1.

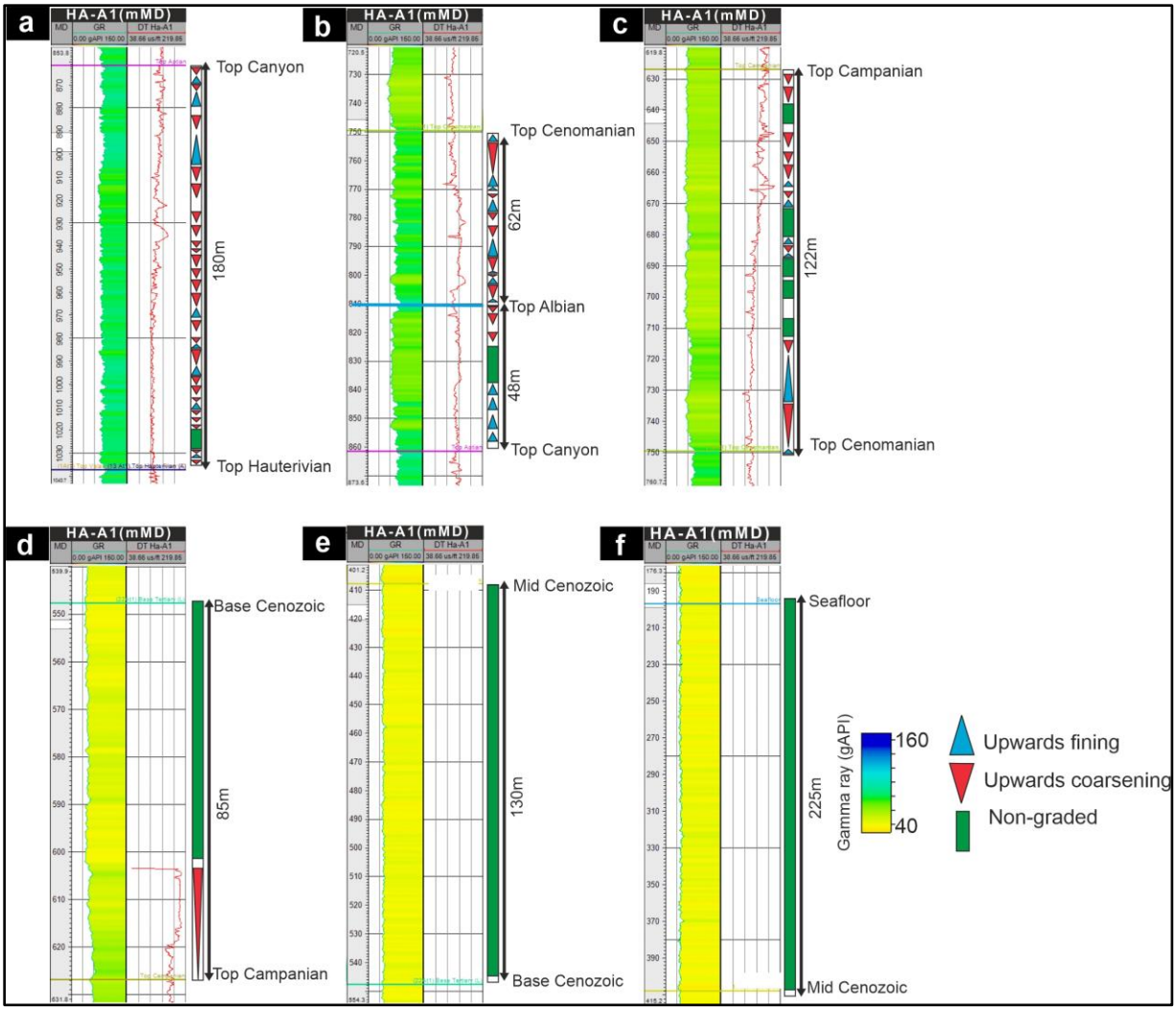

Figure 6.9: Top Hauterivian to Seafloor (Holocene) wireline logs based on borehole Ha-A1 in the Gamtoos Basin. **a** Top Hauterivian to Top Canyon; **b** Top Canyon to Top Cenomanian; **c** Top Cenomanian to Top Campanian; **d** Top Campanian to Base Cenozoic; **e** Base Cenozoic to Mid-Cenozoic; **f** Mid-Cenozoic to Seafloor (for borehole location, see Figure 3.3).

Table 6.1: Top Hauterivian to Seafloor (Holocene) wireline summary based on borehole HA-A1.

Stratigraphic interval	GR values (API)	Summary of vertical grain size trends
Mid-Cenozoic to Seafloor	30–40	Alternating coarsening- and fining-upward as well as non-graded units. Overall, appears to be non-graded
Base Cenozoic to Mid-Cenozoic	34–40	Mostly non-graded successions, with fining-upward units at the base and a few coarsening-upward units at the top
Top Campanian to Base Cenozoic	40–65	Coarsening-upward unit at the base, overlain by a non-graded unit
Top Cenomanian to Top Campanian	45–70	Coarsening- and fining-upward as well as non-graded units
Top Albian to Top Cenomanian	60–90	Coarsening- and fining-upward as well as non-graded units
Top Canyon to Top Albian	70–94	Non-graded unit (low GR)
Top Hauterivian to Top Canyon	92–143	Non-graded unit (low GR)

6.2.2 Surface and thickness map

6.2.2.1 Pre-Aalenian to upper Valanginian

The succession between the Basement D to Holocene reflector is a ~8000-m-thick sediments package in the Gamtoos Basin that is confined to a N-S striking depocenter (Figure 6.9a). The lower most succession, which is between Basement D to Top Kimmeridgian reflectors, also shows a N-S strike orientation and attains a maximum thickness of 3000 m (Figure 6.9b). The Tithonian succession attains a maximum thickness of 900 m and has a N-S striking depocenter (Figure 6.9c). The Berriasian succession is 1400-m-thick and its depocenter is in the NW part of the basin where it strikes in NW-SE direction (Figure 6.9d). The lower Valanginian depocenter also shows a NW-SE strike and attains a maximum thickness of 1400 m (Figure 6.9e). Unlike the underlying stratigraphic units, the Top Valanginian is not limited or bound by the Gamtoos Fault towards the west, and instead, this surface appears to be regional, extending into the Algoa Basin as well. The upper Valanginian succession has a NW-SE striking depocenter, and while it attains a maximum thickness of 3500 m in few places, its average thickness is ~1030 m (Figure 6.9f).

The Kimmeridgian to Tithonian depocenter shows a dominant N-S strike, indicating that the rates of accommodation space increase were higher closer to the N-S trending segment of the Gamtoos Fault. However, from the late Tithonian/Berriasian the orientation of the depocenter assumes a NW-SE strike, located towards the proximal part of the fault. This change in orientation indicates increased rates in accommodation space along the NW-SE segment of the Gamtoos Fault, and a decrease in the rates of accommodation space creation in the S.

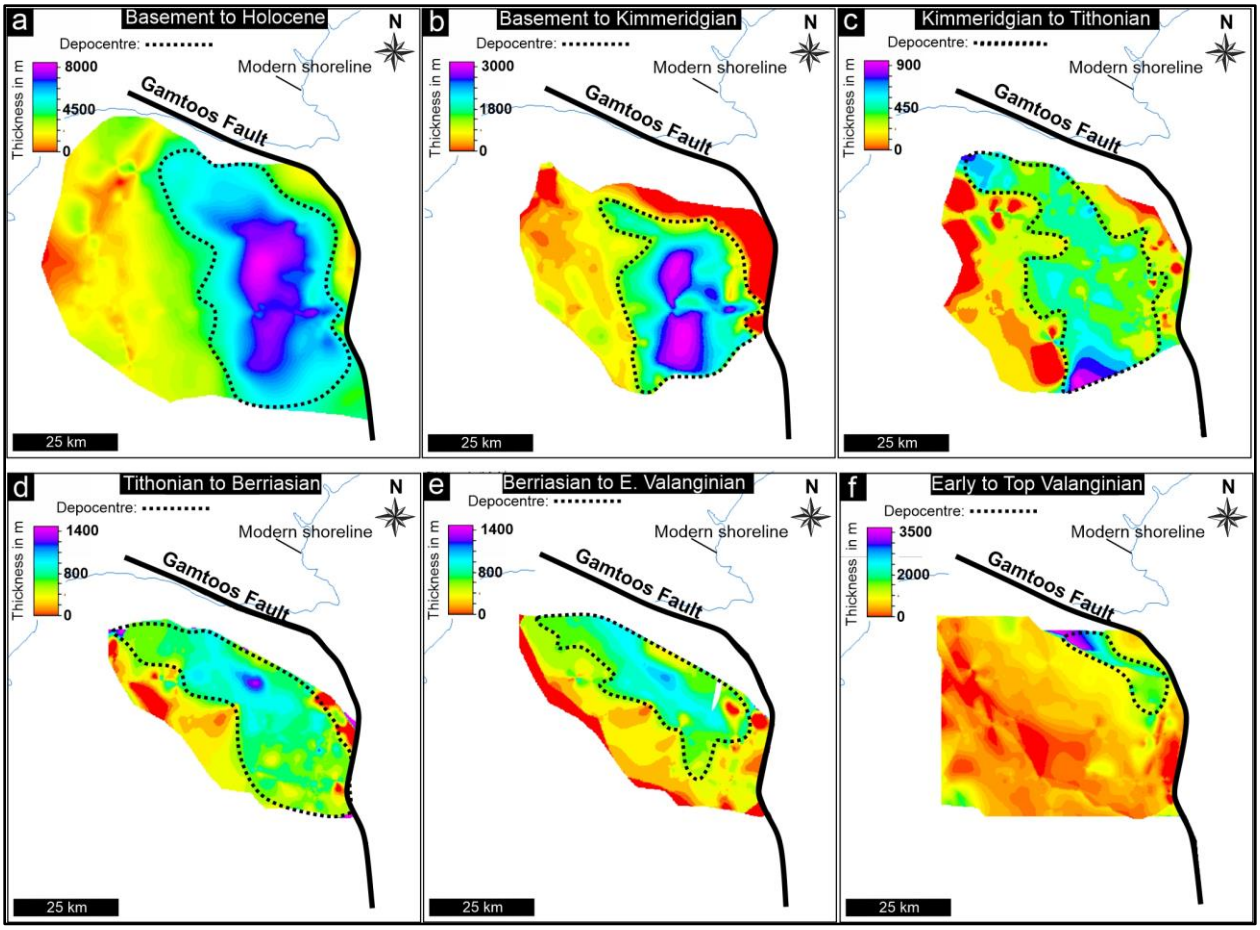

Figure 6.10: a Thickness map from syn-rift to Holocene, highlighting the main depocenters during basin infill. **a** Isopach map from the Basement to Holocene succession. **b** Pre-Aalenian to Kimmeridgian thickness map, showing a dominant N-S striking depocenter. **c-f** NW-SE striking depocenter from the Tithonian to Top Valanginian.

6.2.2.2 Post-Valanginian to lower Albian

In the Gamtoos Basin, the main accommodation space for the Hauterivian succession is situated near the Gamtoos Anticline (Figure 6.11a; Thomson, 1999). The NW-SE striking major depocenter towards the NE attains a maximum thickness of 1800 m (Figure 6.11a). The main Hauterivian depocenter is located in the Gamtoos Syncline, which formed due to a late Valanginian to early Hauterivian tectonic inversion (Thomson, 1999). Folding that resulted from the inversion created accommodation space for the Hauterivian succession. In contrast to the Algoa Canyon, the Gamtoos Canyon is smaller, and has a maximum thickness of 700 m, with a NW-SE striking depocenter (Figure 6.11b). The lateral extent of the Gamtoos Canyon relative to the Algoa Canyon suggest that the uplift in the Gamtoos Basin was less severe relative to the Algoa Basin, probably influenced by the Gamtoos Anticline, which also allowed the preservation of the Hauterivian successions in the Gamtoos Basin.

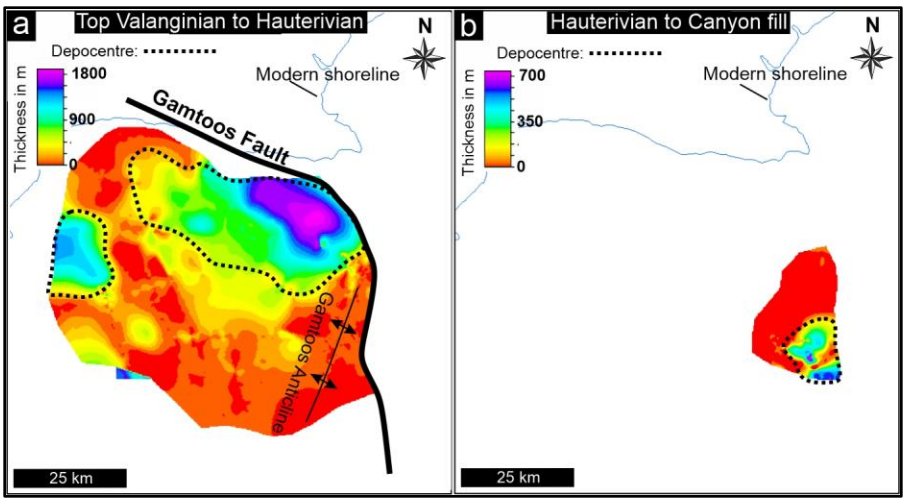

Figure 6.11 a-b Transitional phase thickness maps representing sediments deposited in the Gamtoos Basin from the Hauterivian to early Albian. The Hauterivian depocenter is controlled by the geometry of the Gamtoos Anticline.

6.2.2.3 Albian to Holocene

Although there is not much lateral thickness change on the shelf during the Albian, the depocenter appear to have a NE-SE strike, with average thickness of ~200 m and maximum thickness of 1200 m (Figure 6.12a). Top Cenomanian depocenters are orientated at N-S and W-E, and attain maximum thickness of 350 m (Figure 6.12b). Notwithstanding that within the Campanian succession the thickness does not vary significantly across the shelf, there is still evidence of a subtle depocenter towards the S, which has a maximum thickness of 900 m (Figure 6.12c). The Upper Cretaceous succession, which is bound at the top by the Base Cenozoic (22At1) reflector does not show an obvious depocenter, and the average thickness is ~100 m (Figure 6.12d). The Lower to Upper Cenozoic succession has a NW-SE striking depocenter towards the SW and attains a maximum thickness of 400 m (Figure 6.12c). The younger Upper Cenozoic succession has an average thickness of ~200 m, increasing towards the S, closer to the shelf edge, with NE-SW striking depocenter. Unlike the syn-rift and transitional phase deposits, in which the depocenter has a dominant NW-SE strike on the shelf, the drift phase main depocenters are located towards the shelf edge/slope. The location of the depocenters suggests that on average, accommodation space was primarily higher in the slope during the drift phase.

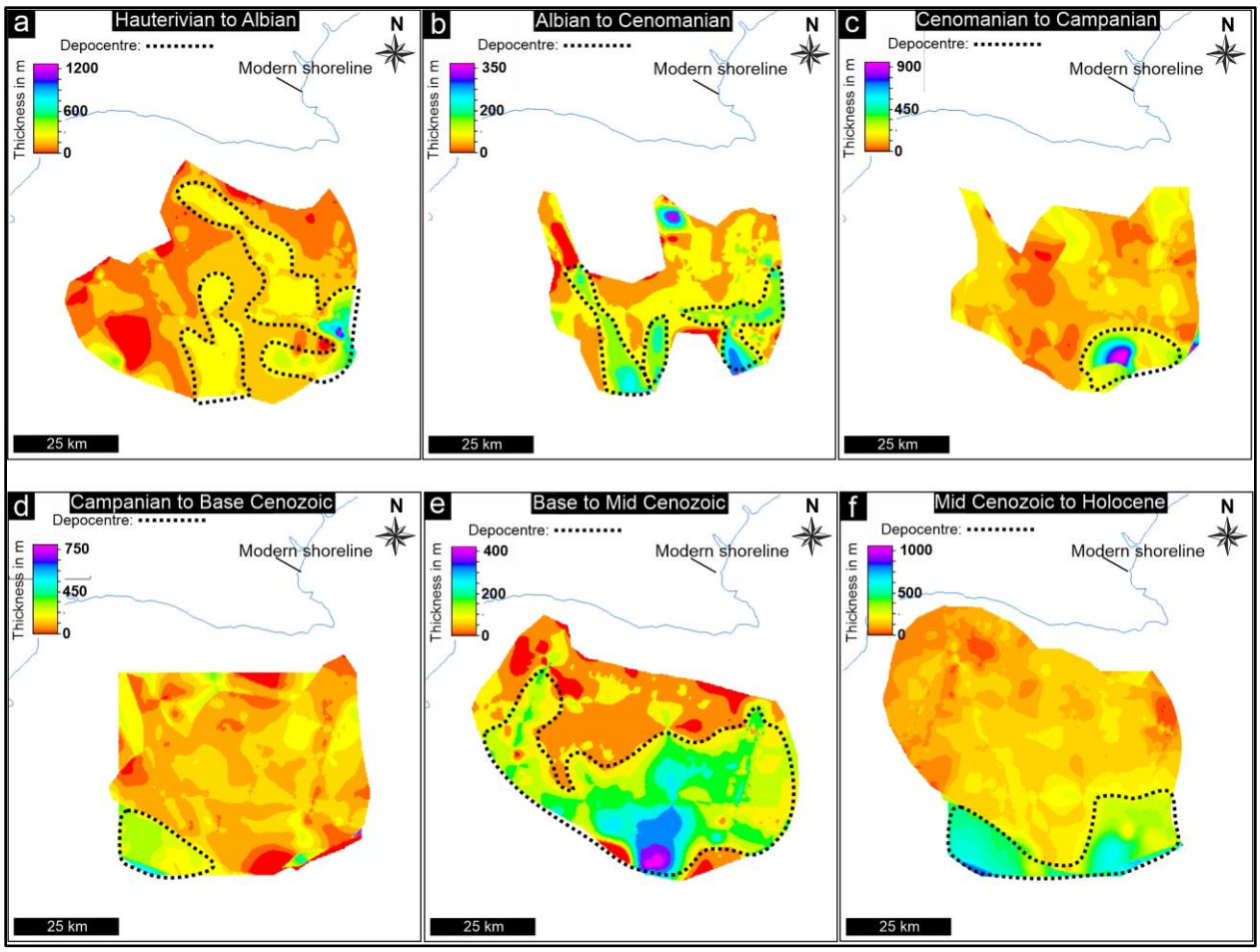

Figure 6.12: a-f Drift phase thickness maps representing sediments deposited in the Gamtoos Basin from the late Albian to Holocene. Drift-phase depocenters are located mainly towards the shelf edge.

6.2.3 Seismic interpretation

6.2.3.1 Pre-Aalenian to upper Kimmeridgian

Unlike in the Algoa Basin, the syn-rift succession is well preserved in the Gamtoos Basin, and shows thickening and folding towards the Gamtoos Fault, in addition to westward pinching near borehole HA-J1 (Figure 6.13A-A', E-E'). There is also evidence of clinoforms prograding from the W towards the Gamtoos Fault (Figure 6.13B-B'). This prograding succession is overlain by dimming chaotic reflectors, which are then overlain by subparallel and continuous reflectors of the upper Kimmeridgian succession (Figure 6.13B-B'). During this interval the fault has a smaller offset relative to the overlying succession (Figure 6.13D-D').

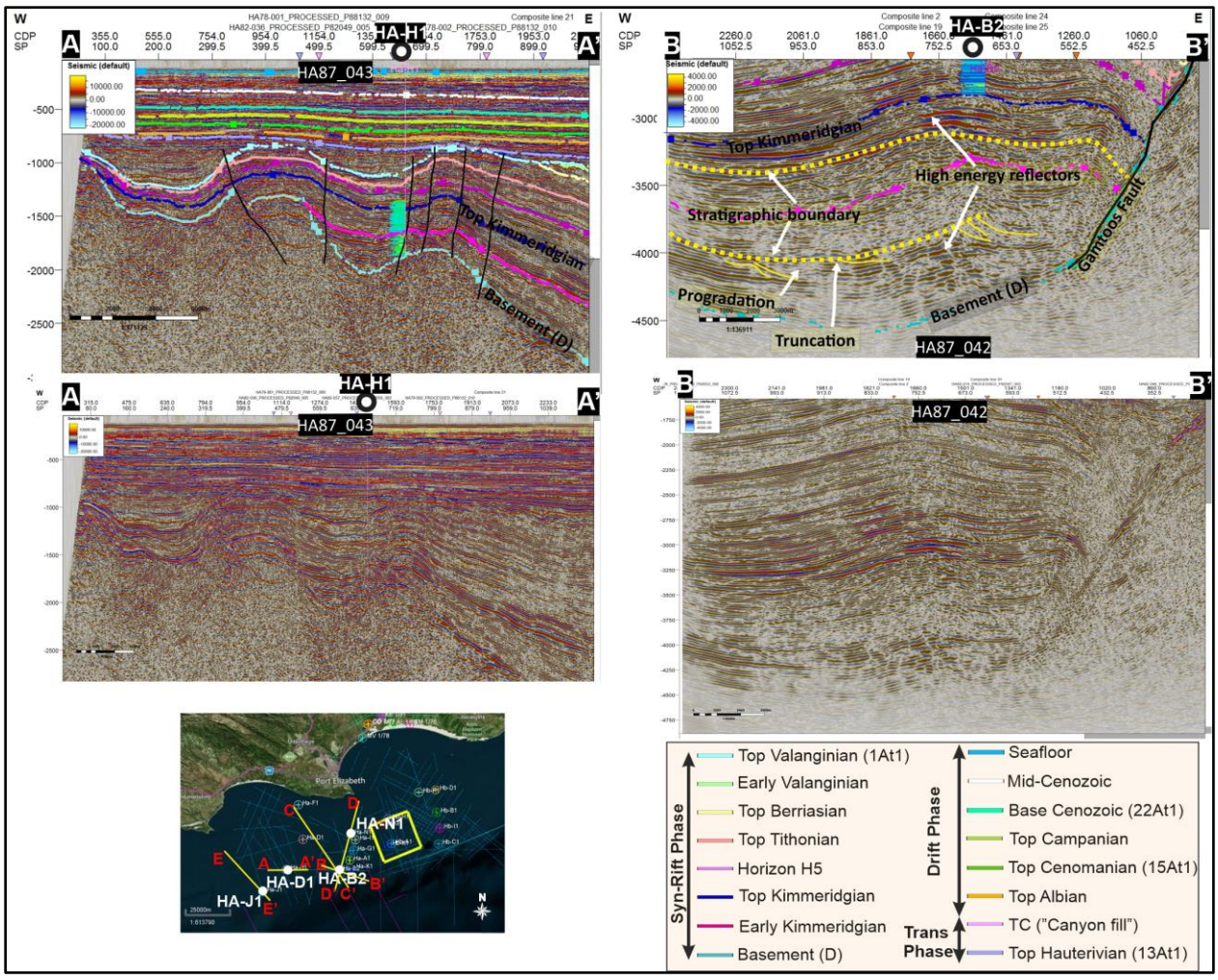
HA-H1
HA87_043
Top Kimmeridgian
Basement (D)
HA-B2
Top Kimmeridgian
High energy reflectors
Stratigraphic boundary
Gamtoos Fault
Progradation
Truncation
Basement (D)
HA87_042
HA-N1
HA-D1
HA-J1
Port Elizabeth
Top Valanginian (1At1)
Early Valanginian
Top Berriasian
Top Tithonian
Horizon H5
Top Kimmeridgian
Early Kimmeridgian
Basement (D)
Syn-Rift Phase
Seafloor
Mid-Cenozoic
Base Cenozoic (22At1)
Top Campanian
Top Cenomanian (15At1)
Top Albian
TC ("Canyon fill")
Top Hauterivian (13At1)
Drift Phase
Trans Phase

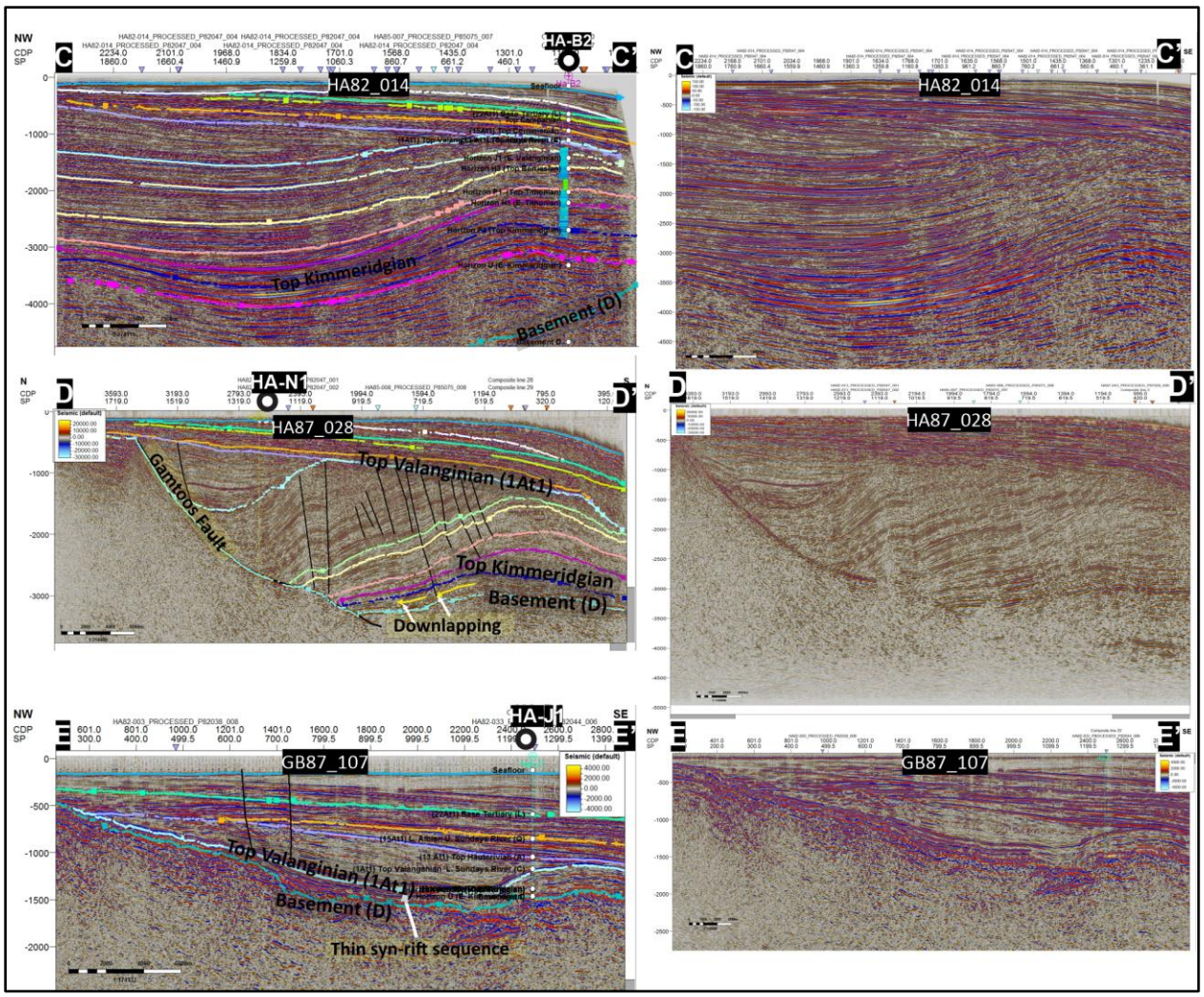

Figure 6.13: A-A' Kimmeridgian succession pinching towards the west. **B-B'** Prograding and truncated reflectors in the Middle Jurassic. **C-C'** Parallel and continuous reflectors in the NW-SE direction. **D-D'** N-S cross-section along the Gamtoos Fault. **E-E'** Syn-rift sequence pitchout towards the west. Base map data ©2020 Google, Maxar Technologies, AfriGIS (Pty) Ltd.

6.2.3.2 Post-Kimmeridgian to upper Tithonian

Although this succession is poorly imaged in some parts of the Gamtoos Basin, the Tithonian reflectors are bright, parallel and laterally continuous (Figure 6.14A-A'). In the W-E direction, the base Tithonian reflectors onlaps on the Top Kimmeridgian reflector (Figure 6.14A-A'). This succession also shows thinning towards the W and seems to be truncated by the 1At1 reflector (Figures 6.13A-A' and 6.14B-B'). Moreover, folding (which is likely early Hauterivian) of the Tithonian succession near the Gamtoos Fault defines the Gamtoos Anticline (Figure 6.13B-B'; Thomson, 1999).

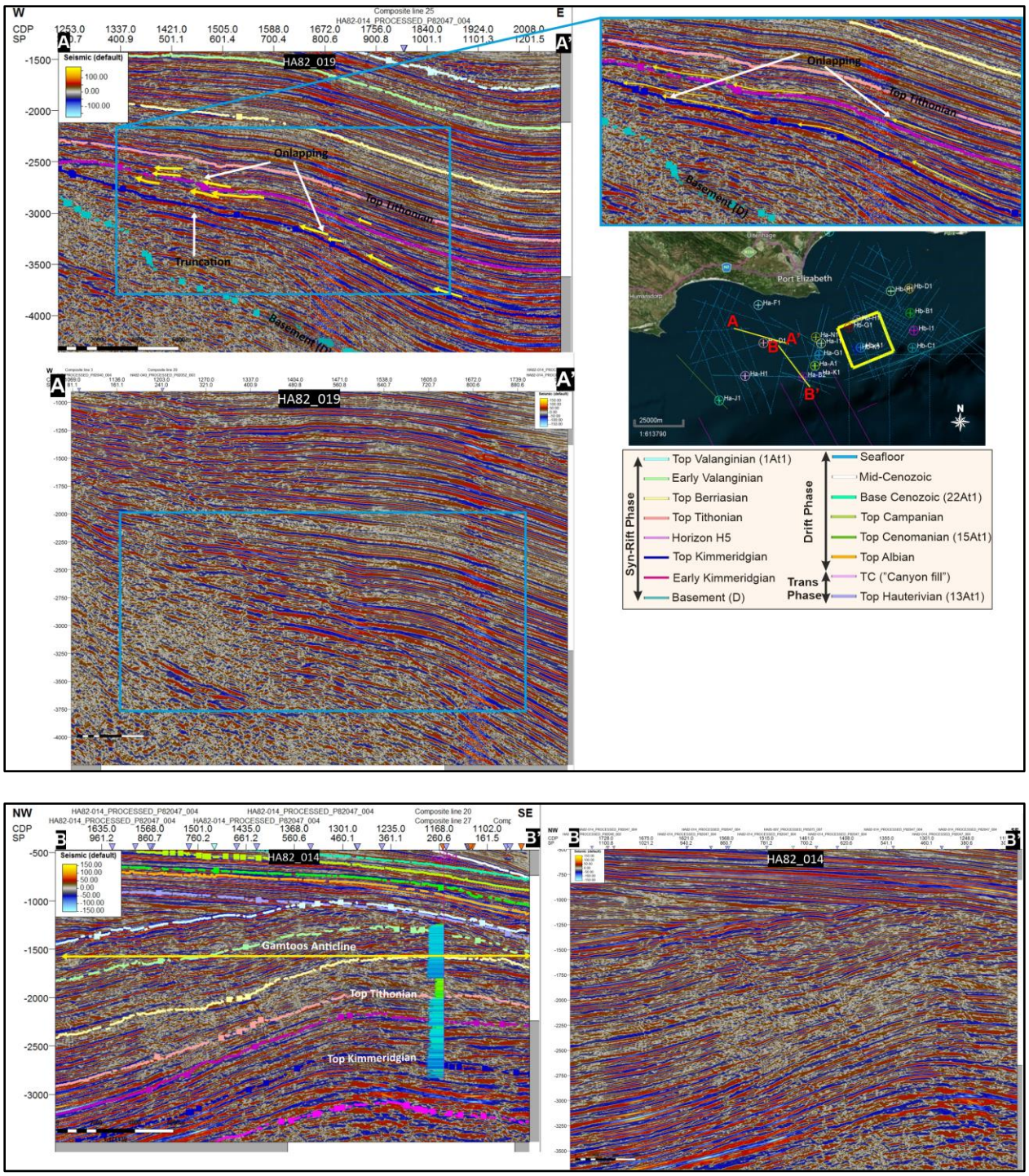

Figure 6.14: A-A' Post-Kimmeridgian to upper Tithonian succession, showing onlapping geometries on the Top Kimmeridgian reflector. **B-B'** Tithonian succession forming part of the Gamtoos Anticline. Base map data ©2020 Google, Maxar Technologies, AfriGIS (Pty) Ltd.

6.2.3.3 Post-Tithonian to upper Berriasian

The base of the Berriasian succession onlaps on the underlying Top Tithonian reflector (Figure 6.15A-A', B-B'). Similar to the underlying successions, the Berriasian succession is also folded, especially near the Gamtoos Fault (Figure 6.15B-B'). Some seismic lines show evidence of incised geometry (Figure 6.15A-A'). Although the Berriasian succession reflectors are mostly parallel and discontinuous, the Top Berriasian reflector appears to be truncational in some places (Figure 6.15C-C'). Towards the W, this succession is also truncated by the 1At1 reflector (Figure 6.13A-A').

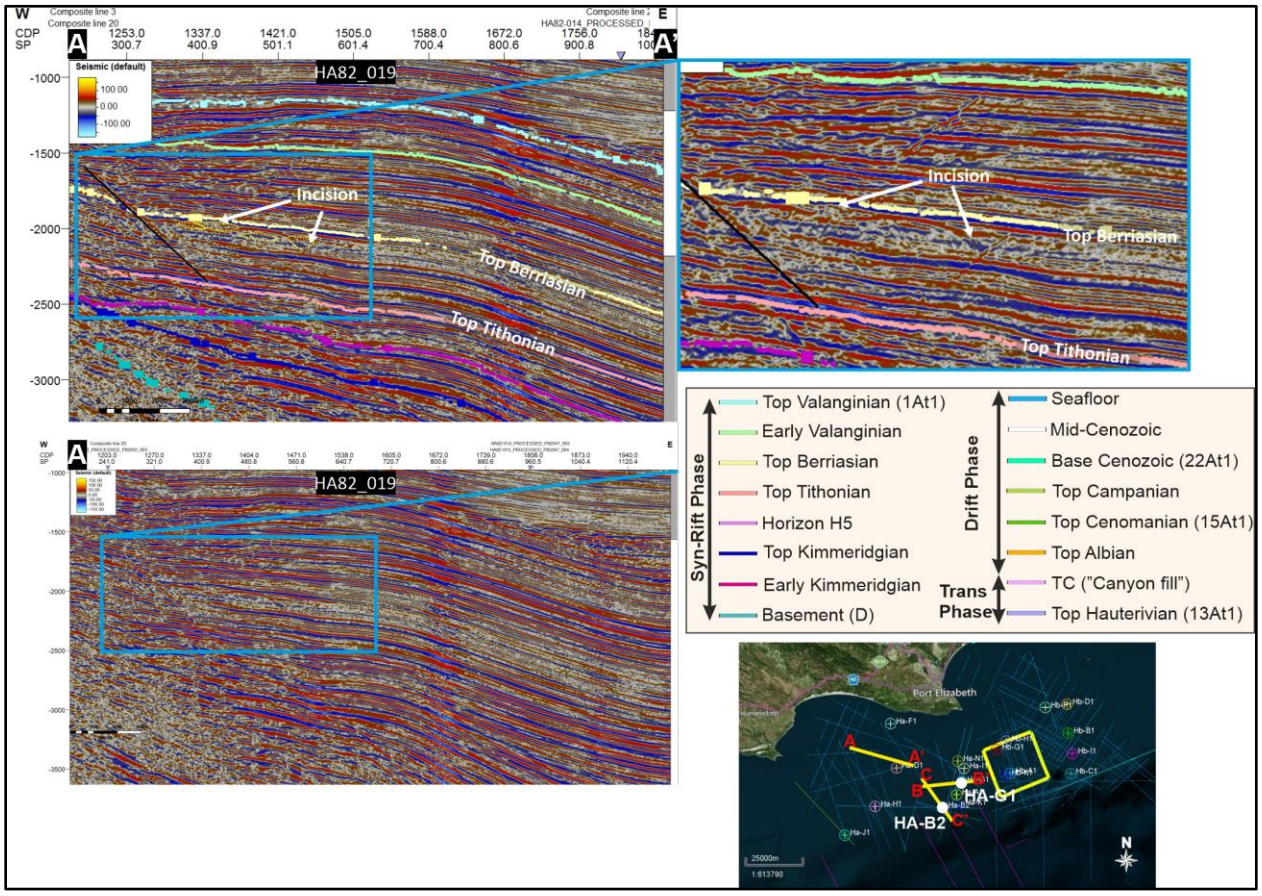

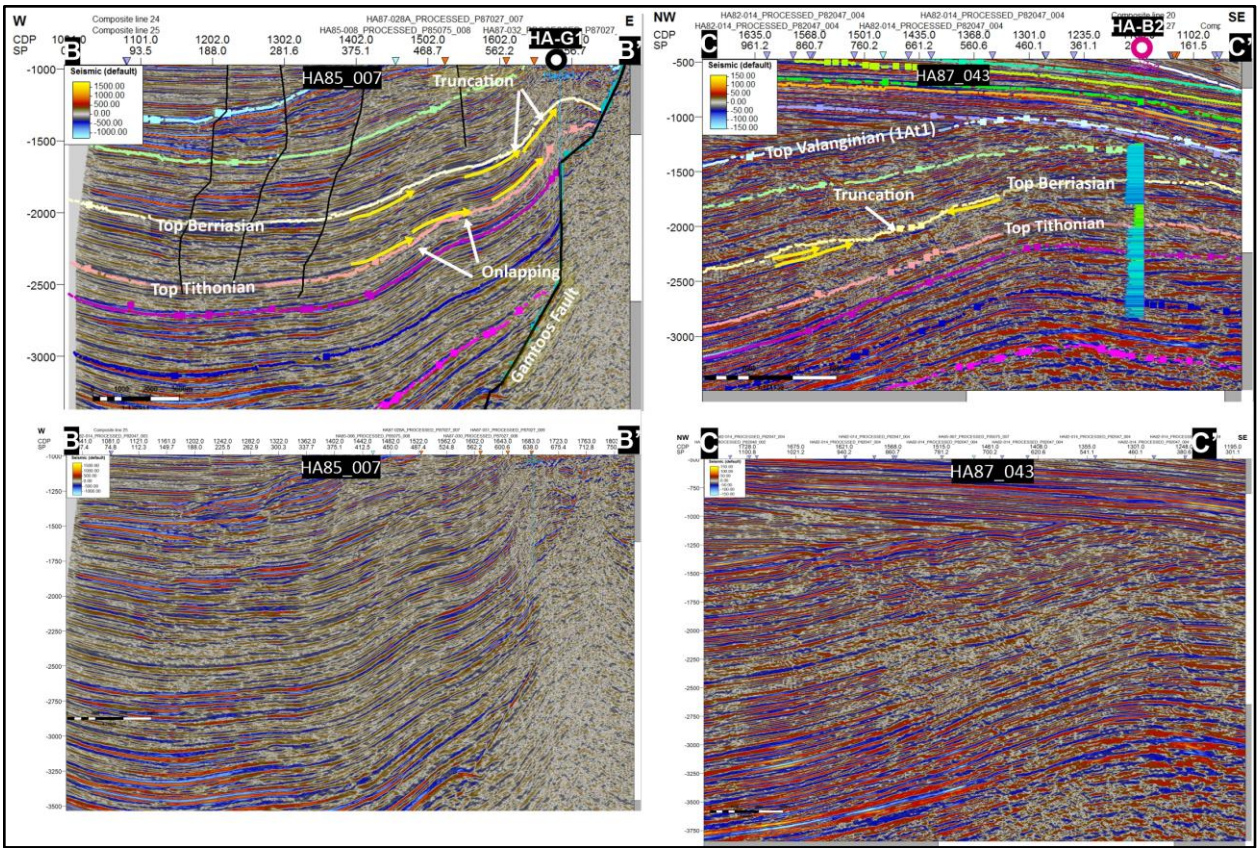

Figure 6.15: A-A' Post-Tithonian to upper Berriasian succession showing incised geometries near the top of the succession. **B-B'** Onlapping nature of the Kimmeridgian to Tithonian succession. **C-C'** The Top Berriasian reflector showing evidence of truncation. Base map data ©2020 Google, Maxar Technologies, AfriGIS (Pty) Ltd.

6.2.3.4 Post-Berriasian to upper Valanginian

The Top Berriasian to early Valanginian reflectors are subparallel, continuous and brighter (high energy) relative to the underlying reflectors (Figure 6.16A-A'). The base of the lower Valanginian succession onlaps on the Top Berriasian reflector (Figure 6.16B-B'), a common feature in these syn-rift successions. Furthermore, in the N-S cross-section, this succession increases in thickness closer to the Gamtoos Fault.

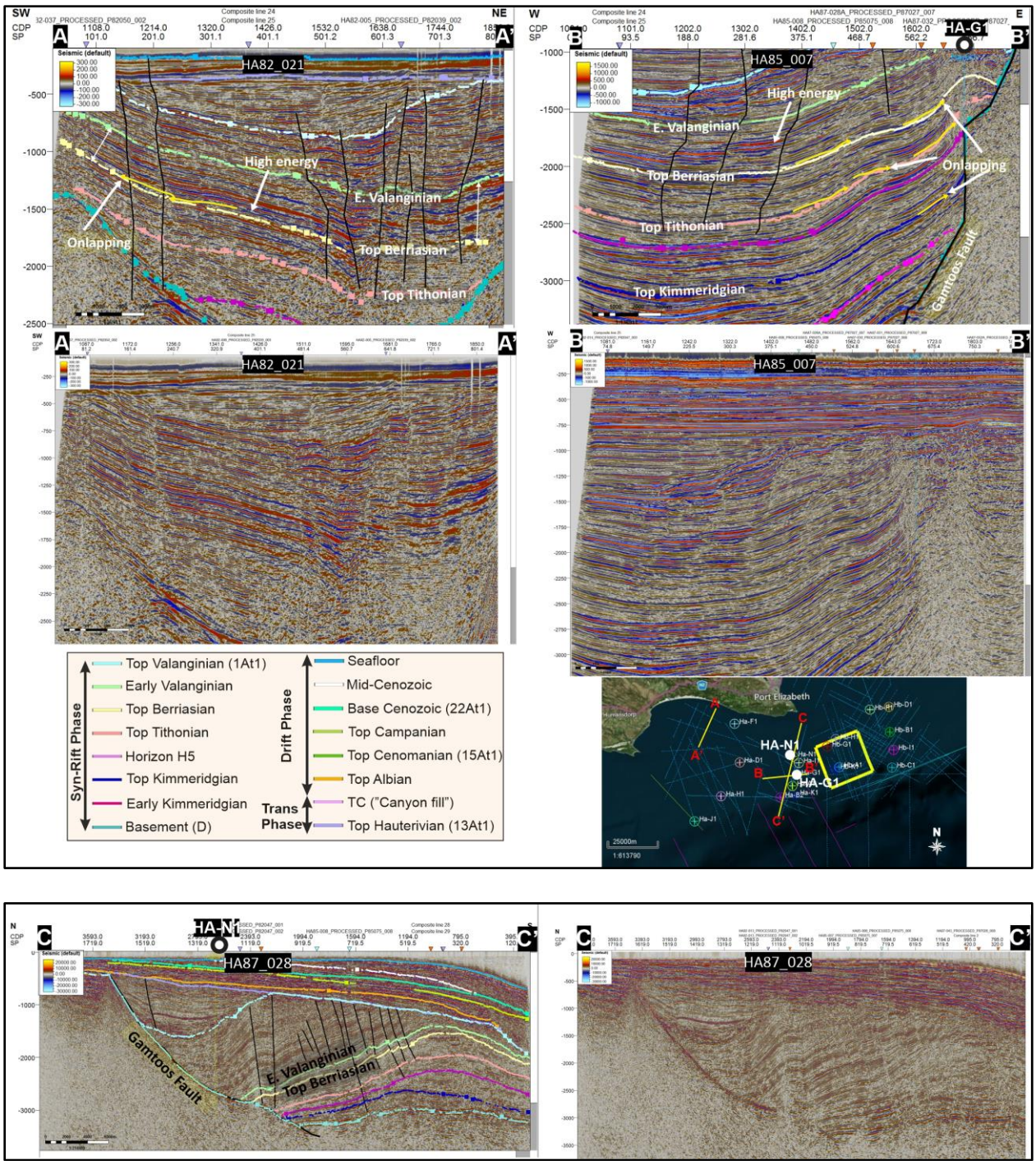

Figure 6.16: A-A', B-B' Lower Valanginian succession onlapping on the Top Berriasian reflector. **c** Faulting appear to be affecting this succession more than the underlying stratigraphy.

The Top Valanginian reflector (1At1) truncates the underlying syn-rift reflectors at the acute angle, especially in the W (in the tilted hanging walls) and N (Figures 6.1 and 6.13A-A', B-B'). The Valanginian succession is also truncated by the Top Hauterivian (13At1) surface, especially in the S near the Gamtoos

Anticline (Figure 6.17A-A'). This severely faulted succession also shows thinning towards the W and onlapping stratal terminations in W-E cross-sections (Figure 6.17A-A', C'-C).

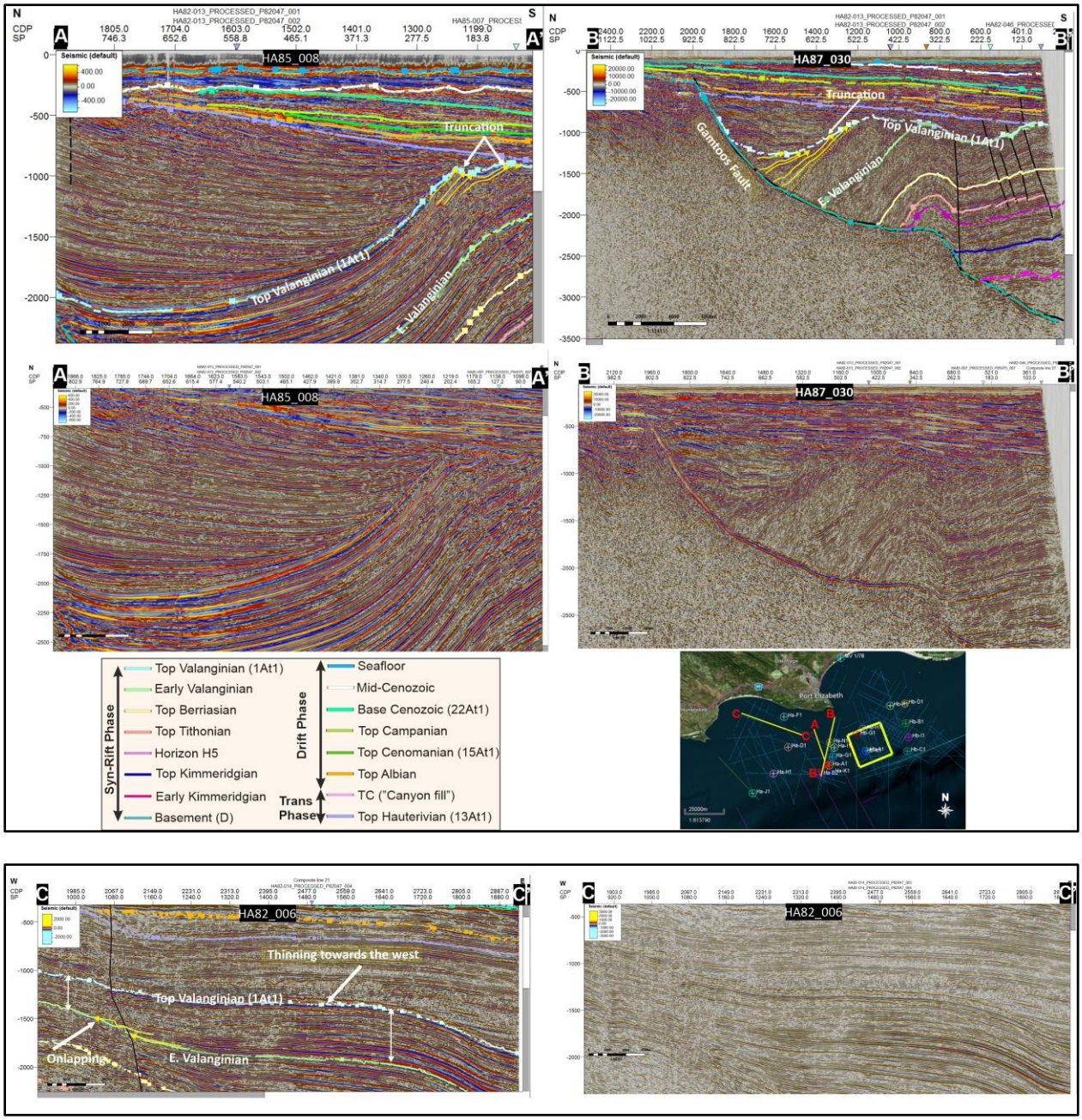

Figure 6.17: A-A' Top Valanginian reflector truncating underlying succession. **B-B'** The upper Valanginian succession thinning towards the west. **C-C'** N-S cross-section showing termination nature of the Top Valanginian reflector against the underlying stratigraphy. Base map data ©2020 Google, Maxar Technologies, AfriGIS (Pty) Ltd.

The syn-rift successions in the Gamtoos Basin shows similar architecture and depositional geometries to that in the Algoa Basin, except for the basal pre-Kimmeridgian successions, which shows evidence of

progradation from the W. Since progradation in a nearshore depositional context, is typically a transitional to marine process, prograding clinoforms are taken as evidence for a pre-Kimmeridgian marine incursion in the Gamtoos Basin (Figure 6.13). However, progradational units are eroded at the top, indication a period where the shoreline shifts basinwards (Figure 6.13). Moreover, the sequence boundary truncating the prograding clinoforms is the only evidence of subaerial unconformity observed in the syn-rift succession in the available dataset. The post-Kimmeridgian syn-rift sequences are dominated by onlapping stratal geometries at the base of stratigraphic unit (i.e., Top Tithonian, Top Berriasian). These onlapping stratal terminations can be used to infer landwards migrating shoreline in a shallow marine setting, probably as response of increased accommodation space during the displacement of the Gamtoos Fault. This increasing accommodation space is evident from the larger sediment thicknesses near the Gamtoos Fault implying increased accommodation towards the E, closer to the Gamtoos Fault. On the other hand, the thinning of the succession towards the W shows the depositional limit of the syn-rift sequence. The erosional features observed at the top of these stratigraphic units (i.e., Top Tithonian, Top Berriasian) appear to be localised in few places, without obvious features to suggests subaerial unconformities (e.g., truncation over several seismic lines, change in dip of the seismic reflectors). Although it is recognised that subaerial unconformities could be below seismic resolution, the localised truncations suggest a submarine erosion, probably from wave scouring as the shoreline retreat landwards. The folding in this syn-rift succession is associated with the late Valanginian to early Hauterivian tectonic inversion, which resulted in the Gamtoos Anticline (Thomson, 1999). The Top Valanginian reflector marks the late syn-rift sequence (Malan et al., 1990; Bate and Malan, 1992; McMillan et al., 1997; Paton and Underhill, 2004), with Top Valanginian reflector truncating the underlying syn-rift reflectors and forming an angular unconformity between pre-Aalenian (Basement D) and Early Valanginian reflector (Figure 6.17).

6.2.3.5 Post-Valanginian to upper Hauterivian

In places where the Hauterivian succession is preserved, the reflectors are dim, parallel and semi-continuous (Figure 6.18). The basal reflectors onlap on the Top Valanginian reflector (Figure 6.18A-A') with two types of geometries: 1) the divergent onlaps in the lower section; and 2) the subparallel onlaps in the upper succession (Figure 6.18A-A'). The Hauterivian succession also shows evidence of accretional stratal geometries, especially in W-E and NW-SE cross-sections (Figure 6.18B-B',C-C'). In the proximal setting, the Hauterivian reflectors exhibit progradation from the NE to SW (Figure 6.18D-D'). Although,

relative to the Algoa Basin, this succession is better persevered in the Gamtoos Basin, the upper succession is truncated here too by the Top Hauterivian (13At1) reflector, which in some places also truncates and amalgamates with the 1At1 reflector (Figure 6.18).

In contrast to the syn-rift successions, which are folded and form the Gamtoos Anticline (Thomson 1999), this Hauterivian succession onlaps onto the Gamtoos Anticline and appears to be syn-tectonic in the lower part of the succession (6At1?; Figure 6.18A-A'). Although the stress field responsible for the formation of the Gamtoos Anticline is poorly understood (Thomson, 1999), this structural feature shows a period of inversion within the syn-rift succession that probably formed during the Hauterivian to Aptian uplift episode (see Thomson 1999 his fig. 9). The accretional stratal geometries observed might be indicative of fluvial aggradational processes as the basin was uplifted. The prograding clinoforms in the proximal setting can be used to infer a NW sediment provenance.

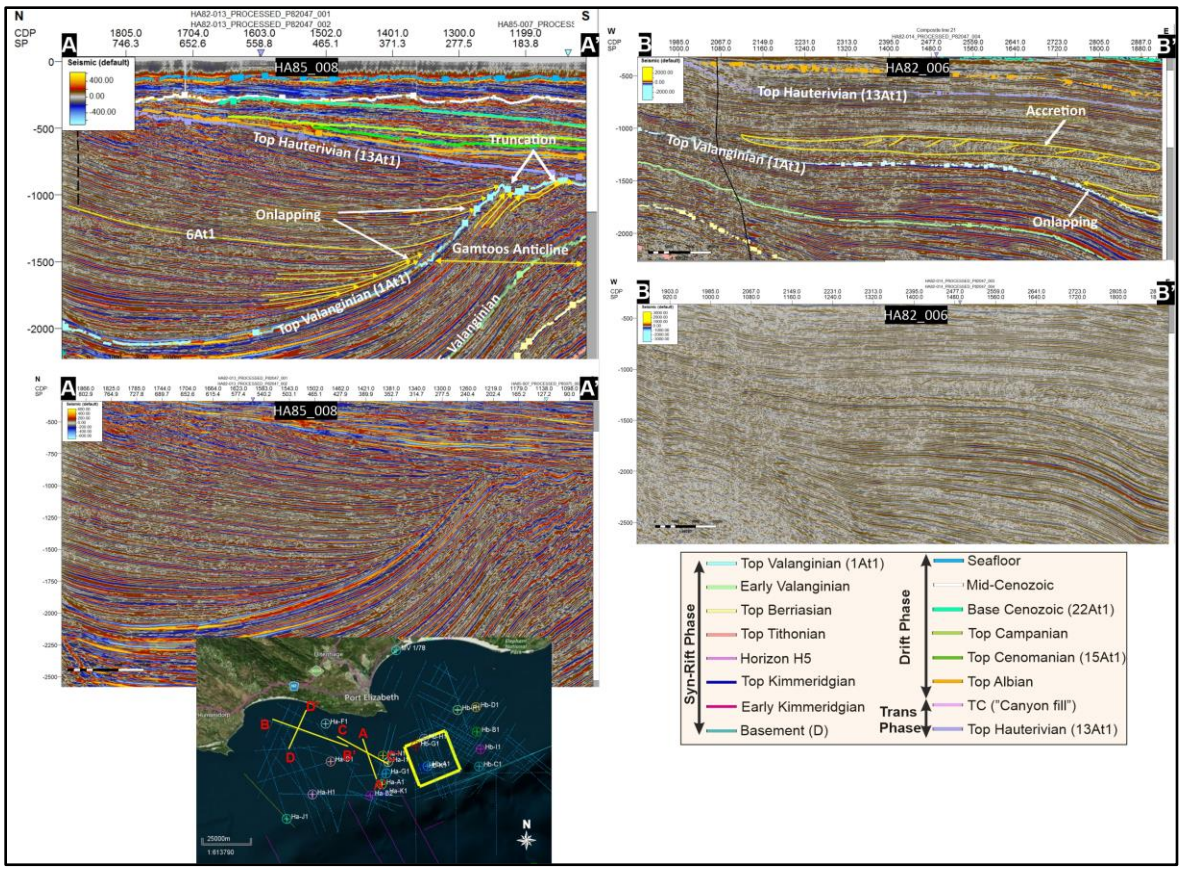

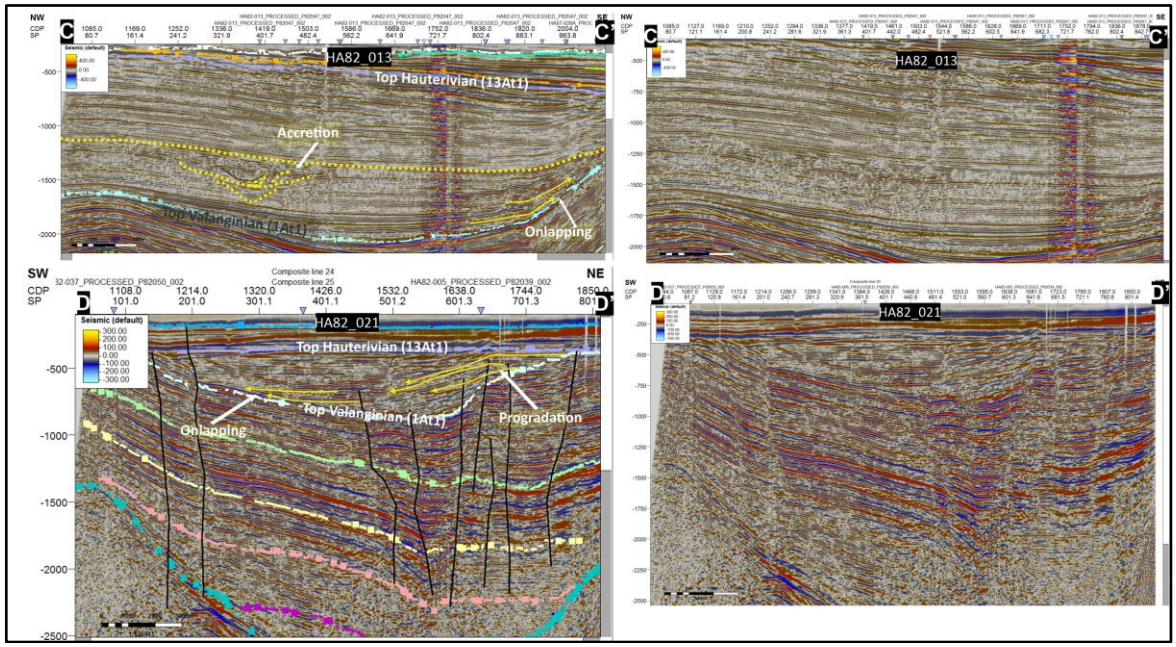

Figure 6.18: A-A' The Hauterivian succession onlapping on the 1At1 reflector. **B-B', C-C'** Accretional stratal geometries identified in the Hauterivian succession. **D-D'** Top Hauterivian reflector (13At1) truncating underlying stratigraphy. Base map data ©2020 Google, Maxar Technologies, AfriGIS (Pty) Ltd.

6.2.3.6 Post-Hauterivian to "Canyon-fill" (lower Albian)

"Canyon fill" sediments onlap onto the basal Top Hauterivian reflectors, and are overlain by eastward prograding clinoforms, in contrast to the co-eval clinoforms in the Algoa Basin, which dip to the S-SE (Figure 6.19). There is also evidence an incision, which are truncated the prograding clinoforms (Figure 6.19A-A').

Unlike the Algoa Canyon, where provenance was primarily from the N-NW, Gamtoos "Canyon fill" was sourced from the W. Moreover, the younger channel-like feature that truncated the "Canyon fill" clinoforms may be takes as evidence for increased depositional energy in the early Albian (i.e., a change from marine to fluvial setting).

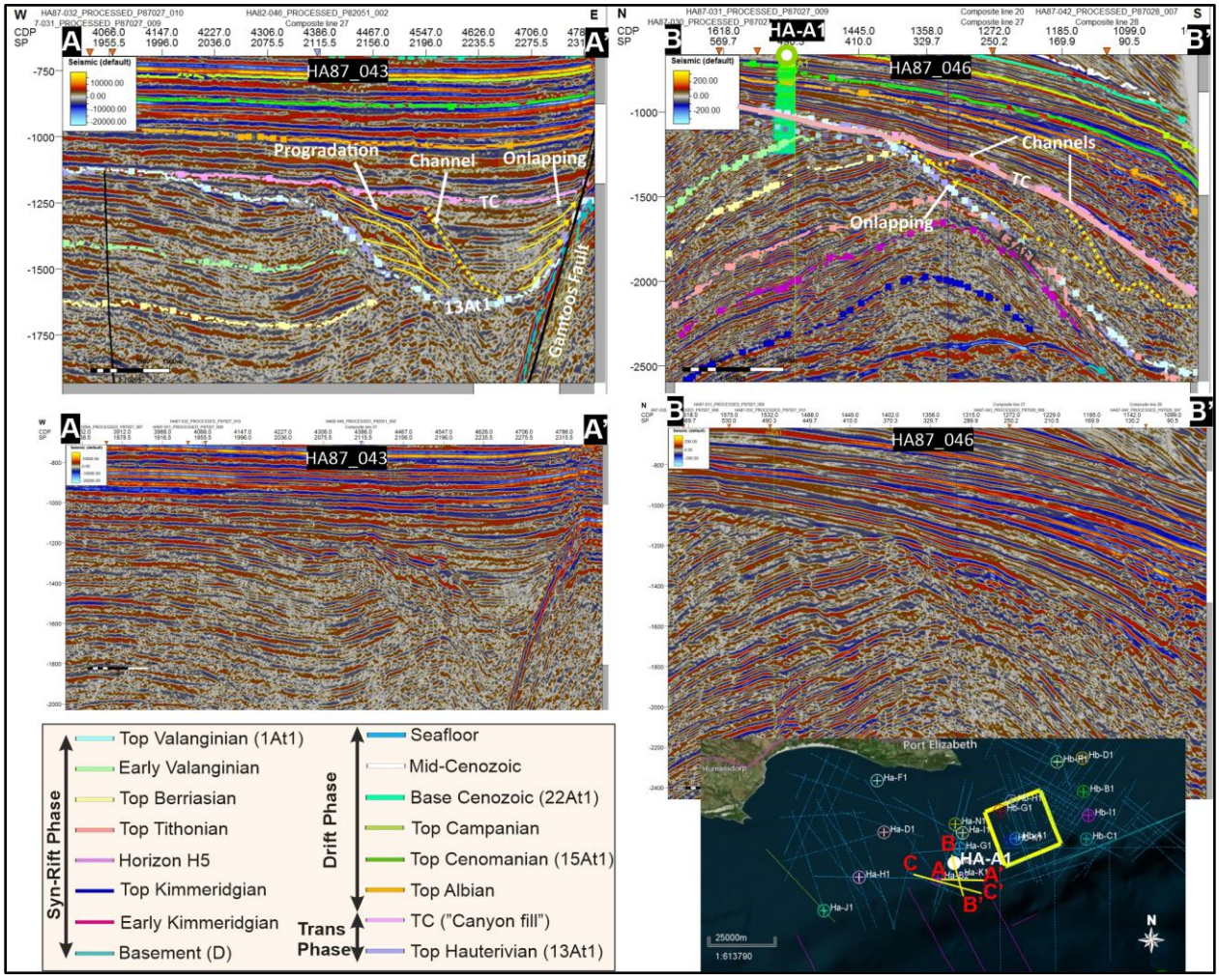

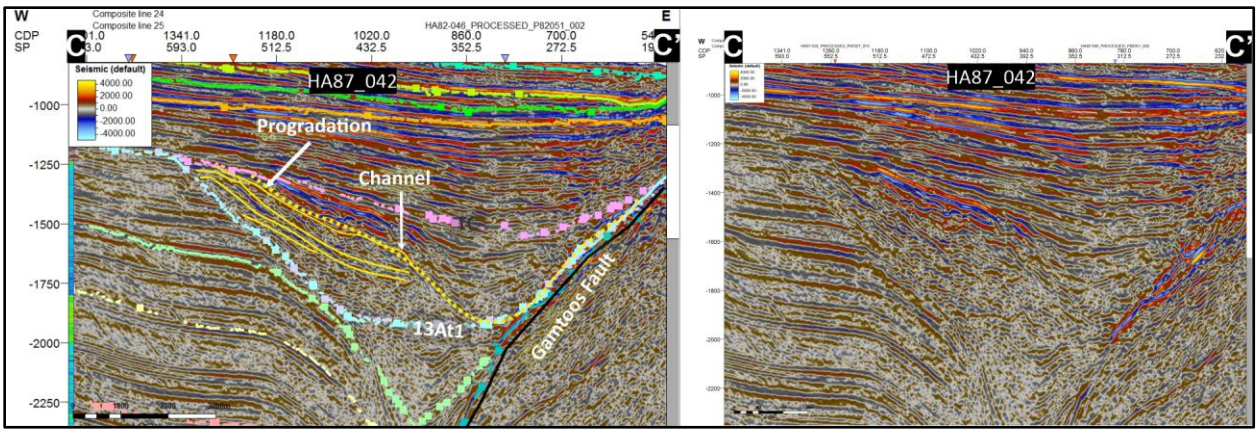

Figure 6.19: A-A', B-B', C-C' The Top Canyon (TC) reflectors exhibit prograding stratal geometries in the W-E direction, which incised stratal geometries truncating across the progradational units. Base map data ©2020 Google, Maxar Technologies, AfriGIS (Pty) Ltd.

6.2.3.7 Post-Hauterivian/"Canyon fill" to upper Albian

This succession, which marks the start of the drift phase (Malan et al., 1990; Bate and Malan, 1992; McMillan et al., 1997; Paton and Underhill, 2004), contains horizontal, continuous reflectors that downlap on the Top Hauterivian reflector (Figure 6.20). The downlapping stratal geometries are mostly observed in the N-S cross-section, with clinoforms prograding to the S. However, these reflectors, which thin towards the N-NE also onlap on the Hauterivian reflectors along strike and show toplaps stratal geometries (Figure 6.20B-B'). The southward prograding clinoforms that dominate the Albian indicate a regressive shift of the shoreline towards the basin. These toplaping clinoforms, which pinch out towards the N, indicate the depositional limit of the Albian succession in the middle shelf. The onlapping stratal geometries along the W-E cross-section suggest increasing accommodation space in the early Albian.

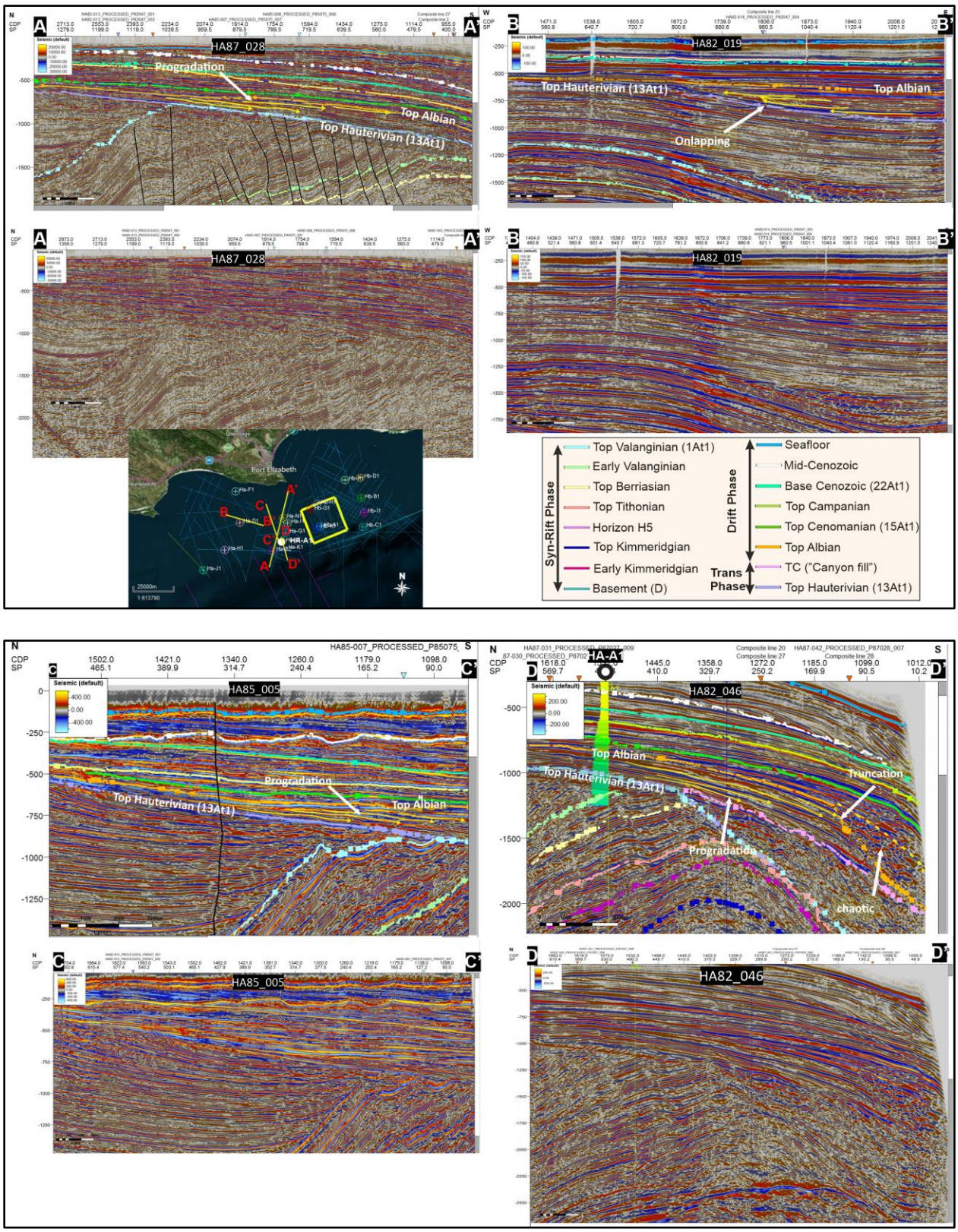

Figure 6.20: A-A' Post-Hauterivian to upper Albian prograding clinoforms from the N. **B-B'** W-E cross-section showing Top Albian onlapping on the Top Hauterivian. **C-C', D-D'** Prograding clinoforms from the N towards the shelf edge. Base map data ©2020 Google, Maxar Technologies, AfriGIS (Pty) Ltd.

6.2.3.8 Post-Albian to upper Cenomanian

This succession progrades from the N and downlaps on the Top Albian reflector (Figure 6.21A-A'). Accretional stratal geometries are also observed on the shelf along the NW-SE cross-section (Figure 6.20B-B'). The Top Cenomanian reflector truncates into the underlying strata, which is more evident towards the shelf-break/slope area, where the successions increase in thickness (Figure 6.21A-A'). Towards the shelf break/slope, this interval shows chaotic character at the base, and then it gives way to prograding clinoforms that dip to the S (Figure 6.20A-A', B-B'). The dominant prograding clinoforms on the shelf suggest a period during the Cenomanian where the shoreline regressed basinwards, likely due to high sedimentation from the N. These clinoforms terminate towards the shelf break, where they are overlain by another prograding unit. The prograding succession towards the shelf edge/slope was probably deposited during forced regression as the shoreline moved basinwards due to the late Cenomanian uplift (Figure 6.20A-A'; Baby et al., 2018). Moreover, the accretional stratal geometries in Figure 6.20B-B' might indicate proximal channelised bodies that were generated during the uplift in the late Cenomanian.

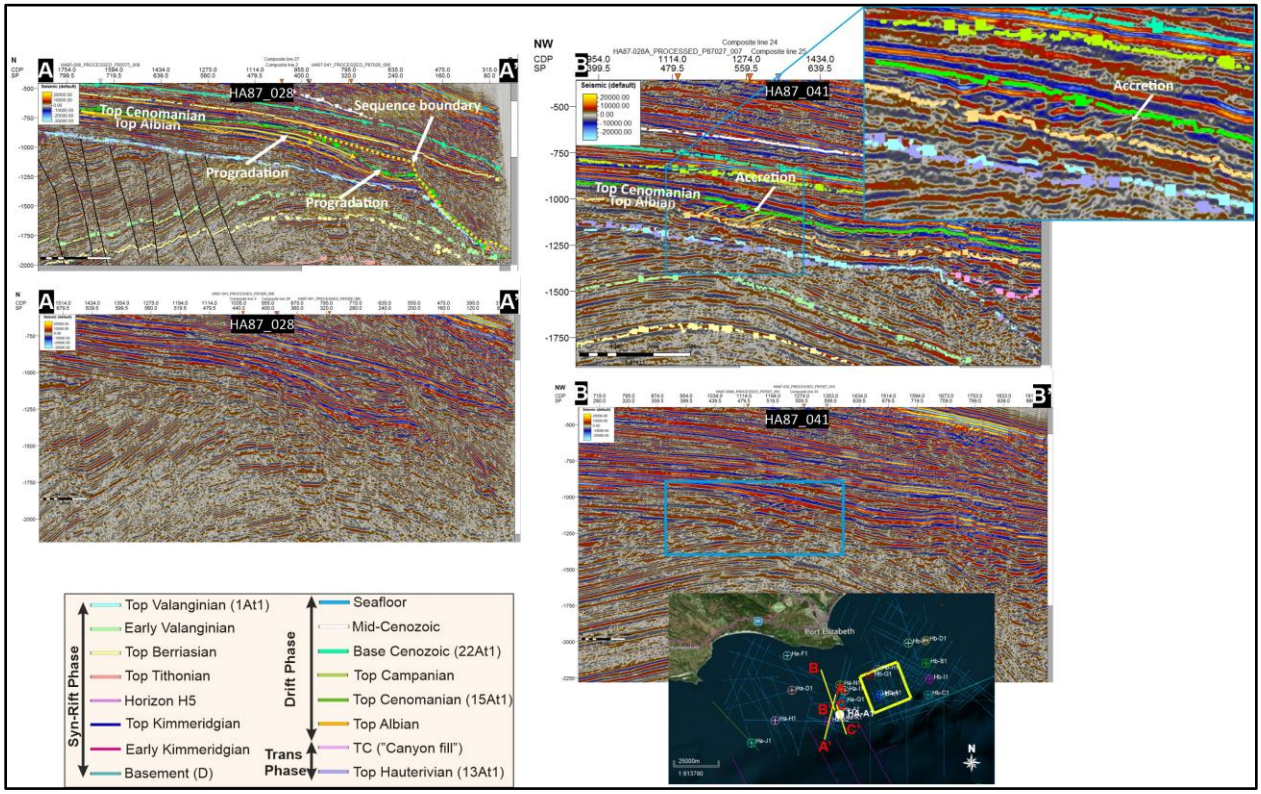

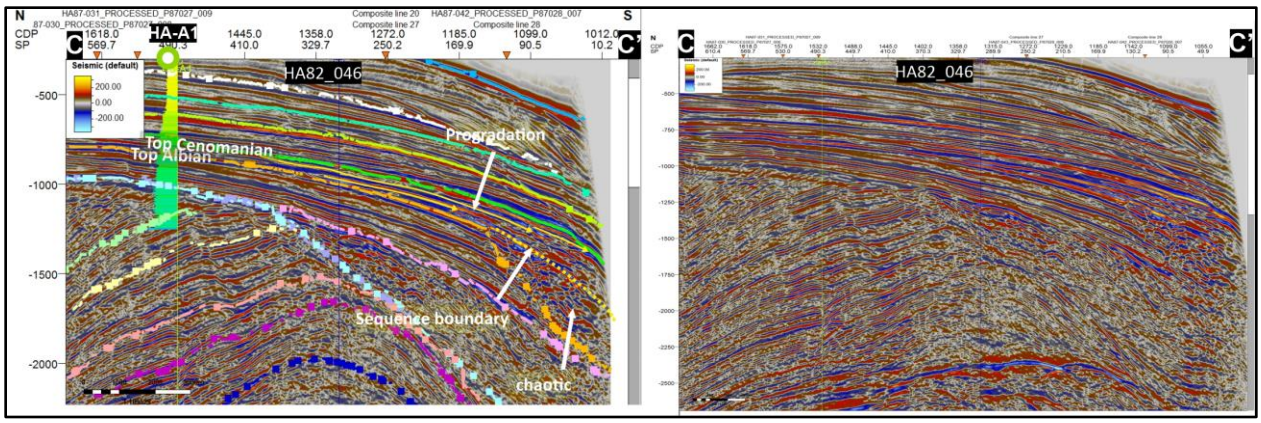

Figure 6.21: A-A' The Albian to Cenomanian succession prograde and downlap on the Top Albian reflector in the shelf-break. **B-B'** Accretional stratal geometries, cross-cutting across the succession in the shelf. **C-C'** N-S prograding stratal geometries observed in the shelf-break/slope. Base map data ©2020 Google, Maxar Technologies, AfriGIS (Pty) Ltd.

6.2.3.9 Post-Cenomanian to upper Campanian

This Upper Cretaceous succession also shows primarily prograding stratal geometries coming from the N and W (Figure 6.22). In most part, these reflectors are parallel, continuous and downlap on the Top Campanian reflector along the shelf. Much like the underlying Campanian succession, this uppermost Cretaceous succession shows that the shoreline shifted basinwards, probably due to increased sedimentation rates on the shelf, and steady/low rate of accommodation space change.

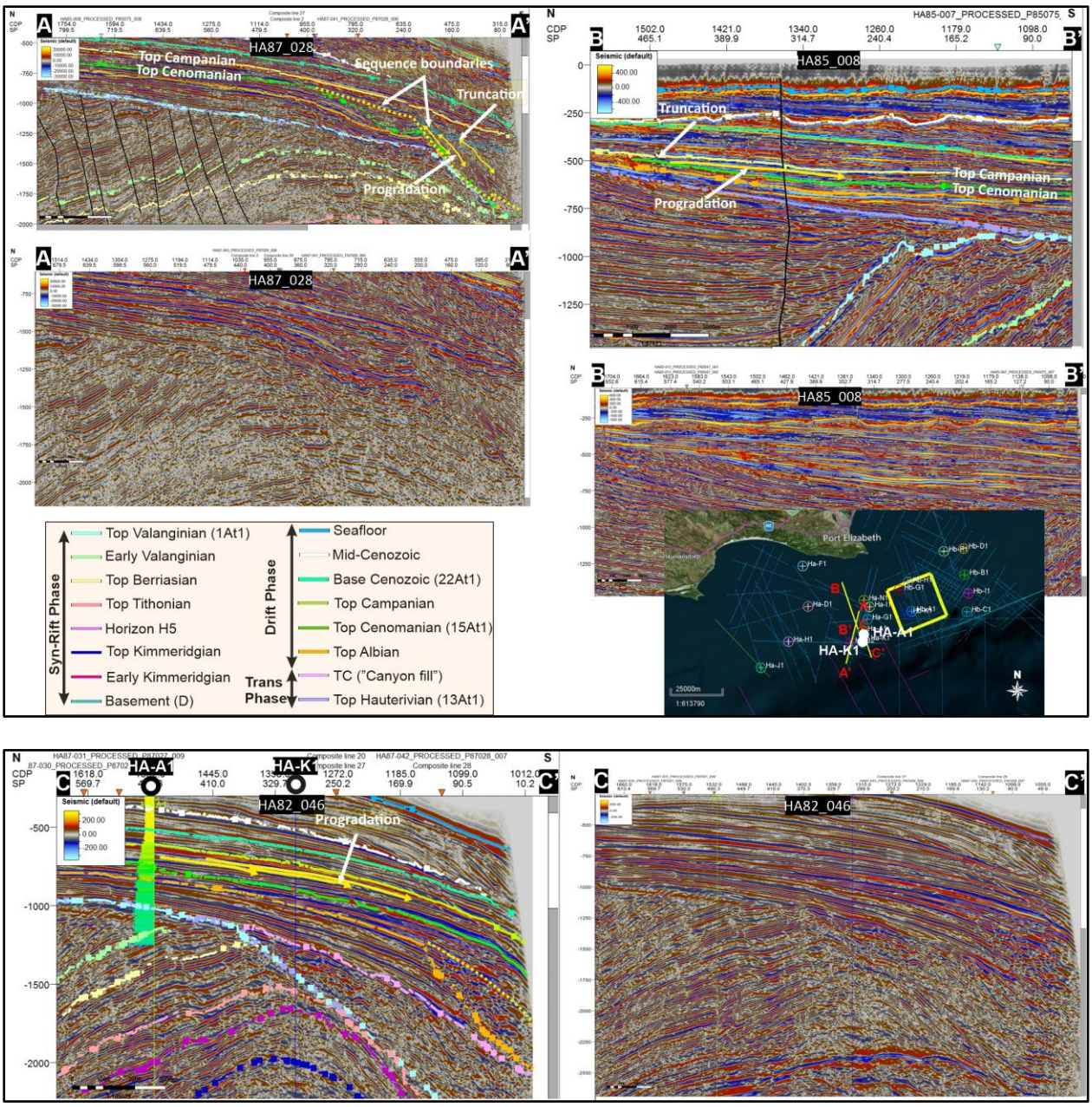

Figure 6.22: Post-Cenomanian to upper Campanian succession. **A-A'** The Campanian succession prograde and downlap on the Top Cenomanian reflector in the shelf-break. **B-B', C-C'** Prograding clinoforms from the N dominating the Campanian shelf. Base map data ©2020 Google, Maxar Technologies, AfriGIS (Pty) Ltd.

6.2.3.10 Post-Campanian to Lower Cenozoic

This Upper Cretaceous sequence also shows primarily prograding stratal geometries coming from the N and W, which downlaps on the Top Campanian reflector (Figure 6.23). In most part, these reflectors are parallel, continuous and downlap on the Top Campanian reflector along the shelf. The commonly

prograding units indicate a regressive shoreline probably due to high sediment input in the Gamtoos Basin. Similar to the underlying Campanian succession, this upper Cretaceous succession shows a shoreline retreating basinwards, probably due to increased sedimentation rates on the shelf, and steady/low rates of accommodation space change.

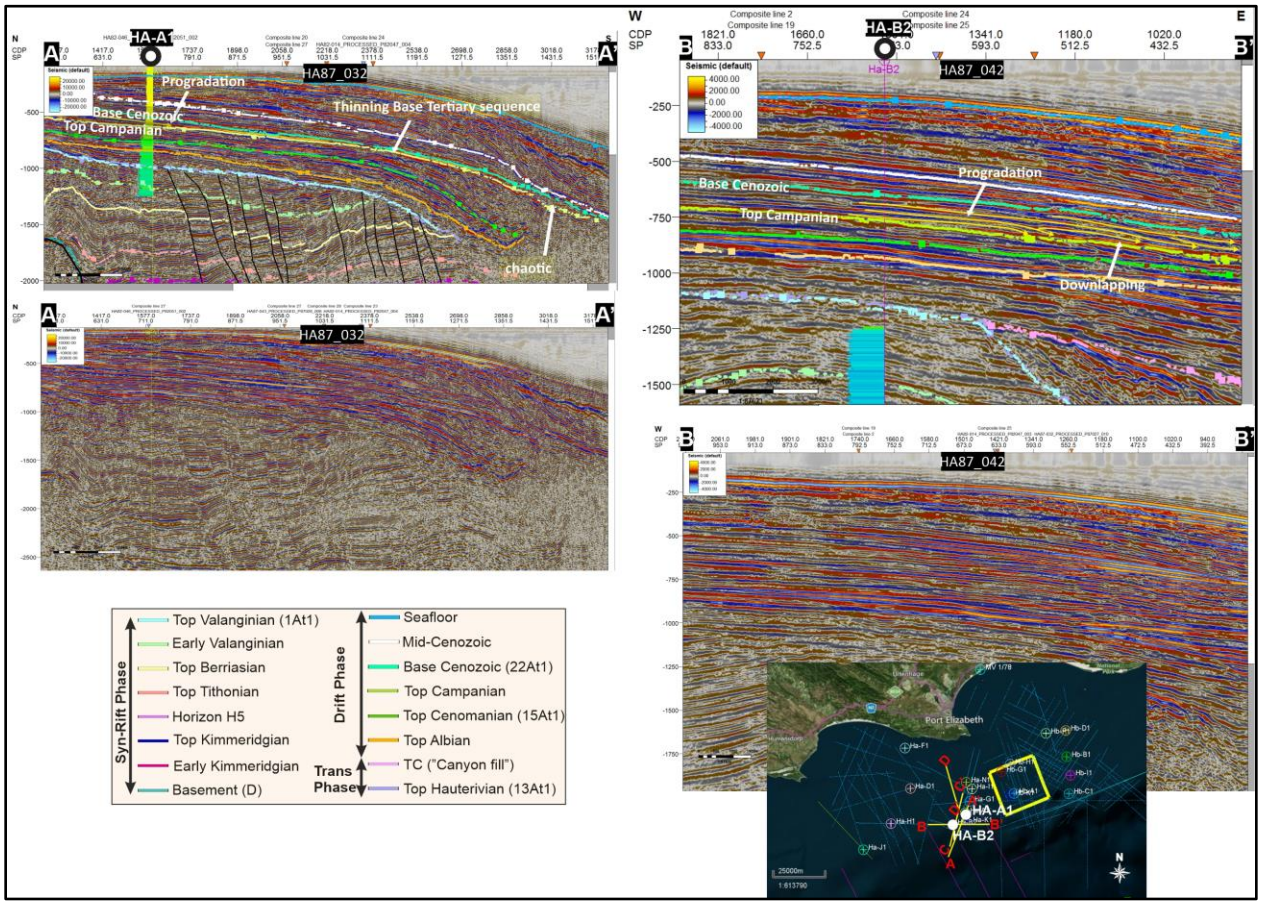

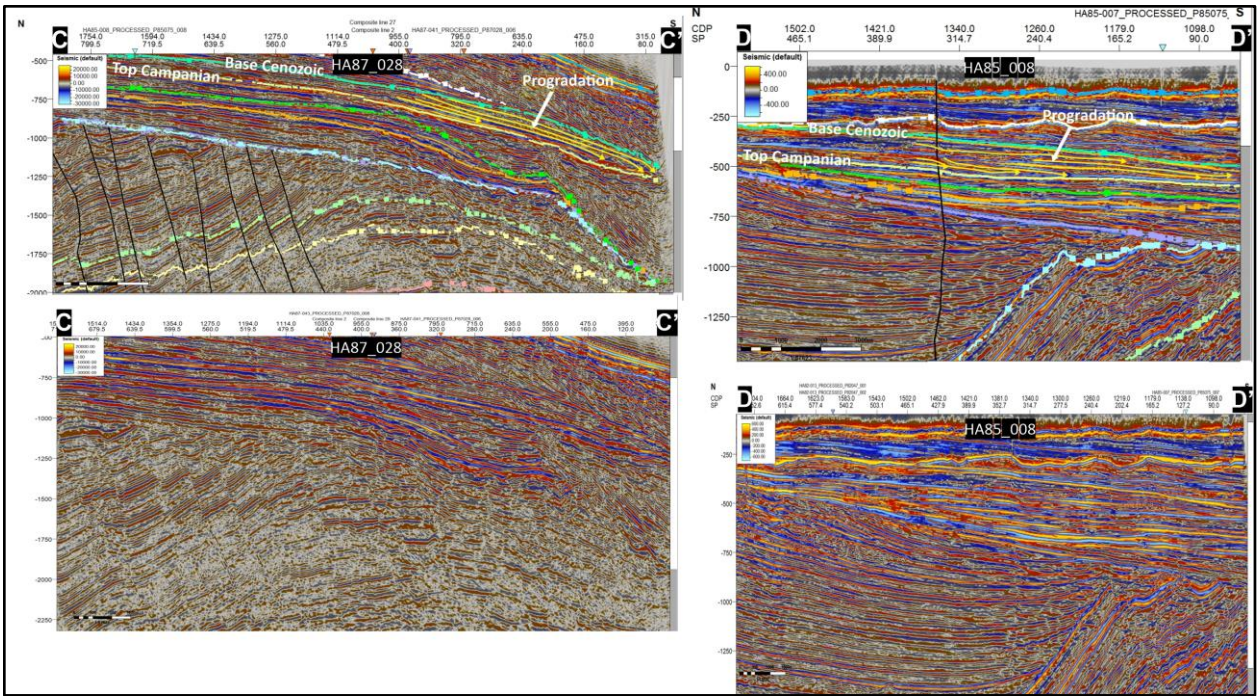

Figure 6.23: A-A', B-B', C-C', D-D' Cross section examples showing the predominantly prograding clinoforms during the post-Campanian to Lower Cenozoic succession in the Gamtoos Basin. Base map data ©2020 Google, Maxar Technologies, AfriGIS (Pty) Ltd.

6.2.3.11 Lower to Middle Cenozoic

The internal geometry of this succession consists of continuous and parallel reflectors, prograding and downlapping on the Base Cenozoic reflector, however, in some places, chaotic geometries are also observed especially on the slope (Figure 6.24a). The Mid-Cenozoic reflector truncates the underlying succession (all post-rift) at an acute angle (Figure 6.24b-d). This truncation is also notable towards the shelf edge/slope (Figure 6.24b-d). The prograding clinoforms indicating a basinwards shoreline shift, probably due to high sedimentation rates. However, these clinoforms were partially eroded during basin tilt in the Middle Cenozoic (Baby et al., 2018; Hatthing, 2001), which also resulted in a regressive shoreline and scouring of the shelf.

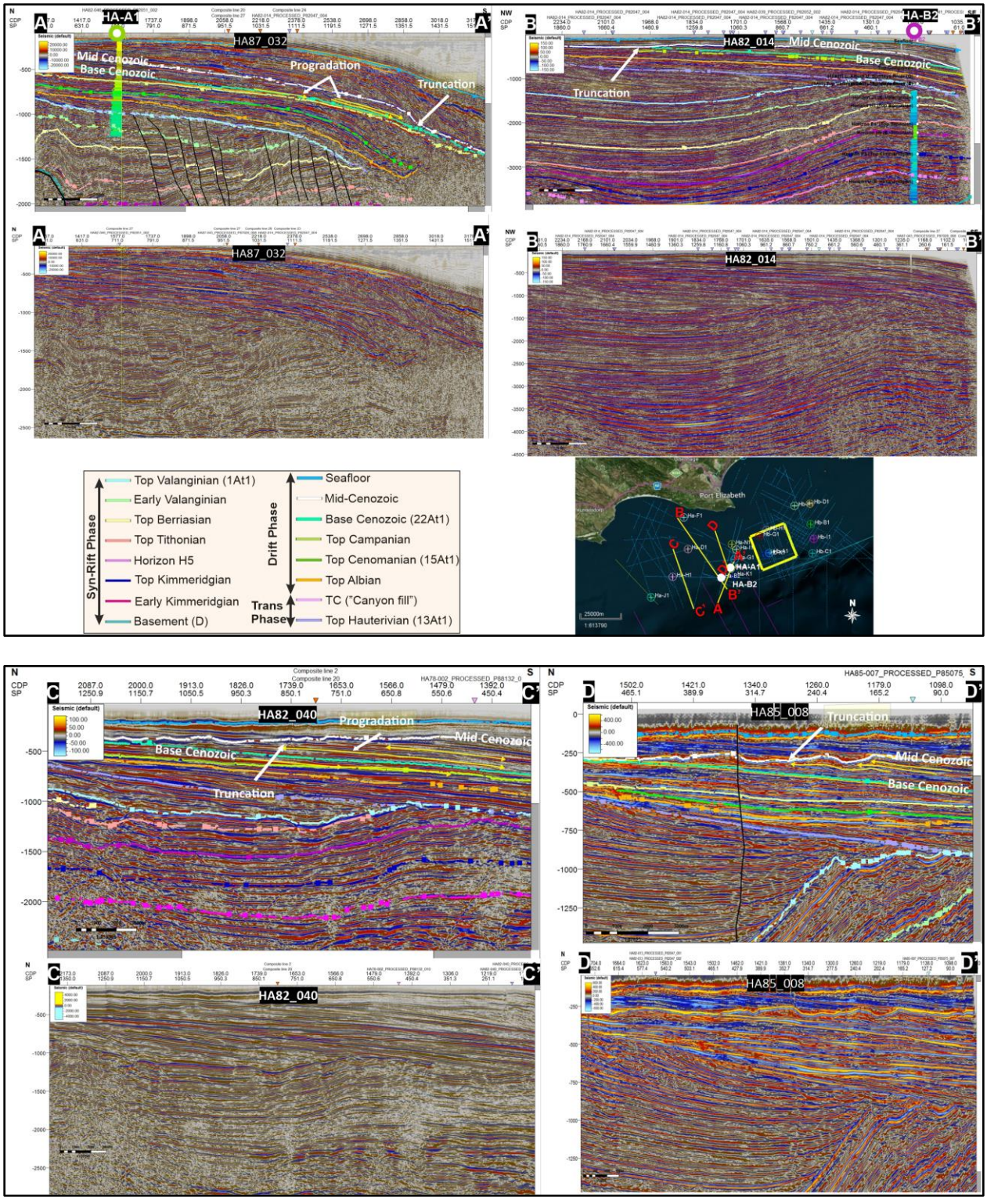

Figure 6.24: a Lower Cenozoic progrades downlapping on the Base Cenozoic reflector. **b-d** Younger successions terminating against the Mid-Cenozoic reflector. Base map data ©2020 Google, Maxar Technologies, AfriGIS (Pty) Ltd.

6.2.3.12 Upper Cenozoic

The Upper Cenozoic, including the Holocene succession, onlaps onto the Mid-Cenozoic reflector, and this is more evident in the slope region, where the succession is thicker (Figure 6.25a). Although the succession is generally thin on the shelf (and below resolution in some seismic lines), there is some evidence for prograding clinoforms, which dip from N to S (Figure 6.25c). Internally, this succession is made up of laterally continuous and parallel reflectors (Figure 6.25). The onlapping stratal geometries shows a period of landwards movement of the shoreline, likely during the late Eocene/Miocene. This flooding event in the Eocene/Miocene could be inferred to be associated with the transgression that resulted in the shallow marine, shark-teeth-bearing limestones of the Bathurst Formation (found ~300m above the present shoreline) in the onshore portion of the Algoa Basin (e.g., Hattingh, 2001). Subsequently, the shoreline regressed basinwards due to the Pliocene/Pleistocene glaciation events (Hattingh, 2001) resulting in erosion in the hinterlands and high sedimentation rates on the shelf. Although the Eocene to Holocene outcrops onshore the Algoa Basin show evidence for several, high frequency transgressive and regressive events, the resolution of the current seismic dataset is not suitable to accurately image this cyclicity that has been linked to glacioeustasic sea level changes in this region (e.g., Le Roux, 1987, 1989, 1990; Illenberger, 1992; Hattingh, 2001; Roberts et al., 2006).

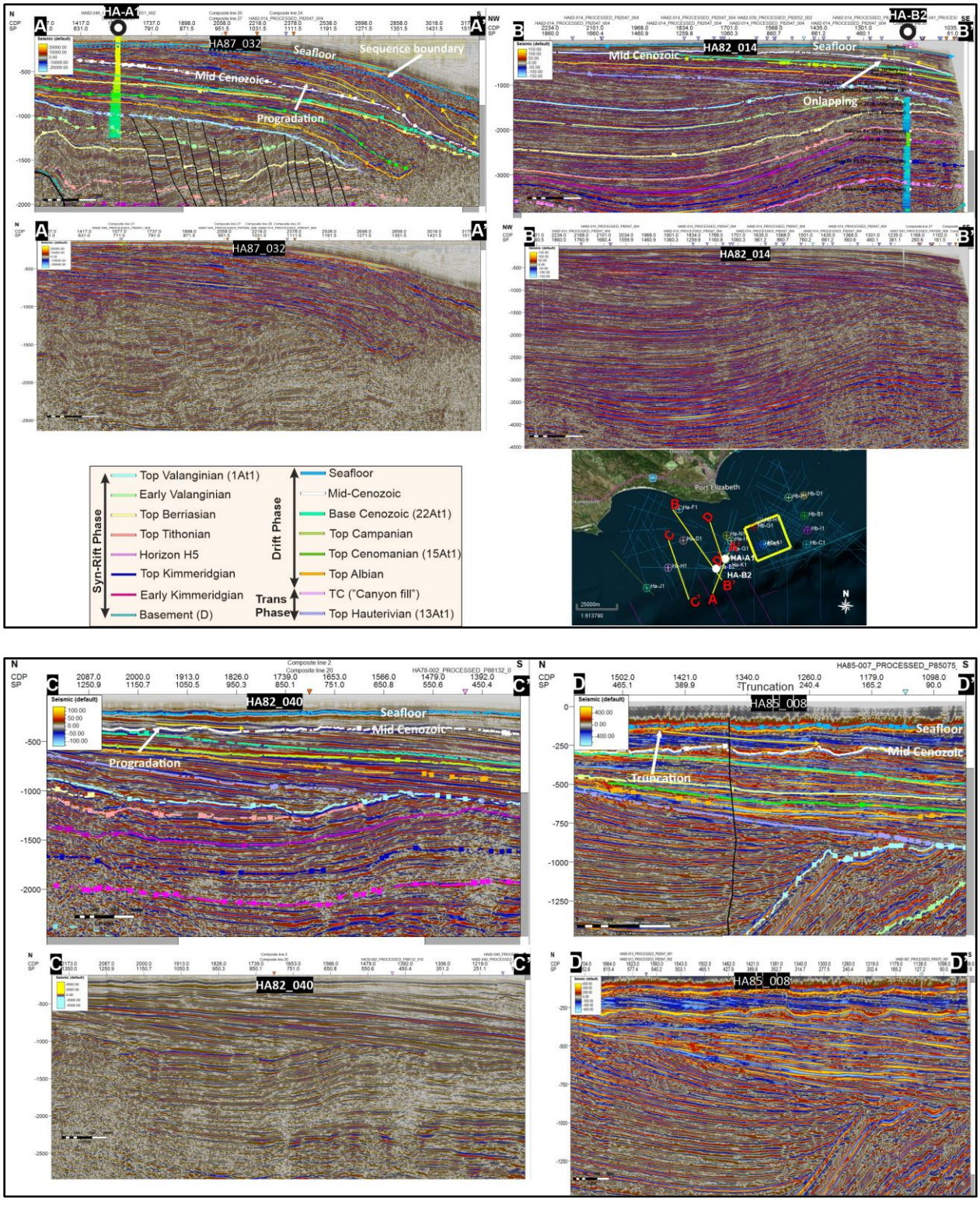

Figure 6.25: a Upper Cenozoic progrades downlapping on the Mid-Cenozoic reflector. **b** Younger successions truncating against the Seafloor reflector. Base map data ©2020 Google, Maxar Technologies, AfriGIS (Pty) Ltd.

7 Discussion

7.1 Syn-rift phase: Pre-Aalenian to upper Valanginian

In the Algoa and Gamtoos Basins, the syn-rift interval is marked by stratigraphic units deposited in half-grabens that formed during the separation of East and West Gondwana in the late Early Jurassic (McLachlan and McMillan, 1976; Dingle et al., 1983; Ben-Avraham et al., 1993; Malan et al., 1990; McMillan et al., 1997; Tinker et al., 2007; Thompson et al., 2019; Muir et al., 2020). In the study area, proximal syn-rift deposits are predominantly conglomerates and sandstones of the Enon Formation, which are overlain by mudstones and sandstones of the Kirkwood Formation (McLachlan and McMillan, 1976; Dingle et al., 1983; McMillan et al., 1997; Broad et al., 2012; Muir et al., 2017a). These continental strata are overlain by the regionally extensive marine Lower Cretaceous Sundays River Formation (McLachlan and McMillan, 1976; Dingle et al., 1983; McMillan et al., 1997; Broad et al., 2012; Muir et al., 2017a). Onshore the Algoa Basin, the mid-Mesozoic Uitenhage Group (Enon, Kirkwood and Sundays River Formations) is unconformably overlain by the Eocene to Holocene Algoa Group (e.g., McMillan and McMillan 1976; Du Toit, 1979; Le Roux, 1987, 1989, 1990, 1991, 1992, 2000; Illenberger, 1992; McMillan, 1990; McMillan et al., 1997; Hattingh, 2001; Broad et al., 2012; Lockley et al., 2021). Using an integrated approach of incorporating well and seismic data, supplemented by inferences from the literature, gross depositional environment maps (GDE) were generated to provide the developmental history for the Algoa and Gamtoos Basins from the late Early Jurassic to Holocene.

7.1.1 Pre-Aalenian to upper Kimmeridgian

In the Algoa Basin, borehole HB-P1 intersected a succession with high net sand-to-shale ratio, while the more distal HB-C1 shows limited sand input (Figure 5.4). The presence of isolated coarsening-upward sandstones within the shaley interval in the distal borehole HB-C1 could represent prograding delta mouth bars, or sediments eroded from the basement subcrops. The combination of coarsening- and fining-upward units as well as clay interbeds suggest that the depositional setting was probably alternating between coastal floodplains and shallow marine waters during a period characterized by fluctuating sediment supply and a slowly rising RSL (Figure 7.1). This fluctuation is attributed to short lived tectonic

pulses in syn-rift settings, resulting in increasing accommodation space (transgression), followed by longer period of tectonic quiescence, which allowed for the progradation of sediments (Martins-Neto and Catuneanu, 2010). According to McMillan et al. (1997), borehole HB-A1 in the Port Elizabeth Trough is dominated by a microfauna that suggest a shallow marine-transitional setting, while borehole HB-K1 contains continental red beds, pebbly sandstone and lignite bearing claystones (Figure 5.4). Although these boreholes are close to each other, their different facies suggest contrasting marine and continental settings, with the red beds and lignite bearing units possibly having formed on emergent basement highs (Figure 7.2).

Most of the basal early rift sediments are not intersected by boreholes and the seismic resolution is very poor in the study area, consequently the interpretation of this succession is reliant on the onshore geological studies (e.g., Muir et al., 2015, 2017b; Muir, 2019). These studies show that in the Algoa and Gamtoos Basins, the Basement to Top Kimmeridgian, conglomerate-dominated succession of the Enon Formation was deposited primarily in high-energy, alluvial fan and braided river setting proximal to basin margin extensional faults, whereas its more distal facies equivalent, the mudstone and sandstone-bearing Kirkwood Formation, was a product of meandering rivers with vast floodplains that supported large, freshwater lakes. Due to the limited data resolution and data coverage, stratal geometry of this succession in the Algoa Basin remains largely unknown.

There is significant lateral lithological heterogeneity in the Gamtoos Basin wireline data, with logs showing varying inferred grain-size and facies trends across the basin, a feature common in highly compartmentalized syn-rift successions (e.g., Chorowicz, 2005; Holz et al., 2017). The lower part of borehole HA-J1 is dominated by shaley facies, overlain by well-defined, channelized, fining-upward sandstones (Figure 6.3). In contrast, the lower part of borehole HA-H1 is dominated by proximal high-energy, coarsening- and fining-upward sandstones, which are overlain by a flooding surface and fine-grained sediments that are characteristic of low-energy settings. Although the upper half of the borehole shows an overall coarsening-upward trend, the very low net sand-to-shale ratio suggests either decreased sedimentation rate or a shoreline advancing landwards at faster rate than sediment input, which is typical during transgression (Figure 7.1; Catuneanu, 2006). In borehole HA-B2, the interval is dominated by mostly claystones, inferred to represent a predominantly low-energy, distal marine depositional environment, with isolated sandstones representing rare events of higher energy sedimentation, possibly as basin floor fans in a deeper water setting (Figure 7.2). The proximity of borehole HA-K1 to the Recife

Arch (Figure 7.2) suggests that the coarsening-upward sandstones were probably eroded from the basement high and deposited as alluvial fans (Figure 5.22B-B').

In the Gamtoos Basin, the pre-Aalenian to upper Kimmeridgian succession thickens towards S of the Gamtoos Fault, indicating active faulting during deposition of this succession (Figure 7.2). The N-S striking, southern part of the fault was probably more active, creating larger accommodation space in S than in the N. Seismic data (Figure 6.13b) shows eastward prograding reflectors (clinoforms) above the Basement D reflector, overlain by chaotic seismic reflectors. Since progradation in a nearshore depositional context is typically a transitional to marine process, prograding clinoforms (Figure 6.13b) are taken as evidence for a pre-Kimmeridgian marine incursion in the Gamtoos Basin. However, due to the unavailability of borehole data intersecting these progrades, the possibility of these progrades representing a transitional deltaic environment cannot be ruled out.

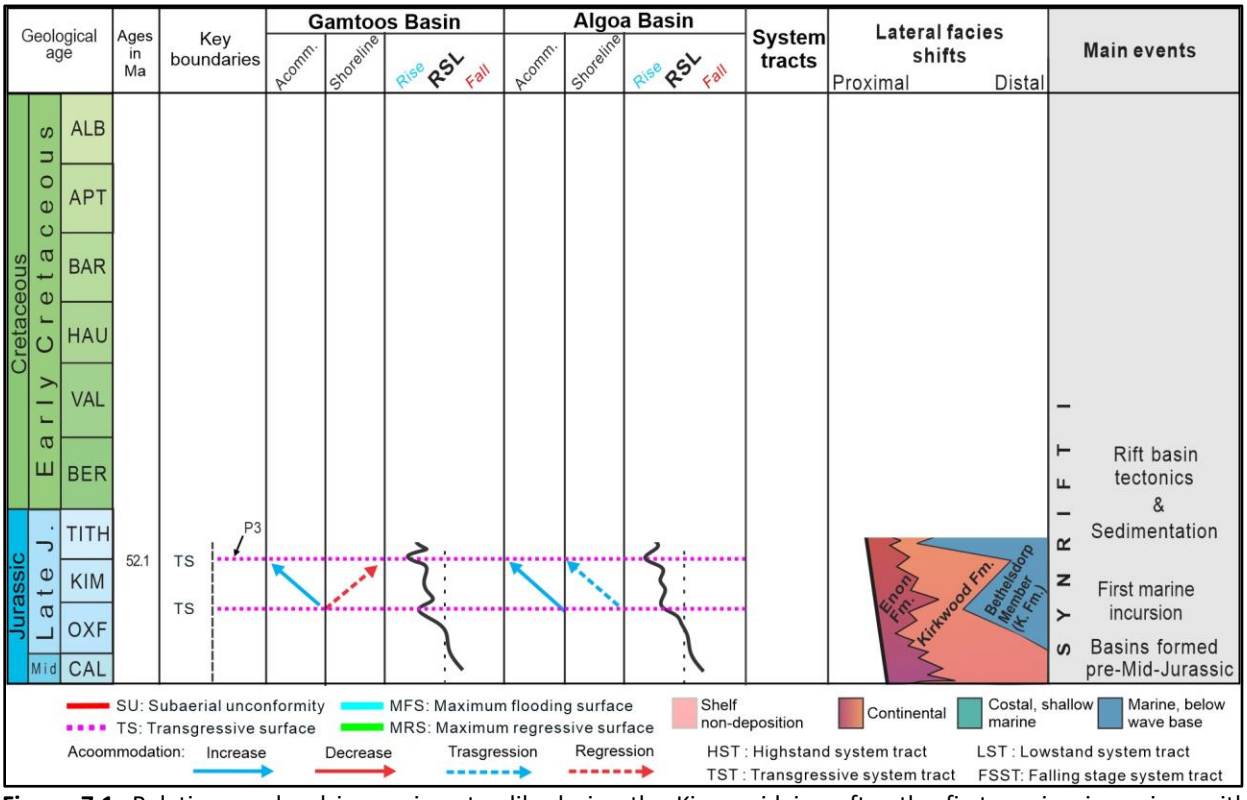

Figure 7.1: Relative sea level increasing steadily during the Kimmeridgian after the first marine incursion, with accommodation space driven by the local tectonic. Prograding clinoforms in the Gamtoos Basin suggest a regressive shoreline during in the Late Jurassic (modified from Brown et al.1995; McMillan et al., 1997; Broad et al., 2012; Baby et al., 2018; Muir et al., 2020).

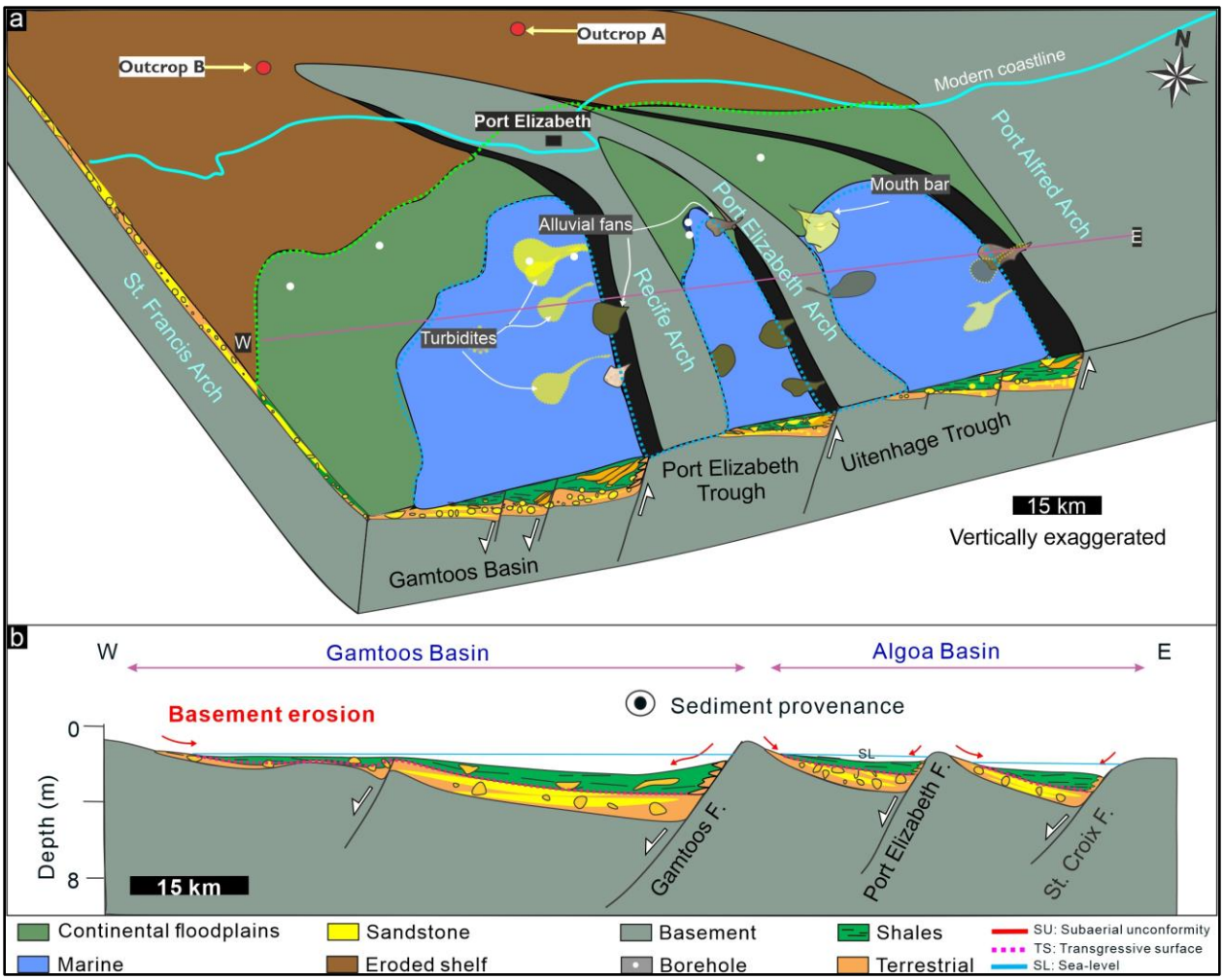

Figure 7.2: a Kimmeridgian gross depositional model after the Middle Jurassic marine incursion. **b** West-East cross section of the Algoa and Gamtoos Basins, with sediments coming into the section. See Figure 2.2 for Enon Formation outcrop A and B.

7.1.2 Post-Kimmeridgian to lower Valanginian

Dataset from this succession supports the widespread fluvial floodplain setting of the Kirkwood Formation established from outcrops studies (Muir et al., 2015, 2017b and references therein). The main depocenters appear to be localised near the NW-SE striking hanging walls, from the late Tithonian to early Valanginian (Figure 5.16 and 6.10). Unlike in the earlier depositional phase, when sedimentation was mainly along the N-S trending sector of the Gamtoos Basin, isopach maps shows active faulting along NW-SE strike from the Tithonian to Valanginian (Figure 5.16 and 6.10). This created accommodation space for marine conditions as the shoreline advanced landwards (Figure 7.3). This increase in accommodation could have resulted from the fault strain following pre-existing crustal-scale structure of the underlying

Palaeozoic Cape Supergroup (Martin et al., 1981; de Wit, 1992; Paton and Underhill, 2004; Muir et al., 2020). Seismic mapping suggests that the sediments were supplied from the NW to S-SE, which is consistent with Kirkwood Formation provenance studies (Shone, 1976). Although Muir et al. (2015) reported a localized SW to NE paleocurrent direction, this discrepancy likely due to the meandering nature of the rivers in the Kirkwood Formation. According to McMillan et al. (1997) and Muir et al. (2017b, 2020), microfossils in the Kirkwood Formation also show evidence for low-energy, lacustrine environments (Colchester Member) that were, among others, inhabited by freshwater algae, and thus these organic matter-rich lake deposits are also potential source rocks in the study area. Data also suggest that the lacustrine environment by this time was probably due to oxbow lakes on the floodplain and drowning estuaries during transgression (Figure 7.4). In addition to the lacustrine setting, the Bethelsdorp Member in the lower Kirkwood Formation indicate the presence of low-energy conditions, albeit in a marine setting, due to sea incursion during the Late Jurassic (McLachlan and McMillan, 1976; McMillan et al., 1997; McMillan, 2010; Muir et al., 2017b). This marine flooding appears to have coincided with the change to NW-SE trending depocenters during the Late Valanginian to Early Berriasian (Figure 5.16 and 6.10). The newly created accommodation space could have aided the marine flooding in the proximal onshore setting as the shoreline advanced towards N. The Bethelsdorp Member, which is a bioturbated, grey shaley succession, outcropping onshore in the Uitenhage Trough (e.g., near Jachtvlakte) attains thickness of 400 m (Muir et al., 2017b). It also contains tabular sandstone beds that lack terrestrial fossils or red palaeosols, contrary to the rest of the units in the Kirkwood Formation (Almond, 2012; Muir et al., 2017b). This Late Jurassic marine influence in the early rift during does not de facto suggests the presence of an ocean floor in the area (McLachlan and McMillan, 1976; Jungslager, 1996; Koopmann et al., 2014; Muir et al., 2017b, 2020), however evidence for a failed, pre-Tithonian (~178 Ma old), mid-oceanic ridge (MOR) was shown in the Falklands (Malvinas) Plateau Basin (Schimschal and Jokat, 2019), which is a region placed near the study area in most palaeogeographic reconstructions (e.g., Lovecchio et al., 2020; Muir et al., 2020).

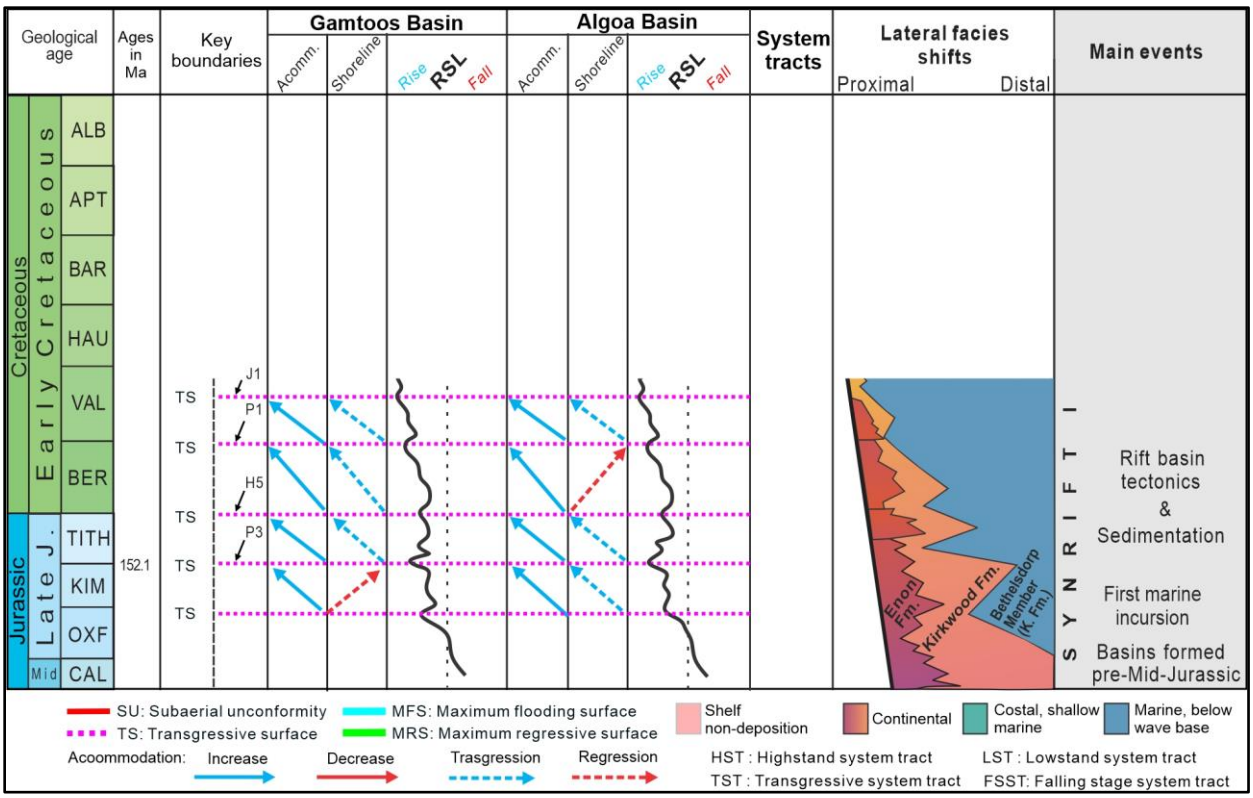

Figure 7.3: Relative sea level increasing steadily from the post-Kimmeridgian to the early Valanginian, accommodation space driven by the local tectonic activities. Wireline logs suggest a regressive shoreline in the Uitenhage Trough during the Berriasian (modified from Brown et al., 1995; McMillan et al., 1997; Broad et al., 2012; Baby et al., 2018; Muir et al., 2020).

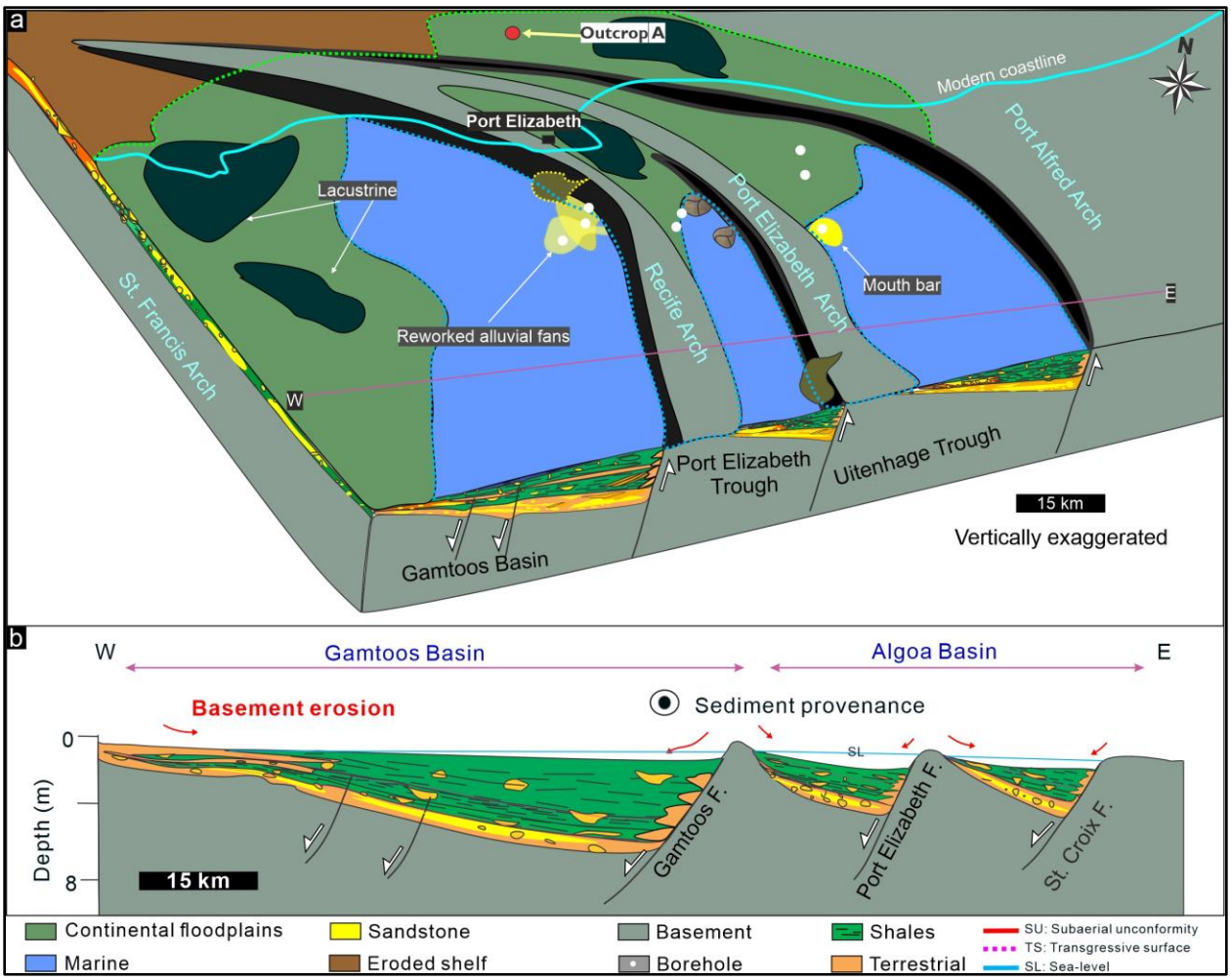

Figure 7.4: a Kimmeridgian to early Valanginian GDE map. **b** West-East cross section of the Algoa and Gamtoos Basins. See Figure 2.3 for Kirkwood Formation outcrop A and B.

7.1.3 Early Valanginian to upper Valanginian (1At1)

Based on sedimentological and palaeontological characteristics (e.g., ammonites, belemnites, bivalves, gastropods, echinoids, crustaceans, polychaetes, corals), the depositional environment of the Valanginian-Hauterivian Sundays River Formation was reconstructed to span a range of marine settings from shallow-marine, tidally influenced, estuarine to deltaic environments to shelf and continental slope settings (Shone, 2006; Muir, 2019 p. 14-15).

Wireline data is dominated by fine-grained units, with a prominent shallow marine retrogradational stacking trend evident in borehole HB-I1 (Figure 5.7). In most places, this interval has been eroded (mostly on the tilted hanging walls), where only the lower part of the succession is preserved in some boreholes.

For example, the sandy facies in the lower parts of boreholes HB-B1 and HB-C1 (Figure 5.7) might represent a period in the Valanginian before the onset of the marine transgression, when deposition was still predominantly occurring on fluvial or coastal floodplains (Figures 7.5 and 7.6). In the Gamtoos Basin, borehole data is dominated by fine-grained successions, and is assumed to represent the dominant marine phase of deposition associated with the Sundays River Formation (Figure 7.6). The coarsening-upward sandy facies in the upper part of borehole HA-D1 could represent a deltaic or river mouth bar setting (Figures 6.7and 7.6). Overall borehole data reflect the marine to nearshore character of the deposition that was previously suggested for the Sundays River Formation (e.g., Shone, 2006; Muir, 2019).

Though this interval is severely eroded in the Algoa Basin, isopach maps in both the Algoa and Gamtoos Basins show NW-SE (Figure 5.16) directed depocenters, suggesting that the syn-rift faults were still active during the later parts of the Valanginian. In the Port Elizabeth and Uitenhage Troughs, this succession is folded, probably due to reactivation of the St. Crox and Uitenhage Faults, respectively, during later tectonic inversion (Thomson, 1999). Because this succession, which can be up to 2500-m-thick, has been intersected by few boreholes (Figures 5.7 and 6.7), its lateral and vertical facies are poorly understood. In both basins, this succession marks a major transgressive event (1At1), which erodes large tracts of syn-rift deposits represented by the Enon and Kirkwood Formations (Figures 5.22, 6.16, 7.5 and 7.6). This boundary marks a period when the Algoa and Gamtoos Basins were physically connected for the first time. It is thus a major flooding surface (i.e., a maximum flooding surface - MFS) that separates the older continental from the younger marine deposits (i.e., the Enon-Kirkwood Formations from the Sundays River Formation), as attested by outcrops of the Sundays River that are rich in marine fossils across the southern half of the Algoa Basin (Figure 7.6). It is noteworthy that while the Bethelsdorp Member (in the lower Kirkwood Formation) and the Sundays River Formation are lithologically alike and are both underlain by marine flooding surfaces due to their similar marine origin (e.g., Almond, 2012; Muir et al., 2017b; Muir, 2019), the older Bethelsdorp Members has a more localized occurrence, whereas the Sundays River Formation is regionally extensive (and coeval with the upper Kirkwood Formation).

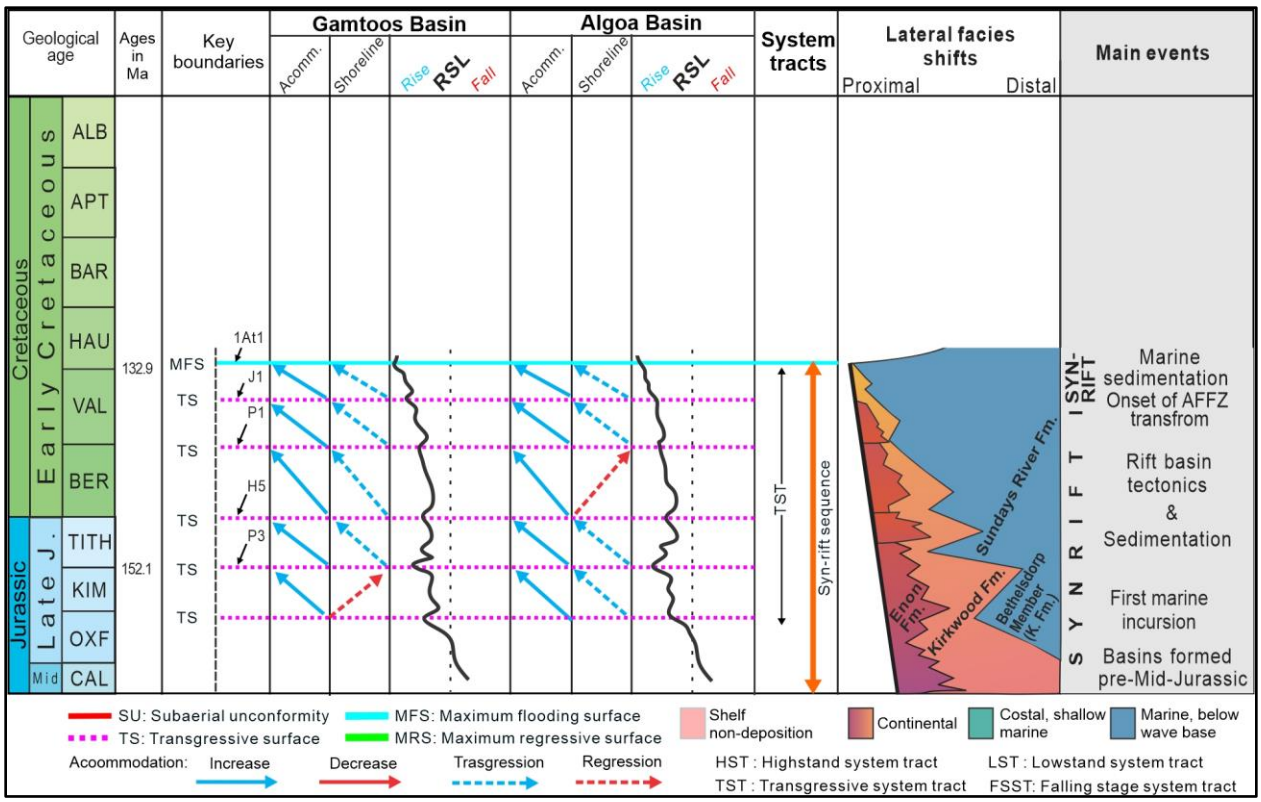

Figure 7.5: Relative sea level increased steadily until the Top Valanginian, with accommodation space driven by the activation of the Agulhas-Falkland Fracture Zone (AFFZ) during the Valanginian. The 1At1 boundary marks the maximum flooding surface in the Algoa and Gamtoos Basins (modified from Brown et al., 1995; McMillan et al., 1997; Broad et al., 2012; Baby et al., 2018; Muir et al., 2020).

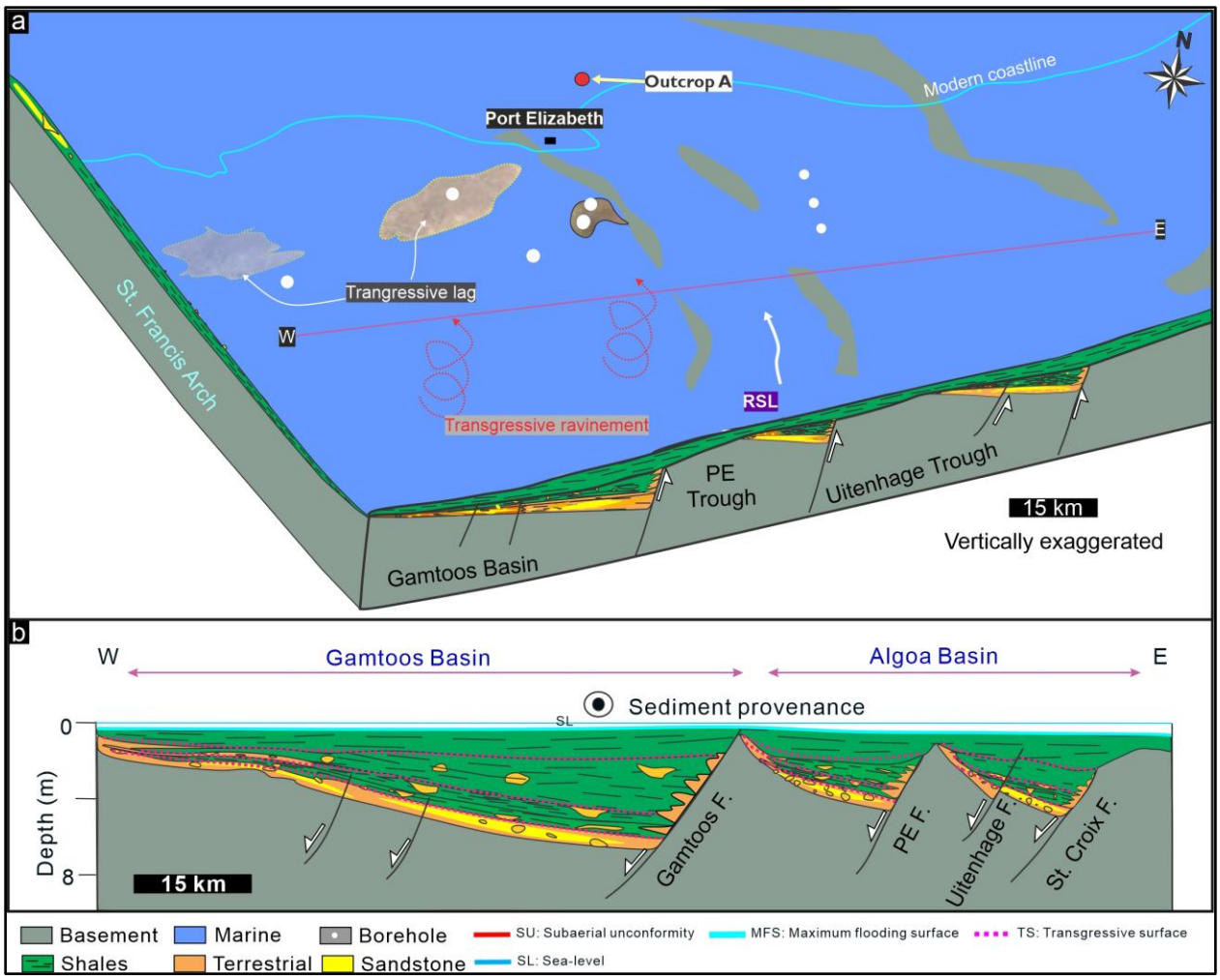

Figure 7.6: a Early to late Valanginian GDE map, showing increasing RSL, which resulted in the 1At1 maximum flooding surface corresponding to the break-up unconformity. **b** West-East cross section of the Algoa and Gamtoos Basins. See Figure 2.4 for Sundays River Formation outcrop A.

7.2 Transitional phase: post-Valanginian to early Albian

This interval represents sediment deposited during reduced (negative) accommodation space in the Algoa and Gamtoos Basins, as a result of a drop in RSL (Malan, 1993; Brown et al., 1995; Thomson, 1999; Paton and Underhill, 2004). The uplift of the basin, which was caused by the dextral (right lateral) AFFZ transform motion, resulted in a regressive shoreline (Malan, 1993; Brown et al., 1995; Thomson, 1999; Paton and Underhill, 2004). This period of uplift, which eroded up to 1000 m of underlying sediments, lasted from the late Hauterivian to early Aptian (6At1 to 13At1), resulting in the Algoa and Gamtoos Canyons and other erosional features across the basins (Bate and Malan, 1992; McMillan et al., 1997; Broad et al., 2012).

7.2.1 Post-Valanginian to upper Hauterivian

In borehole HB-B1, the basal coarsening-upward trend suggest a regressive shoreline, overlain by what appears to be stacked fining-upward successions (Figure 5.8). These upward-fining deposits are likely fluvial in origin, and indicate increased depositional energy, probably during the initiation of the uplift in the late Hauterivian (McLachlan and McMillan, 1976; Dingle et al., 1983; Malan, 1993; Brown et al., 1995; Thompson, 1999; Paton and Underhill, 2004). In the Gamtoos Basin, this succession shows low-energy facies that lacks sandy interbeds in both boreholes HA-J1 and HA-D1 (Figure 6.18), and thus was probably deposited when the basin was still experiencing marine condition during the early Hauterivian before the late Hauterivian/Aptian uplift and erosion (Figures 7.7 and 7.8). Seismic data show that the late Hauterivian unconformity was widespread across the basin, and when it formed, large tracts of the underlying syn-rift succession were eroded in both basins (but especially in the Algoa Basin; Figures 5.24 and 7.8). In the Port Elizabeth Trough, where the erosion was less severe, the onlapping lower Hauterivian seismic reflectors indicate an increasing accommodation space during the early Hauterivian (Figures 5.24 and 7.8). A common feature within this succession is a lateral change in seismic facies, where the brighter (higher energy) reflectors might indicate the presence of sands and dimmer facies indicating shales/clays (Figure 5.24).

In the Gamtoos Basin, accretional stratal geometries are observed towards the upper Hauterivian succession, which could be due to migrating bypass channels, with sediments making their way to the distal setting. The Top Hauterivian reflector (13At1) is highly erosive, and in some places, this reflector forms a composite unconformity with the 1At1 (Top Valanginian reflector). In places the Top Hauterivian reflector also erosively cuts into the syn-rift/transitional phase sediments (Figure 5.24). Towards the S, in the N-S trending part of the Gamtoos Fault, this succession onlaps on the Gamtoos Anticline (McMillan et al., 1997; Thomson, 1999) and appears to be syn-tectonic in the lower part of the succession (Figure 6.18; 6At1?). Although the stress field responsible for the formation of the Gamtoos Anticline is poorly understood (Thomson, 1999), this structural feature shows a period of inversion, which probably formed during the Hauterivian to Aptian uplift episode (see Thomson, 1999 his fig. 9). The presence of canyons and truncational features on the shelf collectively suggest that the shoreline was pushed to the shelf edge during a RSL fall in the late Hauterivian (Figure 7.8). The shelf edge shoreline means that most sediments were being deposited basinward as high-density basin floor fans, outboard of the Algoa and Gamtoos Basins (Figure 7.8). This basinwards deposition is estimated to be similar in age to the recently discovered Brulpadda and Luiperd prospects in the Outeniqua Basin (Africa Energy Corp, 2020). In the shelf regions

of Algoa and Gamtoos Basins, bypass channels with limited coarse-grained sediment content are expected. The higher intensity of this erosion in the fill of the Algoa Basin suggests that the Algoa Basin was more uplifted than the Gamtoos Basin.

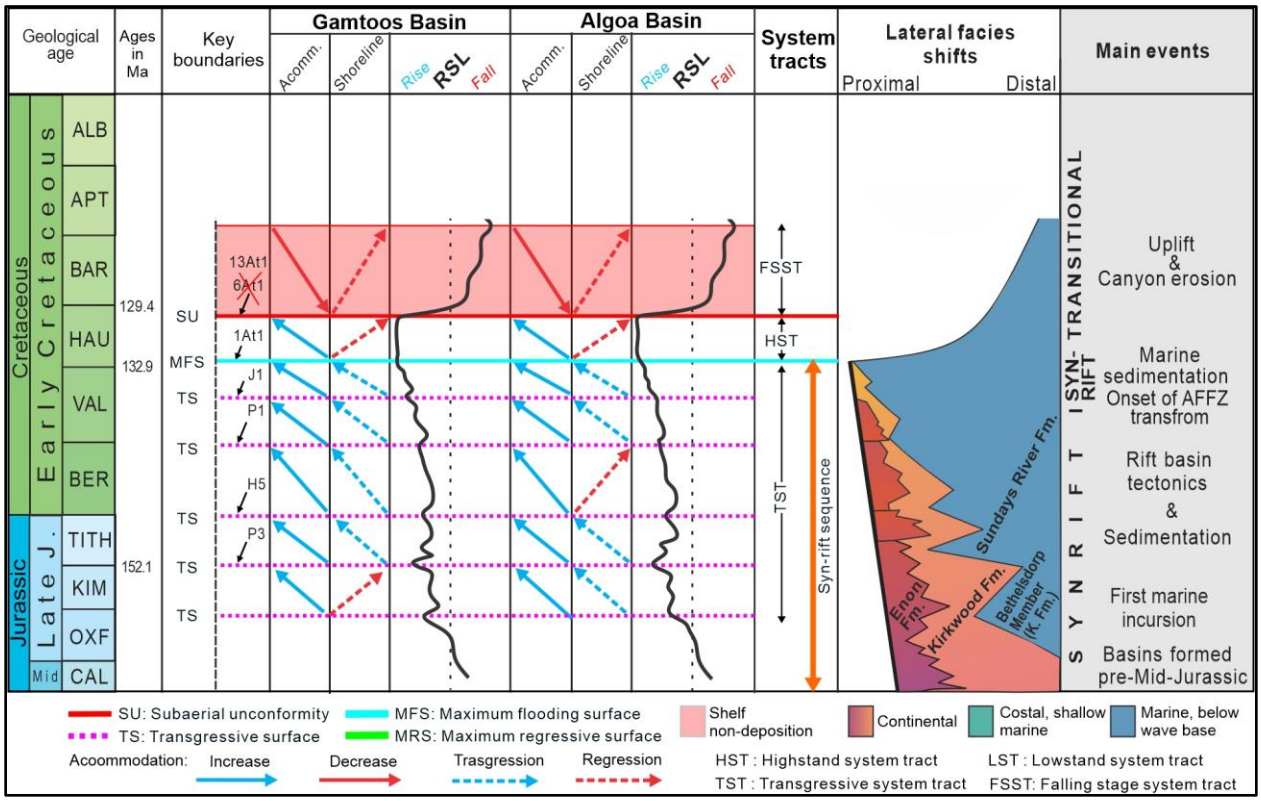

Figure 7.7: Relative sea level curve during the Hauterivian to Aptian, indicating a period of non-deposition and erosion in the Algoa and Gamtoos as the RSL falls and forces the shoreline basinwards, resulting in the Algoa and Gamtoos Canyons. The 6At1 boundary is absent in most part of the basin due to the Hauterivian erosion (modified from Brown et al., 1995; McMillan et al., 1997; Broad et al., 2012; Baby et al., 2018; Muir et al., 2020).

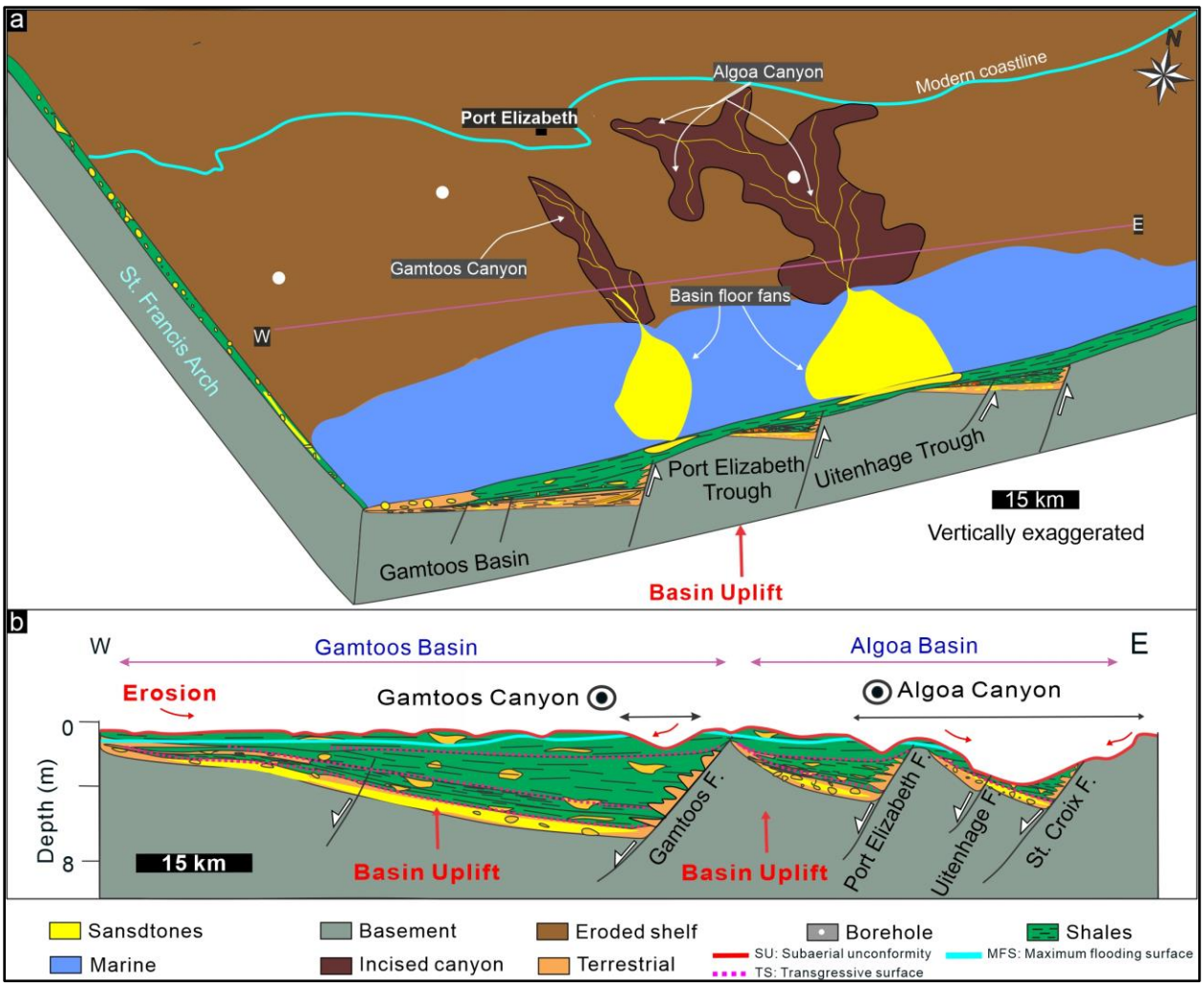

Figure 7.8: a Top Hauterivian to early Aptian GDE map during of a drop in RSL, as a response to the basin uplift, resulting in the Algoa and Gamtoos Basins and possible deposition of basin floor fans in the distal setting. **b** West-East cross section of the Algoa and Gamtoos Basins.

7.2.2 Post-Hauterivian to lower Albian ("Canyon fill")

In the Algoa Basin, this interval is intersected in boreholes HB-H1, HB-B1, HB-I1 and HB-C1 (Figure 5.9). Borehole HB-H1 in the Port Elizabeth Trough is dominated by very fine-grained, coarsening-upward sands and does not show any marine influence (Figure 5.9). Boreholes HB-B1, HB-H1 and HB-C1 on the other hand are dominated by low-energy sediments (possibly marine), with very limited sand input (Figure 5.9). However, unlike boreholes HB-B1 and HB-I1, in which isolated thin, very fine coarsening-upward sands are present, borehole HB-C1 is sand free, and thus can potentially indicate a marine setting in the Uitenhage Trough, at a time when the Port Elizabeth Trough was dominated by fluvial processes. In the Gamtoos Basin, this interval is intersected by borehole HA-A1, which shows an overall non-graded profile,

consisting of coarsening- and fining-upward units (Figure 6.9). “Canyon fill” isopach map in the Algoa Basin depicts a NW-SE trending depocenter, within which sediments thicken towards the SE (Figure 5.17). The base of this succession onlaps onto the Top Hauterivian reflector, indicating a period of increasing accommodation space, whereas the upper succession is dominated by channel accretion geometries in the canyon (Figures 7.9 and 7.10). Basal onlapping stratal geometries on the Top Hauterivian reflector indicate a landward moving shoreline due to possible increased accommodation space linked to a presumed rise in RSL (Figure 7.10). The upper “Canyon fill” is dominated by channel incisions and infill followed by clinoforms prograding to SE, which were deposited during normal regression. In the Gamtoos Basin, “Canyon fill” sediments are confined and laterally limited, and appear to show lateral accretion W, which may have been a possible sediment entry point (Figure 6.19). These eastwards prograding clinoforms appear to be eroded by a younger channel indicating an increase in environmental energy and concomitant shift from marine to fluvial conditions.

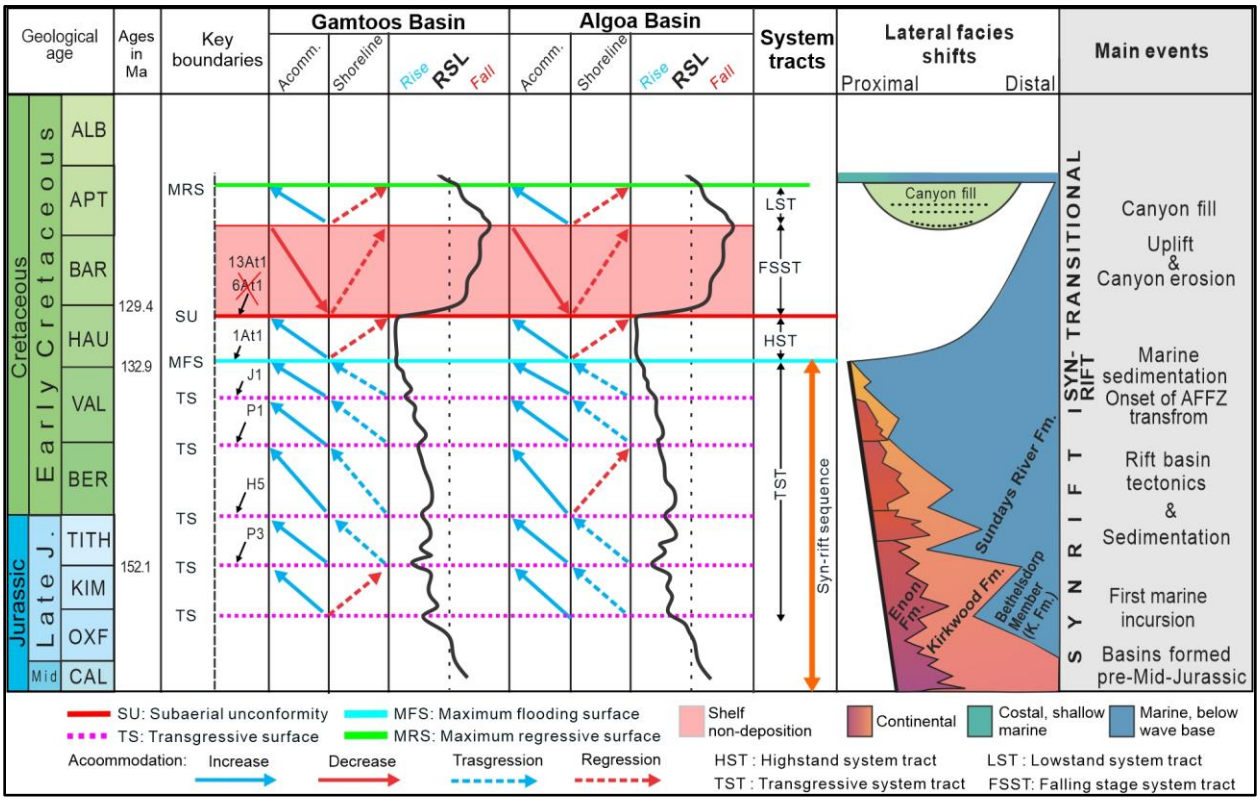

Figure 7.9: Relative sea level curve during the early Albian “Canyon fill”, due to increasing RSL (modified from Brown et al., 1995; McMillan et al., 1997; Broad et al., 2012; Baby et al., 2018; Muir et al., 2020).

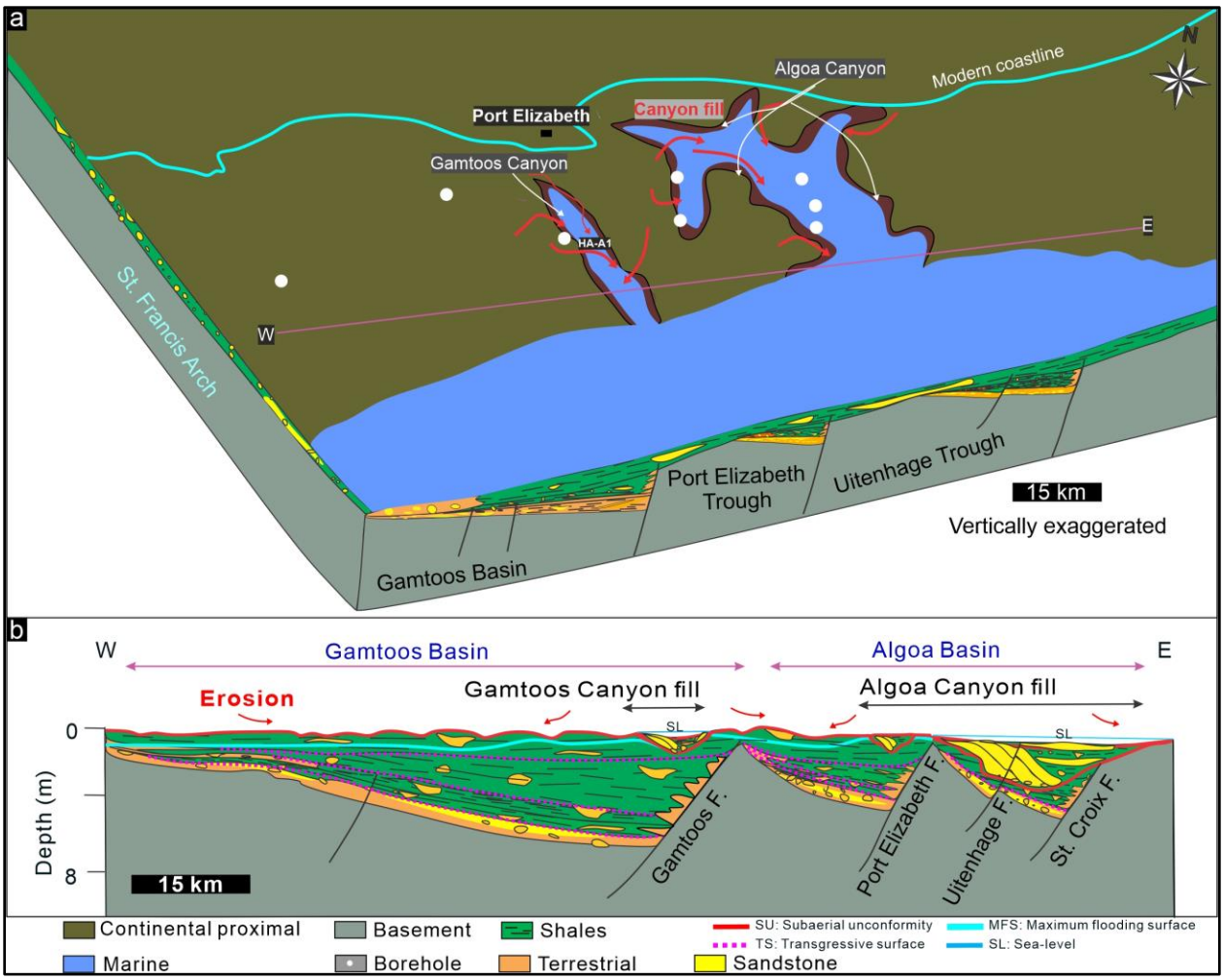

Figure 7.10: a Albian "Canyon fill" GDE map, showing increasing accommodation space in the Algoa and Gamtoos Basins. **b** West-East cross section of the Algoa and Gamtoos Basins.

7.3 Syn-rift to transitional phase sequence stratigraphic models

7.3.1 Analogue

Like every rifting system, the Algoa and Gamtoos Basins developed in a continental setting during the Early Jurassic (McLachlan and McMillan, 1976; Dingle et al., 1983; Malan, 1993; Ben-Avraham et al., 1993; Baby et al., 2018; Muir et al., 2020). However, during the Mid (possibly latest Early) Jurassic (Muir et al., 2020) rifting in the Outeniqua Basin advanced, with the orientation of the faults in the basin supporting the N/NE-S/SW extension and separation from South America (Lovecchio et al., 2020). During the Middle to Late Jurassic, the Outeniqua Basin was part of a failed rift (analogous the North Sea Viking Graben), which formed as part of a triple junction during the breakup of the eastern half of Gondwana (Jungslager,

1996 his figure 14). Basin fill in these rift types (Bosworth and Burke, 2005 their fig.8) are typically influenced by Milankovitch cycles, with RSL changes contending with sediment supply (Gawthorpe and Leeder, 2000). Although there is no perfect modern-day analogue for this type of rift, the closest analogue is the Gulf of Suez, in which rifting was initiated during the Oligo-Miocene period (Gawthorpe and Leeder, 2000; Bosworth et al., 2005; Bosworth and Burke, 2005 their figs.3-12). Similar to the Outeniqua Basin during the Middle (or earlier) Jurassic, the Gulf is assumed to have formed during flooding when the Red Sea opened, and thus marine sediments in the Gulf of Suez predate the rifting phase (Gawthorpe and Leeder, 2000; Bosworth et al., 2005; Bosworth and Burke, 2005 their figs. 3-12). Evidence of marine setting in southern Africa during the Late Jurassic is documented in the Falkland Plateau Basin, where Schimschal and Jokat (2019) argue for a possible MOR below the Tithonian marine sediments. The prograding clinoforms in the Gamtoos Basin suggests that the marine incursion in the Gamtoos Basin occurred sometime before the Top Kimmeridgian (possibly Middle Jurassic). Although these marine influenced rifts might become isolated from the main ocean bodies during lowstand, resulting in restricted environments (Gawthorpe and Leeder, 2000), the Outeniqua Basin and the Gulf of Suez are not associated with a restricted, laterally extensive lacustrine environment during syn-rift (such as those observed in EARS– e.g., Chorowicz, 2005). This implies that the Middle Jurassic to Early Cretaceous rift system of the Algoa and Gamtoos Basins was in constant communication with global oceans (i.e., assuming increasing eustatic levels as the palaeo-Indian Ocean formed due to East Gondwana break-up; Jungslager, 1996).

A close modern-day analogue for Algoa and Gamtoos Basins during the Valanginian rifting episode is the Gulf of California transform margin, located between the Pacific and North America plates, in Guaymas Mexico (Figure 7.11). Similar to the Outeniqua Basin, the Gulf of California is a right-lateral transform margin (Alvarez et al., 2009), with sub-basins bounded by normal faults. The Gulf of California is also compartmentalised, and the alluvial to marine sedimentation appears to be controlled by basement outcrops (Figure 7.11). Due to compartmentalisation, each of the depocenter has a unique sedimentation style relative to the adjacent depocenters (Figure 7.11).

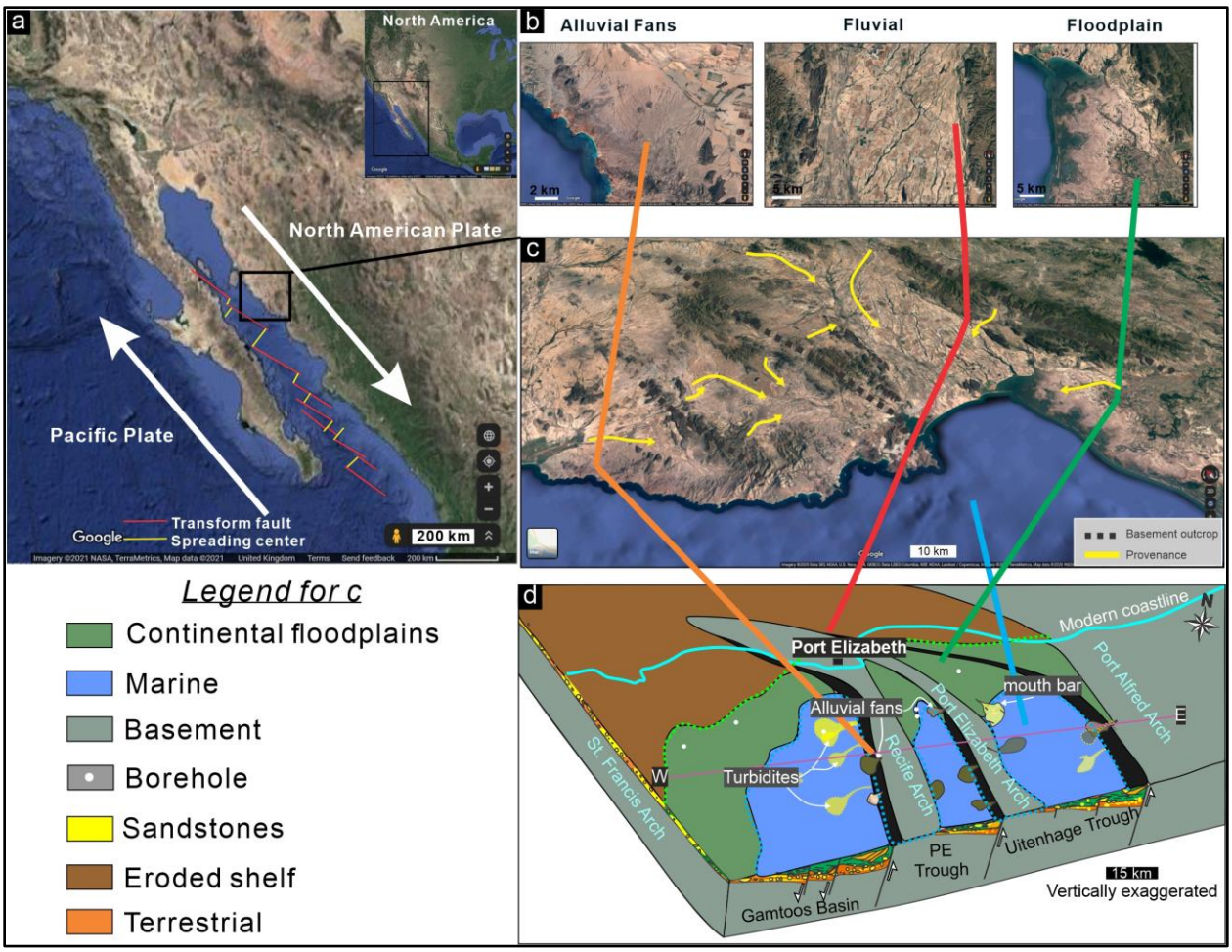

Figure 7.11: Modern-day analogue for the Valanginian deposition is the Gulf of California transform margin, located in Guaymas Mexico. **a** Tectonic element superimposed on Google Earth Image (adapted from Alvarez et al., 2009) show that the Gulf of California is a right lateral transform rift. **b** Geological environments associated with the Gulf if California transform margin. **c** zoomed-in ariel map of the analogue area. **d** Algoa and Gamtoos Basins GDE during the Early Cretaceous. See section 2.3 on outcrop images in the Algoa and Gamtoos Basin associated with the geological settings above. Base map data ©2020 Google, Maxar Technologies, AfriGIS (Pty) Ltd.).

A modern-day analogue, which best represent the Hauterivian to Aptian uplift and erosion is the Melville Island, Arctic Canada, where the shoreline is shifts basinwards due to the Holocene post-glacial isostatic rebound (Figure 7.12; Catuneanu, 2006, p. 187 his figs. 5.29; 5.30). In contrast to the isostatic rebound in the Melville Island, the uplift in the Outeniqua Basin shelf was related to the dextral AFFZ transpression motion, and resulted in the forced regression of the shoreline, canyon scours and sediment bypass on the shelf (Malan, 1993; Brown et al., 1995; Thomson, 1999; Paton and Underhill, 2004). The same sequence of events is detected in the Algoa and Gamtoos Basins (Figure 7.12).

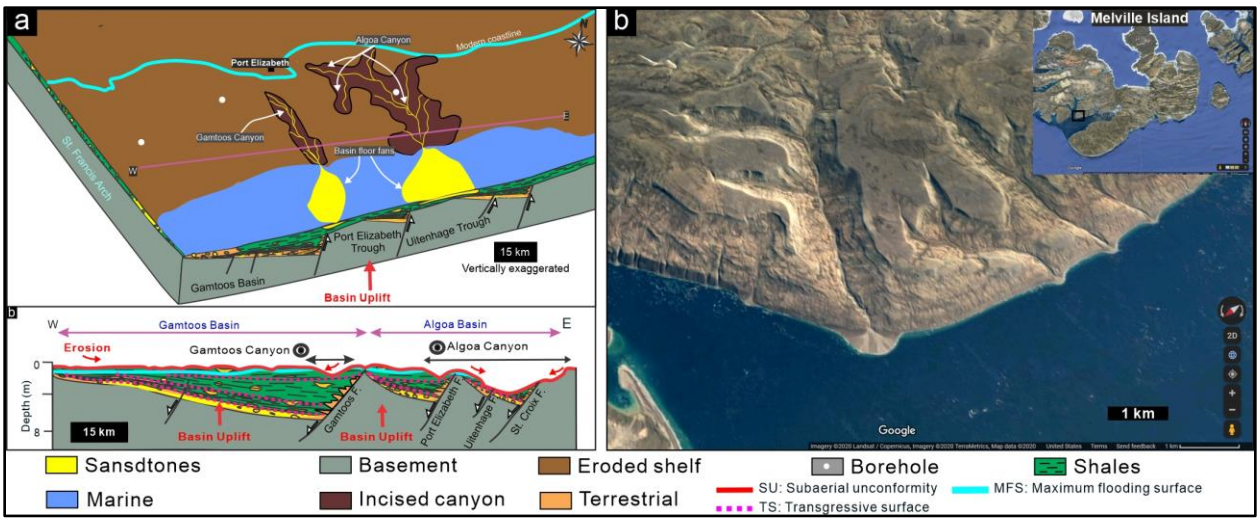

Figure 7.12: a Top Hauterivian to early Aptian GDE map during of a drop in RSL. **b** Melville Island, Arctic Canada as a modern-day analogue for the Hauterivian to Aptian uplift and erosion. Base map data ©2020 Google, Maxar Technologies, AfriGIS (Pty) Ltd.).

7.3.2 Stratigraphic models

7.3.2.1 Syn-rift phase: Aalenian to upper Valanginian

Lateral variability of syn-rift successions mostly results from the differential movements of syn-rift faults. This variability makes it challenging to use the passive margin-based system tracts to predict lateral facies changes in largely continental rift-basins (e.g., Prosser, 1993; Chorowicz, 2005; Holz et al., 2017). Current dataset, previous studies (e.g., Shone, 2006; Muir et al., 2020) as well as studies from the Falkland Plateau Basin (Schimschal and Jokat, 2019) collectively suggest that by Late Jurassic a marine system was established in this region and relative sea level changes started influencing the shoreline trajectories and near shore sedimentary processes. In the Algoa and Gamtoos Basins, the syn-rift sequence is dominated by the alluvial to fluvio-lacustrine Enon and Kirkwood Formations, which spans a depositional period from ~ 170 to about ~135 Ma (Muir et al., 2020). Considering the total average thickness of these units being a few thousand metres (Muir et al., 2017 a, b), it is very likely that their combined succession contains several subaerial unconformities (Sus). However, the detection of these unconformities remains elusive both in outcrops and in the sparse, low resolution subsurface data.

Given the foregoing, it is possible to assume a diachronous advancement of shoreline during the syn-rift until the Top Valanginian breakup unconformity (1At1), which can be classified as a second-order maximum flooding surface (MFS; i.e., high magnitude, low frequency event; e.g., Vail et al., 1977; Vail et al., 1991; Embry, 2009a, p. 59; Catuneanu, 2006, p. 327; Catuneanu, 2019a, b; Catuneanu and Zecchin,

2020). Rift basins are associated with short tectonic pulses, which create accommodation space (i.e., transgression), followed by periods of tectonic quiescence, which allow sediments to prograde (highstand) along the dipping hanging blocks (Martins-Neto and Catuneanu, 2010; Holz et al., 2017). Generally, in the syn-rift successions, formation tops are picked on flooding surfaces (wave-ravinement surfaces; Martins-Neto and Catuneanu, 2010; Catuneanu and Zecchin, 2020; Figure 7.13). Although it could be argued that these third order flooding surfaces in the Algoa and Gamtoos Basins may be MFSs (separating third-order HST and TST), the 1At1 unconformity marks the most landward position of the shoreline in the syn-rift succession, and thus it is the higher rank (i.e., second-order) MFS (e.g., Catuneanu and Zecchin, 2020). In some instances, rift systems can be associated with progradation due to high sedimentation rates, however, increasing accommodation space, due to syn-depositional faulting, eventually results in a basin wide transgressive shoreline (Martins-Neto and Catuneanu, 2010; Holz et al., 2017). Therefore, the low-order/higher rank (low frequency, high magnitude) RSL increase is accompanied by high-order/lower rank transgressive and regressive (e.g., Milankovitch) cycles. Consequently, the syn-rift interval in this study does not contain the "traditional" system tracts as observed in classical depositional sequence models, which were derived from passive margin setting (Martins-Neto and Catuneanu, 2010; Holz et al., 2017).

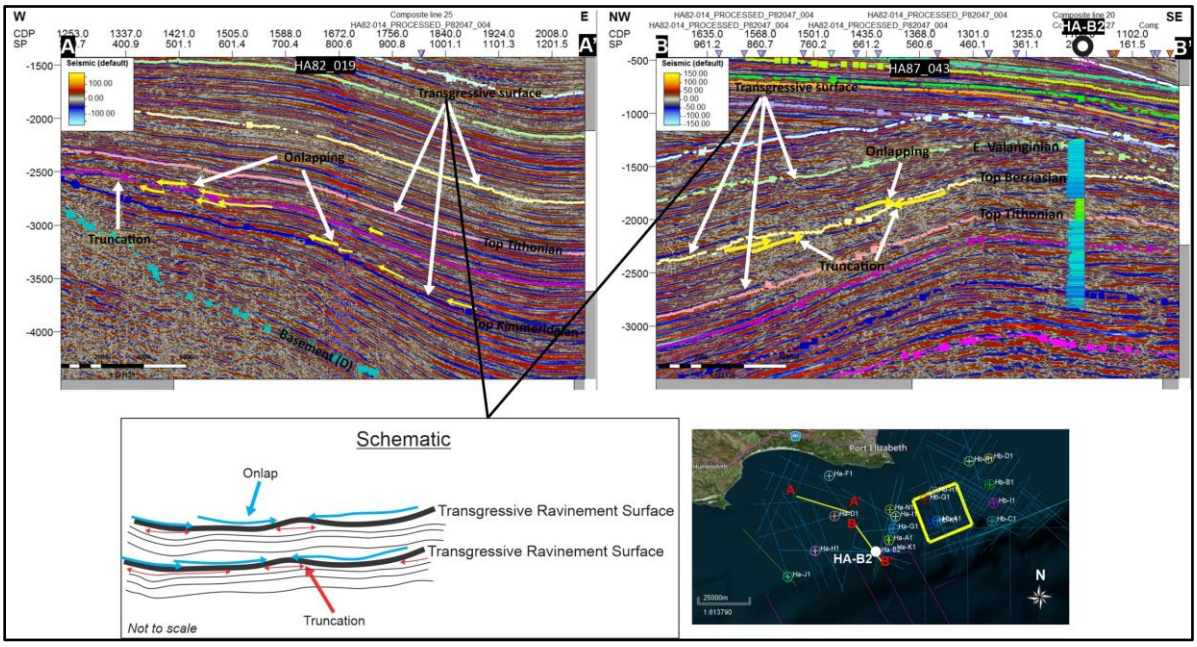

Figure 7.13: Transgressive ravinement surface observed at the end of syn-rift sequence boundaries (i.e., Top Kimmeridgian, Top Tithonian, Top Berriasian), indicating an advancing shoreline accompanied by wave scouring.

Correlating the syn-rift sequences across the Algoa and Gamtoos Basins is challenging, because these successions are laterally constrained by paleo-basement heights due to compartmentalization common in rift basins (e.g., Chorowicz, 2005). The dominant fluvial system in rift basins is controlled by the dipping landscape towards the main faults or paleo-basement highs (Martins-Neto and Catuneanu, 2010). However, as RSL continues to increase, sedimentation becomes more dominant towards the proximal setting, leaving the distal footwalls in the deeper waters sediment starved (Martins-Neto and Catuneanu, 2010). Also, the alluvial, fluvial and lacustrine deposits, due to their inherent laterally and vertically heterogenous nature make the correlation of rock units from one well to the other nearly impossible (e.g., Nádor and Sztanó, 2011). The absence of easily detectable, laterally continuous SUs within the subsurface syn-rift succession limits the use depositional sequence models II, III and IV and T-R sequence model, which depend on the recognition of SUs as sequence boundaries (Catuneanu, 2006; Embry et al., 2007; Catuneanu et al., 2011; Catuneanu, 2019a, b). Holz et al. (2017) proposed the concept of tectonic system tracts, however their model assumes the development of shallow to deep rift lakes during early syn-rift phase. Although there is evidence of lacustrine environment during the deposition of the Kirkwood Formation (Muir et al., 2017b), there is no evidence to suggests that this lacustrine setting occupied the whole half-graben (rift basin) (such as those in the East African Rifts System – e.g., Chorowicz, 2005). Since the above models are limited for explaining the syn-rift evolution in the Algoa and Gamtoos Basins, the question remains: which other model best fits the data in this area? Galloway's (1989) genetic sequence stratigraphic model, in which sequence boundaries are defined by the transgressive MFS unconformity (also known as the breakup unconformity in syn-rift successions – e.g., Holz et al., 2017) is the only model that closely matches the observations in the study area. However, contrary to Galloway's (1989) model, in which both the basal and top sequence boundaries are MFSs, the base of syn-rift is typically a SU atop of the basement rocks (i.e., "rift onset unconformity" in Falvey, 1974 or "syn-rift unconformity" in Bosence, 1998). In the Galloway's model, where MFS are used as sequence boundaries, the SU is included within the succession and is thus not a sequence boundary (*sensu* Vail et al., 1977; Mitchum et al., 1977; Posamentier et al., 1988). It has been repeatedly shown that stratigraphic boundaries should not only be limited to SUs, but to surfaces that mark a full cycle of genetically related sequences (e.g., Catuneanu 2019a,b; Catuneanu and Zecchin, 2020). In this way, the genetically related facies of the syn-rift succession is bound by the key stratigraphic surfaces (e.g., SU at the base, transgressive ravinement surfaces, MFS; Figure 7.14) that satisfy the upper half of Galloway's model, without being limited to SUs as stratigraphic boundaries. The Galloway model does not include system tracts of the conventional depositional sequence models and omitting system tracts limits lateral facies prediction in sequence stratigraphy.

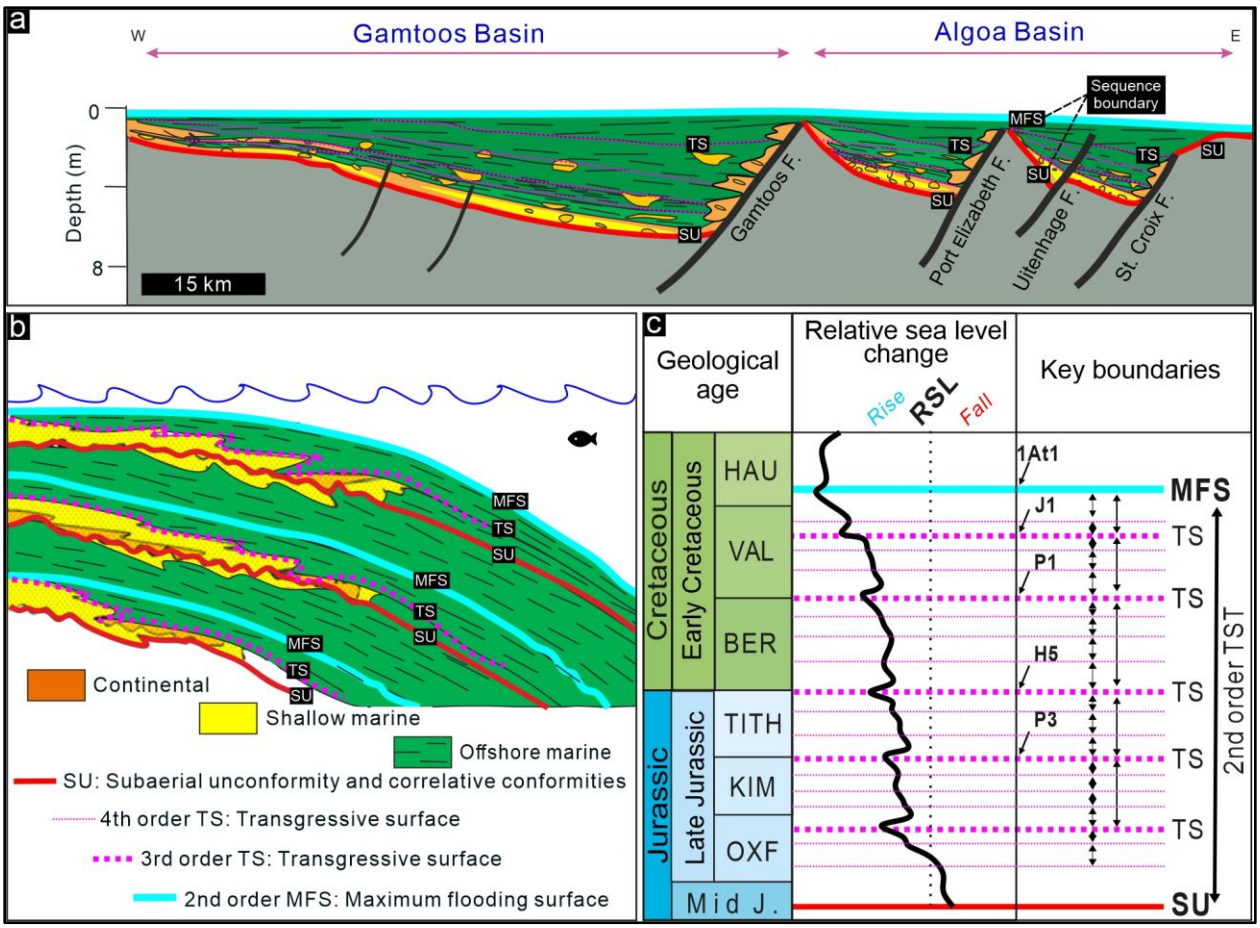

Figure 7.14: a Simplified cross-section of the syn-rift sequence in the Algoa and Gamtoos Basins, showing the main stratigraphic surfaces. **b** Summary of Galloway's model (1989), which is a genetic sequence stratigraphic model approach that uses the maximum flooding surface (MFS) as sequence boundary (modified from Embry et al., 2007). **c** RSL curve and the associated system tracts and their bounding surfaces in the Algoa and Gamtoos Basins.

7.3.2.2 Transitional phase: post-Valanginian to early Albian

This interval represents sediments that were deposited during reduced (negative) accommodation space in the Algoa and Gamtoos Basins, when, due to regional uplift, the RSL dropped and the shoreline regressed (McLachlan and McMillan, 1976; Malan, 1993; Brown et al., 1995; Thomson, 1999; Paton and Underhill, 2004). The strata of this infrequently preserved succession overlie the low order 1At1 MFS, are dominated by clinoforms that prograde towards SW, and show coarsening-upward and non-graded trends in boreholes HB-B1, BA-J1 and HA-A1. These observations suggest a high stand system tract (HST) between the low order 1At1 MFS at the base and the low order 13At1 SU at the top (Figure 7.7). The regional uplift event, which resulted in the 15At1 sequence boundary was triggered by dextral motion along the AFFZ (Malan, 1993; Brown et al., 1995; Thomson, 1999; Paton and Underhill, 2004). This period of uplift, which

lasted from the early Aptian to late Hauterivian (6At1 to 13At1), resulted in the Algoa and Gamtoos Canyons and other erosional features across the shelf area in the region (Bate and Malan, 1992; McMillan et al., 1997; Broad et al., 2012). In contrast to the older syn-rift sequence, the thickness maps (Figures 5.17 and 6.11) show depocenters that do not follow the geometry of the underlying structure. This suggests that the basin infilling during this period was primarily driven by RSL changes, as a function of eustatic sea level change and the motion of AFFZ (Dingle et al., 1983; Ben-Avraham et al., 1993; Malan et al., 1990; Brown et al., 1995; McMillan et al., 1997; Broad et al., 2012; Baby et al., 2018), and less dependent on the Cape Supergroup anisotropy. Moreover, during this period of uplift and erosion, the shoreline retracted towards the distal setting, while the inner to middle shelf was a place of bypass. Because this basinward shoreline shift was primarily driven by the regional uplift, independent of sediment supply, a case for forced regression can be made (Figure 7.8; Hodgson et al., 2018 their fig. 10b), and the processes associated with long lived falling stage system tract (FSST) are expected to have occurred. Therefore, it is expected that in the continental portion (i.e., northern half) of the basin low order SUs were generated, whereas in the marine portion (i.e., southern half) of the basin, sediments bypassed on the shelf and became deposited as high-density, basin-floor fans (e.g., Hunt and Tucker, 1992, 1995; Helland-Hansen and Gjelberg, 1994; Plint and Nummedal, 2000; Catuneanu, 2006, p. 178). Consequently, high potential for the development of reservoirs is expected outboard of the study area. It is noteworthy that this uplift and associated basinal deposition are similar in overall mechanism and age to processes that led to the formation of the hydrocarbon-bearing rocks in the Outeniqua Basin (i.e., Brulpadda and Luiperd discovery in Block 11B/12B; Africa Energy Corp, 2020).

The Aptian to early Albian “Canyon fill” sediments in the shelf overlie the FSST and are characterized by fluvial incisions and prograding stratal geometries (Figure 7.10). These “Canyon fill” sediments are bound by a subaerial uniformity at the base and a transgressive surface at the top (Figures 7.9 and 7.10). These observations are consistent with the definition of the lowstand system tract (LST) on the shelf (Figures 7.9 and 7.10; Catuneanu, 2006 his fig. 5.6) in depositional models II, III and IV. Although there are some low-density basin floor fans that might form during the normal regression, most of the sediments are trapped in the incised valleys during the LST, such as those in the Algoa and Gamtoos Basins. This is because sediments, before making their way to the distal part of the basin, first tend to fill in the proximal topographic irregularities (i.e., nearshore incised valleys) that were carved out during the forced regression (Catuneanu, 2002, 2006). Boreholes HB-B1, HB-I1 and HB-C1 in the Algoa Canyon are characterized by very fine-grained, silty to shaley sediments that formed during this phase of deposition.

The sediments deposited in the incised canyons appear to be dominated by fine grain sizes and small channels with a low net sand-to-shale ratio, and thus are unsuitable as hydrocarbon reservoirs. The more proximal borehole HB-H1 is dominated by clean sandy facies near the canyon head, however these sandy facies (likely bay-head deltas) do not appear to extend toward the distal part of the Algoa Canyon. The Top Canyon reflector marks a maximum regressive surface (MRS), overlying “Canyon fill” sediments that were generated during normal regression.

7.4 Drift phase: upper Albian to Holocene

This interval marks a fully marine influenced setting, where both the Algoa and Gamtoos Basins were hydrologically in communication and became the shelf of the Indian Ocean. Contrary to syn-rift succession, where sedimentation was primarily influenced by syn-rift faults and constrained by basement highs, basin fill in the drift phase is controlled by accommodation space created as a function drift phase thermal subsidence and sediment input. Although the drift phase assumes the geometry of a passive margin, post transitional phase, there are two major uplifts observed in the basins during the Santonian to Late Cretaceous (Malan, 1993) and during late Paleogene (Hattingh, 2001; Baby et al., 2018).

7.4.1 Post-Hauterivian/”Canyon fill” to upper Albian

This interval represents the first succession to be deposited over both the Algoa and Gamtoos Basins post the Top Hauterivian erosional event (Figure 7.15; McMillan and McMillan, 1976; McMillan et al., 1997). This late Albian interval is dominated by inner to middle shelf marine foraminifera (McMillan et al., 1997). In the Algoa Basin, this interval is intersected by boreholes Hb-C1 and Hb-I1, both boreholes indicating a regressive shoreline, evident by the overall coarsening-upward sequences (Figure 7.15). The base of this regressive sequence in borehole Hb-C1 is dominated by low energy clays and shales (flooding surface), overlain by clean sands. However, borehole Ha-A1 in the Gamtoos Basin shows aggradational, relatively high gamma ray readings, indicating the presence of low-energy sediments as opposed to the Hb-C1 borehole dominated by sandy facies. Borehole data suggests that the fill of the Algoa Basin is sandier than of the Gamtoos Basin, most likely because the Algoa Basin was closer to a paleo-source area (Figure 7.16).

The base Albian reflectors onlaps on the Top Canyon/Top Hauterivian reflector in the E-W direction, and progrades from the N direction. The basal onlapping stratal geometries represent a period of flooding in the basin, where RSL increase was higher than sediment input. These onlapping strata are overlain by prograding clinoforms indicating a regressive shoreline. Seismic and well data suggests a period of high sedimentation into the basin, which overwhelmed the RSL rise, resulting a normal shoreline regression. The upper Albian prograding clinoforms are truncated by the Top Albian reflector. However, the truncation appears to be a toplaps indicating possible proximal sedimentation limit (Figure 7.16).

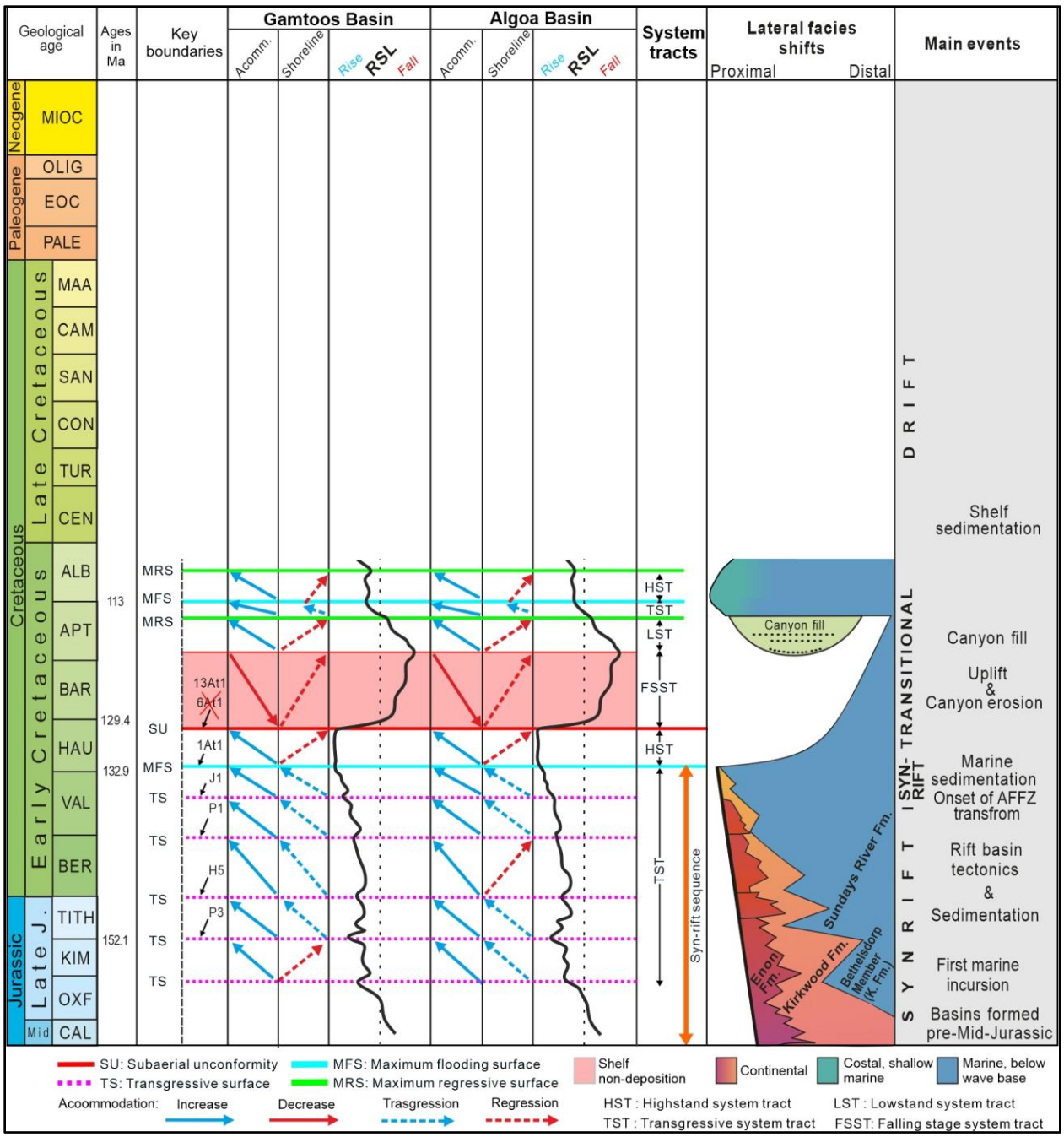

Figure 7.15: Relative sea level increasing steadily during the Albian. With both basins show evidence of a regressive shoreline due to high sedimentation on the shelf (modified from Brown et al., 1995; McMillan et al., 1997; Broad et al., 2012; Baby et al., 2018; Muir et al., 2020).

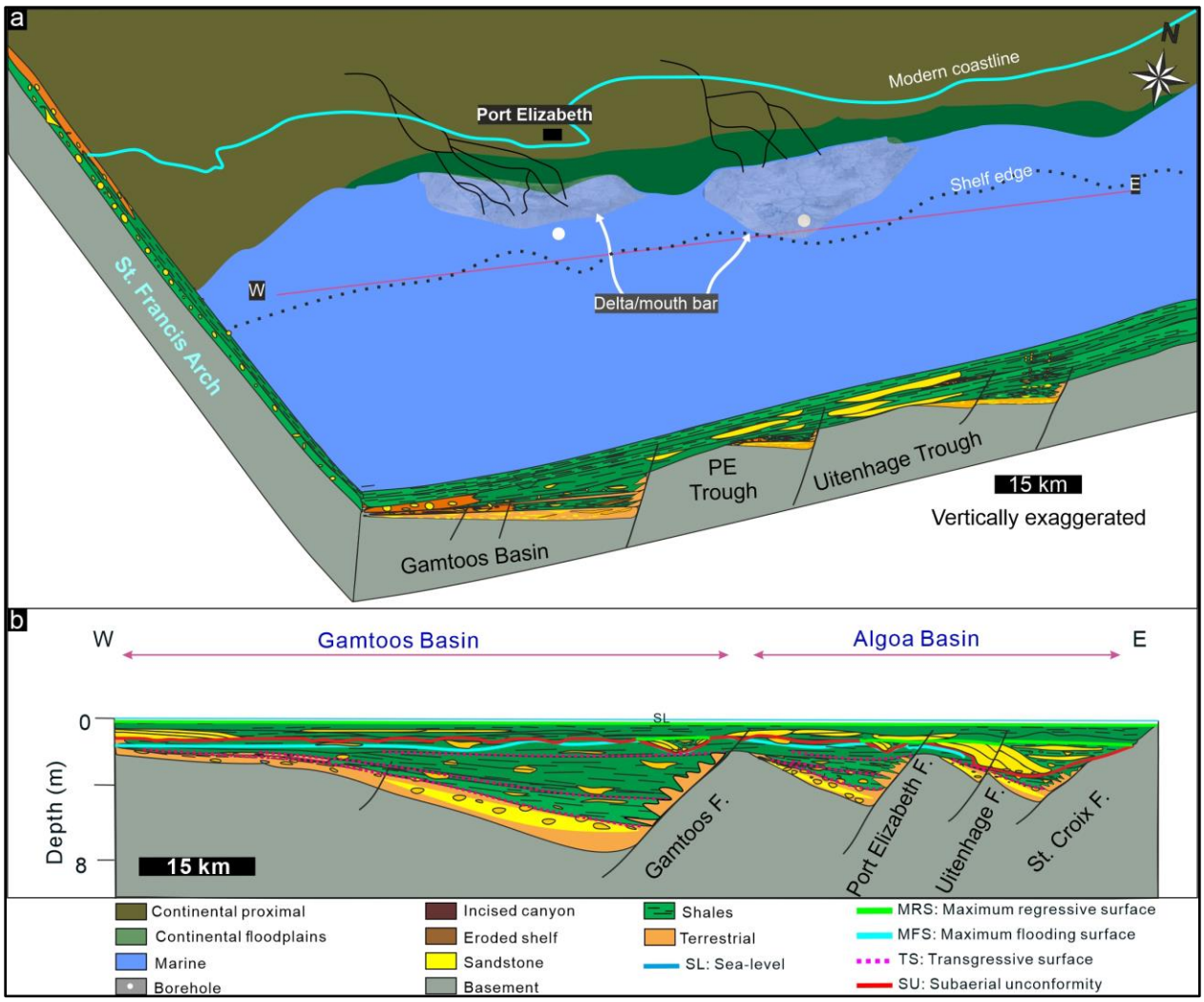

Figure 7.16: a Top Hauterivian/Top Canyon to Early Albian GDE map during a period of increasing accommodation space. **b** West-East cross section of the Algoa and Gamtoos Basin.

7.4.2 Post-Albian to upper Cenomanian (15At1)

In the Gamtoos Basin, this interval was most likely deposited on the shelfal setting, as suggested by the persistence of glauconitic claystones (McMillan et al., 1997). The lower portions of boreholes HB-C1 and HA-A1 are dominated by shaley facies, which were probably deposited during a flooding event after the Albian shoreline regression (Figure 7.17). In contrast, this interval appears to be sandier in the Algoa Basin, evident by the low GR readings in the distal borehole HB-C1 (and borehole HB-I1; McMillan et al., 1997). The base of this succession onlaps on the Top Albian reflector (more so in the distal setting) and is overlain by southward prograding clinoforms that downlap on the Top Albian reflector (more evident in the proximal setting). The onlapping stratal terminations and the flooding event overlying the Top Albian

boundary indicate a shoreline transgression during the early Cenomanian, which could be associated with an increasing RSL (Figures 7.17 and 7.18). The southward prograding clinoforms and sandy facies overlying the transgressive sediments indicate increased sedimentation rates causing shoreline regression in the late Cenomanian. These prograding clinoforms are truncated by the highly erosive Top Cenomanian (15At1) unconformity, which forms an irregular topography in seismic data indicative of strong incision (Figures 7.17 and 7.18). Towards the shelf edge, the Top Cenomanian unconformity is observed to erode into the syn-rift sequence. The uplift associated with this unconformity was accompanied by more than 100 m drop in sea level in the Outeniqua Basin (Baby et al., 2018). Whilst this Top Cenomanian erosional event did not result in as deeply incised canyons as the 13At1 erosional event, it left much of the shelf scoured. This means the shoreline was probably pushed towards the shelf edge sometime during the Late Cretaceous (Turonian to early Campanian?), resulting in shelf sediment bypass with a possibility of depositing the sands as basin floor fans (Figures 7.17 and 7.18). Although the source of this uplift is still uncertain (Baby et al., 2018), the 15At1 unconformity is thought to have been a result of thermal subsidence in the distal offshore, which caused uplift in the proximal setting (Malan, 1993).

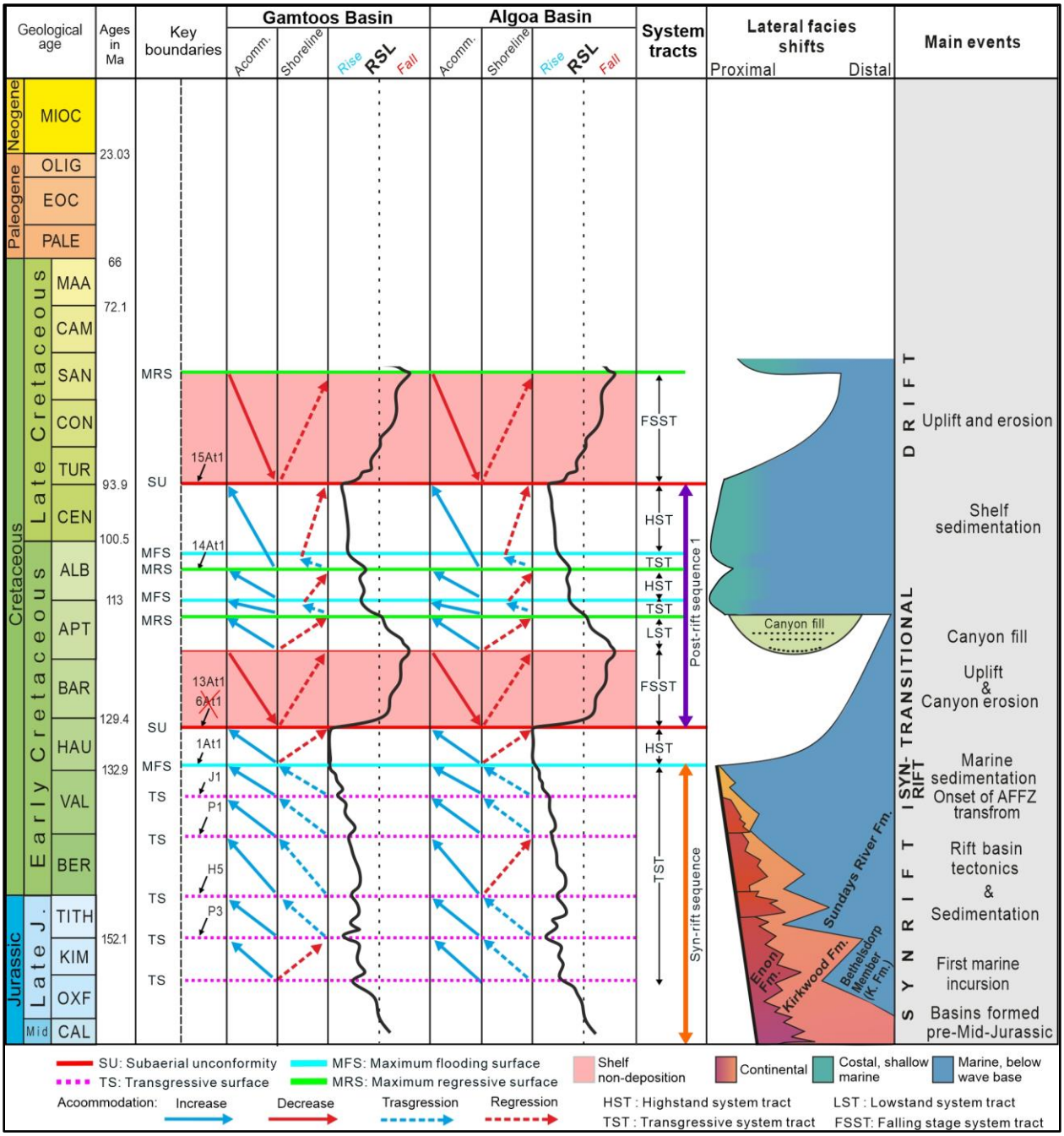

Figure 7.17: Relative sea level fall during the Late Cretaceous resulting in a forced regressive shoreline accompanied by shelf sediment bypass and basinwards deposition (modified from Brown et al., 1995; McMillan et al., 1997; Broad et al., 2012; Baby et al., 2018; Muir et al., 2020).

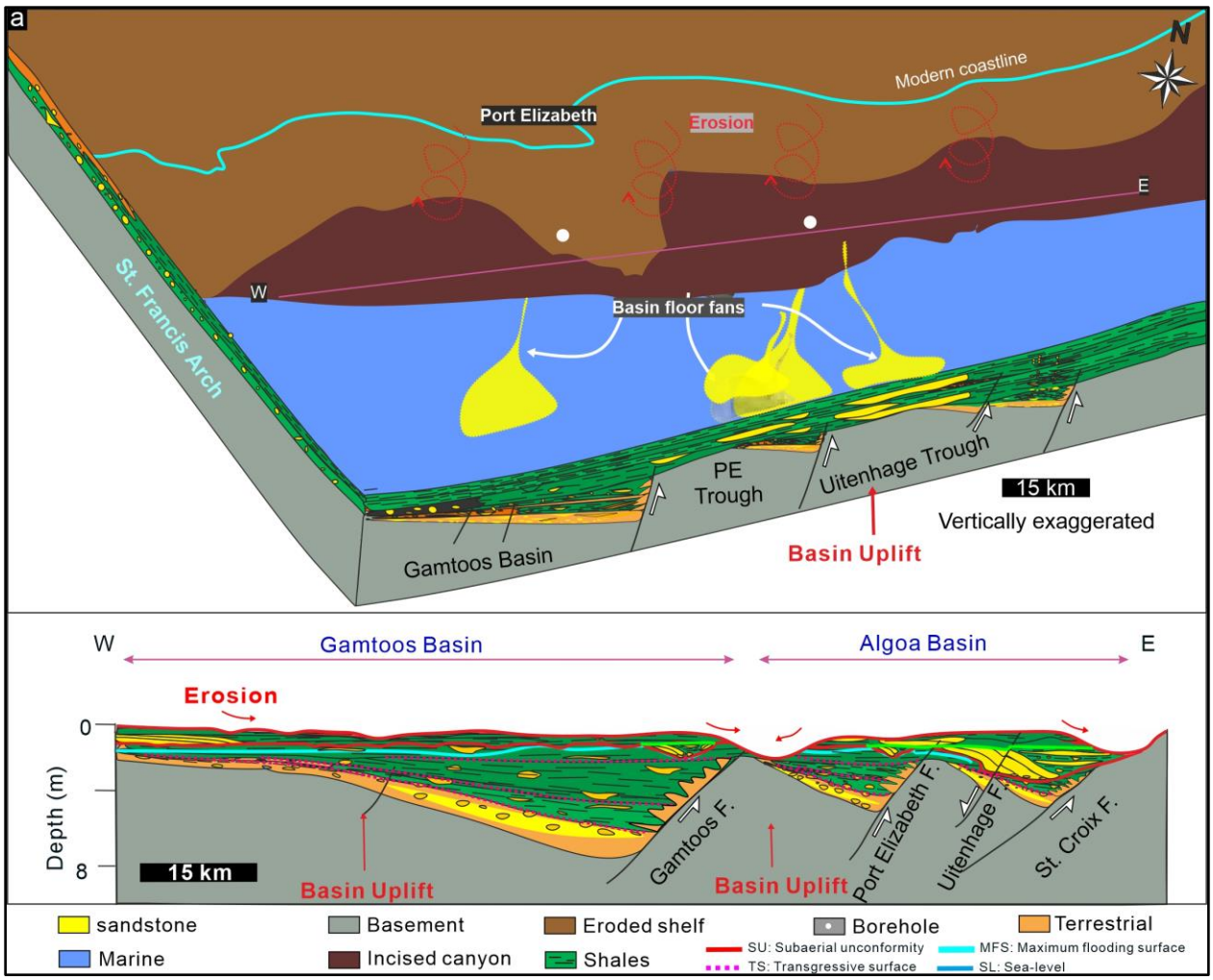

Figure 7.18: a Lower Cenomanian GDE during uplift and erosion of the shelf in the Late Cretaceous, which resulted in the 15At1 Top Cenomanian unconformity. **b** West-East cross section of the Algoa and Gamtoos Basins.

7.4.3 Post-Cenomanian (15At1) to Lower Cenozoic (22At1)

Overlying the Top Cenomanian reflector, clinoforms of the slope setting are prograding towards SE and indicate the position of the shoreline after the RSL fall (Figure 7.19). Relative sea level began to increase during the Late Cretaceous and in some places the shoreline appears to have moved onshore, a short distance N of the modern shoreline (Baby et al., 2018). This major transgressive period was caused by subsidence during the Campanian (McLachlan and McMillan, 1976; McMillan et al., 1997). The contact between the Upper Cretaceous and the Lower Cenozoic is gradational, and thus it is challenging to identify it on lithological grounds, however changes in microfauna from the Cretaceous and the Cenozoic are significant enough to diagnose this contact on biostratigraphic grounds.

In the Algoa Basin, the retrogradational stacking pattern in borehole HB-C1 points to a transgressive shoreline during the Late Cretaceous in contrast to the older progradational successions (i.e., regression from the Albian to the Top Campanian; Figure 7.19). According to Hattingh (2001), the Lower Cenozoic succession in the Algoa Basin was deposited during high sea level, which is consistent with the observations herein. The lack of fluvial deposits in the Algoa Basin from the Late Cretaceous to Early Cenozoic (Hattingh, 2001) could explain why this interval is relatively sand free. In the proximal setting, this high sea level caused a reduction in the gradient and eventual termination (drowning) of the fluvial system in the Algoa Basin (Hattingh, 2001). Although this interval is relatively thin, it is dominated by aggradational stacking of clinoforms, while the base of the succession onlaps on the Top Campanian reflector in the slope setting, representing a period of increased accommodation space (Figure 7.19). In contrast, in the borehole HA-A1 of the Gamtoos Basin, this interval shows evidence for a regressive shoreline, probably due to an active, nearby sediment source in this basin. Moreover, this succession mostly progrades and downlaps on the Top Campanian reflector without any obvious onlapping stratal terminations. Therefore, although RSL was increasing, sedimentation rates were high in the Gamtoos Basin, causing the shoreline to regress, while the Algoa Basin was undergoing transgression (Figures 7.19 and 7.20).

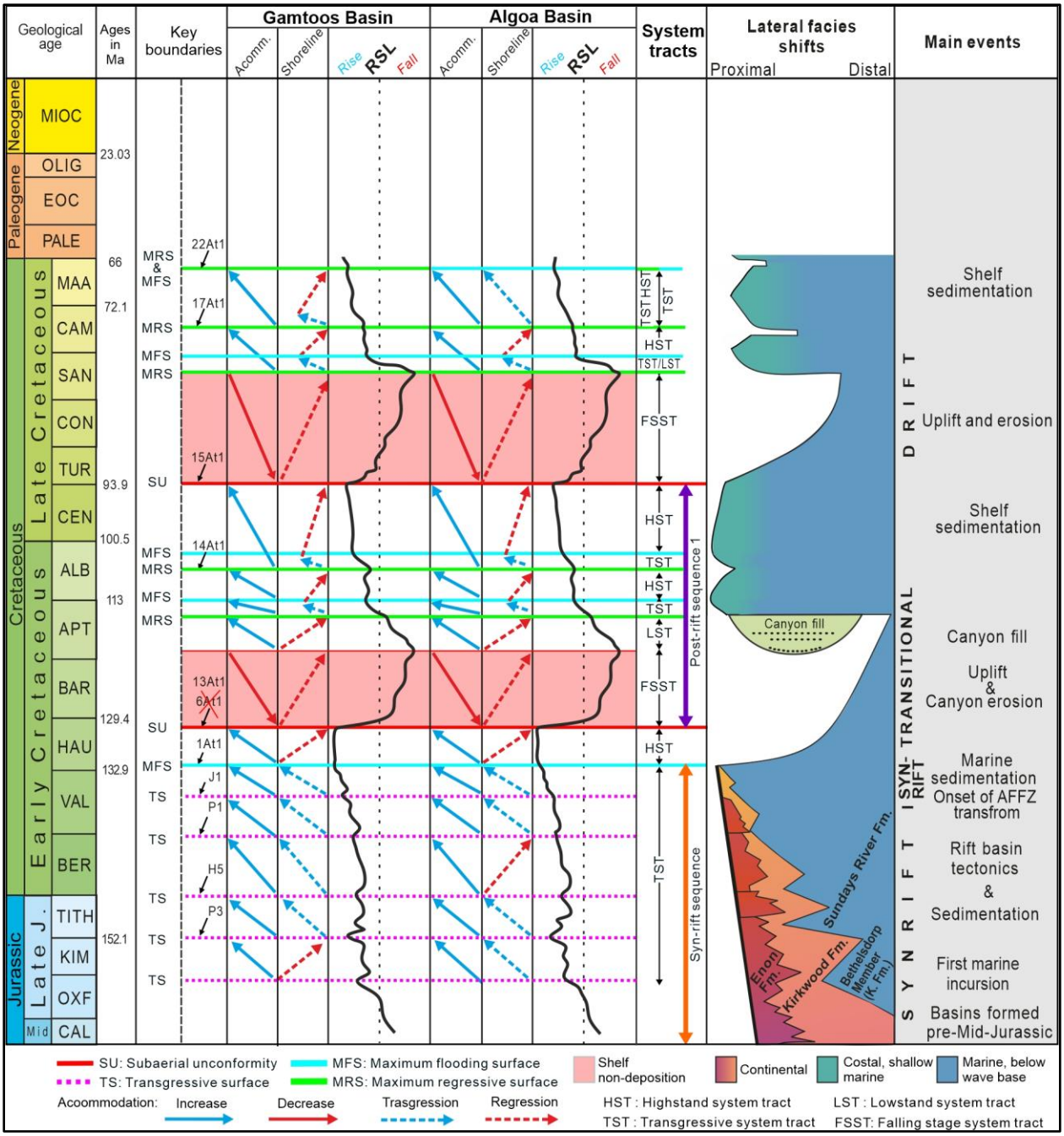

Figure 7.19: Relative sea level rise during the Late Cretaceous/Early Cenozoic, however, the Gamtoos Basin shows a regressive shoreline due to high sedimentation, while the Algoa Basin shows a transgressive shoreline (modified from Brown et al., 1995; McMillan et al., 1997; Broad et al., 2012; Baby et al., 2018; Muir et al., 2020).

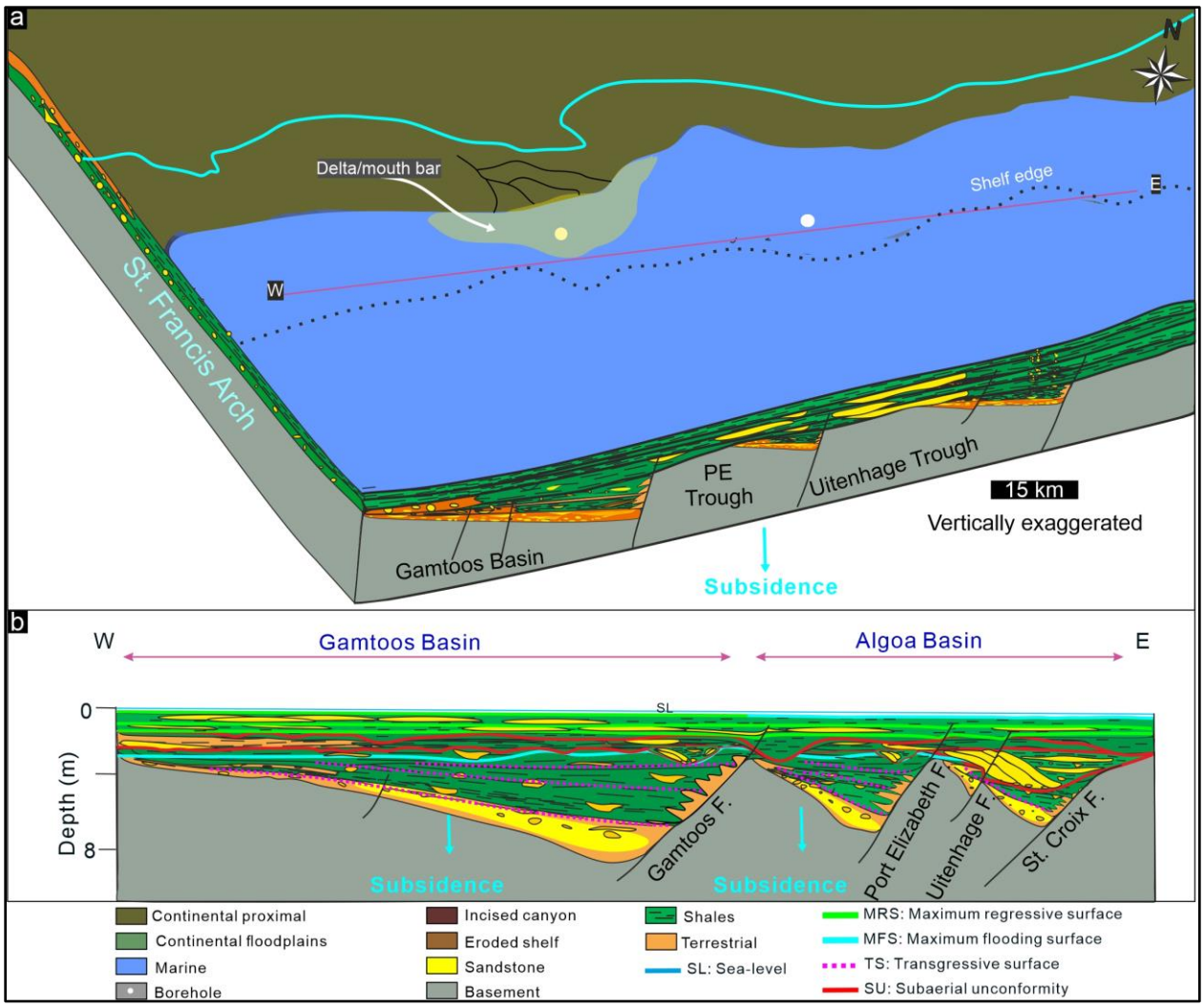

Figure 7.20: a Lower Cenozoic GDE map, showing a period of transgression in the Algoa Basin, while the Gamtoos Basin was undergoing shoreline regression. **b** West-East cross section of the Algoa and Gamtoos Basins.

7.4.4 Lower to Middle Cenozoic

This succession is associated with an uplift, which resulted in a major erosional event observed regionally on seismic data. This erosion was due to the second uplift of the Southern African Plateau and probably lasted from the Eocene to early Oligocene (Hattingh, 2001; Baby et al., 2018). This period of shelf scouring reactivated the fluvial system (notably the Baakens and Shark River valleys) in the Algoa Basin, which became more prominent after the Eocene uplift (Hattingh, 2001). This succession has been completely eroded onshore, where the Miocene Algoa Group unconformably overlay the Mesozoic succession (McMillan and McMillan, 1976; Du Toit, 1979; Le Roux, 1987, 1989, 1990, 1991, 1992, 2000; Illenberger, 1992; McMillan, 1990; McMillan et al., 1997; Hattingh, 2001; Broad et al., 2012; Roberts et al., 2006;

Claassen, 2014; Lockley et al., 2021). According to McMillan et al. (1997), this interval is thicker relative to the underlying Lower Cenozoic succession and is dominated by silty clays, however, borehole data (HB-C1) shows an overall coarsening-upward sandy unit, probably sourced from the reactivated fluvial system. Similarly, borehole HA-A1 in the Gamtoos Basin is also dominated by clean sandy facies throughout (Figure 6.9). The sand at the top of borehole HB-C1 could indicate a reactivated sandy sediment source in the Algoa Basin.

In both basins, shelfal seismic reflectors appear to prograde from N to S, and downlap on the Base Cenozoic reflector (Figures 5.30 and 5.24). Borehole and seismic data suggest a period of high sedimentation resulting in shoreline regression. This surface truncates the drift phase succession in a similar manner as the 1At1 unconformity truncates the syn-rift succession. However, this unconformity was caused by basin wide tilting (uplift) during the late Paleogene (Figures 7.21 and 7.22; Hattingh, 2001; Baby et al., 2018). This unconformity is also observed in Zululand Basin in the E and along the Atlantic margin in the W (Stevenson and McMillan, 2004; Baby et al., 2018). In the study region, tilting of the older rocks appear to be dominant along the N-S strike, with the northern side of the basin being highly eroded, which would explain the missing Upper Cretaceous succession onshore the Algoa and Gamtoos Basin (Figure 7.22).

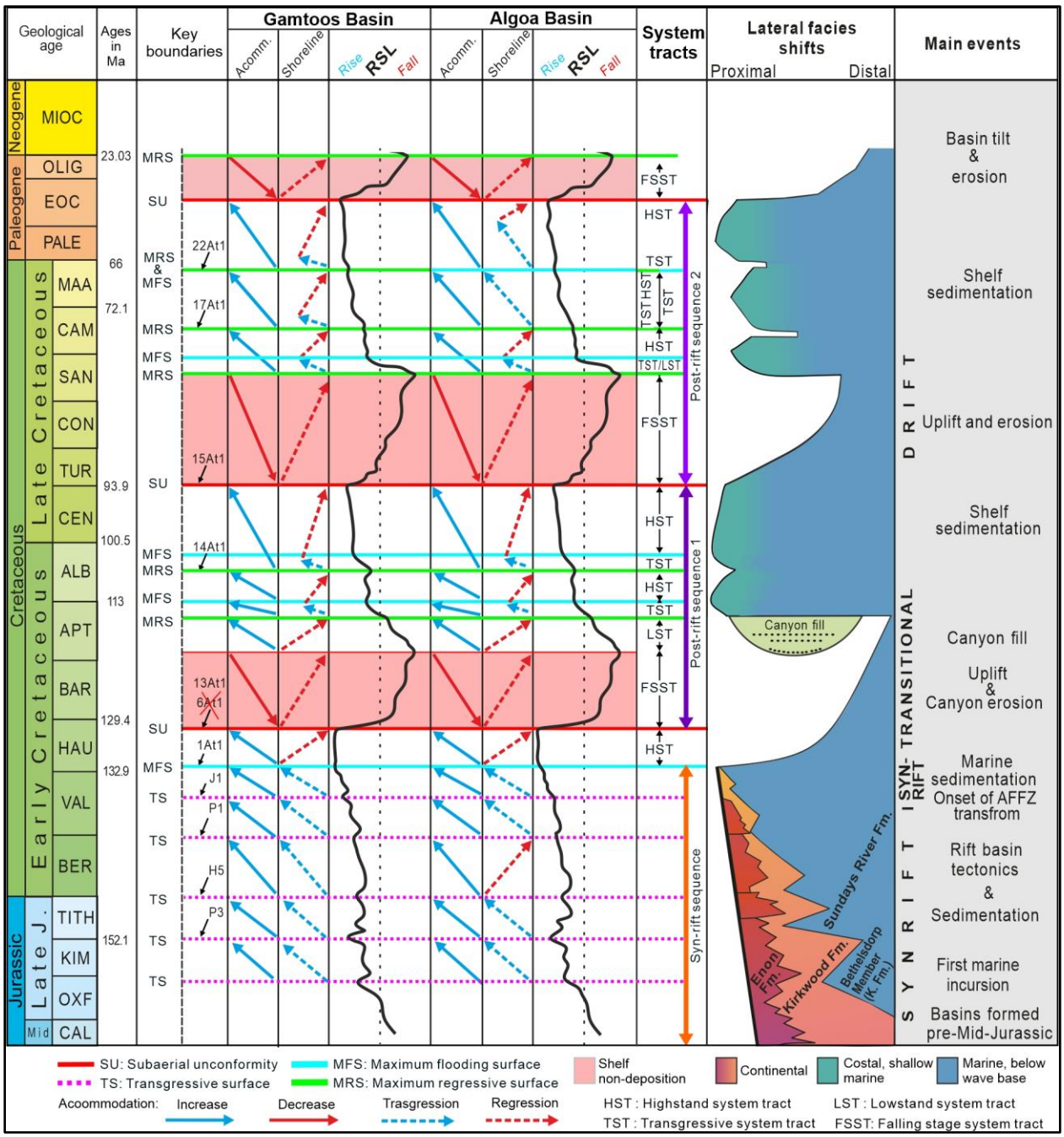

Figure 7.21: Relative sea level fall in the late Paleogene, as a result of basin tilt and uplift resulting in erosion in the Algoa and Gamtoos Basins (modified from Brown et al., 1995; McMillan et al., 1997; Broad et al., 2012; Baby et al., 2018; Muir et al., 2020).

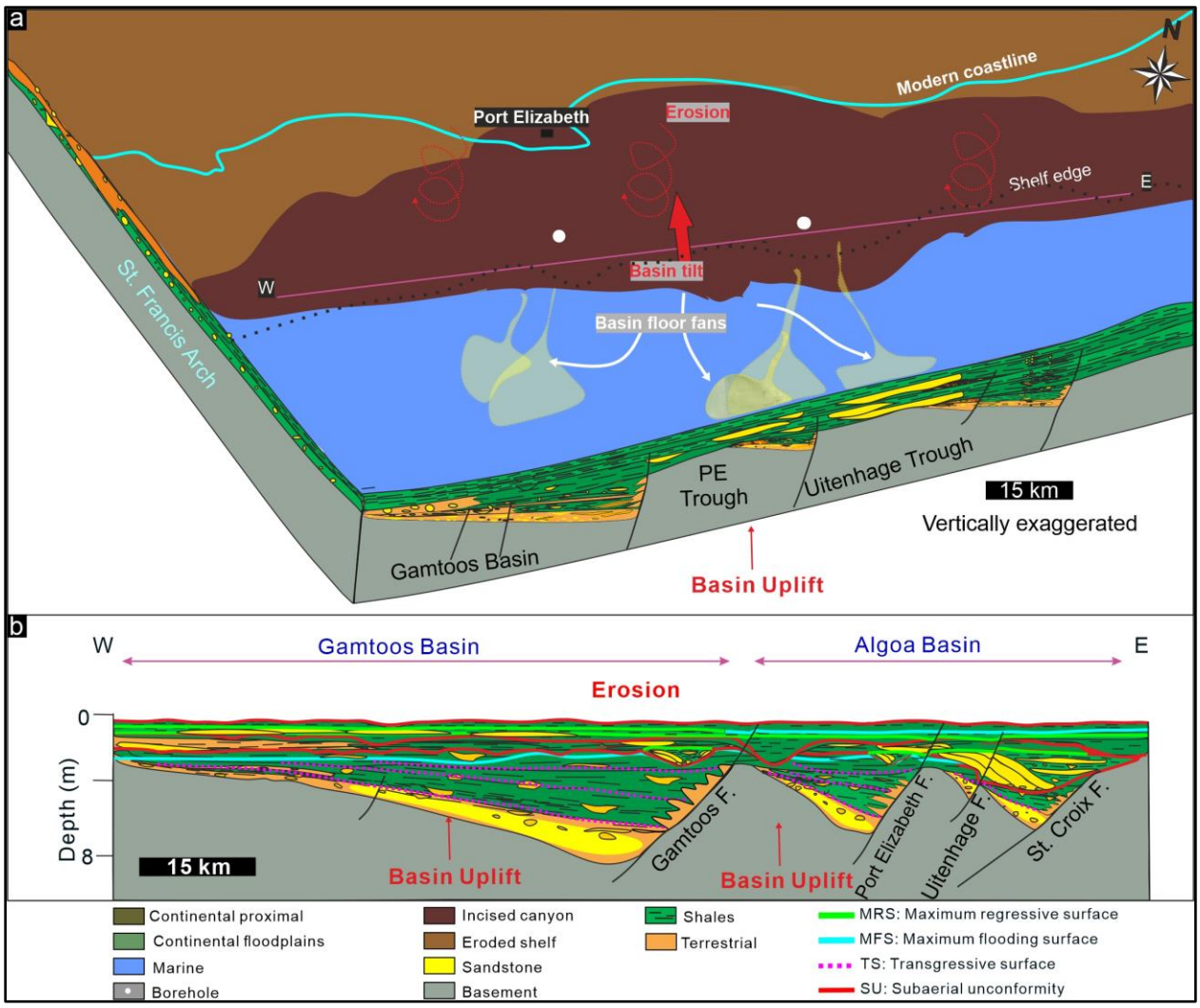

Figure 7.22: a Middle Cenozoic uplift and erosion depositional setting, which was a result of N tilting (Hattingh, 2001; Baby et al., 2018) of the basin. **b** West-East cross section of the Algoa and Gamtoos Basins.

7.4.5 Upper Cenozoic

Onshore, this interval is made up of the Algoa Group, consisting of successions deposited during glacio-eustatic sea level fluctuations (Le Roux, 1987, 1989, 1990, 1991, 1992, 2000; Illenberger, 1992; Roberts et al., 2006; Claassen, 2014). These Upper Cenozoic successions were deposited as a series of transgressive and regressive units in aeolian-to- coastal and shallow marine settings (Le Roux, 1987, 1989, 1990, 1991, 1992, 2000; Illenberger, 1992). After the Eocene to Oligocene uplift, onshore studies (e.g., Hattingh, 2001; Roberts et al., 2006) also suggest that the RSL increased to 300 m higher than the current sea level from the Late Miocene to Holocene, indicating the most landward position of the shoreline before it regressed to its modern-day position (Figures 7.23 and 7.24). This regression (forced?) was probably due to glaciations in the Pleistocene and was responsible for creating present day terraces onshore the Algoa Basin and high sedimentation on the shelf (Hattingh, 2001). The Eocene/Miocene transgression observed on dataset could be inferred to be associated with the limestones of the Bathurst Formation onshore the Algoa Basin. Unfortunately, much of the post-Oligocene succession is below seismic resolution for us to confidently correlate with onshore studies, with available wireline logs showing homogenous, non-graded low GR readings for this interval.

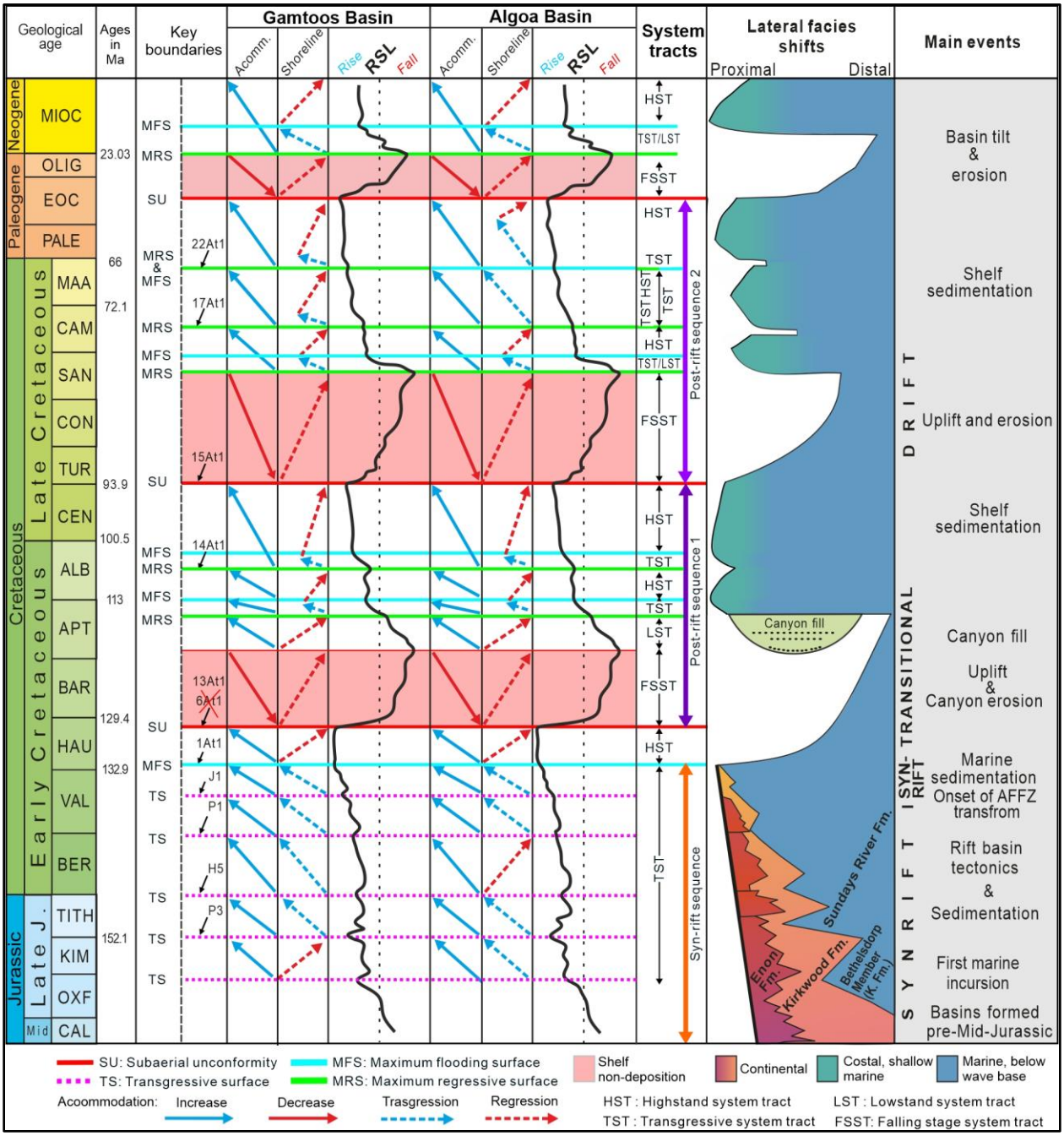

Figure 7.23: Relative sea level rise from the late Paleogene to Holocene in the Algoa and Gamtoos Basin*s* (modified from Brown et al., 1995; McMillan et al., 1997; Broad et al., 2012; Baby et al., 2018; Muir et al., 2020).

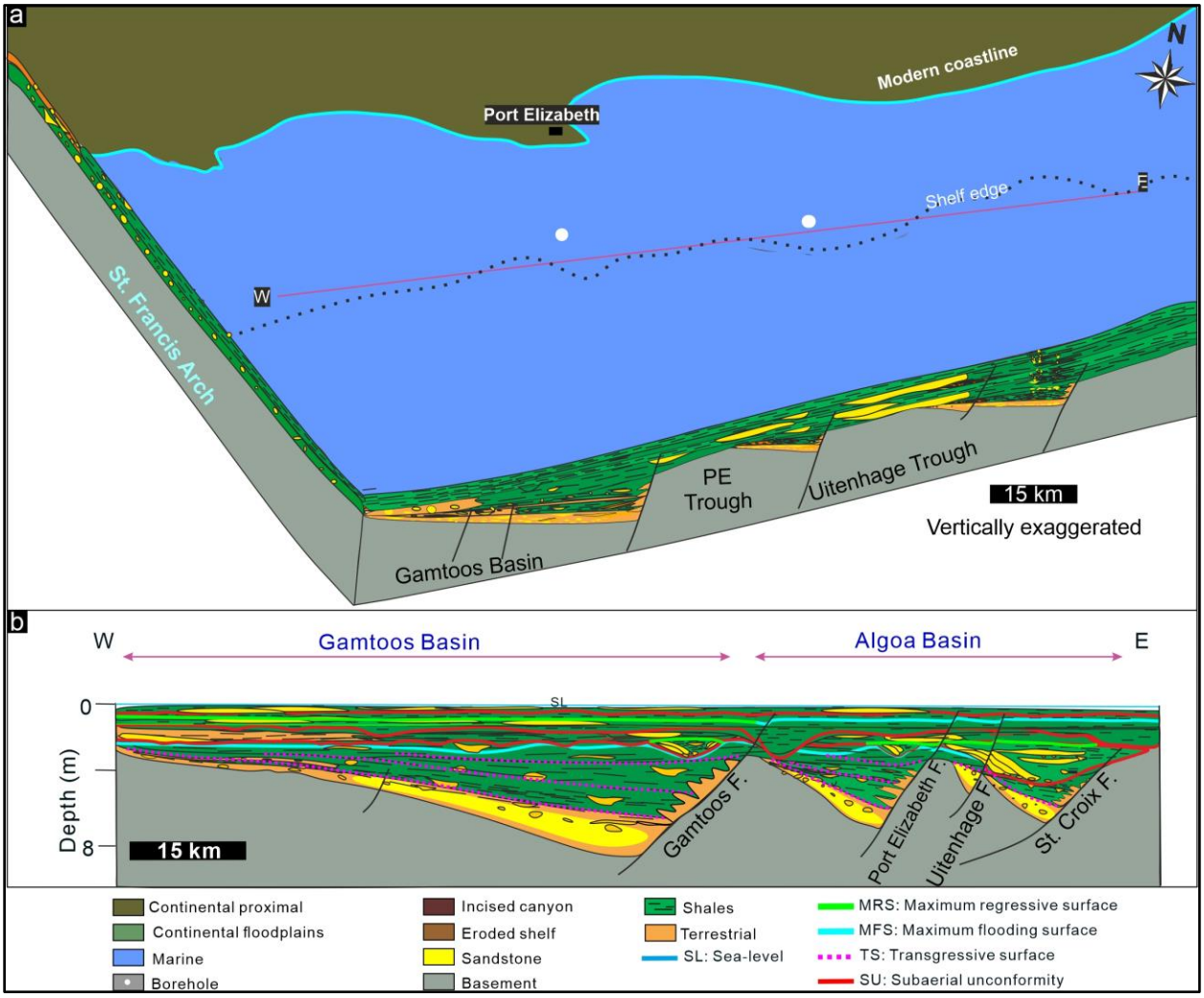

Figure 7.24: a Present-day shoreline position. **b** West-East cross section of the Algoa and Gamtoos Basins.

7.5 Drift phase sequence stratigraphic models

7.5.1 Analogue

The drift phase interval marks a period after the transgressional break-up unconformity, where deposition follows passive margin depositional trends, with basin tectonics having been predominately driven by thermal subsidence (McMillan et al., 1997; Cainelli and Mohriak, 1999; Gawthorpe and Leeder, 2000; Baby et al., 2018). The Outeniqua Basin assumed the passive margin geometry after the Falkland Plateau separated from Africa during the Cenomanian (McMillan et al., 1997; Baby et al., 2018). Basin fill in the drift phase is influenced by RSL change and sedimentation rates, and less dependent on the morphology of syn-rift shoulders (Figure 7.25; Baby et al., 2018).

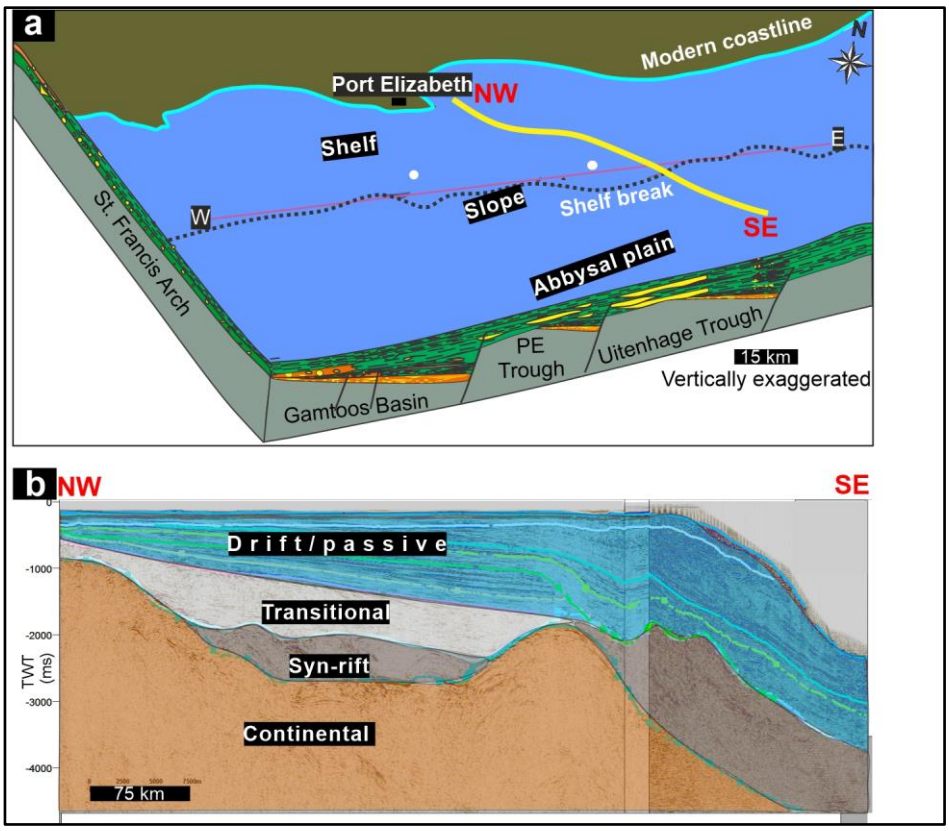

Figure 7.25: a Present-day topography in the Algoa and Gamtoos Basins. **b** NW/SE Arbitrary reflection seismic line (highlighted in yellow) across the Algoa Basin showing passive margin nature of the drift phase successions.

7.5.2 Stratigraphic models

7.5.2.1 "Canyon fill" (lower Albian) to upper Albian

The Top Canyon MRS is overlain by thin (below seismic resolution), lower Albian transgressive system tract (TST; observable at the base of boreholes HB-B1 and HA-A1 as high GR, fining-upward shaly facies), which are then overlain by prograding, normal regressive units (i.e., HST), which mark the Top Albian (Figure 7.15). It has been repeatedly shown that system tracts can form independent of scale and that seismic data might not always resolve high frequency sequence boundaries (e.g., Catuneanu, 2019a, b; Catuneanu and Zecchin, 2020). Unlike the products of an idealized, full relative sea level cycle comprising of fully developed LST-TST-HST-FSST (Figure 7.15; Hunt and Tucker, 1992, 1995; Plint and Nummedal, 2000; Catuneanu, 2002, 2006, 2019a,b; Catuneanu et al., 2011), the current dataset does not resolve any SUs (that formed during forced regression) in the post-Albian, which might suggest a drop in RSL (if the RSL dropped at all, it was most likely very short lived) or slow RSL rise when lowstand deposits formed. As

a result, the Albian highstand is bound at the top by a regressive surface (maximum?), and not a SU in the shelf (which could be there, but below seismic resolution). These observations are consistent with the T-R sequence models, where maximum regressive surfaces are used as sequence boundaries (Figure 7.15; *sensu* Embry and Johannessen, 1992; Embry, 1993). To the likeness of T-R sequence models, toplaps are observed in the proximal setting indicating some bypass, while the shelf and distal setting suggests a MRS.

7.5.2.2 Post-Albian to upper Cenomanian (15At1)

The Cenomanian succession overlies the Top Albian regressive surface and shows evidence for increasing accommodation space in the early Cenomanian. The basal Cenomanian succession in boreholes HB-C1 and HA-A1 is dominated by shales and clays facies, which could represent an early Cenomanian flooding event. This is supported by onlapping stratal geometries in the Algoa Basin shelf. However, the flooding surface associated with this transgression is unresolvable on the seismic lines in the Gamtoos Basin due to the resolution of the data. Consequently, the lower transgressive Cenomanian deposits are separated from the Top Albian highstand deposits by a high order MRS (Figures 7.17 and 7.18; e.g., Catuneanu, 2006, p. 327, 2019a his fig. 3, 2019b). A TST-HST-TST succession like this typically forms during positive accommodation and high sedimentation rates (Galloway, 1989; Catuneanu, 2019a his fig. 3, 2019b; Catuneanu and Zecchin, 2020 their fig. 13). The early Cenomanian transgressive deposits are overlain by two coarsening-upward successions separated by a high order flooding surface in borehole HB-C1, and these represent a period when sedimentation outpaced the RSL rise (Figure 7.17). In both basins, the coarsening-upward units in the boreholes are associated, in the seismic lines, with prograding clinoforms, which downlap on the Top Albian MRS. Taken together, the prograding clinoforms and the coarsening-upward units indicate a normal regressive (likely HST) shoreline during the Cenomanian.

The Cenomanian succession is truncated by a low order erosional boundary (15At1), which in some places erodes into the syn-rift sequence (Figure 5.27). Overall, this suggests that the Cenomanian succession was deposited during normal regression and thus represents a HST that formed when the shelf was dominated by sand deposition and the more distal parts of the basin were dominated by suspension settling (i.e., shales and clays; Figures 7.17 and 7.18). Although the origin of the Late Cretaceous event is still unclear, it has been linked with thermal subsidence in the distal part of the basin, uplift in the shelf and forced regression of the shoreline (e.g., Malan, 1993; Baby et al., 2018). At this time, the shelf area was severely scoured, and at least in the Gamtoos Basin, bypass channels were generated (Figures 5.27 and 6.1). There

are clear downlaps on a surface that might be interpreted as a basal surface of forced regression towards the shelf edge/slope (Figure 7.18; *sensu* Hunt and Tucker, 1992, 1995; Posamentier and Allen, 1999). The Top Cenomanian SU is joined with a correlative conformity (*sensu* Hunt and Tucker, 1992, 1995) towards the shelf edge (Figure 7.18). This correlative conformity is visible on the 2D seismic lines on the slope and is associated with RSL fall. The nature of the 15At1 unconformity is similar to the Hauterivian 131At surface, and thus, again, basin floor fans were likely deposited during this phase of forced regression from the Turonian to Santonian (Figure 7.18; Hodgson et al., 2018 their fig. 10b).

7.5.2.3 Post-Cenomanian (15At1) to Lower Cenozoic (22At1)

In contrast to the transitional phase, where scoured out canyons are filled by deposits of the LST, evidence for normal regressive deposits on the shelf, above Top Cenomanian unconformity (15At1), is lacking. This could either be due to the sediments being too thin and thus below seismic resolution or having been eroded during the subsequent transgression. However, evidence of prograding strata downlapping on the Top Cenomanian in the slope suggests that the LST was preserved basinwards. On the shelf, the Upper Cretaceous succession shows evidence for progradation and downlap on the Top Campanian MRS, while evidence of onlapping is observed in the slope and shelf edge regions (Figure 7.20). Whilst the Base Cenozoic reflector does not appear to be erosional in the Algoa Basin, the seismic data (Figure 7.20) in the Gamtoos Basin shows some evidence for minor erosion, especially in the proximal areas. Alternatively, this supposed erosional feature could be toplaps, indicating the depositional limits of clinoforms in the updip area. Borehole data in the Gamtoos Basin show coarsening-upward clean sands, while the Algoa Basin is dominated by retrogradational strata. These observations may suggest that the Base Cenozoic reflector marks a MFS that is underlain by transgressive deposits in the Algoa Basin, and a MRS that is underlain by a HST in the Gamtoos Basin (Figures 7.19 and 7.20). This sequence cyclicity is similar to the Albian period, when the basin experienced increased accommodation space and high sedimentation (i.e., TST-HST-TST; Figure 7.19; e.g., Galloway, 1989; Catuneanu, 2019a his fig. 3, 2019b). Moreover, the increasing accommodation space is likely a low order event, which occurred on a regional scale. Much like the Albian bounding surfaces, these observations are consistent with the T-R sequence models, where regressive and flooding surfaces are used as sequence boundaries (Figure 7.19; *sensu* Embry and Johannessen, 1992; Embry, 1993)

7.5.2.4 Lower to Middle Cenozoic

Wireline data from borehole HB-C1 record silty clays at the base of the succession, which probably formed during the Late Cretaceous/Early Cenozoic transgression in the Algoa Basin. The flooding surface associated with this transgression is overlain by prograding sandy deposits in borehole HB-C1. The sandy facies is also observed in the borehole HA-A1 in the Gamtoos Basin. This indicates increased sediment supply into the basins and a regressive shoreline. In both basins, seismic reflectors are predominantly prograding and downlapping onto the Lower Cenozoic MRS in the Gamtoos Basin and MFS in the Algoa Basin. These observations suggest that this interval was deposited as a HST in the Gamtoos Basin and TST in the Algoa Basin, until the basin was tilted (Figure 7.21; Hattingh, 2001; Baby et al., 2018) during the late Paleogene. The basin tilting event, which uplifted the shelf, resulted in a forced regression, which pushed the shoreline to the shelf edge, resulting in deposition in the distal basin and bypass on the shelf. Towards the shelf edge in the Algoa Basin, a correlative conformity in the distal setting joining with the low order SU is tentatively expected, where the underlying rock units prograde and downlap onto the basal surface of forced regression. These observations are consistent with the predictions of the depositional sequence IV model. This means, at this period, the eroded shelfal sediments were deposited basinwards, probably as basin floor fans (Figure 7.22). Although there is great potential for reservoir development in the distal setting, the depth to burial of these reservoirs is very shallow limiting hydrocarbon prospectivity. Similar to the 15At1 sequence boundary in the late Cenomanian (Figure 7.21), the Mid-Cenozoic unconformity is overlain by prograding Miocene clinoforms in the slope region, indicating the distal limits of the shoreline during the normal regression that ensued after the uplift and erosion in the Eocene and Oligocene.

7.5.2.5 Upper Cenozoic

Although onshore Algoa Basin outcrop studies of Le Roux (1987, 1989, 1990), Illenberger (1992) and Hattingh (2001) show evidence for several high order transgressive and regressive cycles from the late Miocene to Holocene, corresponding to an overall RSL change of over 300 m (Hattingh, 2001 his fig.5.1), the limited resolution of the current dataset does not allow the identification of these cycles (i.e., their stacking patterns, associated key stratigraphic surfaces; e.g., Catuneanu, 2019a; Catuneanu and Zecchin, 2020). Nonetheless, the offshore equivalent of these outcrops is shown as prograding clinoforms, which correspond to the clean coarsening-upward sands (e.g., boreholes HB-C1 and HA-A1) that were probably deposited during a low order regression (likely HST) phase in the post-Miocene.

8 Conclusions

Depositional models in this study, which encompasses the Algoa and Gamtoos Basins of South Africa, were based on a vintage dataset that is in dire need for further reprocessing in order to improve imaging, especially for the syn-rift section. Although the data quality varies from poor to moderate, the integration of different datasets into the stratigraphic framework provided reasonable insights for the generation of GDE maps and interpretation of the overall geological history of the shoreline's movement in this region. The dataset in the Gamtoos Basin suggest a marine incursion following the onset of rifting as early as in the early Middle Jurassic. This inference is supported by recent radioisotopic dating in the region (Muir et al., 2020) as well as the postulation of a pre-Tithonian mid-ocean ridge succession near the Falkland Plateau Basin (Schimschal and Jokat, 2019), which was nearby prior and during the early phases of Gondwana breakup. This marine incursion also suggests that the sedimentation in the southern Cape was influenced by marine processes and relative sea level changes since early syn-rift phase.

Three main depositional sequences are identified in the study area. The first regional sequence occurs in the syn-rift succession, which is bound by an Early Jurassic subaerial unconformity at the base and the second-order Valanginian maximum flooding surface at the top. The sequence is made up of third and fourth-order transgressive and regressive cycles in the marine sector and formed during the diachronous advancement of the shoreline (i.e., a rapid relative sea-level rise leading to transgression) until the formation of the late Valanginian second-order maximum flooding surface. Well-established stratigraphic models are difficult to apply for the continental sector of the syn-rift sequence, and thus far, the best fitting model for the current stratigraphic framework is a modified version of the genetic sequence stratigraphic model. The second regional succession is the post-rift low-order sequence 1 (*sensu* Vail et al., 1977; Mitchum et al., 1977; Posamentier et al., 1988), which is bound at the base by a major third-order Hauterivian unconformity (surface 13At1) at the base and the late, third-order Cenomanian unconformity (surface 15At1) at the top. Unconformably overlying the post-rift sequence 1, the third and final regional succession is the post-rift second-order sequence 2 that is bound by the third order-Mid-Cenozoic (Eocene) unconformity at the top. All major forced regressive periods appear to tectonically triggered. The post-rift sequence contains several systems tracts that can be identified as FSST-LST-TST-HST (Hunt and Tucker, 1992; 1995; Plint and Nummedal, 2000; Catuneanu, 2002, 2019a, b) contained by low-order key stratigraphic boundaries. Although, these sequences are bound by subaerial

unconformities, some intervals within them are bound by flooding and regressive surfaces (i.e., the Campanian to Lower Cenozoic succession; Galloway, 1989; Catuneanu, 2019a,b). In these flooding-surface-bound third- or even fourth-order successions, the T-R sequence model (*sensu* Embry and Johannessen, 1992; Embry, 1993) is valid.

This study shows, yet again, that sequence stratigraphic models are sensitive to depositional scale (Catuneanu, 2019a,b), which is an idea rooted in the Sedimentation Rate Scale concept of Miall (2015). Thus, just like in the other branches of stratigraphy, the careful consideration of the concept of scale in sequence stratigraphy cannot be emphasized enough, because as others (e.g., Catuneanu, 2019a) also pointed out : 1) the building blocks of sequences, the system tracts form at any scale of deposition; 2) stratigraphic bounding surfaces should not be limited to low-order subaerial unconformities (*sensu* depositional model II, III, IV), but should encompass all surfaces that bound genetically related successions at the same scale (Catuneanu, 2019a, 2020). This is because low-order flooding surfaces (which *sensu* genetic and T-R sequence stratigraphic models are the MFS and MRS) can be contained within subaerial unconformity bound depositional sequence models. Therefore, when applying sequence stratigraphic models, it is important to consider the resolution of the successions (and *inter alia* the resolution of the available datasets) within the regional stratigraphic framework, because certain models are more scale dependent than others.

9 References

Allen, J. P., Fielding, C. R., Gibling, M. R., and Rygel, M. C., 2002. Recognizing products of palaeoclimate fluctuation in the fluvial stratigraphic record: an example from the Pennsylvanian to lower Permian of Cape Breton Island, Nova Scotia. Sedimentology 61 (5), 1332–1381.

AAPG, 2018 http://archives.aapg.org/slide_resources/schroeder/7/index.cfm Accessed 11 Feb. 2018.

Africa Energy Corp., 2020. Oil and Gas Exploration in Africa, Operations, South Africa, Block 11b/12b https://www.africaenergycorp.com/operations/south-africa-block-11b-12b/ Accessed 07 Dec. 2020.

Almond, J.E., 2012. Proposed Jachtvlakte Precinct Human Settlement Plan, Nelson Mandela Bay Municipality, Eastern Cape. Natura Viva c, Palaeontological Assessment: Combined Desktop and Scoping Study, 22p.

Alvarez, L.G., Suárez-Vidal, F., Mendoza-Borunda, R. and González-Escobar, M., 2009. Boletín de la Sociedad Geológica Mexicana, 61, 129–141.

Atherstone, W.G., 1857. Geology of Uitenhage: Eastern Province Monthly Magazine, 1, 518–532.

Ayodele, O., Chatterjee, T. And Donker, J.V.B., 2020. Seismic Stratigraphic Analyses of Early Cretaceous (Valanginian) Sediments of Gamtoos Basin, Offshore South Africa. Journal of Basic and Applied Research International, 26, 1–14.

Baby, G., Guillocheau, F., Boulogne, C., Robin, C. and Dall'Asta, M., 2018. Uplift history of a transform continental margin revealed by the stratigraphic record: The case of the Agulhas transform margin along the Southern African Plateau. Tectonophysics, 731–732, 104–130.

Bacon, M., Simm, R., Redshaw, T., 2003. 3-D Seismic Interpretation, Cambridge University Press.

Bate, K. J. and J. A. Malan., 1992. Tectonostratigraphic evolution of the Algoa, Gamtoos and Pletmos Basins, offshore South Africa. In: M. J. De Wit and I. G. D. Ransome (Eds.). Inversion Tectonics of the Cape Fold Belt, Karoo ad Cretaceous Basins of Southern Africa. Balkema, Rotterdam, 61–73.

Ben-Avraham, Z., Hartnady, C.J.H. and Kitchin, K.A., 1997. Structure and tectonics of the Agulhas-Falkland fracture zone. Tectonophysics, 282, 83–98.

Ben-Avraham, Z., Hartnady, C.J.H., Malan, J.A., 1993. Early tectonic extension between the Agulhas Bank and the Falkland Plateau due to the rotation of the Lafonia microplate. Earth Planet Scientific Letters, 117, 43–58.

Bishop, T.N. and Nunns, A.G., 1994. Correcting amplitude, time and phase mis-ties in seismic data. Geophysics, 59, 946–953.

Boggs, S., 2006. Principles of sedimentology and stratigraphy (4th edition). Pearson Prentice Hall, Upper Saddle River, NJ.

Bosence, D.W.J., 1998. Stratigraphic and sedimentological models of rift basins In: Purser, B.H., Bosence, D.W.J. (Eds.), Sedimentation and Tectonics of Rift Basins Red Sea—Gulf of Aden. Chapman & Hall, London. 630 pp.

Bosworth, W. and Burke, K., 2005. Evolution of the Red Sea—Gulf of Aden Rift System. In, Petroleum Systems of Divergent Continental Margin Basins, Post, P.J., Rosen, N. C., Olson, D. L., Palmes, S.L., Lyons, K.T., and Newton, G. B. SEPM Society for Sedimentary Geology, 25, 324–372.

Bosworth, W., Huchon, P. and McClay, K., 2005. The Red Sea and Gulf of Aden basins. Journal of African Earth Sciences, 43, 334–378.

Broad, D.S., 1990. Petroleum geology of the Gamtoos and Algoa basins. Ext. Abstract Geocongress 90, Geological Society of South Africa, Abstract, 60–63.

Broad, D.S., Jungslager, E.H.A., McLachlan, I.R., Roux, J. and van der Spuy, D., 2012. South Africa's offshore Mesozoic basins. Phanerozoic Passive Margins, Cratonic Basins and Global Tectonic Maps. Elsevier, 535–560.

Brown, A., 1999. Interpretation of Three-Dimensional Seismic Data, Fifth Edition. AAPG Memoir 42 SEG Investigations in Geophysics, 9, 355.

Brown Jr., L.F. and Fisher, W.L., 1977, Seismic stratigraphic interpretation of depositional systems: examples from Brazilian rift and pull apart basins. In: Payton, C.E. (Ed.), Seismic Stratigraphy—Applications to Hydrocarbon Exploration, American Association of Petroleum Geologists Memoir, 26, 213–248.

Brown, L.F. Jr., Benson, J.M., Brink, G.J., Doherty, S., Jollands, A., Jungslager, E.H.A., Keenan, J.H.G., Muntingh, A. and Van Wyk, N.J.S., 1995. Sequence stratigraphy, in offshore South African divergent basins. An atlas on exploration for Cretaceous lowstand traps by Soekor (Pty) Ltd. American Association of Petroleum Geologists, 41.

Brownfield, M.E., and R.R. Charpentier., 2006. Geology and total petroleum systems of the west-central coastal province (7203), West Africa: U.S. Geological Survey Bulletin, 2207-B, 60.

Burgess, M.P., Allen, A.P. and Steel, R.J., 2016. Introduction to the future of sequence stratigraphy: evolution or revolution? Journal of the Geological Society, 173, 801–802.

Cainelli, C., Mohriak, W.U., 1999. Some remarks on the evolution of sedimentary basins along the Eastern Brazilian continental margin. Episodes, 22, 206–216.

Caku, N., Gwavava, O., Liu, K. and Baiyegunhi, C., 2020. An integration of magnetic, gravity and seismic data in Evaluating the Algoa Basin in the Eastern Cape Province of South Africa for stratigraphic and structural geodynamics. Pure and Applied Geophysics, 177, 4177–4205.

Cant, D.J., 1992. Subsurface facies analysis. Facies models, pp.27–45.

Catuneanu, O., 2002. Sequence stratigraphy of clastic systems: concepts, merits, and pitfalls. Journal of African Earth Sciences, 35, 1–43.

Catuneanu, O., 2006. Principles of sequence stratigraphy, Elsevier, Amsterdam 375.

Catuneanu, O., 2007. Comments on the ISSC draft report on sequence stratigraphy. http://www.sepmstrata.org/CMS_Files/Catuneanu_com_ISSC_Report_Sequence_Stratigr.pdf Accessed 12 Jan. 2017.

Catuneanu, O., 2019a. Model-independent sequence stratigraphy. Earth-science reviews, 188, 312–388.

Catuneanu, O., 2019b. Scale in sequence stratigraphy. Marine and Petroleum Geology, 106, 128–159.

Catuneanu, O., Galloway, W.E., Kendall, C., Miall, A., Posamentier, H. W., Strasser, A. and Tucker, M.E., 2011. Sequence stratigraphy: methodology and nomenclature. Newsletters on Stratigraphy, Stuttgart, 44, 173–245.

Catuneanu, O. and Zecchin, M., 2016. Unique vs. non-unique stratal geometries: Relevance to sequence stratigraphy. Marine and Petroleum Geology, 78, 184–195.

Catuneanu, O. and Zecchin, M., 2020. Parasequences: Allostratigraphic misfits in sequence stratigraphy. Earth-Science Reviews, p.103289.

Chopra, S., Castagna, J.P. and Portniaguine, O., 2006. Seismic resolution and thin-bed reflectivity inversion. CSEG Recorder, 31, 19–25.

Chorowicz, J., 2005. The east African rift system. Journal of African Earth Sciences, 43(1–3), 379–410.

Christie-Blick, N., 1991. Onlap, offlap, and the origin of unconformity-bounded depositional sequences. Marine Geology, 97, 35–56.

Claassen, D., 2014. Geographical controls on sediment accretion of the Cenozoic Algoa group between Oyster Bay and St. Francis, Eastern Cape coastline, South Africa. South African Journal of Geology, 117, 109–128.

Davids, A.C., van Bloemenstein, C. and Roux, J., 2017. Play Analysis of the Gamtoos Basin, off the south coast of South Africa – from concept to portfolio. 79th EAGE Conference & Exhibition 2017 Submission ID 42714, Workshop 10: Play Analysis – From Concept to Portfolio.

De Wit, M.J., 1992. The Cape fold belt: a challenge for an integrated approach to inversion tectonics. In: Inversion tectonics of the Cape Fold Belt, Karoo and Cretaceous Basins of Southern Africa (Ed. by M.J. de Wit & I.G.D. Ransome), 3–14. Balkema, Rotterdam.

Dingle, R.V. and Scrutton, R. A., 1974. Continental break-up and the development of post-Palaeozoic sedimentary basins around southern Africa. Bulletin of the Geological Society of America, 85, 1467–1474.

Dingle, R.V., Siesser, W.G. and Newton, A.R., 1983. Mesozoic and Tertiary Geology of Southern Africa. A.A. Balkema, Rotterdam, 375.

Doveton, J.H., 1994. Geologic log interpretation. SEPM Society for Sedimentary Geology, 29, 91.

Du Toit, S.R., 1979. The Mesozoic history of the Agulhas Bank in terms of plate tectonic theory. Geokongres 77. Geological Society of South Africa Special Publication, 6, 197–203.

Einsele, G., Ricken, W. and Seilacher, A., 1991. Cycles and events in stratigraphy. Springer-Verlag, Berlin, Heidelberg, New York, 955.

Embry, A.F., 1993. Transgressive-regressive (T-R) sequence analysis of the Jurassic succession of the Sverdrup Basin, Canadian Arctic Archipelago. Canadian Journal of Earth Sciences, 30, 301–320.

Embry, A.F., 1995. Sequence boundaries and sequence hierarchies: problems and proposals, In: Steel, R.J., Felt, F.L., Johannessen, E.P. and Mathieu, C., (eds)., Sequence stratigraphy on the northwest European margin: NPF Special Publication, 5, 1–11.

Embry, A.F., 2009a. Practical sequence stratigraphy. Canadian Society of Petroleum Geologists, Online at www.cspg.org, 81.

Embry, A. F., 2009b. Lowstand systems tract – a problematic stratigraphic unit. Frontiers + Innovation – 2009 CSPG CSEG CWLS Convention.

Embry, A., Johannessen, E., Owen, D., Beauchamp, B., Gianolla. P., 2007. Sequence stratigraphy as a "concrete" stratigraphic discipline. Report of the ISSC Task Group on Sequence Stratigraphy.

Emery, D. and Myers, K.J., 1996. Sequence stratigraphy. London: Blackwell Science, 297pp.

Embry, A. F. and Johannessen, E. P., 1992. T–R sequence stratigraphy, facies analysis and reservoir distribution in the uppermost Triassic-Lower Jurassic succession, western Sverdrup Basin, Arctic Canada. In Arctic Geology and Petroleum Potential (T. O. Vorren, E. Bergsager, O. A. Dahl-Stamnes, E. Holter, B. Johansen, E. Lie and T. B. Lund, Eds.), p. 121–146. Norwegian Petroleum Society (NPF), Special Publication 2.

Falvey, D.A., 1974. The development of continental margins in plate tectonic theory. Journal of the Australian Petroleum Production & Exploration Association, 14, 95–106.

Feder, J., 2019. Offshore: making a comeback after the downturn. Journal of Petroleum Technology, 71, 27–31.

Fletcher, O., 1971a. Geological well report of borehole KE 1/71. Unpublished report of the Southern Oil Exploration Corporation (Pty.) Limited (now PetroSA), Parow, Western Cape, 1–27.

Fletcher, O., 1971b. Geological well report of borehole CO 3/71. Unpublished report of the Southern Oil Exploration Corporation (Pty.) Limited (now PetroSA), Parow, Western Cape, 1–23.

Frazier, D.E., 1974. Depositional episodes: their relationship to the Quaternary stratigraphic framework in the north western portion of the Gulf basin. Geological Circular. University of Texas at Austin, Bureau of Economic Geology, 1, 28.

Frisch, W., Meschede, M. and Blakey, R., 2011. Passive continental margins and abyssal plains. Plate Tectonics, 43–57. Springer, Berlin, Heidelberg.

Galloway, W.E., 1989. Genetic stratigraphic sequences in basin analysis. I. Architecture and genesis of flooding-surface bounded depositional units. American Association of Petroleum Geologists Bulletin, 73, 125–142.

Gawthorpe, R. and Leeder, M., 2000. Tectono-sedimentary evolution of active extensional basins: Basin Research, 12, 195–218.

Hampson, D. and Galbraith, M., 1981. Wavelet extraction using sonic log correlation. The J. Canadian Society for Exploration Geophysics, 17, 24–42.

Hampson, G. J., 2016. Towards a sequence stratigraphic solution set for autogenic processes and allogenic controls: Upper Cretaceous strata, Book Cliffs, Utah, USA. Journal of the Geological Society, 173, 817–836.

Haq, B.U., Hardenbol, J. and Vail, P.R., 1987. Chronology of fluctuating sea levels since the Triassic. Science, 235, 1156–1166.

Hattingh, J., 2001. Late Cenozoic drainage evolution in the Algoa basin with special reference to the Sundays River Valley. Bulletin of the Council for Geoscience 128, 141pp.

Helland-Hansen, W. and Gjelberg, J. G., 1994. Conceptual basis and variability in sequence stratigraphy: a different perspective. Sedimentary Geology, 92, 31–52.

Hernández-Molina, F.J., Llave, E. and Stow, D.A.V., 2008. Continental slope contourites. Developments in Sedimentology, 60, 379–408.

Hodgson, D. M., Browning, J. V., Miller, K. G., Hesselbo, S. P., Poyatos-More, M. and Mountain, G. S., 2018. Sedimentology, stratigraphic context, and implications of intrashelf bottomset deposits, offshore New Jersey. Geosphere, 14, 95–114.

Holz, M., Vilas-Boas, D.B., Troccoli, E.B., Santana, V.C. and Vidigal-Souza, P.A., 2017. Conceptual models for sequence stratigraphy of continental rift successions. Stratigraphy & Timescales, 2, 119–186.

Hubral, P., Schleicher, J., Tygel, M. and Hanitzsch, C., 1993. Determination of Fresnel zones from traveltime measurements. Geophysics, 58, 703–712.

Hunt, D. and Tucker, M.E., 1992. Stranded parasequences and the forced regressive wedge systems tract: deposition during base-level fall. Sedimentary Geology, 81, 1–9.

Hunt, D. and Tucker, M. E., 1995. Stranded parasequences and the forced regressive wedge systems tract: deposition during base-level fall – reply. Sedimentary Geology, 95,147–160.

Illenberger, W. K., 1992. Lithostratigraphy of the Schlemm Hoek formation (Algoa Group). Institute for Coastal Research, University of Port Elizabeth.

Jacobs, Z. and Roberts, D.L., 2009. Last Interglacial age for aeolian and marine deposits and the Nahoon fossil human footprints, southeast coast of South Africa. Quaternary Geochronology 4, 160–169.

Johnson, J.G. and Murphy, M.A., 1984. Time-rock model for Siluro-Devonian continental shelf, western United States. Geological Society of America Bulletin, 95, 1349–1359.

Jungslager, E.H.A., 1996. Geological Evaluation of the Remaining Prospectivity for Oil and Gas of the Pre-1At1 “Synrift” Succession in Block 9, Republic of South Africa. Unpublished SOEKOR Report, 63pp.

Keogh, K.J., Martinius, A.W. and Osland, R., 2007. The development of fluvial stochastic modelling in the Norwegian oil industry: A historical review, subsurface implementation and future directions. Sedimentary Geology, 202, 249–268.

Koopmann, H., Franke, D., Schreckenberger, B., Schulz, H.,Hartwig, A., Stollhofen, H. and di Primio, R., 2014. Segmentation and volcano-tectonic characteristics along the SW African continental margin, South Atlantic, as derived from multichannel seismic and potential field data. Marine and Petroleum Geology, 50, 22–39.

Le Roux, F.G., 1987. Lithostratigraphy of the Alexandria Formation. South African Committee for Stratigraphy (SACS), Lithostratigraphic Series 1, 1–18.

Le Roux, F.G., 1989. The lithostratigraphy of Cenozoic deposits along the south-east Cape coast as related to sea-level changes. Unpublished PhD thesis, Stellenbosch University, 243pp.

Le Roux, F.G., 1990. Palaeontological correlation of Cenozoic marine deposits of the southeastern, southern and western coasts, Cape Province. South African Journal of Geology, 93, 514–518.

Lockley, M.G., Helm, C.W., Cawthra, H.C., De Vynck, J.C. and Perrin, M.R., 2021. Pleistocene golden mole and sand-swimming trace fossils from the Cape coast of South Africa. Quaternary Research, 1–18.

Long, A., 2003. Marine acquisition: moving beyond the signal-to-noise ratio. First Break, 21, 67–70.

Lovecchio, J.P., Rohais, S., Joseph, P., Bolatti, N.D. and Ramos, V.A., 2020. Mesozoic rifting evolution of SW Gondwana: A poly-phased, subduction-related, extensional history responsible for basin formation along the Argentinean Atlantic margin. Earth-Science Reviews, 203, 103138.

Malan, J.A., 1993. Geology, potential of Algoa, Gamtoos Basins of South Africa. Oil & Gas Journal. Soekor (Pty.) Ltd.

Malan, J.A., Martin, A.K. and Cartwright, J.A., 1990. The structural and stratigraphic development of the Gamtoos and Algoa Basins, offshore South Africa. Geological Society of South Africa, Abstract, Geoscience 90, 328–331.

Martin, A.K. and Hartnady, C.J.H., 1986. Plate tectonic development of the south west Indian Ocean: A revised reconstruction of East Antarctica and Africa. Journal of Geophysical Research, 91, 4767–4786.

Martin, A.K., Hartnady, C.J.H. and Goodlad, S.W., 1981. A revised fit of South America and South-Central Africa. Earth Planet, Science Letters, 54, 293–305.

Martins-Neto, M.A. and Catuneanu, O., 2010. Rift sequence stratigraphy. Marine and Petroleum Geology, 27, 247–253.

McLachlan, I.R. and McMillan, I.K., 1976. Review and stratigraphic significance of southern Cape Mesozoic palaeontology. Transactions of the Geological Society of South Africa, 79, 197–212.

McMillan, I. K., Brink, G.J., Broad, D.S. and Maier, J. J., 1997. Late Mesozoic sedimentary basins off the south coast of South Africa. In Selly, R.C. (ed), African Basins, Sedimentary Basins of the World. Elsevier, Amsterdam, 319–376.

McMillan, I.K., 2010. The Foraminifera of the Portlandian (Late Jurassic) Bethelsdorp Formation of the onshore Algoa Basin, Eastern Cape Province. Les Rosalines Press, Clovelly, 176pp.

Merkel, R. H., 1979. Well log formation evaluation. Continuing education course note series #14. American Association of Petroleum Geologists Martin, J., Toothill, S., CGG Veritas and Mousavou, R. 2009. Hunting the pre-salt. Geo expo December 2009, frontier exploration.

Miall, A.D., 1992. Exxon global cycle chart: an event for every occasion? Geology, 20, 787–790.

Miall, A.D., 2009. Correlation of sequences and the global eustasy paradigm: A Review of Current Data. Frontiers + Innovation – 2009 CSPG CSEG CWLS Convention, 123–126.

Miall, A.D., 2014. The emptiness of the stratigraphic record: a preliminary evaluation of missing time in the Mesaverde Group, Book Cliffs, Utah, USA. Journal of Sedimentary Research, 84(6), 457–469.

Miall, A.D., 2016. The valuation of unconformities. Earth Science Reviews, 163, 22–71.

Miall, A.D. and Strasser, A., 2018. Standards for publications in the field of basin analysis in Earth-Science Reviews. Earth Science Reviews, 177, 1.

Mitchum, R. M. Jr., Vail, P. R. and Thompson, S., III., 1977. Seismic stratigraphy and global changes of sea-level, part 2: the depositional sequence as a basic unit for stratigraphic analysis. In Seismic Stratigraphy–Applications to Hydrocarbon Exploration (C. E. Payton, Ed.), American Association of Petroleum Geologists Memoir, 26, 53–62.

Mitchum, R.M., Jr., 1977. Seismic stratigraphy and global changes of sea level, part 11: Glossary of terms used in seismic stratigraphy. In: (C.E. Payton, Ed.), Seismic Stratigraphy-- Applications to Hydrocarbon Exploration: American Association of Petroleum Geologists, 26, 205–212.

Mudaly, K., Turner, J., Escorcial, F. and Higgs, R., 2009. FO GasField, Offshore South Africa–an Integrated Approach to Field Development. American Association of Petroleum Geologist (AAPG) Search and Discovery Article, 20070.

Muir, R.A., 2019. Recalibrating the breakup history of SW Gondwana: The first U-Pb chronostratigraphy for the Uitenhage Group, South Africa. Unpublished PhD thesis, University of Cape Town, 415pp.

Muir, R., Bordy, E.M. and Prevec, R., 2015. Lower Cretaceous deposit reveals first evidence of a post-wildfire debris flow in the Kirkwood Formation, Algoa Basin, Eastern Cape, South Africa. Cretaceous Research, 56, 161–179.

Muir, R.A. and Bordy, E.M., 2016. Stratigraphic framework for the Kirkwood Formation in the southern Cape region: invertebrate biostratigraphy and zircon geochronology. In: 19th Palaeontological Society of South Africa biennial conference, Stellenbosch University, 65.

Muir, R., Bordy, E.M., Reddering, J.S.V. and Viljoen, J.H.A., 2017a. Lithostratigraphy of the Enon Formation (Uitenhage Group), South Africa. Geological Society of South Africa, 120.2, 273–280.

Muir, R., Bordy, E.M., Reddering, J.S.V. and Viljoen, J.H.A., 2017b. Lithostratigraphy of the Kirkwood Formation (Uitenhage Group), including the Bethelsdorp, Colchester and Swartkops Members, South Africa. Geological Society of South Africa, 120.2, 281–293.

Muir, R., Bordy, E.M., Mundi, R. and Frei, D., 2020. Recalibrating the breakup history of SW Gondwana: U–Pb radioisotopic age constraints from the southern Cape of South Africa. Gondwana Research, 84, 177–193.

Muto, T., Steel, R.J. and Burgess, P.M., 2016. Contributions to sequence stratigraphy from analogue and numerical experiments. Journal of the Geological Society, 173, 837–844.

Neal, J.E., Risch, D. and Vail, P., 1993. Sequence stratigraphy-a global theory for local success. Oil Field Review, 5, 51–62.

Neal, J. and Abreu, V., 2009. Sequence stratigraphy hierarchy and the accommodation succession method. Geology, 37, 779–782.

Neal, J.E., Abreu, V., Bohacs, K. M., Feldman, H.R. and Pederson, K.H., 2016. Accommodation succession (δA/δS) sequence stratigraphy: observational method, utility and insights into sequence boundary formation. Journal of the Geological Society, 173, 803–816.

New Age Global Energy., 2018. Offshore South Africa, Algoa Gamtoos licence (Algoa, Gamtoos ad South Outeniqua Basins) Farm-out opportunity report. http://envoi.co.uk/wp-content/uploads/2018/09/P253NewAge(SouthAfrica)IntroFlyer.pdf Accessed 11 Dec 2020.

Paton, A.D. and Underhill, J. R., 2004. Role of crustal anisotropy in modifying the structural and sedimentological evolution of extensional basins: the Gamtoos Basin, South Africa. Basin Research, 16, 339–359.

Petroleum Agency SA., 2012. Petroleum exploration in South Africa information and opportunities.

Petroleum Agency SA., 2020. https://geoportal.petroleumagencysa.com [Date accessed 03/03/2020]

Platon, C., 2017. Guyana-Suriname Basin, South America: Hot Ultra-Deepwater Exploration Opportunities and Liza Field: Worldwide Largest 2015–2016 Hydrocarbon Discovery. In AAPG Annual Convention and Exhibition, Houston, Texas, April 2-5, 2017.

Plint, A.G. and Nummedal, D., 2000. The falling stage systems tract: recognition and importance in sequence stratigraphic analysis; in Sedimentary Responses to forced regressions; D. Hunt and R. Gawthorpe, eds., Geological Society of London, Special Publications, 172, 1–17.

Posamentier, H.W., Jervey, M.T. and Vail, P.R., 1988. Eustatic controls on clastic deposition. I. Conceptual framework. In: Wilgus, C.K., Hastings, B.S., Kendall, C.G.St.C., Posamentier, H.W., Ross, C.A., Van Wagoner, J.C. (Eds.), Sea Level Changes—An Integrated Approach. SEPM Special Publication, 42, 110–124.

Posamentier, H. W., Allen, G. P., James, D. P. and Tesson, M., 1992. Forced regressions in a sequence stratigraphic framework: concepts, examples, and exploration significance. American Association of Petroleum Geologists Bulletin, 76, 1687–1709.

Posamentier, H.W. and Allen, G.P., 1999. Siliciclastic sequence stratigraphy: concepts and applications. SEPM Concepts in Sedimentology and Paleontology, 7, 210pp.

Prosser, S., 1993. Rift-related linked depositional systems and their seismic expression. In: Williams, G.D., Dobb, A. (Eds.), Tectonics and seismic sequence stratigraphy Geological Society Special Publication, 71, 35–66.

Reeves, C.V., 2018. The development of the East African margin during Jurassic and Lower Cretaceous times: a perspective from global tectonics. Petroleum Geoscience, 24, 41–56.

Ridente, D., 2016. Releasing the sequence stratigraphy paradigm. Journal of the Geological Society, 173, 845–853.

Rigassi, D.A. and Dixon, G.E., 1972. Cretaceous of the Cape Province, Republic of South Africa. In: T.F.J. Dessauvagie and A.J. Whiteman (Editors). African Geology. Geology Department, University of Ibadan, Nigeria, 513–527.

Roberts, D.L., 2008. Last interglacial hominid and associated vertebrate fossil trackways in coastal eolianites, South Africa. Ichnos, 15, 190–207.

Roberts, D.L., Botha, G.A., Maud, R.R. and Pether, J., 2006. Coastal Cenozoic deposits. Pp. 605 – 628 in Johnson, M.R., Anhaeusser, C.R. & Thomas, R.J. (Eds.) The geology of South Africa. Geological Society of South Africa, Johannesburg & Council for Geoscience, Pretoria.

Schimschal, C.M. and Jokat, W., 2019. The Falkland Plateau in the context of Gondwana breakup. Gondwana Research, 68, 108–115.

Schlumberger Wireline and Testing., 1989. Log interpretation principles applications sugarland, Texas. Schlumberger, Laredo, TX, 251 pp.

Shanley, K. W. and McCabe, P. J., 1994. Perspectives on the Sequence Stratigraphy of Continental Strata. AAPG Bulletin, 78, 544–568.

Shanmugam, G., 1988. Origin, recognition and imprudence of erosional unconformities in sedimentary basins. In: K. Kleinspehn, C Paola (editors): New Perspectives in Basin Analysis, Springer Verlag, New York, 83–108.

Sheriff, E.G. and Geldart, L.P., 1995. Exploration Seismology. Cambridge University Press, Cambridge, 592pp.

Sheriff, R.E., 1977. Limitations on resolution of seismic reflections and geologic detail derivable from them. In: Payton (Ed.), Seismic Stratigraphy: Application to Hydrocarbon Exploration. American Association of Petroleum Geologists, 26, 3–14.

Shone, R.W., 1976. The sedimentology of the Mesozoic Algoa Basin. Unpublished M.Sc. thesis, University of Port Elizabeth, 48pp.

Shone, R.W. and Johnson, M.R., 2006. Onshore post-Karoo Mesozoic deposits. The Geology of South Africa, 541–552.

Shone, R.W., 1978. A case for lateral gradation between the Kirkwood and Sundays River Formations, Algoa Basin. Transactions of the Geological Society of South Africa, 81, 319–326.

Shone, R.W., 2006. Onshore post-Karoo Mesozoic deposits. In: M.R. Johnson, C.R. Anhaeusser and R.J. Thomas (Editors). The Geology of South Africa, Geological Society of South Africa, Johannesburg, and Council for Geoscience, Pretoria, 541–571.

Sims, R. and Bacon, M., 2014. Seismic amplitude an interpreter's handbook. UK: Cambridge University Press.

Singh, V., Brink, G.J. and Winter, H.D.L.R., 2005. New interpretation reveals potential in onshore Algoa basin, South Africa. Oil and Gas Journal, 103, 34–39.

Sloss, L., Krumbein, W. and Dapples, E., 1949. Integrated facies analysis, In: Longwell, C., (ed.), Sedimentary facies in geologic history. Geological Society America, 39, 91–124.

Soares, D.M., Alves, T.M. and Terrinha, P., 2012. The breakup sequence and associated lithospheric breakup surface, their significance in the context of rifted continental margins (West Iberia and Newfoundland margins, North Atlantic). Earth and Planetary Science Letters, 355–356, 311–326.

Stevenson, I.R. and McMillan, I.K., 2004. Incised valley fill stratigraphy of the Upper Cretaceous succession, proximal Orange Basin, Atlantic margin of southern Africa. Journal of the Geological Society, London, 161, 185–208.

Thompson, J.O., Moulin, M., Aslanian, D., de Clarens, P. and Guillocheau, F., 2019. New starting point for the Indian Ocean: Second phase of breakup for Gondwana. Earth-Science Reviews, 91, 26–56.

Thomson, K., 1999. Role of continental break-up mantle plume developments and fault reactivation in the evolution of the Gamtoos Basin, South Africa. Marine Petroleum Geology, 16, 409–429.

Vail, P.R., Hardenbol, J. and Todd, R.G., 1984. Jurassic unconformities, chronostratigraphy and sea-level changes from seismic stratigraphy and biostratigraphy. In Interregional Unconformities and Hydrocarbon Accumulation (J. S. Schlee, Ed.), 129–144.

Vail, P. R., Audemard, F., Bowman, S. A., Eisner, P. N. and Perez-Cruz, C., 1991. The stratigraphic signatures of tectonics, eustasy and sedimentology – an overview. In: Einsele, G., Ricken, W., Seilacher, A. (eds), Cycles and Events in Stratigraphy. Springer–Verlag, 617–659.

Vail, P. R., Todd, R. G. and Sangree, J. B.., 1977a. Seismic stratigraphy and Global Changes of Sea Level: Part 5. Chronostratigraphic Significance of Seismic Reflections: Section 2. Application of Seismic Reflection Configuration to Stratigraphic Interpretation, 26, 99–116.

Vail, P.R., Mitchum, R.M., Jr. and Thompson, S., III., 1977b. Seismic stratigraphy and global changes of sea level, Part 4: Global cycles of relative changes of sea level. In: Payton, C.E. (ed.) Seismic Stratigraphy—Applications to Hydrocarbon Exploration. AAPG Memoirs, 26, 83–97.

Van Wagoner, J. C., Posamentier, H. W., Mitchum, R. M. Jr., Vail, P. R., Sarg, J. F., Loutit, T. S. and Hardenbol, J., 1988. An overview of sequence stratigraphy and key definitions. In Sea Level Changes–An Integrated Approach C. K. Wilgus, B. S. Hastings, C. G. St. C. Kendall, H. W. Posamentier, C. A. Ross and J. C. Van Wagoner, Eds.). SEPM Special Publication, 42, 39–45.

Van Wagoner, J. C., Mitchum, R. M. Jr., Campion, K. M. and Rahmanian, V. D., 1990. Siliciclastic sequence stratigraphy in well logs, core, and outcrops: concepts for high-resolution correlation of time and facies. APPG Methods in Exploration Series, 7, 55.

Veeken, P.C.H., 2007. Handbook of geophysical exploration – seismic stratigraphy, basin analysis and reservoir characterization. Elsevier, 37, 523pp.

Viljoen, J.H.A., Stapelberg, F.D.J. and Cloete, M., 2011. Technical report on the geological storage of carbon dioxide in South Africa. Council for Geoscience, http://www.ccsconference.co.za/images/presentations/thinus_cloete.pdf. Accessed 21 December 2020.

Walker, R.G., 1990. Facies modelling and sequence stratigraphy. Journal of Sedimentary Research, 60, 777–786.

Walker, R.G., 2006. Facies Models Revisited. SEPM (Society for Sedimentary Geology) Special Publication, 84, 1–17.

Winter, H.D.L. R., 1973. Geology of the Algoa Basin, South Africa, In: G. Blant, (Editor). Sedimentary basins of the African coasts, Part 2, South and East Coast. Association of African Geological Surveys, Paris, 17–48.

Winters, S., 1985. Geological well report of borehole Ha-B2. Unpublished report of the Southern Oil Exploration Corporation (Pty.) Limited (now PetroSA), Parow, Western Cape, 1–26.

Appendix

The Appendix is a peer-reviewed and revised manuscript that is based on the results of this PhD and is under editorial consideration at Geo-Marine Letters (manuscript number EMID:4787406fa4983ae4).

Sequence stratigraphy in the Algoa and Gamtoos Basins (South Africa): a shoreline's journey since the Middle Mesozoic

Marvel H. Makhubele* (ORCID: https://orcid.org/0000-0002-4187-5298) and Emese M. Bordy (ORCID: http://orcid.org/0000-0003-4699-0823)

Department of Geological Sciences, University of Cape Town, Private Bag X3, Rondebosch, 7701, South Africa

* – corresponding author's email: mkhmar015@myuct.ac.za

Abstract

Basin evolution models are dependent on high quality subsurface data, normally obtained during hydrocarbon exploration activities. The limited exploration, to-date, has impeded the understanding of the geological evolution of the offshore Algoa and Gamtoos half-graben Basins in the southern Cape region of South Africa. To reconstruct the main geological events of the area since the Early Jurassic, we integrated vintage borehole and seismic data as well as key outcrop observations, generated contemporary gross depositional environment models for the basin fill, and tested the applicability of different sequence stratigraphic models. The studied stratigraphic interval formed since the inception of Gondwana break-up in a syn- and post-rift system that was dominated by marine processes, especially in the distal hanging walls of these compartmentalized half-graben basins. Sedimentation within these depocenters primarily occurred above the hanging walls whilst the footwalls form regions of basement highs. The geological characteristics of the studied succession prevents the application of the depositional sequence model or tectonic system tracts model in the syn-rift succession. Because subaerial unconformities (SUs) in the distal syn-rift sequence are not detectable, a diachronous, northward advancement of relative sea-level until the late Valanginian can be postulated. The observations in the syn-rift sequence, which is bound by a basal SU, followed by third and fourth-order transgressive and regressive cycles and a second-order maximum flooding surface at the top, can be explained with a modified genetic sequence model. In the transitional to drift phase interval, from Hauterivian to Holocene, the successions are bound by SUs and their correlative conformities. In the successions without evidence for subaerial exposure, flooding surfaces could be used as sequence-bounding stratigraphic contacts. This study reaffirms the notion that while the sequence stratigraphic concept is model independent, sequence models are sensitive to depositional scale.

Keywords: sequence stratigraphic models; syn-rift; gross depositional environment models; sequence boundaries

Introduction

The application of sequence stratigraphy in identifying hydrocarbon traps in frontier basins has been successful globally (e.g., ExxonMobil Liza discovery offshore Guyana; Platon 2017; Feder 2019) and to some extent in southern Africa too (e.g., the Brulpadda and Luiperd discoveries in the Outeniqua Basin; Africa Energy Corp. 2020). However, from an economic geology view-point, a solid knowledge of the geological history is important not only for exploiting hydrocarbons while transitioning to alternative energy resources but also for siting deep geological mediums to mitigate the negative impact of anthropogenic climate change (e.g., CO_2 storage, deep burial of hazardous waste; Hong et al. 2015). Moreover, despite serious collaborative scientific efforts in the past decade to stabilize the sequence stratigraphic method (e.g., Catuneanu et al. 2011, Catuneanu 2019a, b, 2020, Catuneanu and Zecchin 2020), terminology is still inconsistently used by different schools of thought not only to define stratigraphic surfaces but also to interpret the geological history of stratigraphic successions. This has resulted in multiple sequence stratigraphic models that interpret the same data differently.

Although a working petroleum system was proven in the Algoa and Gamtoos Basins of South Africa, data acquired to-date yielded limited exploration success unlike in the neighboring Bredasdorp Basin (e.g., Malan 1993; McMillan et al. 1997). Consequently, no robust sequence stratigraphic work exists for the Algoa and Gamtoos Basins (Ayodele et al. 2020; Caku et al. 2020), and this limits, especially in the offshore regions, the understanding of the: a) sedimentary facies distribution, b) basin development history and c) nature of the petroleum systems (Muir et al. 2020). Herein, a mid-Mesozoic to Holocene sequence stratigraphic framework is built in the Algoa and Gamtoos Basins. By integrating a subset of available vintage data (seismic and wireline) and some outcrop studies, the usefulness of a few, selected sequence stratigraphic models is tested for the study area. Moreover, by combining the available data, conceptual models of the gross depositional environments (GDE) are generated and shown as maps. These GDE maps were derived from studying facies change, the vertical stacking pattern of facies in available wireline data, seismic geometries, and also by incorporating recent results from field studies conducted onshore in the Algoa and Gamtoos Basins.

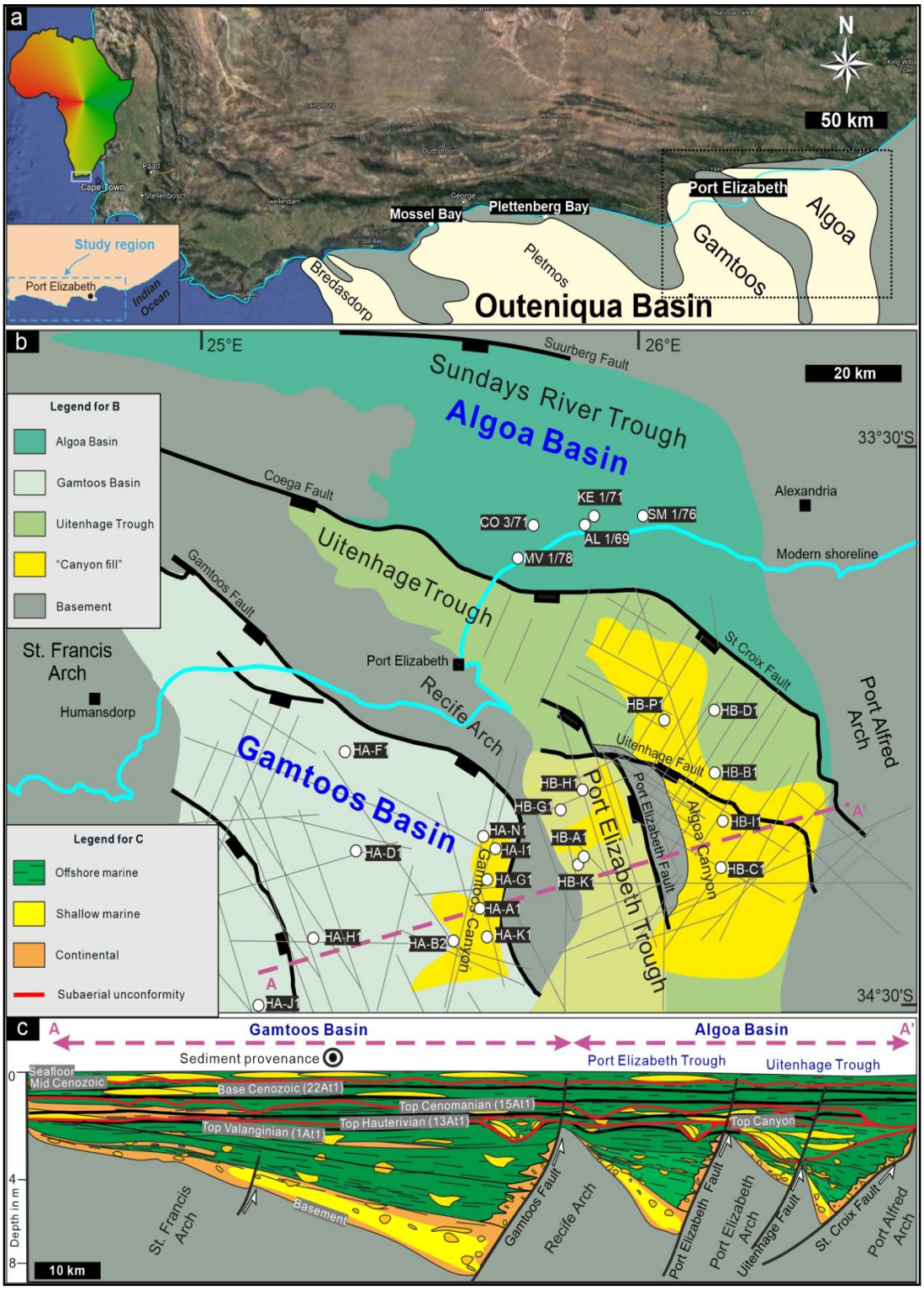

Fig. 1. **a** Regional southern Africa map, showing the location of the greater Outeniqua Basin. **b** Simplified onshore and offshore geological map of the Algoa and Gamtoos Basin. **c** Structural cross-section of the Algoa and Gamtoos Basins (modified from McMillan et al. 1997; Broad et al. 2012; Muir at al. 2020). Base map data ©2020 Google, Maxar Technologies, AfriGIS (Pty) Ltd.

Geological background

Stratigraphic framework

The Algoa and Gamtoos Basins, together with the Pletmos and Bredasdorp Basins form part of the larger Outeniqua Basin, located along the southern coast of South Africa (Fig. 1; Malan 1993; Brown et al. 1995; McMillan et al. 1997; Singh et al. 2005; Thompson et al. 2019; Muir et al. 2020). The Outeniqua Basin is a remnant of extensional basins formed in southern Africa during Gondwana break-up in the Early Jurassic (McLachlan and McMillan 1976; Dingle et al. 1983; McMillan et al. 1997; Thompson et al. 2019; Muir et al. 2020). While the Algoa and Gamtoos Basins are adjacent to each other, sedimentation was primarily influenced by their local structural anisotropy (Broad 1990; McMillan et al. 1997; Muir 2019). The Algoa Basin is compartmentalized into sub-basins or troughs by three major bounding faults, the St Croix, Port Elizabeth and Uitenhage Faults (Fig. 1; McLachlan and McMillan 1976; Dingle et al. 1983; Broad,1990; Bate and Malan 1992; Broad et al. 2012; McMillan et al. 1997). The Gamtoos Basin contains only one major listric-type fault (i.e., Gamtoos Fault), which has a throw of 3 km onshore and 12 km offshore, and was active from Middle to Late Jurassic (Fig. 1; e.g., McLachlan and McMillan 1976; Dingle et al. 1983; Malan et al. 1990; Bate and Malan 1992; McMillan et al. 1997; Paton and Underhill 2004). The basin fill (Fig. 2) can be separated into: 1) pre-Oxfordian to Valanginian rift/syn-rift phase (reflector D to 1At1); 2) Valanginian to Hauterivian early drift phase (transition phase; 1At1 to 6At1/13At1); 3) Aptian to Albian "Canyon fill" (13At1 to 14At1) and; 4) drifting (thermal subsidence) phase (13At1 to Holocene; e.g., McLachlan and McMillan 1976; Dingle et al. 1983; Broad et al. 1990; Bate and Malan 1992; Malan 1993; Brown et al. 1995; McMillan et al. 1997; Broad et al. 2012).

The oldest rocks are conglomerates and subordinate sandstones that belong to the Enon Formation, which was deposited on alluvial fans developed from high-energy rivers during the early Middle Jurassic (or earlier) to the Early Cretaceous (Fig. 2; McLachlan and McMillan 1976; Dingle et al. 1983; Malan 1993; McMillan et al. 1997; Singh et al. 2005; Muir et al. 2017a, 2020). This basal conglomeritic unit, with thickest accumulations in the deepest portions of the sub-basins adjacent to the bounding faults (Fig. 2; Muir et al. 2017a) is coeval with, but occasionally overlain by the variegated mudstones and sandstones of the Kirkwood Formation (Fig. 2; McLachlan and McMillan 1976; Dingle et al. 1983; McMillan et al. 1997; Singh et al. 2005; Muir et al. 2015, 2017b, 2020). The Kirkwood Formation was deposited in the meandering rivers and floodplains along the dipping landscape of the hanging walls of the rift normal faults (Fig. 2; McLachlan and McMillan 1976; Dingle et al. 1983; McMillan et al. 1997; Muir et al. 2015, 2017b, 2020). Onshore, the continental deposits of the Enon and Kirkwood Formations are overlain by the Sundays River Formation. In outcrops, this marine, regionally extensive unit is well known for its age-diagnostic Valanginian foraminifera (McMillan et al. 1997, 2003; Broad et al. 2012; Muir et al. 2017a, b, 2020). Unlike the Enon and Kirkwood Formations, the age of the Sundays River Formation has not been determined with radioisotopic dating methods (see Muir et al. 2020 for discussion). Based on biostratigraphic proxies, its lower part can be considered coeval with the upper Kirkwood and Enon Formations. Despite lacking robust age constraints, the Sundays River Formation is widely considered to mark the end of syn-rift deposition in the study region, chiefly because it is overlain by the Hauterivian to Albian transitional phase succession (McLachlan and McMillan 1976; Dingle et al. 1983; McMillan et al. 1997). These sediments are well preserved in the offshore Gamtoos Basin but not in the Algoa Basin,

where they have been eroded during the late Aptian uplift. Aero-magnetic studies show that the Uitenhage Group in the Algoa Basin can reach a thickness of up to 6 km, especially in the SW part of the basin (Caku et al. 2020). The Hauterivian to Aptian uplift resulted in the Algoa and Gamtoos Canyons (McLachlan and McMillan 1976; Dingle et al. 1983; Malan et al. 1990; Bate and Malan 1992; McMillan et al. 1997; Paton and Underhill 2004), which were subsequently filled with transitional phase late Aptian (13At1) to early Albian (possible early Cenomanian) inner to middle shelf marine claystones with sandstone interbeds (McMillan et al. 1997). The transitional phase succession is truncated by the regionally extensive Top Cenomanian (15At1) unconformity (Fig. 2), which is onlapped by marine-dominated Upper Cretaceous drift phase sediments (McMillan et al. 1997; Broad et al. 2012). Unconformably overlying the Mesozoic successions onshore are various Cenozoic formations comprising of the: Bathurst, Alexandria, Nanaga, Salnova, Nahoon, and Schelm Hoek Formations, which mostly belong to the Eocene to Holocene-age Algoa Group (e.g., McMillan and McMillan 1976; Du Toit 1979; Le Roux 1987, 1989, 1990; McMillan 1990; Illenberger 1992; McMillan et al. 1997; Hattingh 2001; Broad et al. 2012).

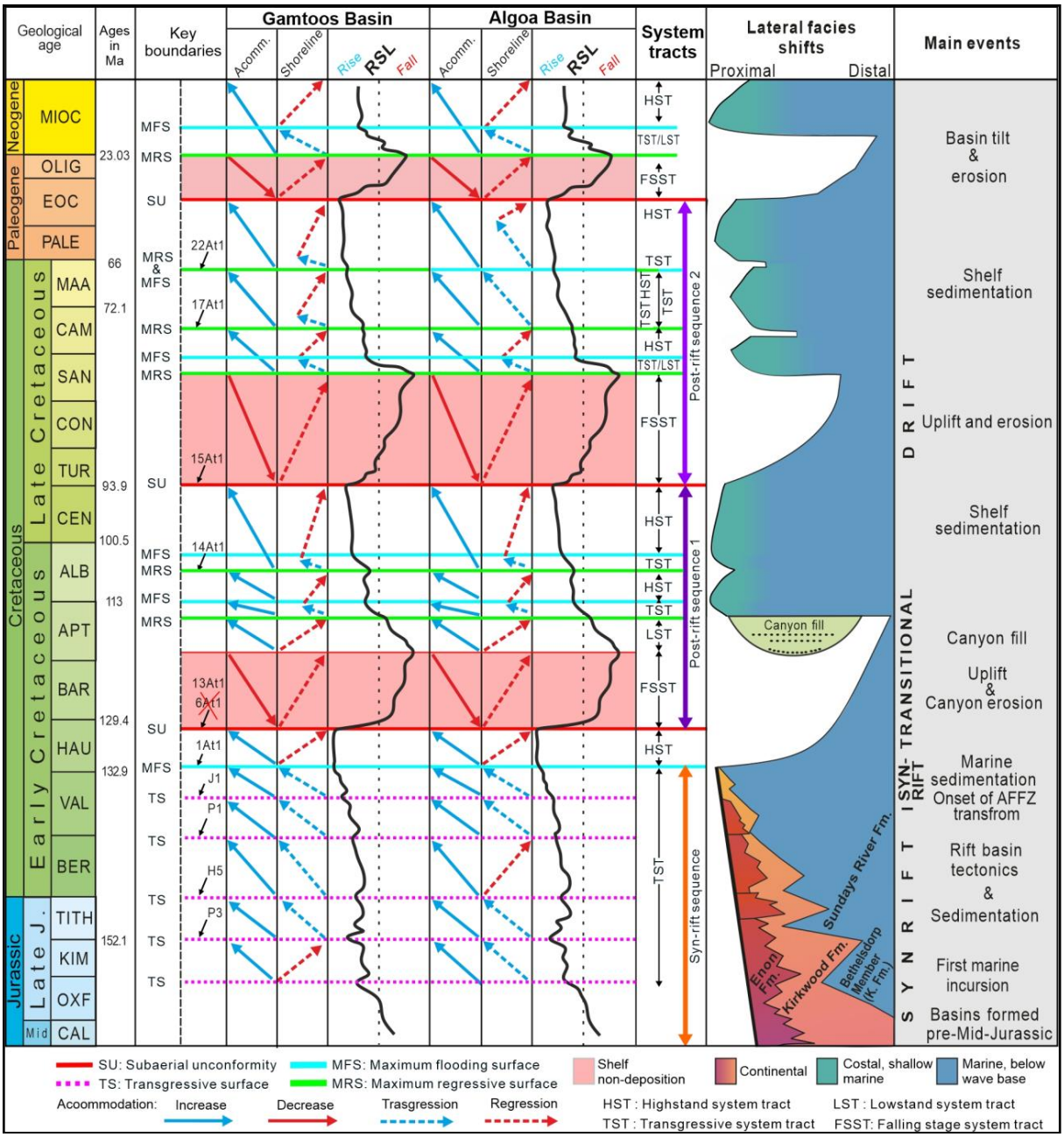

Fig. 2 Stratigraphic succession of the Algoa and Basins showing major geological events from the Late Jurassic to Miocene (modified from Brown et al. 1995; McMillan et al. 1997; Baby et al. 2018; Muir et al. 2020).

Tectonic setting and basin evolution

In the long-lived rift-basin system of the southern Cape, two main rifting episodes were recorded: 1) the opening of west Gondwana during the Early Jurassic, and 2) the Early Cretaceous strike-slip movement along the Agulhas-Falkland Fracture Zone (AFFZ; Fig. 1; Muir et al. 2020). Based on recent U-Pb radioisotopic dating of pyroclastics and resedimented volcaniclastics, Muir et al. (2020) showed that the Uitenhage Group was deposited over a 40 myr-long-period, from the Early Jurassic to the Early Cretaceous. This recent age assessment suggests that the initial rifting in the region occurred pre-Aalenian, during the Early Jurassic as part of the rift system that was generated during the separation of East and West Gondwana, in the initial Gondwana break-up interval (Jungslager 1996; Muir et al. 2020). The second rifting phase occurred in the Early Cretaceous due to transform rifting, which is linked to the initiation of the AFFZ and the opening of the South Atlantic (McLachlan and McMillan 1976; Martin et al. 1981; Dingle et al. 1983; Broad 1990; Bate and Malan 1992; Ben-Avraham et al. 1993; Paton and Underhill 2004; Muir et al. 2020). This second rift phase (late Valanginian transitional phase) was shown to correspond to the M21-M10 magnetic signatures with a radioisotopic age of ~145−122 Ma (Martin and Hartnady 1986). During the post-rifting phase, the basin underwent several uplift events, the first of which occurred during the Barremian−Aptian (6At1 to 13At1; Fig. 2; McLachlan and McMillan 1976; Dingle et al. 1983; Malan 1993; Brown et al. 1995; Thomson 1999; Paton and Underhill 2004). After the syn-rift phase, the second major erosional event caused uplift in the distal/offshore part of the basin in the Late Cretaceous (15At1 to 22At1; Fig. 2; Malan 1993; Baby et al. 2018) and resulted in the "Drift Sequence" (*sensu* Broad et al. 2012; thermal subsidence driven). The last notable uplift event occurred during the Oligocene, when the basin tilted to the N, deeply eroding the drift sediments on the shelf (Hattingh 2001; Baby et al. 2018).

Material and methods

Vintage datasets (Fig. 3), consisting of seismic and borehole data were purchased from the Petroleum Agency SA (PASA). Generally, the wireline data are of moderate to good quality, the two dimensional (2D) seismic data is poor to moderate quality, and three dimensional (3D) seismic data varies from moderate to good quality. This dataset would require reprocessing to further enhance the seismic imaging, eliminate multiples, increase the vertical resolution, and minimise seismic misties between different vintages, however these processes are beyond the scope and budget of this study.

	Algoa Basin	
Data type	**Quantity**	**Years acquired**
Onshore wells	6	1968-1978
Offshore wells	9	1978-1987
Offshore seismic survey (2D)	71 lines	1976-1989
Onshore seismic survey (2D)	6 lines	1968-1977
Offshore seismic survey (3D)	1 X 424 km^2	2001

	Gamtoos Basin	
Data type	**Quantity**	**Years acquired**
Onshore wells	NA	NA
Offshore wells	10	1978-1990
Offshore seismic survey (2D)	20 lines	1975-1987

Fig. 3 Inventory of the dataset from the Algoa and Gamtoos Basins obtained from the archives of the Petroleum Agency of South Africa). Base map data ©2020 Google, Maxar Technologies, AfriGIS (Pty) Ltd.

Interpreted two-way time (TWT) maps were depth converted using multiple methods (i.e., V0k, layered cake and average velocities), following which isopach maps were generated to delineate the stratigraphic thickness variations in the basin. In the Algoa Basin, the complex subsurface successions required a complex velocity model such as the V0k method to depth convert the TWT maps (Fig. 4a). In the Gamtoos Basin, due to its less complicated basin structure, the average velocity model derived from wireline checkshot data yielded favourable maps (Fig. 5b). The limitation of reflection seismic resolution, a challenge in this study, is discussed in Catuneanu (2019a, b) and Catuneanu and Zecchin (2020), and addressed in the Discussion.

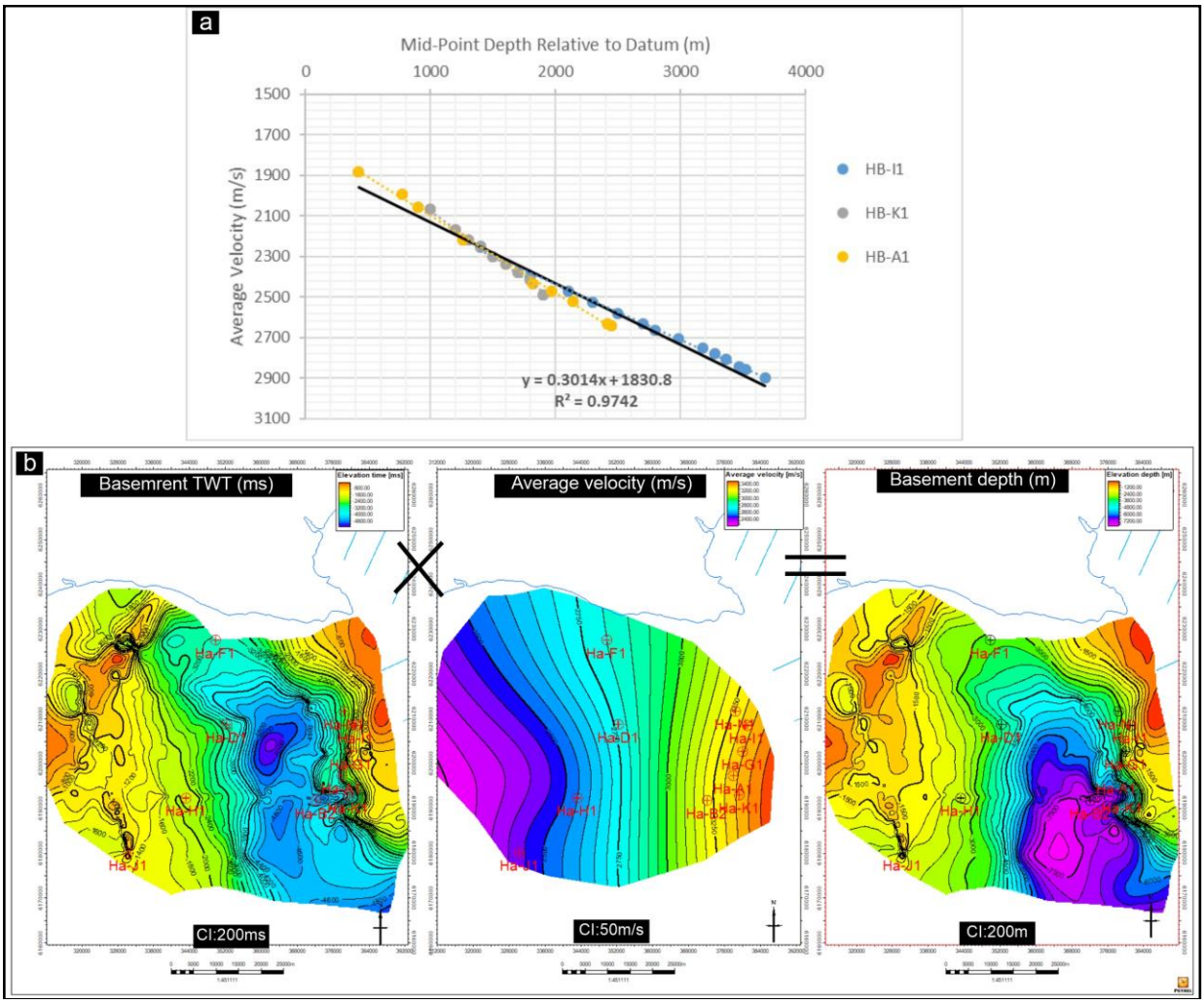

Fig. 6 **a** Interval Velocity vs Mid-Point Depth. Sedimentary rocks in the Algoa Basin show an increase of velocity with depth, without any velocity inversion. V0: 1830 m/s, k:0.3014. Data points are from Hb-I1, Hb-K1 and Hb-A1 wells. **b** Gridded TWT Basement map multiplied by average velocity from check shot data to produce the depth maps in the Gamtoos Basin. This process was repeated for all surfaces.

Understanding of the shoreline trajectories, vertical stacking patterns of the facies, geometry of stratal terminations and spatial facies changes are building blocks of any robust sequence stratigraphic framework (Neal et al. 2016). A reliable evaluation of the rock record is best achieved with those sequence stratigraphic depositional models that integrate different types of datasets (core, outcrop, wireline, seismic surveys, etc.; e.g., Neal and Abreu 2009; Catuneanu et al. 2011). There are currently several conventional stratigraphic models grouped into depositional, genetic and T-R sequence models as shown in Fig. 7. Depositional sequence models use SUs as sequence boundaries, while the genetic and T-R sequence models use shoreline trajectories (MFS and MRS) to define a sequence boundary (e.g., Embry et al. 2007; Catuneanu et al. 2011).

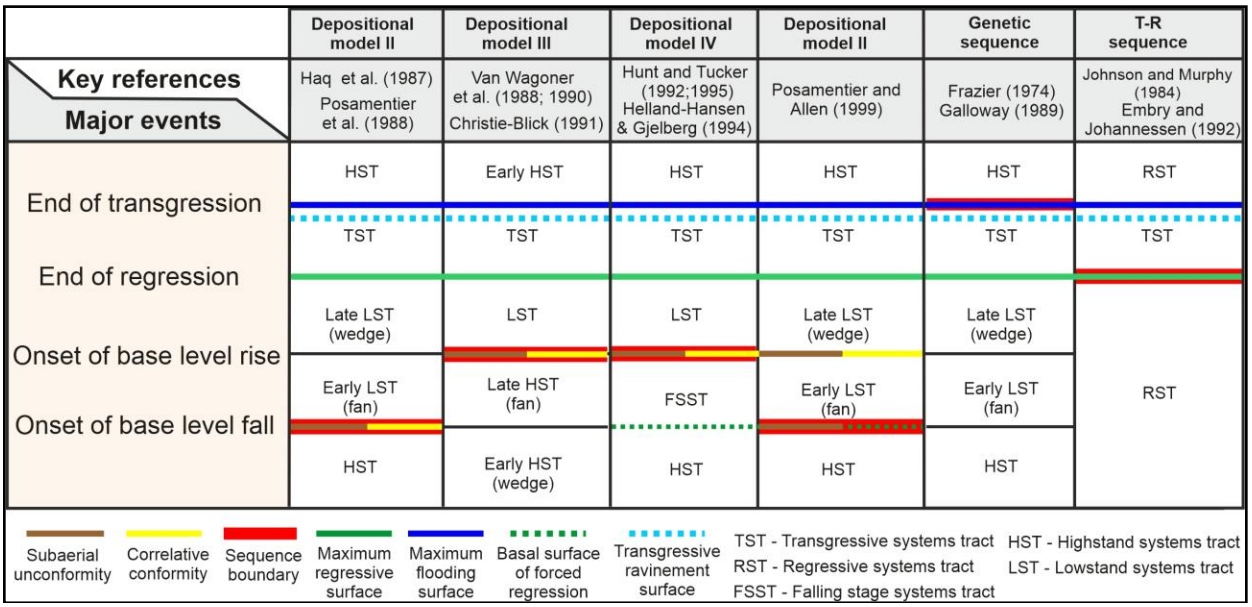

Fig. 7 Sequence models, and their bounding surfaces. Abbreviations: LST—lowstand systems tract; TST—transgressive systems tract; HST—highstand systems tract; FSST—falling-stage systems tract; RST—regressive systems tract; T–R— transgressive-regressive (modified from Catuneanu 2002).

Gross depositional environment modelling in this study followed the workflow presented in Fig. 8. This workflow serves as a set of guidelines, rather than strict rules that can be used from data loading into the data analysis software (Petrel E&P Software Platform), to interpretations, to the final step of gross depositional model building. Concerted effort was made to integrate outcrop, core, wireline, and seismic data in order to achieve comprehensive interpretation of the depositional history.

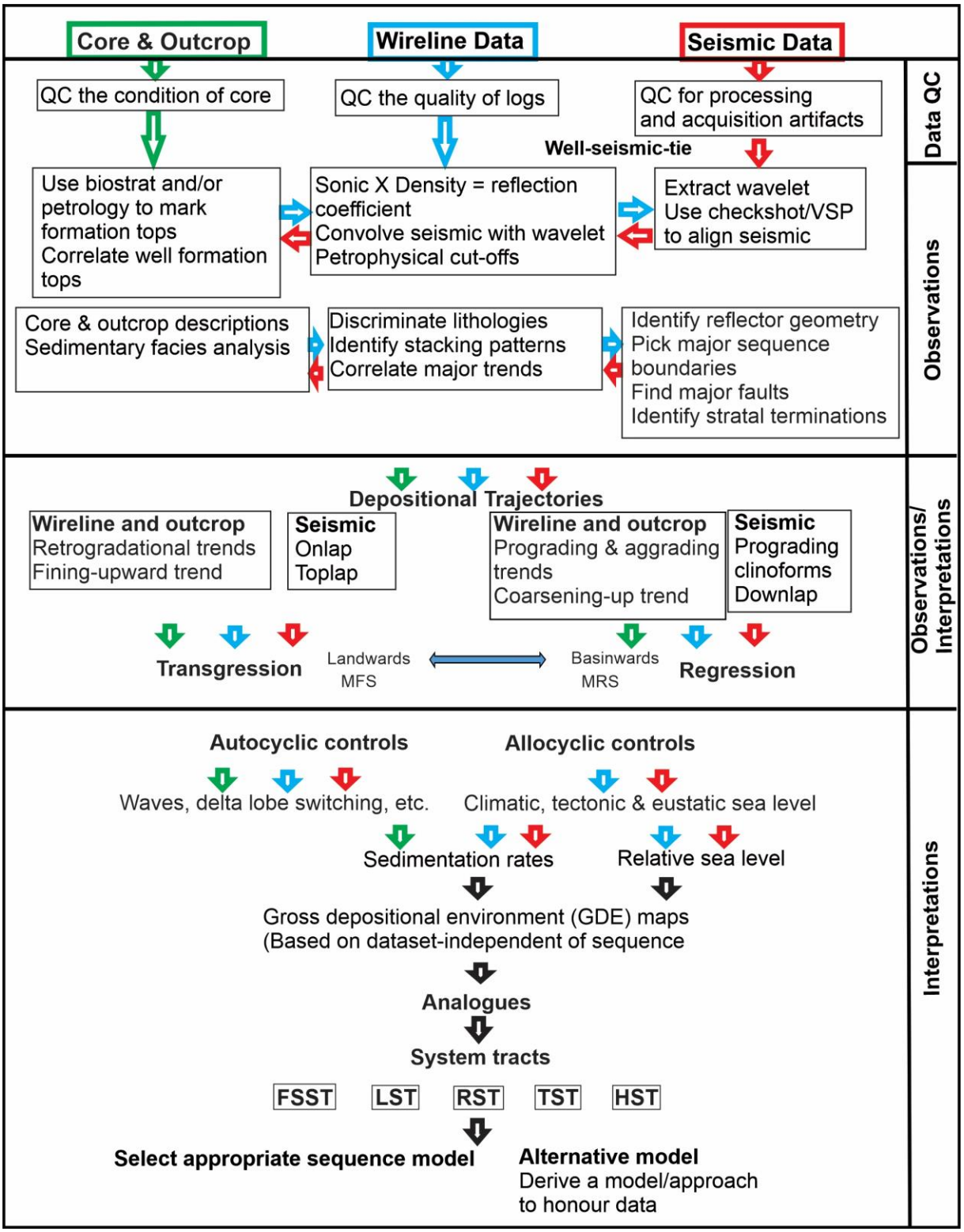

Fig. 8 Proposed workflow for sequence stratigraphic interpretations and building depositional models (adopted from Neal et al. 1993; Catuneanu 2006 p. 6; Miall and Strasser 2018; Neal et al. 2016; Burgess et al. 2016).

Results

Syn-rift I observations

Aalenian to upper Kimmeridgian

The Enon Formation is described from onshore outcrops as a predominantly immature, poorly sorted, pebble to cobble conglomerate with subordinate sandstones (Fig. 9a; Muir et al. 2017b). In the Algoa Basin, this succession shows lateral facies variability shown by alternating low to high gamma-ray (GR) values. In the S borehole HB-C1, the low GR values, ranging from 44 to 151 American Petroleum Institute (API), are detected over a ~85-m-thick unit, with two overall coarsening upwards packages, whereas in the N, high GR values dominate (Fig. 9c). The more proximal HB-P1 is dominated by > 400 m of serrated GR signatures (44 to 151 API) consisting of alternating coarsening-upward and fining-upward trends. Overall, the borehole contains more sandy facies relative to the HB-C1 borehole. The lower part of borehole HA-J1 shows fining-upward trend in shale and clay succession followed by coarsening-upward trend in silty/shaley successions that give way to fining-upward trend in sandstones. Overall, borehole HA-J1 intersected a ~130-m-thick Basement to upper Kimmeridgian succession (GR: 64–180 API). In the center of the Gamtoos Basin, borehole HA-H1 is dominated by > 700-m-thick fining-upward units (GR: 30–112 API). However, the lower part shows a high net sand-to-shale ratio, while the upper succession shows silty and claystones facies. Near the Gamtoos Fault, borehole HA-B2 intersected a > 265-m-thick succession of shales and clays that contain some isolated coarsening-upward sandy facies (GR: 42–145 API). Borehole HA-K1, which is closer to the Recife Basement High contains a > 1720-m-thick succession of predominantly coarsening-upward units (GR: 36–120 API; Fig. 9c).

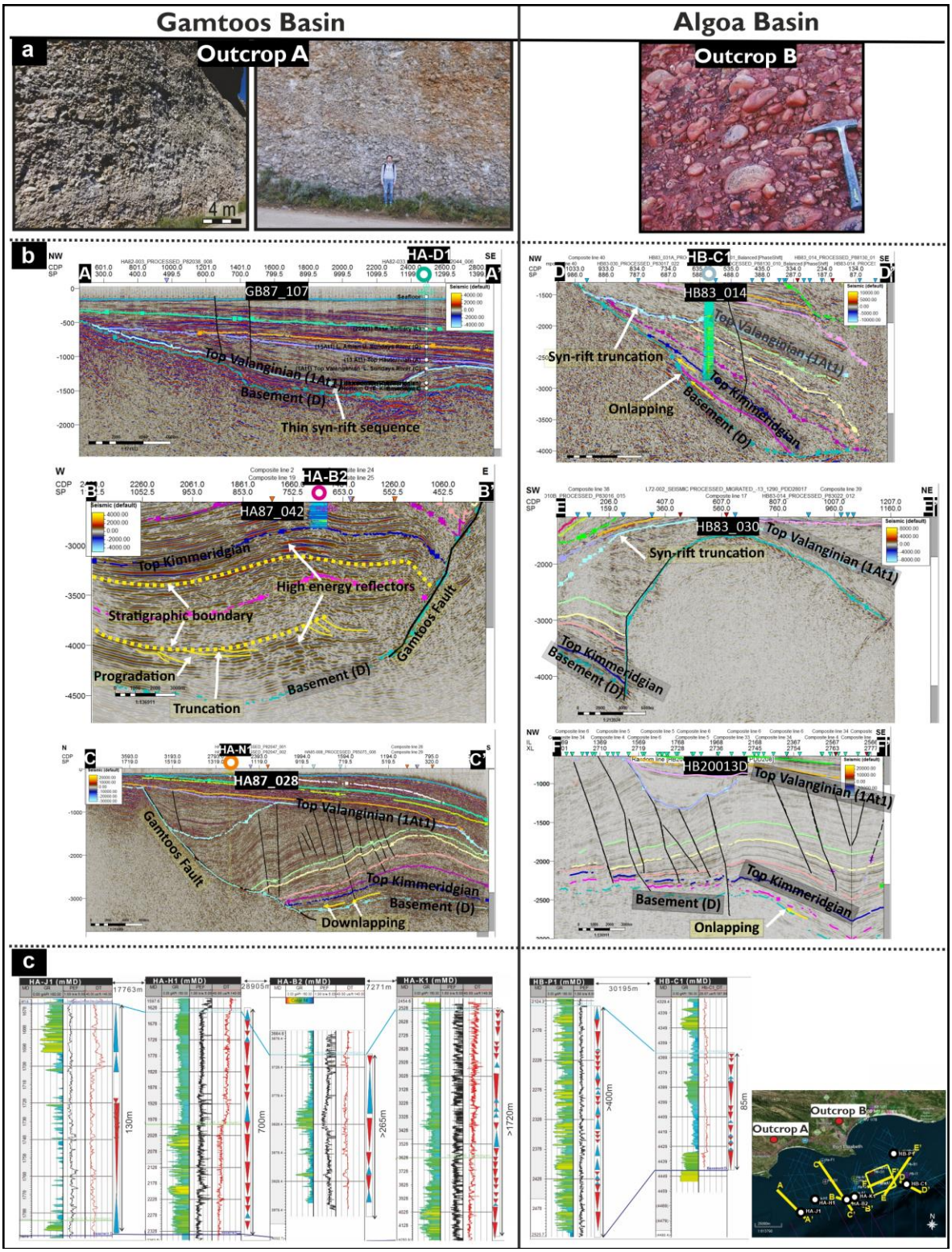

Fig. 9 a Enon Formation outcrop images (taken from Muir et al. 2017b with permission from the author). **b** Seismic lines examples over the Algoa and Gamtoos Basins. **c** Wireline logs intersecting the Kimmeridgian succession in the Algoa and Gamtoos Basins. Base map data ©2020 Google, Maxar Technologies, AfriGIS (Pty) Ltd.

This Aalenian to Kimmeridgian succession onlaps (in some places downlaps) onto the Basement D reflector, generally showing higher energy seismic reflectors than the overlying and the underlying succession (Fig. 9b). The internal reflector geometries are commonly discontinuous and chaotic. This succession has been subject to intense erosion in the Uitenhage Trough, whilst being less eroded in the Port Elizabeth Trough where it terminates against the Basement D Reflector. Although this erosion is extensive in the Algoa Basin, this succession is preserved in some isolated areas, such as borehole HB-P1 location. The absence of this succession in most parts of the Algoa Basin make it challenging to confidently correlate it across the basin (Fig. 9b). In the Gamtoos Basin, the syn-rift succession is better preserved, and shows thickening and folding (due to a later tectonic inversion; Thomson 1999) towards the Gamtoos Fault, in addition to westward pinching near the borehole HA-J1 (Figs. 7 and 8b). A thickness map from seismic mapping (Fig. 10a) shows a prominent depocenter near the N/S trending limb of the Gamtoos Fault. There is also evidence of clinoforms prograding from the W towards the Gamtoos Fault (Fig. 9b). This progradational succession is overlain by dimming chaotic reflectors, which are subsequently overlain by subparallel and continuous reflectors of the upper Kimmeridgian succession (Fig. 9b).

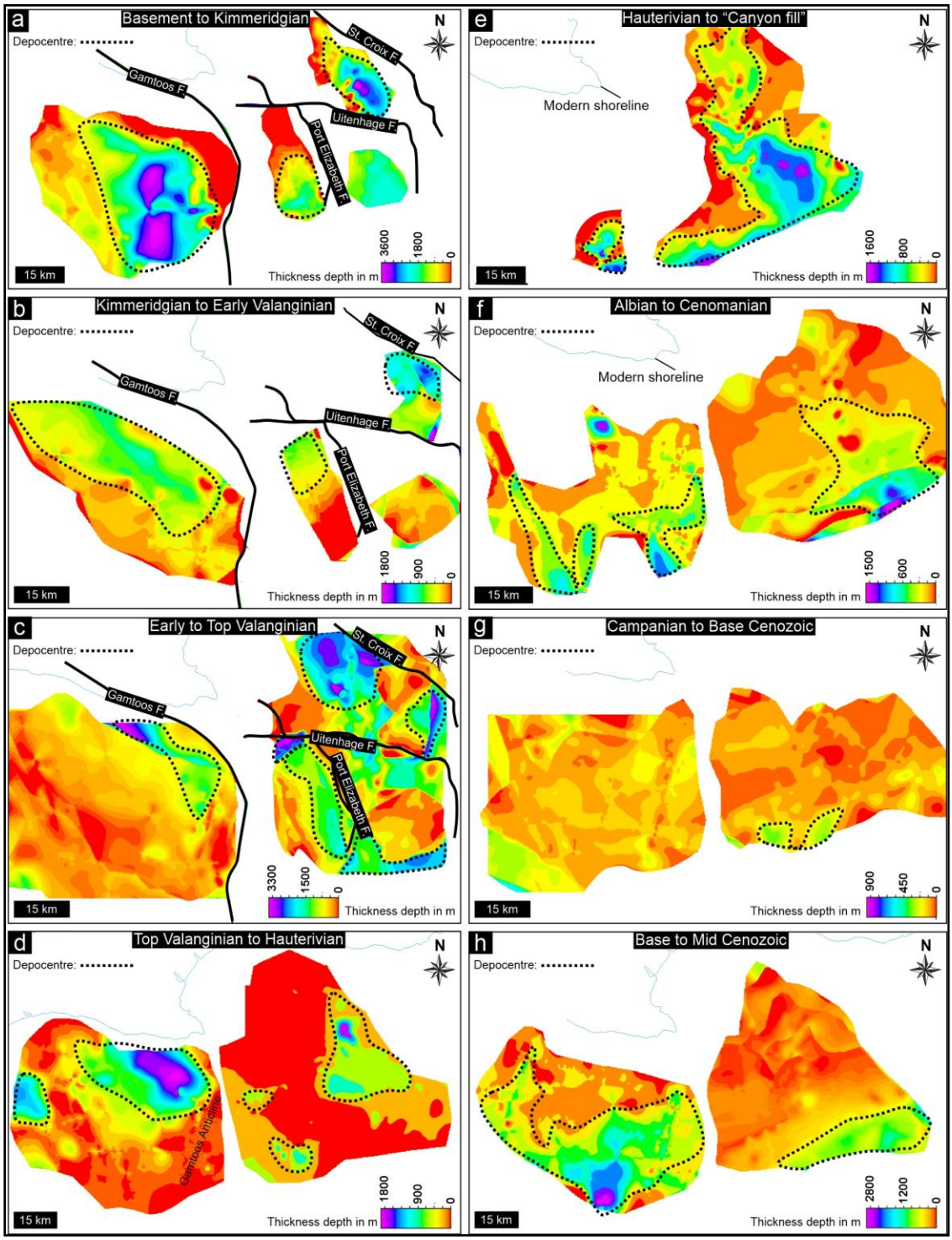

Fig. 10 Thickness maps from syn-rift to Holocene, highlighting the main depocenters during basin infill. **a** Pre-Aalenian to Kimmeridgian thickness map, showing a dominant N-S striking depocenter in the Gamtoos Basin and a NW-SE striking depocenter in the Uitenhage Trough. **b-c** NW-SE striking depocenter in the Gamtoos and Algoa Basins from the Tithonian to upper Valanginian. **d** In the Gamtoos Basin, the depocenter is controlled by the geometry of the Gamtoos Anticline, in the Algoa Basin, the depocenter is a remnant of sediments not eroded during the Hauterivian to Aptian erosional event. **e** The orientation of the main depocenter was influenced by the geometry of the Algoa Canyon. **f-h** Drift-phase depocenters located mainly towards the shelf edge.

Post-Kimmeridgian to Early Valanginian

The most dominant rock unit of this interval is the Kirkwood Formation, which consists of mostly variegated mudstones and sandstones with subordinate conglomerates that formed in meandering rivers with wide floodplains and lakes (Fig. 11a; Muir et al. 2017b). The formation contains a rich and diverse fossil biota (e.g., theropod dinosaurs, freshwater fish, reptile, plants) that further supports the continental nature of the depositional setting (Muir et al. 2017b). The Lower Valanginian thickens towards the S and attains a thickness of ~620 m in borehole HB-C1 (Fig. 11c). Borehole HB-B1 consists of ~320-m-thick, alternating fining-upward and coarsening units with high sand to shale/clays ratio (GR: 35–82 API). The borehole HB-C1 intersected predominantly shales and clays and a 330-m-thick, coarsening-upward sandy unit (GR: 40–140 API) in the lower half of the succession (Fig. 11c). The upper part of borehole HB-C1 is dominated by a ~310-m-thick, shaley succession with very limited sand content (GR: 70–140 API). In the Gamtoos Basin, the general vertical grains size trend is stacked, comprising mostly coarsening-upward and rare fining-upward units (Fig. 11c).

In the Port Elizabeth Trough, where this interval is preserved, seismic reflectors are chaotic and discontinuous in the N-S direction (Fig. 11b). Contrary to the underlying successions, which form a westward pinching wedge in the Port Elizabeth sub-basin, the wedge geometry in this stratal unit is less defined (Fig. 11b). On the seismic lines, most faults appear to propagate from the Top Tithonian, through to the Top Valanginian reflector, with very few faults observed in the older successions (Fig. 11b). Furthermore, thickness maps show a change in the depocenter strike direction from N-S in the Late Jurassic to NW-SE in the Early Cretaceous (Fig. 10). Overall, in the Algoa Basin, this unit shows dimming seismic reflectors in contrast to the surrounding reflectors. In the Gamtoos Basin, the Lower Valanginian unit, which onlap on the Top Berriasian reflector, contains bright reflectors that are subparallel and continuous (Fig. 11b). Towards the W, in the hanging walls, this unit is truncated at the top by the Top Valanginian (1At1) unconformity (Fig. 11b).

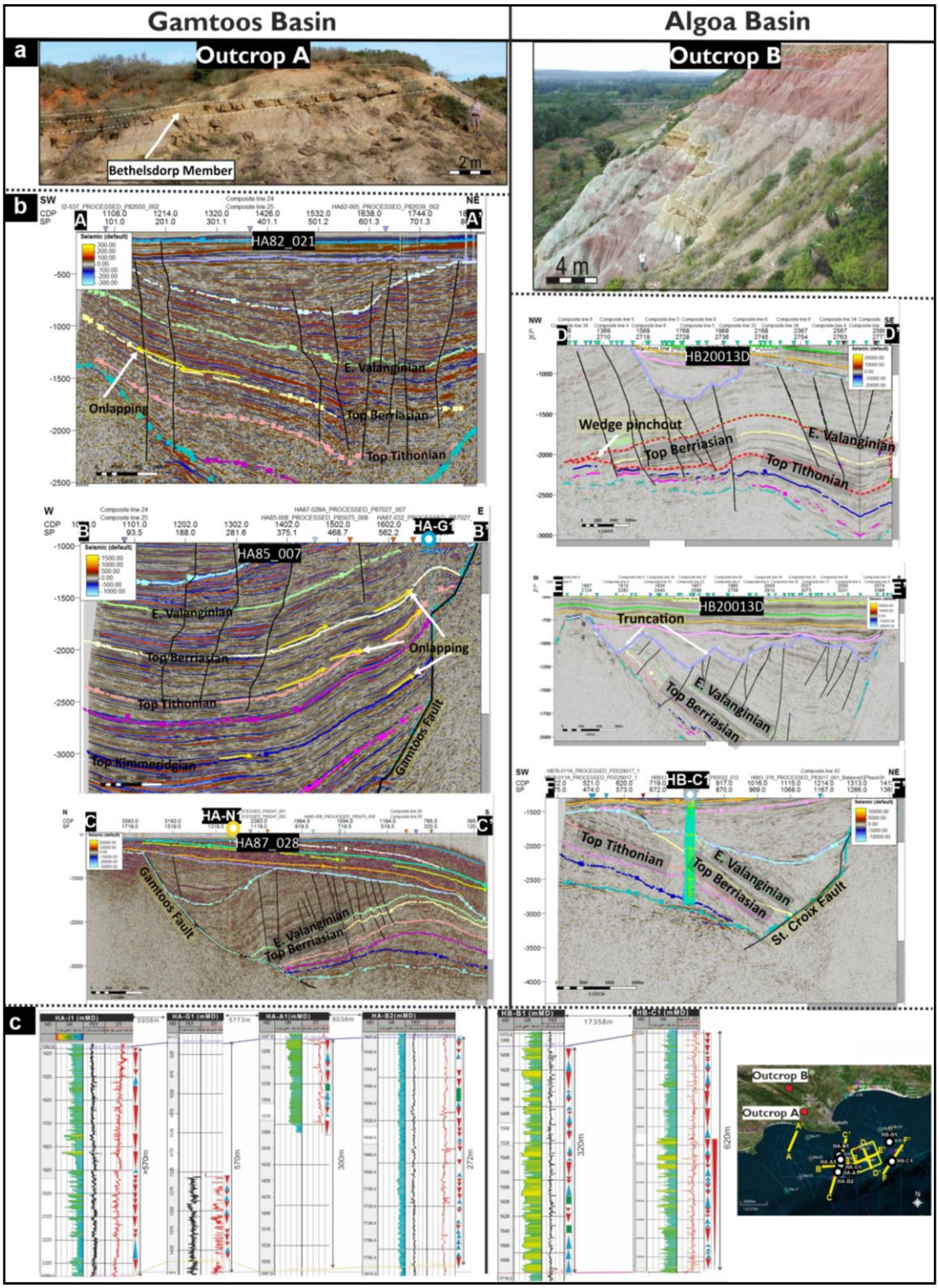

Fig. 11 a Outcrop A- Bethelsdorp member near Jachtvlakte. Outcrop B- Kirkwood Formation outcrop in the
Algoa Basin (taken from Muir 2019; Muir et al. 2017b with permission from the authors). **b** Seismic lines examples over the Algoa and Gamtoos Basins. **c** Wireline logs intersecting the early Valanginian succession in the Algoa and Gamtoos Basins. Base map data ©2020 Google, Maxar Technologies, AfriGIS (Pty) Ltd.

Syn-rift I interpretations

Aalenian to upper Kimmeridgian

In the Algoa Basin, borehole HB-P1 intersected a succession with high net sand-to-shale ratio, while the more distal HB-C1 shows limited sand input (Fig. 9c). The presence of isolated coarsening-upward sandstones within the shaley interval in the distal borehole HB-C1 could represent prograding delta mouth bars, or sediments eroded from the basement subcrops. The combination of coarsening-upward and fining units and clay interbeds suggest that the depositional setting was probably alternating between coastal floodplains and shallow marine environments during a period characterized by fluctuating slow rise of RSL and sediment supply (Fig. 12a). This fluctuation is attributed to short lived tectonic pulses in syn-rift settings, resulting in increasing accommodation space (transgression), followed by longer period of tectonic quiescence which allows progradation of sediments (Martins-Neto and Catuneanu 2010). According to McMillan et al. (1997), borehole HB-A1 in the Port Elizabeth Trough is dominated by a microfauna that suggest a shallow marine-transitional setting, while borehole HB-K1 contains continental red beds, pebbly sandstone, and lignite-bearing claystones. Although these boreholes are close to each other, their different facies suggest contrasting marine vs continental settings, with the red beds and lignite bearing units possibly having formed on emergent basement highs (Fig. 12a).

There is significant lateral lithological heterogeneity in the Gamtoos Basin wireline data, with logs showing varying inferred grain-size and facies trends across the basin, a feature common in highly compartmentalized syn-rift successions (e.g., Chorowicz 2005; Holz et al. 2017). The lower part of borehole HA-J1 is dominated by shaley facies, overlain by well-defined, channelized, fining-upward sandstones (Fig. 9c). In contrast, the lower part of borehole HA-H1 is dominated by proximal high-energy, coarsening- and fining-upward sandstones, which are overlain by a flooding surface and fine-grained sediments that are characteristic of low energy settings. Although the upper half of the borehole shows an overall coarsening-upward trend, the very low net sand-to-shale ratio suggests either decreased sedimentation rates, or a shoreline advancing landwards at faster rate than sediment input, which is typical during transgression (Fig. 2; Catuneanu 2006). In borehole HA-B2, the interval is mostly claystones, inferred to represent a predominantly low energy, distal depositional environment, with isolated sandstones representing rare events of higher energy sedimentation, possibly as basin floor fans in a deeper water setting (Fig. 12a). The proximity of borehole HA-K1 to the Recife Arch (Fig. 1) suggests that the coarsening-upward sandstones were probably eroded from the basement high and deposited as alluvial fans.

Most of the basal early rift sediments are not intersected by boreholes and the seismic resolution is very poor in the study area, consequently the interpretation of this succession is reliant on the onshore geological studies (e.g., Muir et al., 2015, 2017b; Muir, 2019). These studies show that in the Algoa and Gamtoos Basins, the Basement to Top Kimmeridgian, conglomerate-dominated succession of the Enon Formation was deposited primarily in high-energy, alluvial fan and braided river setting proximal to basin margin extensional faults, whereas its more distal facies equivalent, the mudstone and sandstone-bearing Kirkwood Formation, was a product of meandering rivers with vast floodplains that supported large, freshwater lakes. Due to the limited data resolution and data coverage, stratal

geometry of this succession in the Algoa Basin remains largely unknown. In the Gamtoos Basin, the pre-Aalenian to upper Kimmeridgian succession thickens towards S of the Gamtoos Fault, indicating active faulting during deposition of this succession (Fig. 10a). The N-S striking, southern part of the fault was probably more active, creating larger accommodation space in S than in the N. Seismic data ((Fig. 9c).) shows eastward prograding reflectors (clinoforms) above the Basement D reflector overlain by chaotic seismic reflectors. Since progradation in a nearshore depositional context is typically a transitional to marine process, prograding clinoforms ((Fig. 9c).) are taken as evidence for a pre-Kimmeridgian marine incursion in the Gamtoos Basin. However, due to the unavailability of borehole data intersecting these progrades, the possibility of these progrades representing a deltaic environment cannot be ruled out. In which case, these progrades would suggest a transitional setting.

Post-Kimmeridgian to Early Valanginian

Dataset from this succession supports the widespread fluvial floodplain setting of the Kirkwood Formation established from outcrops studies (Muir et al. 2015, 2017b and references therein). The main depocenters appear to be localised near the NW-SE striking hanging walls, from the late Tithonian to early Valanginian (Fig. 10a, b). Unlike in the earlier depositional phase, when sedimentation was mainly along the N-S trending sector of the Gamtoos Basin, isopach maps shows active faulting along NW-SE strike from the Tithonian to Valanginian (Fig. 10a, b). This created accommodation space for marine conditions as the shoreline advanced landwards. This increase in accommodation could have resulted from the fault strain following pre-existing crustal scale structures of the underlying Palaeozoic Cape Supergroup (Martin et al. 1981; de Wit 1992; Paton and Underhill 2004; Muir et al. 2020). Seismic mapping suggests that the sediments were supplied from the NW to S-SE, which is consistent with Kirkwood Formation provenance studies (Shone 1976). Although Muir et al. (2015) reported a localized SW to NE paleocurrent direction, this discrepancy is likely due to the meandering nature of the rivers in the Kirkwood Formation. According to McMillan et al. (1997) and Muir et al. (2017b, 2020), microfossils in the Kirkwood Formation also show evidence for low energy, lacustrine environments (Colchester Member) that were, among others, inhabited by freshwater algae, and thus these organic matter rich lake deposits are also potential source rocks in the study area. However, data suggest that the lacustrine environment by this time was probably due to oxbow lakes on the floodplain and drowning estuaries during transgression (Fig. 12b). In addition to the lacustrine setting, the Bethelsdorp Member in the lower Kirkwood Formation indicate the presence of low energy conditions, albeit in a marine setting, due to sea incursion during the Late Jurassic (McLachlan and McMillan 1976; McMillan et al. 1997; McMillan 2010; Muir et al. 2017b). This marine flooding appears to have coincided with the change to NW-SE trending depocenters during the Late Valanginian to Early Berriasian (Fig. 10a, b). The newly created accommodation space could have aided the marine flooding in the proximal onshore setting as the shoreline advanced towards N. The Bethelsdorp Member, which is a bioturbated, grey shaley succession, outcropping onshore in the Uitenhage Trough (e.g., near Jachtvlakte) attains a thickness of 400 m (Muir et al. 2017b). It also contains tabular sandstone beds that lack terrestrial fossils or red palaeosols, contrary to the rest of the units in the Kirkwood Formation (Almond 2012; Muir et al. 2017b). This Late Jurassic marine influence in the early rift during does not de facto suggests the presence of an ocean floor in the area (McLachlan and McMillan 1976; Jungslager 1996; Koopmann et al. 2014; Muir et al. 2017b, 2020). However, evidence for a failed, pre-Tithonian

(~178 Ma old), mid-oceanic ridge (MOR) was shown in the Falklands (Malvinas) Plateau Basin (Schimschal and Jokat 2019), which is a region placed near the study area in most palaeogeographic reconstructions (e.g., Lovecchio et al. 2020; Muir et al. 2020).

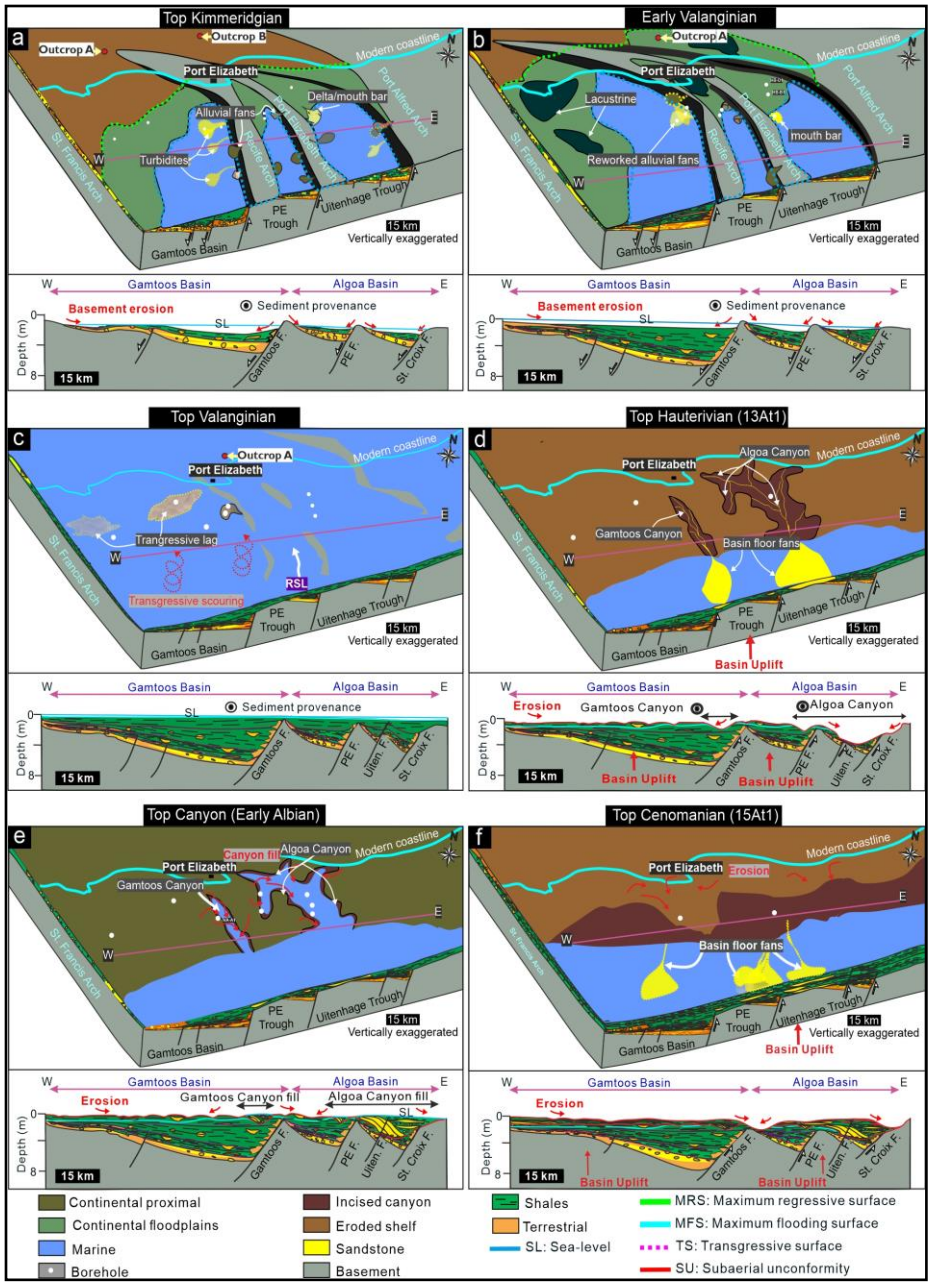

Fig. 12 Aalenian to upper Cenomanian gross depositional models, showing the basin evolution from syn-rift to transitional and then to drift phase. **a-b** syn-rift phase deposition compartmentalized into sub-basins bound by the Gamtoos, Port Elizabeth, St. Croix Fault. **c** Late Valanginian increase in RSL over the Algoa and Gamtoos Basins. **d** Hauterivian to Aptian uplift and erosion, resulting in the Algoa and Gamtoos Canyons. **e** Early Albian "Canyon fill" phase. **f** Late Cretaceous uplift and erosion, resulting in the shelf/shelf edge scouring. (See figs. 7, 9 and 11 for outcrop images noted above)

Syn-rift II observations

The Valanginian–Hauterivian Sundays River Formation is a mostly shallow marine succession, characterized by fossiliferous, green-grey laminated mudstones (Fig. 13a; McLachlan and McMillan 1976; Shone 1978; McMillan 2003; Muir 2019). Syn-rift sequences generally shows lateral facies variability, with the logs dominated by alternating fining-upward and coarsening trends within the same succession. Wireline data from the upper Valanginian succession in the Uitenhage Trough shows a 190-m-thick unit of alternating low and high GR signatures (GR: 51–129 API), with coarsening-upward and fining trends in borehole HB-B1 (Fig. 13c). Borehole HB-I1, contains a > 800-m-thick logged succession dominated by low to high GR readings (GR: 52–145 API; Fig. 13c), with alternating coarsening-and fining-upward trends. In the distal borehole HB-C1, the same interval shows a coarsening-upward trend in a ~50-m-thick succession with relatively low GR signature (GR: 50–104 API). In the Gamtoos Basin, the upper Valanginian succession has a very low net sand-to-shale ratio, which increases towards the SW (Fig. 13b). Borehole HA-J1 is dominated by ~330-m-thick clay- and shale-rich unit that is sand free (GR: 107–142 API), while borehole HA-D1 is dominated by a ~500-m-thick, aggrading sandy and silty unit (GR: 30–95 API; Fig. 13b). However, the uppermost 50 m in borehole HA-D1 intersected two cycles of coarsening-upward clean sands (GR: 20–45 API) separated by a flooding surface. Borehole HA-B2 is dominated by a ~375-m-thick unit of clean shales/clays (GR: 45–120 API) without any sand. Alternating, fining-upward and coarsening silty sands dominate in boreholes HA-G1 and HA-I1 over a thickness of 240 and 657 m with GR values of 69-104 and 50-125 API, respectively (Fig. 13b).

Most of this succession remains unresolved in the seismic data, because where preserved, the succession can be featureless and very thick (e.g., up to 3000 m in the Algoa Basin; Fig. 10c). Closer to the Port Elizabeth Fault, the reflectors in this succession show chaotic character. In the Uitenhage Trough, the succession appears to be folded (due to a later inversion; Thomson 1999) at the top, closer to the Uitenhage Fault (Fig. 13b). In both basins, the Top Valanginian reflector truncates the underlying syn-rift reflectors at the acute angle, especially towards the W (in the tilted hanging walls) and S (Fig. 13b). This succession also shows thinning towards the W and onlapping stratal terminations in W-E cross-sections (Fig. 13b). In the S, within the N-S trending sector of the Gamtoos Fault, the upper Valanginian succession is truncated by the 13At1 unconformity near the Gamtoos Anticline (Bate and Malan 1992; McMillan et al. 1997; Thomson 1999).

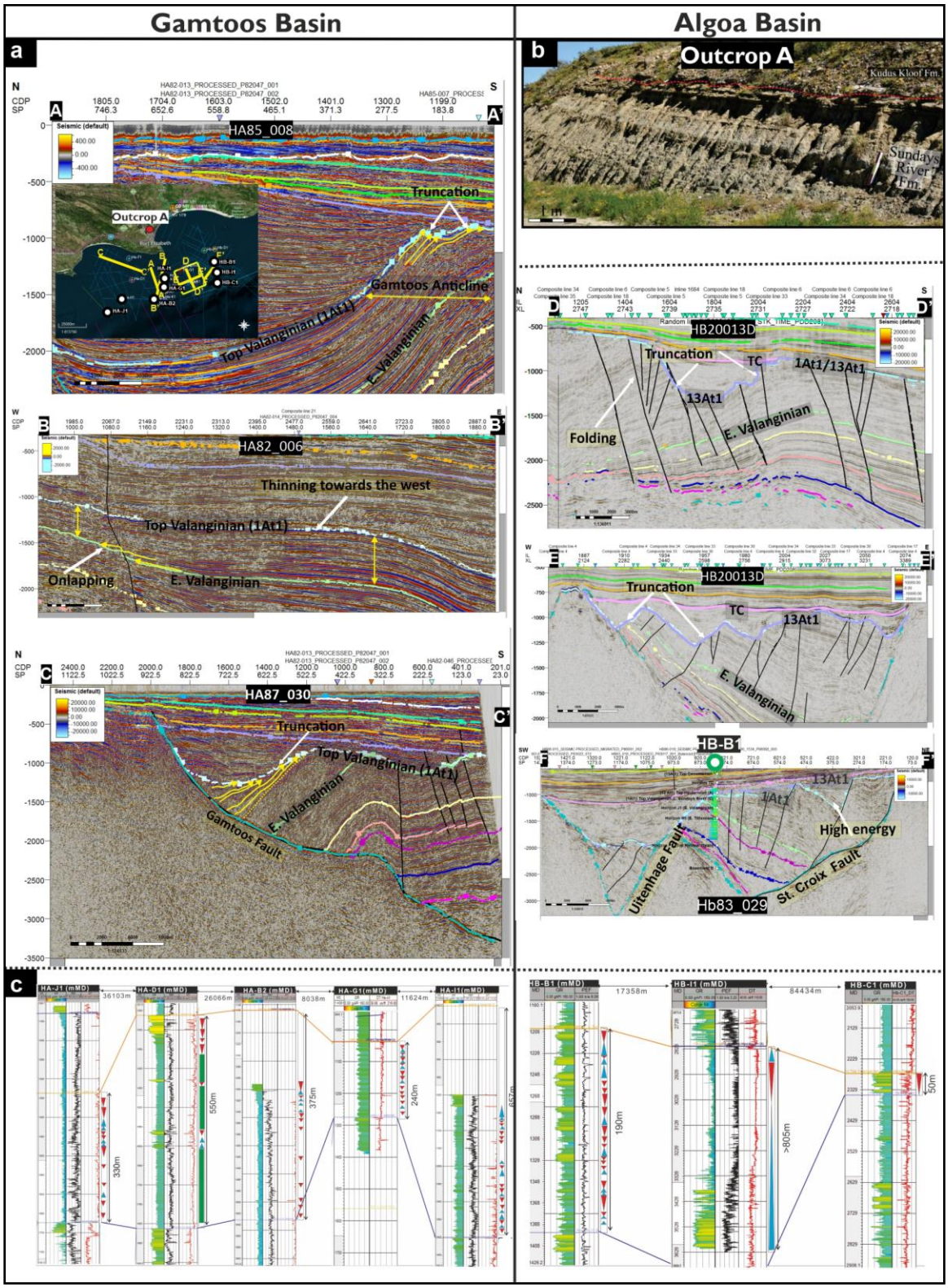

Fig. 13 a Seismic line examples from the Algoa and Gamtoos Basins. **b** Sundays River Formation outcrop images (taken from Muir 2019 with permission from the author). **c** Wireline logs intersecting the Kimmeridgian succession in the Algoa and Gamtoos Basins. Base map data ©2020 Google, Maxar Technologies, AfriGIS (Pty) Ltd.

Syn-rift II interpretations

Based on sedimentological and palaeontological characteristics (e.g., ammonites, belemnites, bivalves, gastropods, echinoids, crustaceans, polychaetes, corals), the depositional environment of the Valanginian-Hauterivian Sundays River Formation was reconstructed to span a range of marine settings from shallow-marine, tidally influenced, estuarine to deltaic environments to deeper water shelf and continental slope settings (Shone 2006; Muir 2019 p. 14-15).

Wireline data is dominated by fine-grained units, with a prominent shallow marine transgressive trend evident in borehole HB-I1 (Figs. 2 and 11c). In most places, this interval has been eroded (mostly on the tilted hanging walls), where only the lower part of the succession is preserved in some boreholes. For example, the sandy facies in the lower parts of boreholes HB-B1 and HB-C1 (Fig. 13c) might represent a period in the Valanginian before the onset of the marine transgression, when deposition was still predominantly occurring on fluvial or coastal floodplains (Fig. 2). In the Gamtoos Basin, borehole data is dominated by fine-grained successions, and is assumed to represent the dominant marine phase of deposition associated with the Sundays River Formation (Fig. 12c). The coarsening-upward sandy facies in the upper part of borehole HA-D1 could represent a deltaic or river mouth bar setting. Overall borehole data reflect the marine to nearshore character of deposition that was previously suggested for the Sundays River Formation (e.g., Shone 2006; Muir 2019).

Though this interval is severely eroded in the Algoa Basin, isopach maps in both the Algoa and Gamtoos Basins show NW-SE (Fig. 10c) directed depocenters, suggesting that the syn-rift faults were still active during the later parts of the Valanginian. In the Port Elizabeth and Uitenhage Troughs, this succession is folded, probably due to reactivation of the St. Crox and Uitenhage Faults, respectively during later tectonic inversion (Thomson 1999). Because this succession, which can be up to 2500-m-thick, has been intersected by few boreholes (Fig. 13c), its lateral and vertical facies are poorly understood. In both basins, this succession marks a major transgressive event (bound at the top by the 1At1 sequence boundary), which erodes large tracts of syn-rift deposits represented by the Enon and Kirkwood Formations (Figs. 2 and 11b). The 1At1 boundary marks a period when the Algoa and Gamtoos Basins were hydraulically connected for the first time. It is thus a major flooding surface (i.e., a maximum flooding surface - MFS) that separates the older continental from the younger marine deposits (i.e., the Enon-Kirkwood Formations from the Sundays River Formation), as attested by outcrops rich in marine fossils across the southern half of the Algoa Basin (Fig. 12c). It is noteworthy that while the Bethelsdorp Member in the lower Kirkwood Formation and the Sundays River Formation are lithologically alike and are both underlain by marine flooding surfaces due to their similar marine origin (e.g., Almond 2012; Muir et al. 2017b; Muir 2019), the older Bethelsdorp Member has a more localized occurrence, whereas the Sundays River Formation is regionally extensive (and coeval with the upper Kirkwood Formation).

Transitional phase observations

Post-Valanginian to upper Hauterivian

Most of this succession has been severely eroded during the late Aptian uplift event (Dingle et al. 1983; Broad 1990; Bate and Malan 1992; McMillan et al. 1997; Broad et al. 2012), as a result, there is very limited data available for this interval. Preserved in a total thickness of 120 m in borehole HB-B1, showing a change from predominantly coarsening-upward at the base (~75-m-thick, GR: 45–110 API; Fig. 14b) to fining-upward at the top (~45-m-thick, GR: 54–125 API; Fig. 14b). In the Gamtoos Basin, boreholes HA-J1 (~208 m-thick, GR: 92–143 API) and HA-D1 (~600 m-thick, GR: 35–105 API) intersected a predominantly fine-grained succession that seems to show a coarsening-upward trend (Fig. 14).

In places, where the Hauterivian succession is preserved, the generally dim reflectors are parallel, semi-continuous and show evidence for a few prograding strata dripping to the SW (Fig. 14a). Moreover, some brighter basal reflectors appear to onlap on the Top Valanginian reflector (Fig. 14a). In contrast to the younger successions, which are folded and form the so-called Gamtoos Anticline (that is more evident in the N-S trending part of the Gamtoos Fault; Thomson 1999), this Hauterivian succession onlaps onto the Gamtoos Anticline. Most of this succession is truncated by the Top Hauterivian (13At1) reflector, which in some places also truncates and forms a composite unconformity with the 1At1 reflector (Fig. 14a).

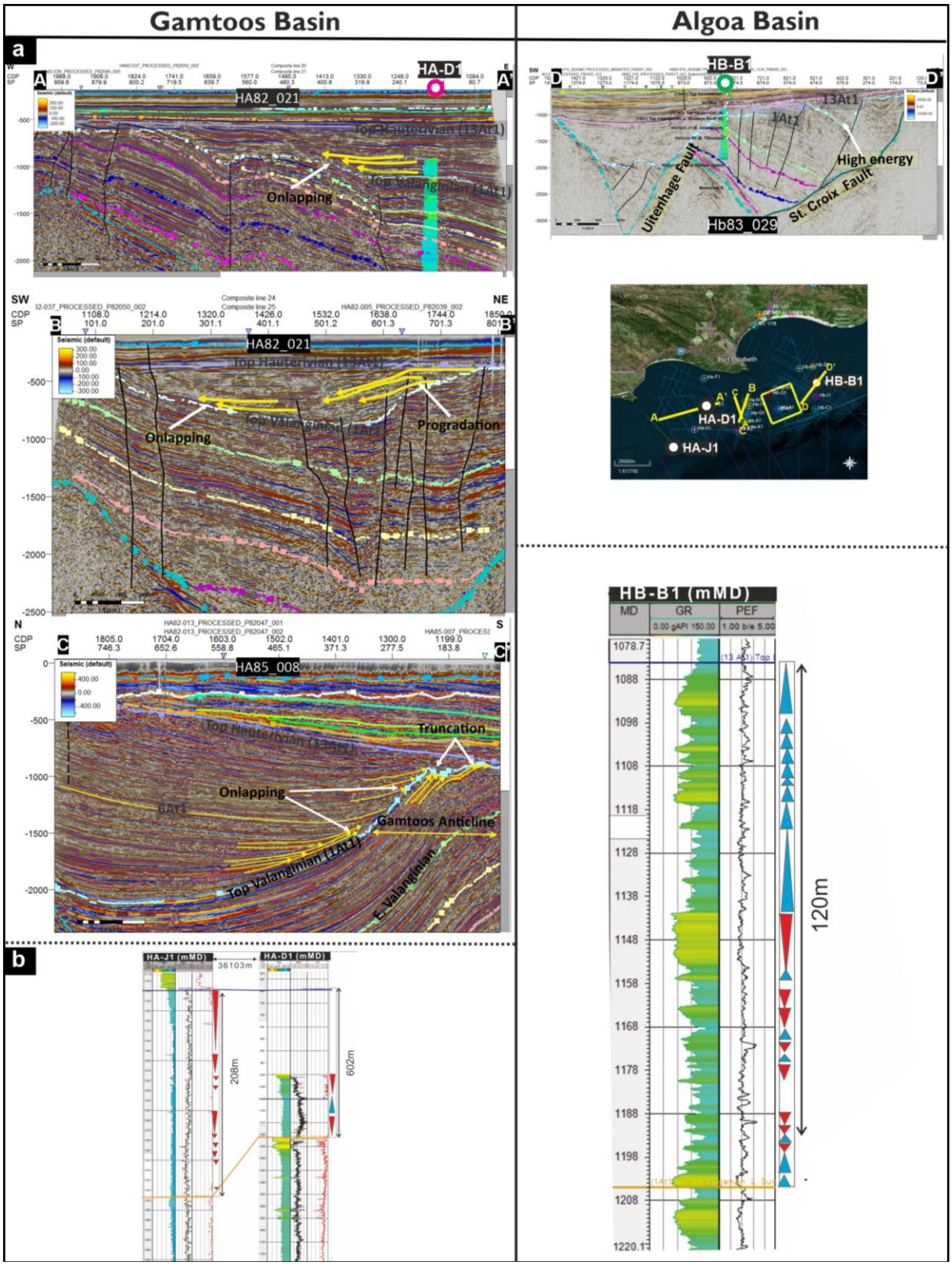

Fig. 14 a Seismic lines examples over the Algoa and Gamtoos Basins. **b** Wireline logs intersecting the Hauterivian succession in the Algoa and Gamtoos Basins. Base map data ©2020 Google, Maxar Technologies, AfriGIS (Pty) Ltd.

Post-Hauterivian to "Canyon fill" (early Albian)

This interval is more prominent in the Algoa Basin, along the Algoa Canyon (Fig. 15a). In the Gamtoos Basin, this succession is laterally constrained to the Gamtoos Canyon, which is significantly smaller than the Algoa Canyon. Borehole HB-H1 in the Port Elizabeth Trough is dominated by a ~65 m-thick sandy unit (GR: 28–62 API), with an overall cylindrical GR shape (Fig. 15b). Although the Uitenhage Trough is dominated by fine-grained sediments (i.e., 200-m- and 1420-m-thick in boreholes HB-B1 and HB-I1, respectively), there are some isolated, thin, coarsening-upward sandstones in this interval. The more distal borehole HB-C1 is intersected a ~470-m-thick, fine-grained unit (GR: 83–116 API) that lacks sandy interbeds (Fig. 15b). Although borehole HB-H1intersected "Canyon fill" sediments, mapping this canyon succession in the Port Elizabeth Trough is challenging, because it is absent in most parts of this trough, and seems to be localized around the borehole itself. This is exacerbated by the overall poor data quality, and therefore this succession is omitted from Fig. 15a in the Port Elizabeth Trough. Along the Algoa Canyon, seismic reflectors are very chaotic and discontinuous in the N-S direction, downlapping on the Top Hauterivian reflector, while a SW-NW cross-section shows onlapping stratal geometries onto the Top Hauterivian reflector (Fig. 15a). The lower part of this succession contains horizontal reflectors, while the top appears to be prograding from the NW to SE; incised features are also observed in this section (Fig. 15a).

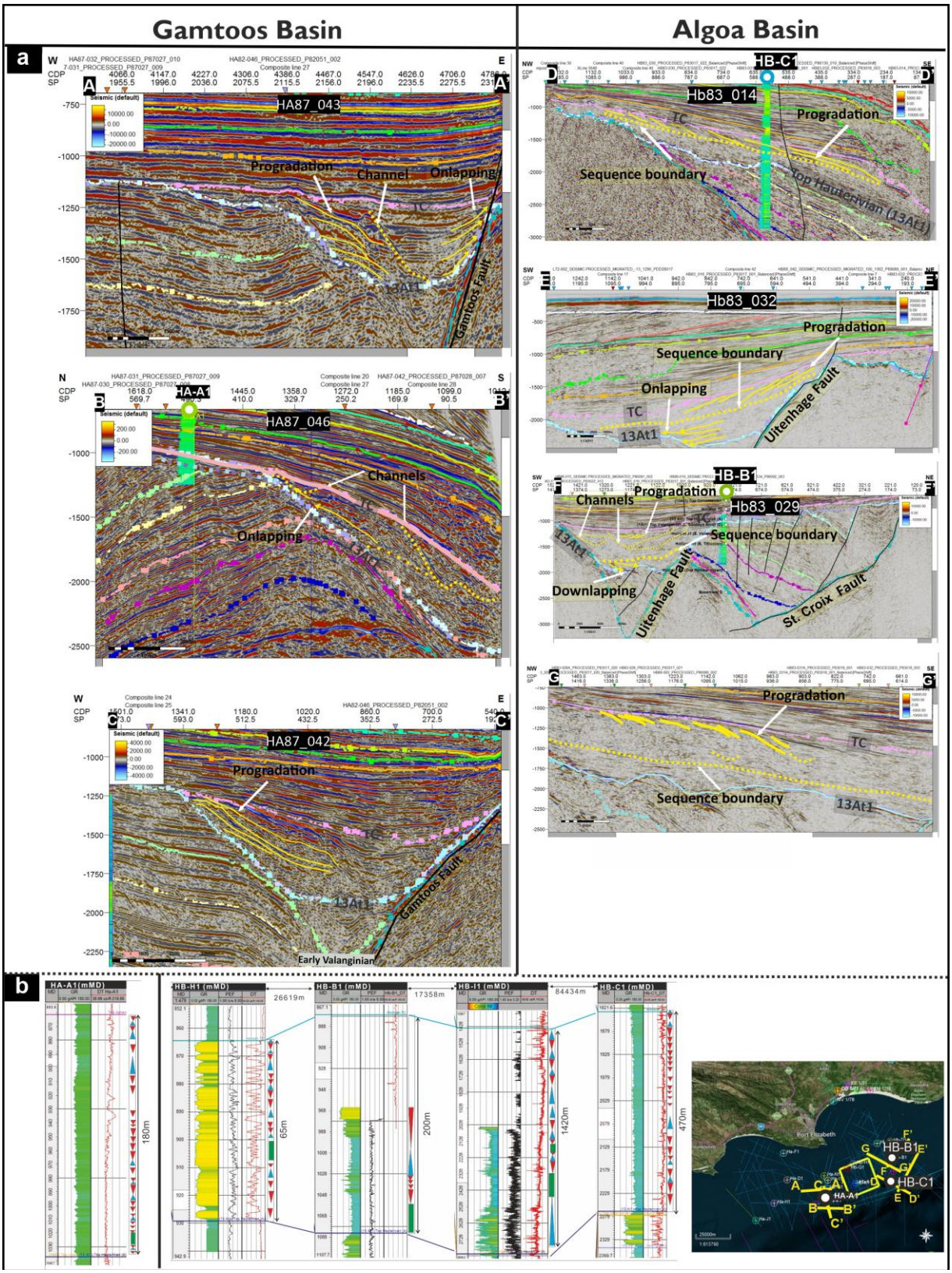

Fig. 15 a Seismic lines examples from the Algoa and Gamtoos Basins. **b** Wireline logs intersecting the "Canyon fill" succession in the Algoa Basin. Base map data ©2020 Google, Maxar Technologies, AfriGIS (Pty) Ltd.

Transitional phase interpretations

Post-Valanginian to upper Hauterivian

In borehole HB-B1, the basal coarsening-upward trend suggests a regressive shoreline, overlain by what appears to be stacked fining-upwards successions (Fig. 2). These fining-upward deposits that are likely fluvial in origin, indicating increased depositional energy, probably during the initiation of the uplift during the late Hauterivian (Fig. 14b; McLachlan and McMillan 1976; Dingle et al. 1983; Malan 1993; Brown et al. 1995; Thompson 1999; Paton and Underhill 2004). In the Gamtoos Basin, this succession shows low energy facies that lacks sandy interbeds in both boreholes HA-J1 and HA-D1, and thus was probably deposited when the basin was still experiencing marine conditions during the early Hauterivian before the late Hauterivian/Aptian uplift and erosion (Figs. 2 and 12b). Seismic data show that the late Hauterivian unconformity was widespread across the basin, and when it formed, large tracts of the underlying syn-rift succession were eroded in both basins (but especially in the Algoa Basin; Figs. 12b and 10d). In the Port Elizabeth Trough, where the erosion was less severe, the onlapping lower Hauterivian seismic reflectors indicate an increasing accommodation space during the early Hauterivian (Fig. 14a). A common feature within this succession is a lateral change in seismic facies, where the brighter (higher energy) reflectors might indicate the presence of sands and dimmer facies indicating shales/clays (Fig. 14b).

In the Gamtoos Basin, accretional stratal geometries are observed towards the upper Hauterivian succession, which could be due to migrating bypass channels, with sediments making their way to the basin. The Top Hauterivian reflector (13At1) is highly erosive, and in some places, this reflector forms a composite unconformity with the 1At1/6At1 reflectors. In places the Top Hauterivian reflector also erosively cuts into the syn-rift/transitional phase sediments (Fig. 14a). Towards the S, in the N-S trending part of the Gamtoos Fault, this succession onlaps on the Gamtoos Anticline (McMillan et al. 1997; Thomson 1999) and appears to be syn-tectonic in the lower part of the succession (6At1?). Although the stress field responsible for the formation of the Gamtoos Anticline is poorly understood (Thomson 1999), this structural feature shows a period of inversion, which probably formed during the Hauterivian to Aptian uplift episode (see Thomson 1999, his fig. 9). The presence of canyons and truncational features on the shelf collectively suggest that the shoreline was pushed to the shelf edge during a RSL fall in the late Hauterivian (Fig. 12d). The shelf edge shoreline means that most sediments were being deposited as high-density basin floor fans in the distal parts of the Algoa and Gamtoos Basins (Fig. 12d). This depositional unit is estimated to be similar in age to the recently discovered Brulpadda and Luiperd prospects in the Outeniqua Basin (Africa Energy Corp 2020). In the shelf regions of Algoa and Gamtoos Basins, bypass channels with limited coarse-grained sediments are expected. The intensity of scouring and canyon features in the Algoa Basin could suggest that the Algoa Basin was more uplifted than the Gamtoos Basin.

Post-Hauterivian to "Canyon fill" (early Albian)

In the Algoa Basin, this interval is intersected in boreholes HB-H1, HB-B1, HB-I1 and HB-C1 (Fig. 15b). Borehole HB-H1 in the Port Elizabeth Trough is dominated by very fine-grained, coarsening-upward sands and does not show any marine influence (Fig. 15b). Boreholes HB-B1, HB-H1 and HB-C1 on the other hand are dominated by low energy sediments (possibly marine), with very limited sand input (Fig. 15b). However, unlike boreholes HB-B1 and HB-I1, in which isolated thin, very fine coarsening-upward sands are present, borehole HB-C1 is sand free, and thus can potentially indicate a marine setting in the Uitenhage Trough, at a time when the Port Elizabeth Trough was dominated by fluvial processes. In the Gamtoos Basin, this interval is intersected by borehole HA-A1, which shows an overall non-graded profile, consisting of coarsening-upward and fining units (Fig. 15b). The "Canyon fill" isopach map in the Algoa Basin depicts a NW-SE trending depocenter, within which sediments thicken towards the SE (Fig. 10e). The base of this succession onlaps onto the Top Hauterivian reflector, indicating a period of increasing accommodation space, whereas the upper succession is dominated by channel accretion geometries in the canyon (Fig. 15a). Basal onlapping stratal geometries on the Top Hauterivian reflector indicate a landwards moving shoreline due to possible increased accommodation space linked to a presumed rise in RSL (Fig. 12e). The upper "Canyon fill" is dominated by channel incisions and contain clinoforms prograding to SE, which were probably deposited during normal regression. In the Gamtoos Basin, "Canyon fill" sediments are confined and laterally limited, and appear to prograde predominantly from the W, which may have been a possible sediment entry point (Fig. 13a and 8e). These eastwards prograding clinoforms appear to be eroded by a younger channel indicating an increase in environmental energy and concomitant shift from marine to fluvial conditions (Fig. 15a).

Drift phase observations

Post-Hauterivian/"Canyon fill" to upper Cenomanian

The Cenomanian is ~440-m-thick and contains two main coarsening-upward successions in borehole HB-C1, with the lower one being dominated by high GR readings between 63-85 API, while the upper one being dominated by relatively low GR signatures of 56-72 API (Fig. 16b). However, unlike the underlying succession, this interval is less sandy (dominated by fining-upward and coarsening silty sands). Borehole HA-A1 in the Gamtoos Basin contains a 62-m-thick Cenomanian succession with relatively high GR readings of 60-90 API and alternating fining-upward and coarsening units (Fig. 16b). Seismic reflectors within this succession are brighter, continuous and onlap onto the Top Albian reflector (Fig. 16a). Seismic data also show lateral accretional stratal geometries from the N-NW towards the S-SE in the more proximal setting (Fig. 16b). The Top Cenomanian reflector truncates the Top Albian reflector and cuts into top of the syn-rift sequence. This truncation is more evident at the shelf break (which appears to have developed in the Albian), where the erosion caused highly irregular topography (Fig. 16a).

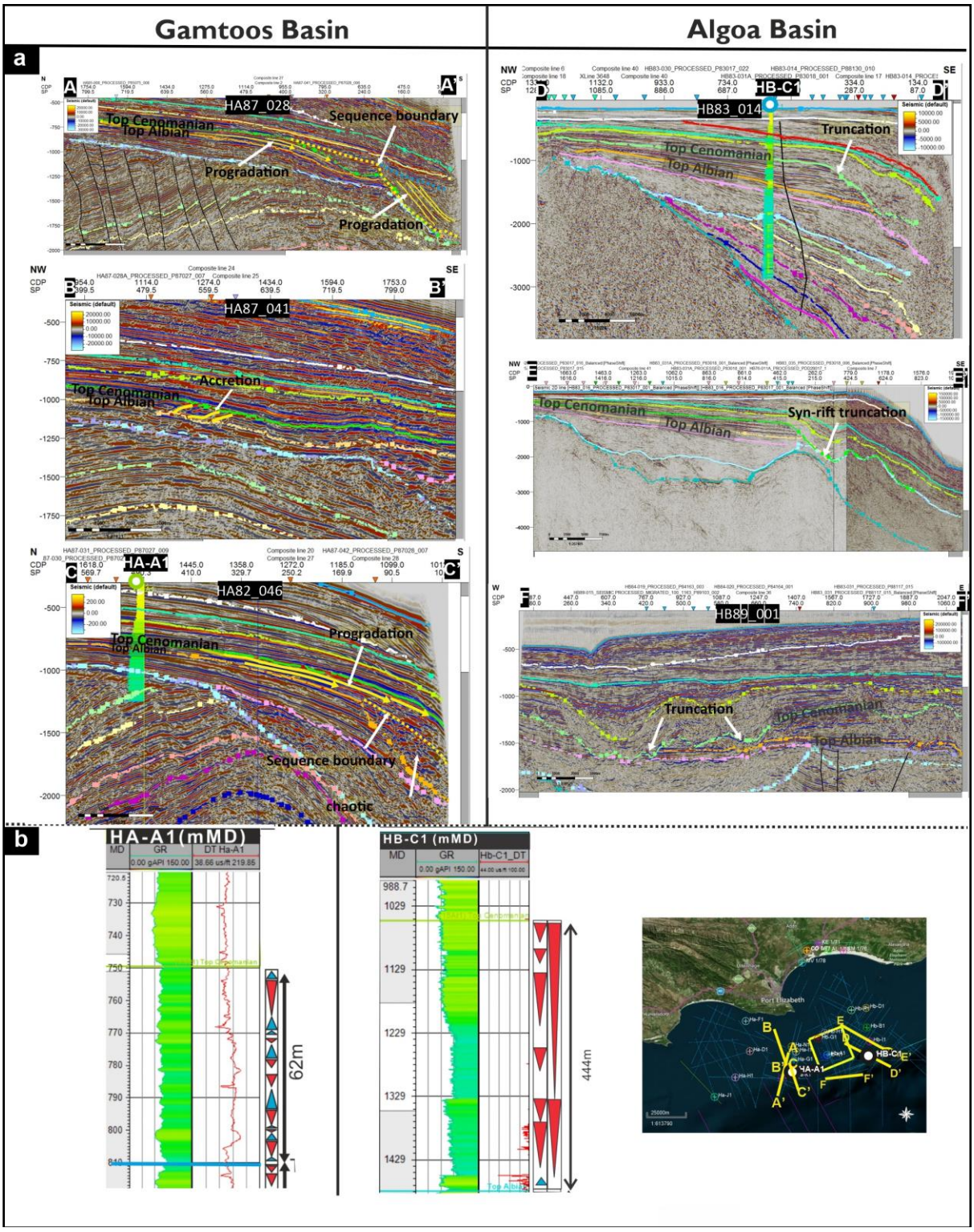

Fig. 16 a Seismic lines examples over the Algoa and Gamtoos Basins. **b** Wireline logs intersecting the Cenomanian succession in the Algoa and Gamtoos Basin. Base map data ©2020 Google, Maxar Technologies, AfriGIS (Pty) Ltd.

Post-Cenomanian to Lower Cenozoic

Contrary to the underlying and overlying successions, the Upper Cretaceous, which is an 80-m-thick unit in HB-C1 in the Algoa Basin, shows relatively high GR readings of 58-97 API and consists of fining-upward and coarsening trends (Fig. 17b). Although the GR readings show fining-upward and coarsening units, there is less sand in the Algoa shelf compared to the one in the Gamtoos Basin, where borehole HA-A1 is dominated by a 85-m-thick unit with low GR readings of 40-65 API (Fig. 17b). On the shelf, the Upper Cretaceous seismic reflectors onlap on the Top Campanian reflector. In the Port Elizabeth Trough, the base of this succession shows chaotic reflectors, closer to the shelf edge. In the slope setting, this succession onlaps onto the Top Campanian reflector and shows evidence of clinoforms that prograde towards SE (Fig. 17a).

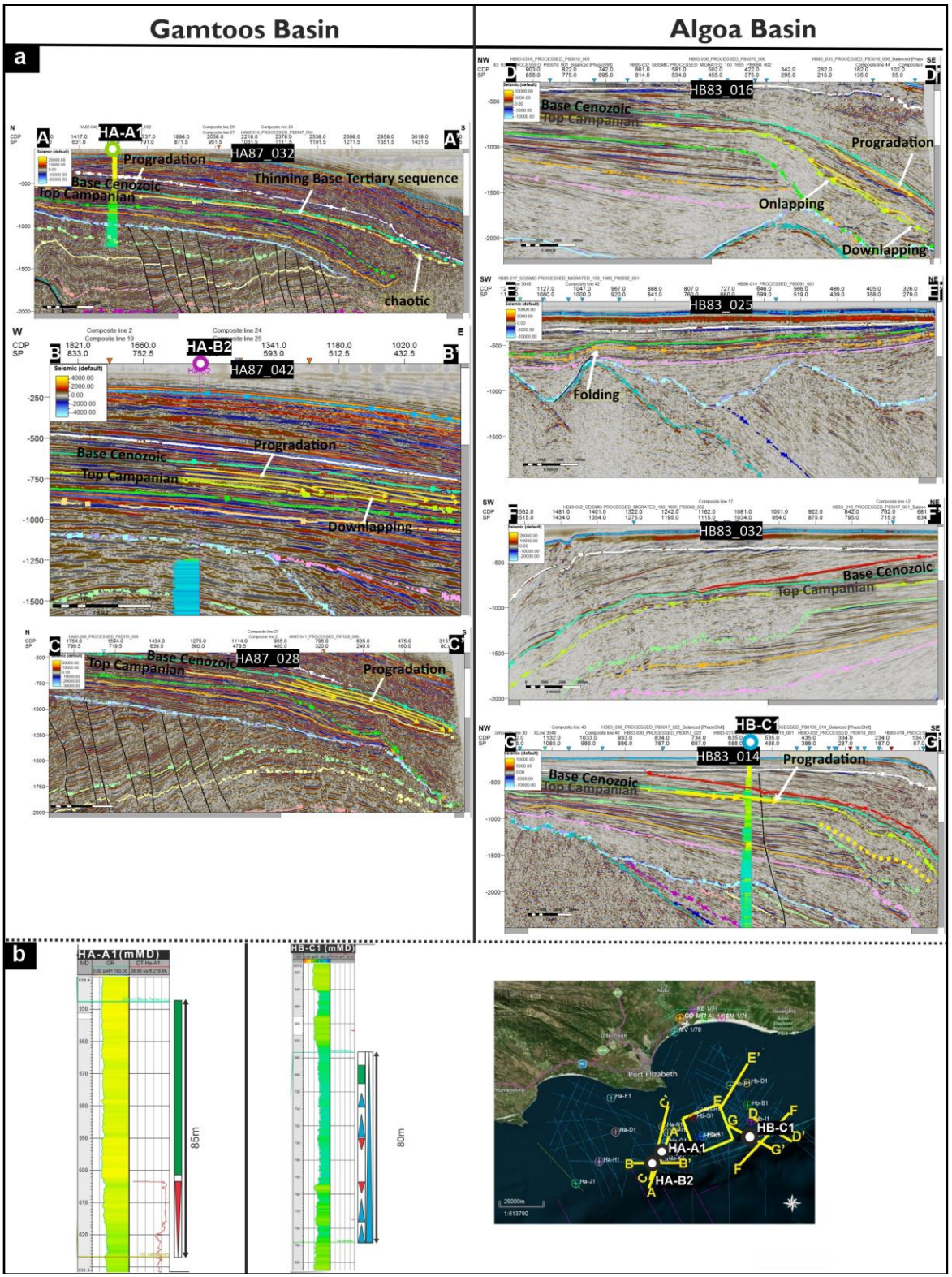

Fig. 17 a Seismic lines examples over the Algoa and Gamtoos Basins. **b** Wireline logs intersecting the Upper Cretaceous/Lower Cenozoic succession in the Algoa and Gamtoos Basin. Base map data ©2020 Google, Maxar Technologies, AfriGIS (Pty) Ltd.

Lower to Middle Cenozoic

In the Algoa Basin, borehole HB-C1 contains one ~356-m-thick, overall coarsening-upward unit with GR readings of 38-93 API (Fig. 18b). Although borehole HA-C1 has an overall coarsening-upward trend, it is made up of smaller alternating fining-upward and coarsening units and its lower portion is dominated by shaley facies. In the Gamtoos Basin, borehole HA-A1 contains one 130-m-thick, aggrading sandy unit that has low GR reading of 30-40 API without any obvious clay or silt content (Fig. 18b).

The Base to Mid-Cenozoic reflectors are semi-continuous and show a dimming character in contrast to the underlying post-rift succession (Fig. 18a). Along a NW-SE section, these reflectors downlap onto the Base Cenozoic reflector along the shelf, while prograding on the slope/shelf edge from the N towards S. The Mid-Cenozoic reflector truncates the underlying, Cretaceous succession at an acute angle (Fig. 18a). This truncation is also notable towards the shelf edge/slope (Fig. 18a).

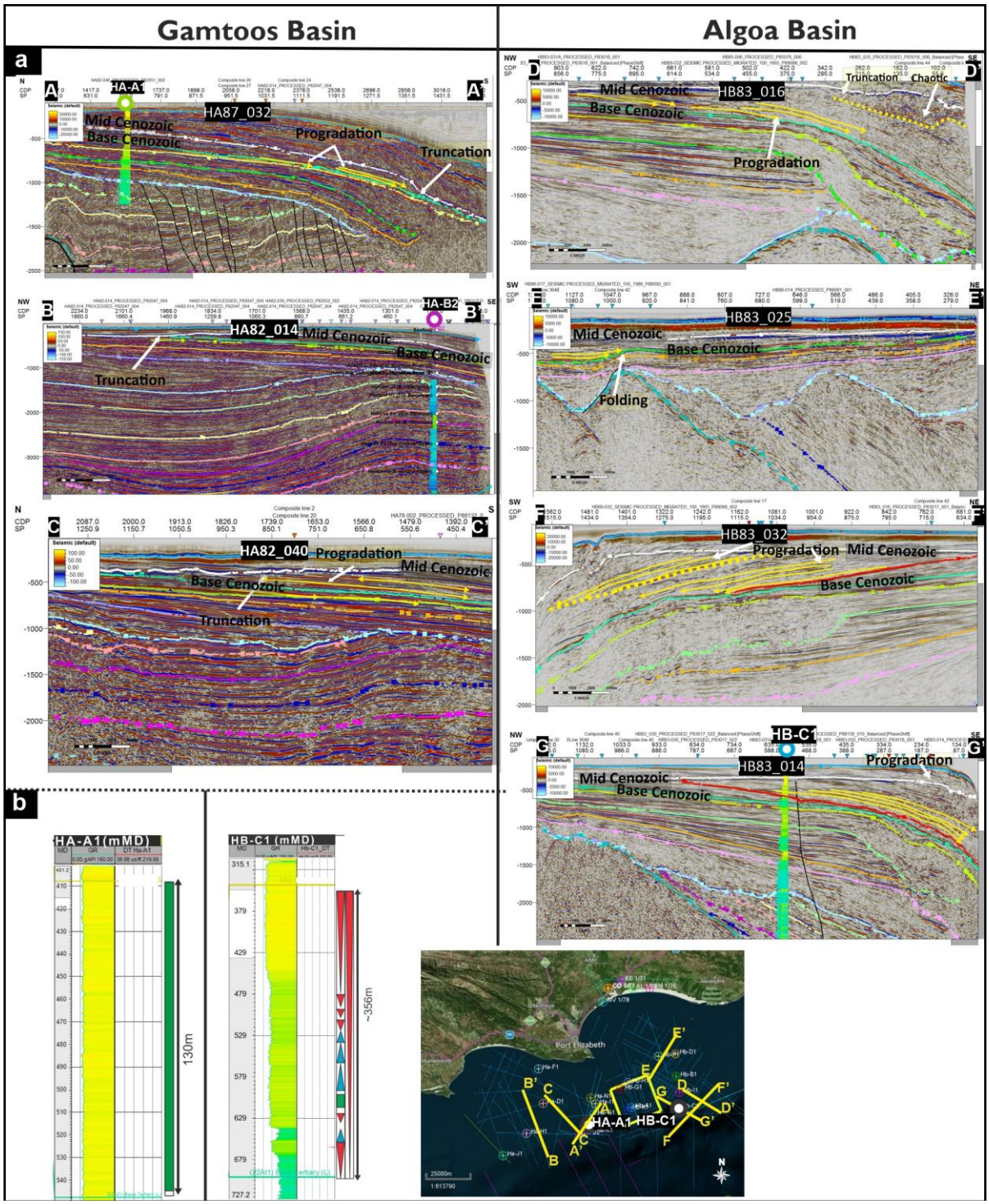

Fig. 18 a Seismic lines examples over the Algoa and Gamtoos Basins. **b** Wireline logs intersecting the Lower to Upper Cenozoic succession in the Algoa and Gamtoos Basin. Base map data ©2020 Google, Maxar Technologies, AfriGIS (Pty) Ltd.

Drift phase interpretations

Post-Hauterivian/ "Canyon fill" to upper Cenomanian

In the Gamtoos Basin, this interval was most likely deposited in a shelfal setting, as suggested by the persistence of glauconitic claystones (McMillan et al. 1997). The lower portions of boreholes HB-C1 and HA-A1 are dominated by shaley facies, which were probably deposited during a flooding event after the Albian shoreline regression (Fig. 2). In contrast, this interval appears to be sandier in the Algoa Basin, evident by the low GR readings in the distal borehole HB-C1 (and borehole HB-I1; McMillan et al. 1997). The base of this succession onlaps on the Top Albian reflector (more so in the distal setting) and is overlain by southward prograding clinoforms that downlap on the Top Albian reflector (more evident in the proximal setting). The onlapping stratal terminations and the flooding event overlying the Top Albian boundary indicate a shoreline transgression during the early Cenomanian, which could be associated with an increasing RSL (Fig. 2). The southward prograding clinoforms and sandy facies overlying the transgressive sediments indicate increased sedimentation rates causing shoreline regression in the late Cenomanian. These prograding clinoforms are truncated by the highly erosive Top Cenomanian (15At1) unconformity, which forms an irregular topography in seismic data indicative of strong incision (Figs. 2, 10f and 14). Towards the shelf edge, the Top Cenomanian unconformity is observed to erode into the syn-rift sequence. The uplift associated with this unconformity was accompanied by more than 100 m drop in the relative sea-level in the Outeniqua Basin (Baby et al. 2018). Whilst this Upper Cretaceous erosional event did not result in as deeply incised canyons as the 13At1 erosional event, it left much of the shelf scoured. This means the shoreline was probably pushed towards the shelf edge sometime during the Late Cretaceous (Turonian to early Campanian?), resulting in shelf sediment bypass with a possibility of depositing the sands as fans in the basin (Figs. 2, 10f and 14). Although the source of this uplift is still uncertain (Baby et al. 2018), the 15At1 unconformity is thought to have been a result of thermal subsidence in the distal offshore, which caused uplift in the proximal setting (Malan 1993).

Post-Cenomanian to Lower Cenozoic

Overlying the Top Cenomanian reflector, clinoforms of the slope setting were prograding towards SE and indicate the position of the shoreline after the RSL fall (Fig. 2). Relative sea-level began to increase during the Late Cretaceous and in some places, the shoreline appears to have migrated to a position geographically inland, a short distance N of the modern shoreline (Baby et al. 2018). This major transgressive period was caused by subsidence during the Campanian (McLachlan and McMillan 1976; McMillan et al. 1997). The contact between the Upper Cretaceous and the Lower Cenozoic is gradational, and thus it is challenging to identify it on lithological grounds, however changes in microfauna from the Cretaceous and the Cenozoic are significant enough to diagnose this contact on biostratigraphic grounds.

In the Algoa Basin, the retrogradational stacking pattern in borehole HB-C1 points to a transgressive shoreline during the Late Cretaceous in contrast to the older progradational successions (i.e., regression from the Albian to the upper

Campanian; Fig. 2). According to Hattingh (2001), the Lower Cenozoic succession in the Algoa Basin was deposited during high sea-level, which is consistent with the observations herein. The lack of fluvial deposits in the Algoa Basin from the Late Cretaceous to Early Cenozoic (Hattingh 2001) could explain why this interval is relatively sand free. In the proximal setting, this high sea-level caused a reduction in the fluvial gradient and the eventual termination (drowning) of the fluvial system in the Algoa Basin (Hattingh 2001). Although this interval is relatively thin, it is dominated by aggradational stacking of clinoforms, while the base of the succession onlaps on the Top Campanian reflector in the slope setting, representing a period of increased accommodation space (Fig. 2). In contrast, in the borehole HA-A1 of the Gamtoos Basin, this interval shows evidence for a regressive shoreline, probably due to an active, nearby sediment source in this basin. Moreover, this succession mostly progrades and downlaps on the Top Campanian reflector without any obvious onlapping stratal terminations. Therefore, although RSL was increasing, sedimentation rates were high in the Gamtoos Basin, causing the shoreline to regress, while the Algoa Basin was undergoing transgression (Figs. 2 and 17a).

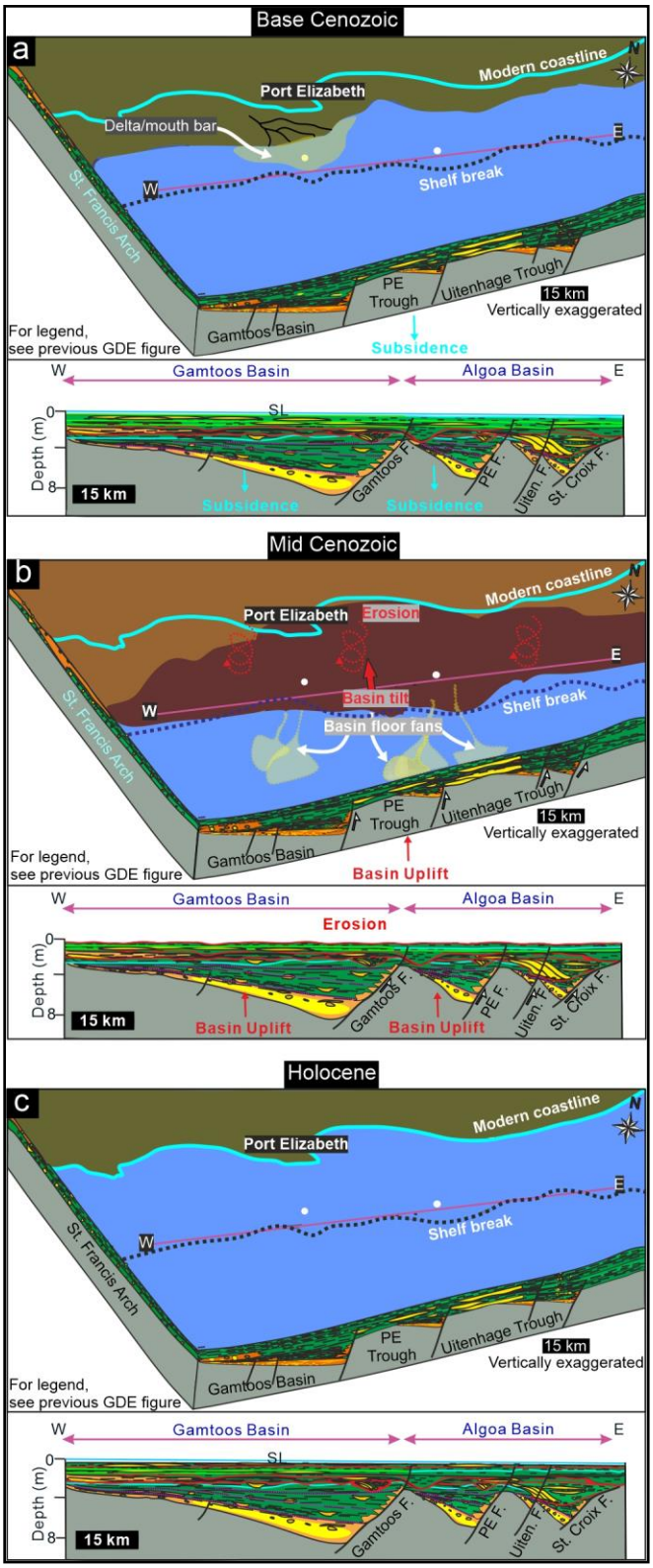

Fig. 19 a-c Upper Cenozoic gross depositional models, showing the basin evolution from syn-rift to transitional to drift phase (see Fig. 10 for legend).

Lower to Middle Cenozoic

This succession is associated with an uplift during the Oligocene (?), which resulted in a major erosional event observed regionally on seismic data. This erosion was due to the second uplift of the Southern African Plateau and probably lasted from the Eocene to early Oligocene (Hattingh 2001; Baby et al. 2018). This period of shelf scouring reactivated the fluvial system (notably the Baakens and Shark River valleys) in the Algoa Basin, which became more prominent after the Eocene uplift (Hattingh 2001). According to McMillan et al. (1997), this interval is thicker relative to the underlying Lower Cenozoic succession and is dominated by silty clays, however, borehole data (HB-C1) shows an overall coarsening-upward sandy unit, probably sourced from the reactivated fluvial system. Similarly, borehole HA-A1 in the Gamtoos Basin is also dominated by clean sandy facies throughout (Fig. 18b). The sand at the top of borehole HB-C1 could indicate a reactivated sandy sediment source in the Algoa Basin. Post the Mid-Cenozoic unconformity (i.e., Miocene to Holocene), GR logs show low reading, homogenous and non-graded profiles. This succession, presently being deposited on the shelf can be correlated with the Algoa Group actively being deposited onshore during over the last 20 Ma (Illenberger 1992; Hattingh 2001).

In both basins, shelfal seismic reflectors appear to prograde from N to S, and downlap on the Base Cenozoic reflector (Fig. 18a). Borehole and seismic data suggest a period of high sedimentation resulting in shoreline regression. This surface truncates the drift phase succession in a similar manner as the 1At1 unconformity truncates the syn-rift succession. However, this unconformity was caused by basin wide tilting (uplift) during the late Paleogene (Figs. 2 and 10b; Hattingh 2001; Baby et al. 2018). This unconformity is also observed in Zululand Basin in the E and along the Atlantic margin in the W (Stevenson and McMillan 2004; Baby et al. 2018). In the study region, tilting of the older rocks appear to be dominant along the N-S strike, with the northern side of the basin being eroded (Fig. 12b). Post the Eocene to Oligocene uplift, Hattingh (2001) onshore studies also suggest that the RSL increased to 300 m higher than the current level from the Late Miocene to Holocene, indicating the landwards most position of the shoreline before it regressed to modern position (Fig. 12c). This regression (forced?) was probably due to the eastwards tilt of the Algoa Basin during the Late Miocene to Holocene and was responsible for creating present day terraces onshore the Algoa Basin (Hattingh 2001). However, unfortunately much of the post-Oligocene succession is below seismic resolution for us to confidently correlate with onshore studies.

Discussion

Syn-rift sequence models

Lateral variability of syn-rift successions is mostly resultant from the differential movements along syn-depositional faults. This high facies and structural variability make it challenging to use the passive margin-based system tracts to predict lateral facies changes in a largely continental rift-basin setting (e.g., Prosser 1993; Chorowicz 2005; Holz et al. 2017). Current dataset, previous studies (e.g., Shone 2006; Muir et al. 2020) as well as studies from the Falkland Plateau Basin (Schimschal and Jokat 2019) collectively suggest that by the Late Jurassic a marine system was established in this region and relative sea-level changes started influencing the shoreline trajectories and nearshore

sedimentary processes. In the Algoa and Gamtoos Basins, the syn-rift sequence is dominated by the alluvial to fluvio-lacustrine Enon and Kirkwood Formations, which spans a depositional period from ~ 170 to about ~135 Ma (Muir et al. 2020). Considering the total average thickness of these units being a few thousand metres (Muir et al. 2017 a, b), it is very likely that their combined succession contains several SUs. However, the detection of these unconformities remains elusive both in outcrops and in the sparse, low resolution subsurface data.

Given the foregoing, it is possible to assume a diachronous advancement of shoreline during the syn-rift until the Top Valanginian breakup unconformity (1At1), which can be classified as a second-order MFS (high magnitude, low frequency event; e.g., Vail et al. 1977; Vail et al. 1991; Embry 2009, p. 59; Catuneanu 2006, p. 327; Catuneanu 2019a, b; Catuneanu and Zecchin 2020). Rift basins are associated with short tectonic pulses, which can create sudden and large accommodation space increases (i.e., transgression), followed by a period of tectonic quiescence, which allows sediments to prograde (highstand) along the dipping hanging blocks (Martins-Neto and Catuneanu 2010; Holz et al. 2017). Generally, in the syn-rift successions, formation tops are picked on flooding surfaces (wave-ravinement surfaces; Martins-Neto and Catuneanu 2010; Catuneanu and Zecchin 2020; Fig. 20). Although it could be argued that these third order flooding surfaces in the Algoa and Gamtoos Basins may be MFSs (separating third-order HST and TST), the 1At1 unconformity marks the most landward position of the shoreline in the syn-rift succession, and thus it is the main higher rank (i.e., second-order) MFS (e.g., Catuneanu and Zecchin 2020). In some instances, rift systems can be associated with progradation due to high sedimentation rates, however, increasing accommodation space, due to syn-depositional faulting, will eventually result in a basin wide transgressive shoreline (Martins-Neto and Catuneanu 2010; Holz et al. 2017). Therefore, the low-order/higher rank (low frequency, high magnitude) RSL increase is accompanied by high-order/lower rank transgressive and regressive (e.g., Milankovitch) cycles. Consequently, the syn-rift interval in this study does not contain the "traditional" system tracts as observed in passive margin depositional sequence models. This is also because depositional sequence models were derived from passive margin setting (Martins-Neto and Catuneanu 2010; Holz et al. 2017).

Correlating the syn-rift sequences across the Algoa and Gamtoos Basins is very challenging, because these successions are laterally constrained by paleo-basement heights due to compartmentalization common in rift basins (e.g., Chorowicz 2005). The dominant fluvial system in rift basins is controlled by the dipping landscape towards the main faults or paleo-basement heights (Martins-Neto and Catuneanu 2010). However, as RSL continues to increase, sedimentation becomes more dominant towards the proximal setting, leaving the distal footwalls in the deep marine sediment starved (Martins-Neto and Catuneanu 2010). Also, the alluvial, fluvial and lacustrine deposits, due to their inherent laterally and vertically heterogenous nature make the correlation of rock units from one well to the other nearly impossible (e.g., Nádor and Sztanó 2011). The absence of easily detectable SUs within the subsurface syn-rift succession limits the use depositional sequence models II, III and IV and T-R sequence model, which depend on the recognition of SUs as sequence boundaries (Catuneanu 2006; Embry et al. 2007; Catuneanu et al. 2011; Catuneanu 2019a, b). Holz et al. (2017) proposed the concept of tectonic system tracts, however their model assumes the development of shallow to deep rift lakes during early syn-rift phase. Although there is evidence of lacustrine environments during the deposition of the Kirkwood Formation (Muir et al. 2017b), there is no evidence to suggests

that this lacustrine setting occupied the whole half-graben (rift basin; such as those in the East African Rifts System – e.g., Chorowicz 2005). Since the above models are limited for explaining the syn-rift evolution in the Algoa and Gamtoos Basins, the question remains: which other model best fits the data in this area? Galloway's (1989) genetic sequence model, in which sequence boundaries are defined by the transgressive MFS unconformity (also known as the breakup unconformity in syn-rift successions – e.g., Holz et al. 2017) is the only model that closely matches the observations in the study area. However, contrary to Galloway's (1989) model, in which both the basal and top sequence boundaries are MFSs, the base of syn-rift is typically a SU atop of the basement rocks (i.e., "rift onset unconformity" in Falvey 1974 or "syn-rift unconformity" in Bosence 1998). In the Galloway's model, where MFS are used as sequence boundaries, the SU is included within the succession and is thus not a sequence boundary. It has been repeatedly shown that stratigraphic boundaries should not only be limited to SUs, but to surfaces that mark a full cycle of genetically related sequences (e.g., Catuneanu 2019a, b; Catuneanu and Zecchin 2020). In this way, the genetically related facies of the syn-rift succession is bound by the key stratigraphic surfaces (e.g., SU at the base, transgressive ravinement surfaces, MFS; Figs. 2 and 18) that satisfy the upper half of Galloway's model, without being limited to SUs as stratigraphic boundaries. The Galloway model does not include system tracts of the conventional depositional sequence models and omitting system tracts limits lateral facies prediction in sequence stratigraphy.

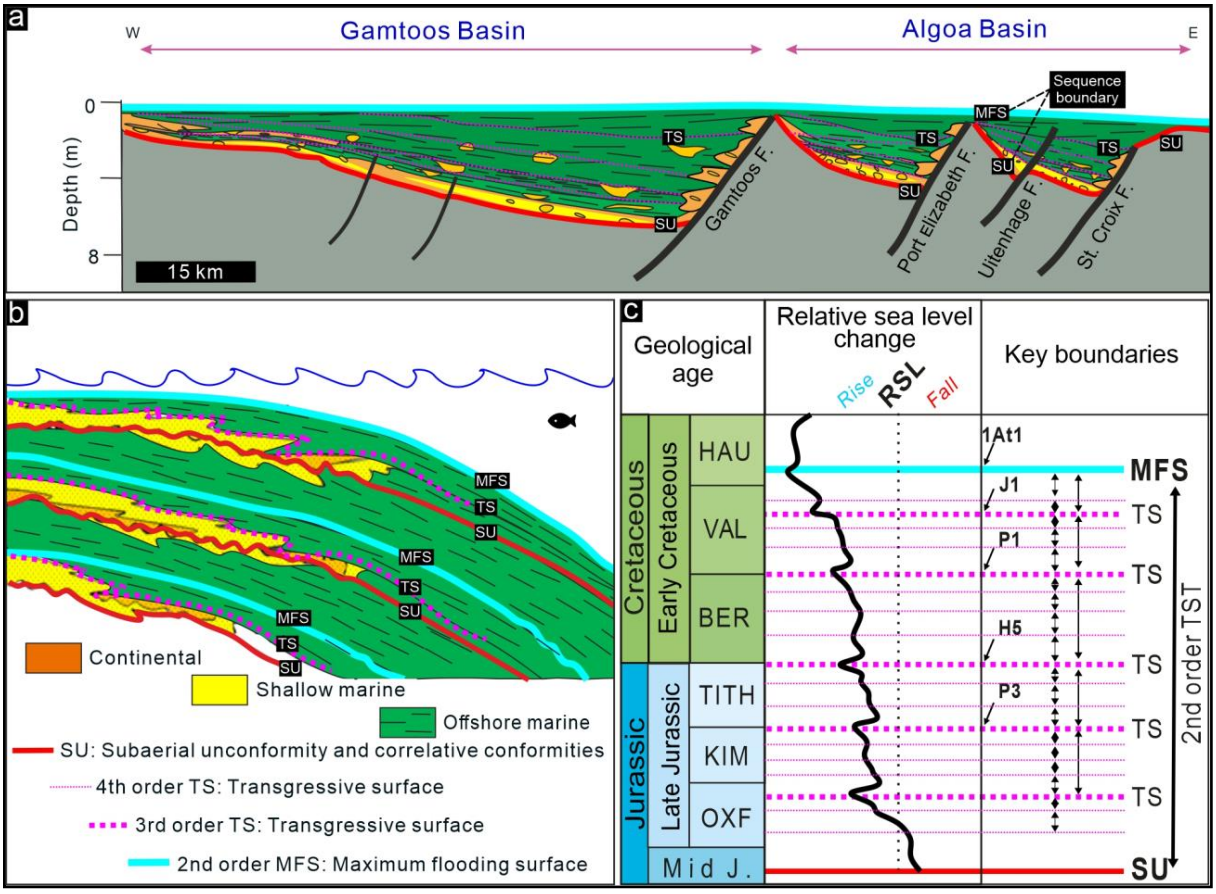

Fig. 20 a Simplified cross-section of the syn-rift sequence in the Algoa and Gamtoos Basins, showing the main stratigraphic surfaces. **b** Summary of Galloway's model (1989), which is a genetic sequence approach that uses the maximum flooding surface (MFS) as sequence boundary (modified from Embry et al. 2007). **c** RSL curve and the associated system tracts and their bounding surfaces in the Algoa and Gamtoos Basins.

Transitional phase sequence models

Post-Valanginian to upper Hauterivian

This interval represents sediments that were deposited during reduced (negative) accommodation space in the Algoa and Gamtoos Basins, when, due to regional uplift, the RSL dropped and the shoreline regressed (McLachlan and McMillan 1976; Malan 1993; Brown et al. 1995; Thomson 1999; Paton and Underhill 2004). The strata of this infrequently preserved succession, which overlie the low order 1At1 MFS, are dominated by clinoforms that prograde towards SW, and show coarsening-upward and non-graded trends in boreholes HB-B1, BA-J1 and HA-A1. These observations suggest a high stand system tract (HST) between the low order 1At1 MFS at the base and the low order 13At1 SU at the top (Fig. 2). The regional uplift event, which resulted in the 15At1 sequence boundary was triggered by dextral motion along the AFFZ (Malan 1993; Brown et al. 1995; Thomson 1999; Paton and Underhill 2004). This

period of uplift, which lasted from the early Aptian to late Hauterivian (6At1 to 13At1), resulted in the Algoa and Gamtoos Canyons and other erosional features across the shelf area in the region (Bate and Malan 1992; McMillan et al. 1997; Broad et al. 2012). In contrast to the older syn-rift sequence, the thickness maps (Fig. 10) show depocenters that do not follow the geometry of the underlying structure. This suggests that the basin infilling during this period was primarily driven by RSL changes, as a function of eustatic sea-level change and the motion of AFFZ (Dingle et al. 1983; Ben-Avraham et al. 1993; Malan et al. 1990; Brown et al. 1995; McMillan et al. 1997; Broad et al. 2012; Baby et al. 2018), and less dependent on the Cape Supergroup anisotropy. Moreover, during this period of uplift and erosion, the shoreline retracted towards the distal setting, while the inner to middle shelf was a place of bypass. Because this basinward shoreline shift was primarily driven by the regional uplift, independent of sediment supply, a case for forced regression can be made (Fig. 12d; Hodgson et al. 2018 fig. 10b), and the processes associated with falling stage system tract (FSST) are expected to have occurred. Therefore, it is expected that in the continental portion (i.e., northern half) of the basin low order SUs were generated, whereas in the marine portion (i.e., southern half) of the basin, sediments bypassed on the shelf and became deposited as high-density, basin-floor fans (e.g., Hunt and Tucker 1992; 1995; Helland-Hansen and Gjelberg 1994; Plint and Nummedal 2000; Catuneanu 2006, p. 178). Consequently, high potential for the development of reservoirs is expected outboard of the study area. It is noteworthy that this uplift and associated basinal deposition are similar in overall mechanism and age to processes that led to the formation of the hydrocarbon-bearing rocks in the Outeniqua Basin (i.e., Brulpadda and Luiperd discovery in Block 11B/12B; Africa Energy Corp. 2020).

Post-Hauterivian to "Canyon fill" (early Albian)

The Aptian to early Albian "Canyon fill" sediments in the shelf overlie the FSST and are characterized by fluvial incisions and prograding stratal geometries (Fig. 15). These "Canyon fill" sediments are bound by a subaerial uniformity at the base and a transgressive surface at the top (Fig. 19). These observations are consistent with the definition of the lowstand system tract (LST) on the shelf (Figs. 2 and 10e; Catuneanu 2006, his fig. 5.6) in depositional models II, III and IV. Although there are some low-density basin floor fans that might form during the normal regression, most of the sediments are trapped in the incised valleys during the LST, such as those in the Algoa and Gamtoos Basins. This is because sediments, before making their way to the distal part of the basin, first tend to fill in the proximal topographic irregularities (i.e., nearshore incised valleys) that were carved out during the forced regression (Catuneanu 2002, 2006). Boreholes HB-B1, HB-I1 and HB-C1 in the Algoa Canyon are characterized by very fine-grained, silty to shaley sediments that formed during this phase of deposition. The sediments deposited in the incised canyons appear to be dominated by fine grain sizes and small channels with a low net sand-to-shale ratio, and thus are unsuitable as hydrocarbon reservoirs. The more proximal borehole HB-H1 is dominated by clean sandy facies near the canyon head, however these sandy facies do not appear to extend toward the distal part of the Algoa Canyon. The Top Canyon reflector marks a maximum regressive surface (MRS), overlying "Canyon fill" sediments that were generated during normal regression. The MRS is overlain by thin (below seismic resolution), lower Albian transgressive system tract (TST; observable at the base of boreholes HB-B1 and HA-A1 as high GR, fining-upward

shaly facies), which are then overlain by prograding, normal regressive sediments (i.e., HST), which mark the Top Albian. It has been repeatedly shown that system tracts can form independent of scale and that seismic data might not always resolve high frequency sequence boundaries (e.g., Catuneanu 2019a, b; Catuneanu and Zecchin 2020). Unlike the "ideal" products of a full relative sea-level cycle comprising of fully developed LST-TST-HST-FSST (Hunt and Tucker 1992; 1995; Plint and Nummedal 2000; Catuneanu 2002, 2006; Catuneanu et al. 2011; Catuneanu 2019a, b), in the current dataset no SU's (that form during forced regression) are resolved in the upper (Late) Albian, which might suggest a drop in RSL or slow RSL rise when lowstand deposits formed. As a result, the Albian highstand is bound at the top by a regressive surface (maximum?), and not a SU (which could be there, but below seismic resolution).

Drift phase sequence models

Lower to upper Cenomanian

The Cenomanian succession overlies the Top Albian regressive surface and shows evidence for increasing accommodation space in the early Cenomanian. The basal Cenomanian succession in boreholes HB-C1 and HA-A1 is dominated by shales and clays facies, which could represent an early Cenomanian flooding event. This is supported by onlapping stratal geometries in the Algoa Basin shelf. However, the flooding surface associated with this transgression is unresolvable on the seismic lines in the Gamtoos Basin due to the resolution of the data. Consequently, the lower transgressive Cenomanian deposits are separated from the upper Albian highstand deposits by a high order MRS (Fig. 2; e.g., Catuneanu 2006, p. 327; Catuneanu 2019a his fig. 3, 2019b). A TST-HST-TST succession like this typically forms during positive accommodation and high sedimentation rates (Galloway 1989; Catuneanu 2019a his fig. 3, 2019b; Catuneanu and Zecchin 2020 their fig. 13). The early Cenomanian transgressive deposits are overlain by two coarsening-upward successions separated by a high order flooding surface in borehole HB-C1, and these represent a period when sedimentation outpaced the RSL rise (Fig. 2). In both basins, the coarsening-upward units in the boreholes are associated, in the seismic lines, with prograding clinoforms, which downlap on the Top Albian MRS. Taken together, the prograding clinoforms and the coarsening-upward units indicate a normal regressive (likely HST) shoreline during the Cenomanian.

The Cenomanian succession is truncated by a low order erosional boundary (15At1), which in some places erodes into the syn-rift sequence (Fig. 16a). Overall, this suggests that the Cenomanian succession was deposited during normal regression and thus represents a HST that formed when the shelf was dominated by sand deposition and the more distal parts of the basin were dominated by suspension settling (i.e., shales and clays; Fig. 2). Although the origin of the Late Cretaceous event is still unclear, it has been linked with thermal subsidence in the distal part of the basin, uplift in the shelf and forced regression of the shoreline (e.g., Malan 1993; Baby et al. 2018). At this time, the shelf area was severely scoured, and at least in the Gamtoos Basin, bypass channels were generated (Fig. 16a). There are clear downlaps on a surface that might be interpreted as a basal surface of forced regression towards the shelf edge/slope (Fig. 16a; *sensu* Hunt and Tucker 1992, 1995; Posamentier and Allen 1999). The Top Cenomanian SU is joined with a correlative conformity (*sensu* Hunt and Tucker 1992, 1995) towards the shelf edge (Fig. 16). This correlative conformity is visible on the 2D seismic lines on the slope and is associated with RSL fall. The nature of

the 15At1 unconformity is similar to the Hauterivian 131At surface, and thus, again, basin floor fans were likely deposited during this phase of forced regression from the Turonian to Santonian (Fig. 12f; Hodgson et al. 2018 their fig. 10b).

Post-Cenomanian to Lower Cenozoic

In contrast to the transitional phase, where scoured out canyons are filled by deposits of the LST evidence for normal regressive deposits on the shelf, above Top Cenomanian unconformity, is lacking. This could either be due to the sediments being too thin and thus below seismic resolution or having been eroded during the subsequent transgression. However, evidence of prograding strata downlapping on the Top Cenomanian reflector in the slope suggests that the LST was preserved basinwards. On the shelf, the Upper Cretaceous succession shows evidence for progradation and downlap on the Top Campanian MRS, while evidence of onlapping is observed in the slope and shelf edge regions (Fig. 17a). Whilst the Base Cenozoic reflector does not appear to be erosional in the Algoa Basin, the seismic data (Fig. 17a) in the Gamtoos Basin shows some evidence for minor erosion, especially in the proximal areas. Alternatively, this supposed erosional feature could be toplaps, indicating the depositional limits of clinoforms in the updip area. Borehole data in the Gamtoos Basin show coarsening-upward clean sands, while the Algoa Basin is dominated by retrogradational strata. These observations may suggest that the Base Cenozoic reflector marks a MFS that is underlain by transgressive deposits in the Algoa Basin, and a MRS that is underlain by a HST in the Gamtoos Basin (Figs. 2 and 10a). This sequence cyclicity is similar to the Albian period, when the basin experienced increased accommodation space and high sedimentation (i.e., TST-HST-TST; e.g., Galloway 1989; Catuneanu 2019a his fig. 3, 2019b). Moreover, the increasing accommodation space is a likely low order event, which occurred on a regional scale.

Lower to Middle Cenozoic

Wireline data from borehole HB-C1 record silty clays at the base of the succession, which probably formed during the Late Cretaceous/Lower Cenozoic transgression in the Algoa Basin. The flooding surface associated with this transgression is overlain by prograding sands in borehole HB-C1. These sandy facies are also observed in the borehole HA-A1 in the Gamtoos Basin. This indicates increased sediment supply into the basins and a regressive shoreline. In both basins, seismic reflectors are predominantly prograding and downlapping onto the Lower Cenozoic MRS in the Gamtoos Basin and MFS in the Algoa Basin. These observations suggest that this interval was deposited as a HST in the Gamtoos Basin and TST in the Algoa Basin, until the basin was tilted (Fig. 2; Hattingh 2001; Baby et al. 2018) during the late Paleogene. The basin tilting event, which uplifted the shelf, resulted in a forced regression, which pushed the shoreline to the shelf edge, resulting in deposition in the distal basin and bypass on the shelf. Towards the shelf edge in the Algoa Basin, a correlative conformity in the distal setting joining with the low order SU is tentatively expected, where the underlying rock units prograde and downlap onto the basal surface of forced regression. These

observations are consistent with the predictions of the depositional sequence IV model. This means, at this period, the eroded shelfal sediments were deposited basinwards, probably as floor fans (Fig. 12c). Although there is great potential for reservoir development in the distal setting, the depth to burial of these reservoirs is very shallow limiting hydrocarbon prospectivity. Similar to the 15At1 sequence boundary in the late Cenomanian (Fig. 2), the Mid-Cenozoic unconformity is overlain by prograding Miocene clinoforms in the slope region, indicating the distal limits of the shoreline during the normal regression that ensued after the uplift and erosion in the Eocene and Oligocene. Although onshore Algoa Basin outcrop studies (e.g., Le Roux 1987, 1989, 1990; Illenberger 1992; Hattingh 2001) show evidence for several high order transgressive and regressive cycles from the late Miocene to Holocene, corresponding to an overall RSL change of over 300 m (see Hattingh 2001 his fig. 5.1), the limited resolution of the current dataset does not allow the identification of these cycles (i.e., their stacking patterns, associated key stratigraphic surfaces; e.g., Catuneanu 2019a; Catuneanu and Zecchin 2020). Nonetheless, the offshore equivalent of these outcrops is shown as prograding clinoforms, which correspond to the clean coarsening-upward sands (e.g., boreholes HB-C1 and HA-A1) that were probably deposited during a low order regression (likely HST) phase in the post-Miocene.

Conclusions

Depositional models in this study, which encompasses the Algoa and Gamtoos Basins of South Africa, are based on a vintage dataset that is in dire need for further reprocessing in order to improve imaging, especially for the syn-rift section. Although the data quality varies from poor to moderate, the integration of different datasets into the stratigraphic framework provided reasonable insights for the generation of GDE maps and interpretation of the overall geological history of the shoreline's movement in this region. The dataset in the Gamtoos Basin suggest a marine incursion following the onset of rifting as early as the early Middle Jurassic. This inference is supported by recent radioisotopic dating in the region (Muir et al. 2020) as well as the postulation of a pre-Tithonian mid-ocean ridge succession near the Falkland Plateau Basin (Schimschal and Jokat 2019), which was nearby prior and during the early phases of Gondwana breakup. This marine incursion also suggests that the sedimentation in the southern Cape was influenced by marine processes and relative sea level changes since early syn-rift phase.

Three main depositional sequences are identified in the study area encompassing the Algoa and Gamtoos Basins of South Africa. The first regional succession is a syn-rift sequence, which is bound by an Early Jurassic subaerial unconformity at the base and the second-order Valanginian maximum flooding surface at the top. The sequence is made up of third and fourth-order transgressive and regressive cycles in the marine sector and formed during the diachronous advancement (transgression) of relative sea-level until the late Valanginian second-order maximum flooding surface. Well-established stratigraphic models are difficult to apply for the continental sector of the syn-rift sequence, and thus far, the best fitting model for the current stratigraphic framework is a modified version of the genetic sequence model. The second regional succession is the post-rift low-order sequence 1, which is bound at the base by a major third-order Hauterivian unconformity (surface 13At1) at the base and the late third-order Cenomanian unconformity (surface 15At1) at the top. Unconformably overlying the post-rift sequence 1, the third and final regional

succession is the post-rift order-order sequence 2 that is bound by the third order-Mid-Cenozoic (Eocene) unconformity at the top. All major forced regressive periods appear to be tectonically triggered. The post-rift sequence contains several high-order systems tracts that can be identified as FSST-LST-TST-HST (Hunt and Tucker 1992; 1995; Plint and Nummedal 2000; Catuneanu 2002, 2019a, b) contained within the low-order boundaries. Although, these sequences are bound by subaerial unconformities, some intervals within them are bound by flooding and regressive surfaces (i.e., the Campanian to Lower Cenozoic succession; Galloway 1989; Catuneanu 2019a, b). In these flooding-surface-bound third- or even fourth-order successions, the T-R sequence model (sensu Embry and Johannessen 1992; Embry 1993) is valid.

This shows, yet again, that these sequence models are more sensitive to depositional scale (also see the Sedimentation Rate Scale concept in Miall 2015; Catuneanu 2019a, b). Thus, this level of the stratigraphic framework can be explained with the concept of scale in sequence stratigraphy (Catuneanu 2019a), where; 1) system tracts form at any scale (i.e., are independent of scale). 2), stratigraphic bounding surfaces should not be limited to just low order subaerial unconformities (*sensu* depositional model II, III, IV), but to surfaces that bound genetically related successions (Catuneanu 2019a, 2020). This is because low order flooding surfaces (MFS and MRS - *sensu* genetic and T-R sequence models) can be contained within subaerial unconformity bound depositional sequence models. Therefore, when applying sequence models, it is important to consider the resolution of the successions within the regional stratigraphic framework, because certain models are more scale dependent than others.

Data availability All dataset generated for this study are included in the article.

Acknowledgments We are grateful to Chris Malaver, David Holmes, Richard Paterson, Gerhard Brinks, Duncan Barkwith and Richard Harris for reviewing various drafts of this manuscript. We also like to thank Petroleum Agency SA for permission to publish this dataset.

Funding information Funding for the project's dataset was provided by REI fund of the Geological Society of South Africa. The dataset was purchased from Petroleum Agency SA.

Compliance with ethical standards Not applicable

Conflict of interest The authors declare that they have no conflict of interest, and that the research was conducted in the absence of any commercial or financial relationships that could be construed as a potential conflict of interest.

Author contributions This paper was developed from the PhD's thesis by MHM. EMB conceptualized idea for research, designed the project, and as the project leader advised MHM during the research. MHM was responsible for data processing, analysis and interpretation, and drafted the initial figures of the manuscript. Both authors performed critical writing and revision of the manuscript for important intellectual content and approved the final manuscript.

References

Africa Energy Corp (2020) Oil and Gas Exploration in Africa, Operations, South Africa, Block 11b/12b https://www.africaenergycorp.com/operations/south-africa-block-11b-12b/ accessed 07 December 2020

Almond JE (2012) Proposed Jachtvlakte Precinct Human Settlement Plan, Nelson Mandela Bay Municipality, Eastern Cape. Natura Viva c,Palaeontological Assessment: Combined Desktop and Scoping Study: 22p

Ayodele O, Chatterjee T, and Donker JVB (2020) Seismic Stratigraphic Analyses of Early Cretaceous (Valanginian) Sediments of Gamtoos Basin, Offshore South Africa. Int j sci: basic appl res, 26(1): 1–14

Baby G, Guillocheau F, Boulogne C, Robin C, Dall'Asta M (2018) Uplift history of a transform continental margin revealed by the stratigraphic record: The case of the Agulhas transform margin along the Southern African Plateau. Tectonophysics 731: 104–130

Bate KJ, Malan JA (1992) Tectonostratigraphic evolution of the Algoa, Gamtoos and Pletmos Basins, offshore South Africa. In: De Wit MJ, Ransome IGD (eds) Inversion Tectonics of the Cape Fold Belt, Karoo ad Cretaceous Basins of Southern Africa. Balkema, Rotterdam, pp. 61–73

Ben-Avraham Z, Hartnady CJH, Malan JA (1993) Early tectonic extension between the Agulhas Bank and the Falkland Plateau due to the rotation of the Lafonia microplate. Earth Planet Sci Lett, 117: 43–58

Bosence DWJ (1998) Stratigraphic and sedimentological models of rift basins. In: Purser, B.H., Bosence, D.W.J. (eds) Sedimentation and Tectonics of Rift Basins Red Sea – Gulf of Aden. Springer, Dordrecht, pp. 630

Broad DS (1990) Petroleum geology of the Gamtoos and Algoa Basins. Geol Soc S Afr, Geocongress 90: 60–63

Broad DS, Jungslager EHA, McLachlan IR, Roux J, van der Spuy D (2012) South Africa's offshore Mesozoic basins. Phanerozoic Passive Margins, Cratonic Basins and Global Tectonic Maps. Elsevier, pp. 535–560

Brown LF Jr, Benson JM, Brink GJ, Doherty S, Jollands A, Jungslager EHA, Keenan JHG, Muntingh A and Van Wyk NJS (1995) Sequence stratigraphy, in offshore South African divergent basins. An atlas on exploration for Cretaceous lowstand traps by Soekor (Pty) Ltd. Am Assoc Pet Geol Stud Geol: 41

Burgess MP, Allen AP Steel RJ (2016) Introduction to the future of sequence stratigraphy: evolution or revolution? J Geol Soc 173: 801–802

Caku N, Gwavava O, Liu K and Baiyegunhi C (2020) An integration of magnetic, gravity and seismic data in Evaluating the Algoa Basin in the Eastern Cape Province of South Africa for stratigraphic and structural geodynamics. Pure and Applied Geophysics 177; 4177–4205

Catuneanu O (2002). Sequence stratigraphy of clastic systems: concepts, merits, and pitfalls. J Afr Earth Sci 35, 1–43

Catuneanu O (2006) Principles of sequence stratigraphy, Elsevier

Catuneanu O (2019a) Model-independent sequence stratigraphy. Earth Sci Rev 188: 312–388

Catuneanu O (2019b) Scale in sequence stratigraphy. Mar Pet Geo 106: 128–159

Catuneanu O, Galloway WE, Kendall C, Miall A, Posamentier HW, Strasser A, Tucker M E (2011) Sequence stratigraphy: methodology and nomenclature. Newsl Stratigr 44/3: 173–245

Catuneanu O, Zecchin M (2020) Parasequences: Allostratigraphic misfits in sequence stratigraphy. Earth Sci Rev, pp.103289

Christie-Blick N (1991) Onlap, offlap, and the origin of unconformity-bounded depositional sequences. Mar Geo 97:35–56

Chorowicz J (2005) The East African rift system. J Afr Earth Sci 43: 379–410

De Wit MJ (1992) The Cape Fold Belt: a challenge for an integrated approach to inversion tectonics. In: De Wit MJ, Ransome IGD (eds) Inversion Tectonics of the Cape Fold Belt, Karoo ad Cretaceous Basins of Southern Africa. Balkema, Rotterdam, pp. 3–14

Du Toit SR (1979) The Mesozoic history of the Agulhas Bank in terms of plate tectonic theory. Geokongres 77. Spec Publ Geol Soc S Afr 6: 197–203

Dingle RV, Siesser WG, Newton AR (1983) Mesozoic and Tertiary Geology of Southern Africa. A.A. Balkema, Rotterdam, 375 pp

Embry AF, Johannessen E, Owen D, Beauchamp B, Gianolla P (2007) Sequence stratigraphy as a "concrete" stratigraphic discipline. Report of the ISSC Task Group on Sequence Stratigraphy

Embry AF (2009) Practical sequence stratigraphy. Can Soc Petroleum Geo Online at www.cspg.org, 81

Galloway WE (1989) Genetic stratigraphic sequences in basin analysis. I. Architecture and genesis of flooding-surface bounded depositional units. Am Assoc Pet Geol Bull 73; 125–142

Embry AF, Johannessen EP (1992) T–R sequence stratigraphy, facies analysis and reservoir distribution in the uppermost Triassic-Lower Jurassic succession, western Sverdrup Basin, Arctic Canada. In: Vorren TO, Bergsager E, Dahl-Stamnes OA, Holter E, Johansen B. Lie E, Lund TB (eds) Arctic Geology and Petroleum Potential. Norw Petrol Soc Spec Pub 2: 121-146

Falvey DA (1974) The development of continental margins in plate tectonic theory. J Aust Pet Explor Ass 14: 95-106

Feder J (2019) Offshore: making a comeback after the downturn. J Pet Technol 71: 27–31

Frazier DE (1974) Depositional episodes: their relationship to the Quaternary stratigraphic framework in the north western portion of the Gulf basin. Geological Circular. University of Texas at Austin, Bureau of Economic Geology 1: 28

Hattingh J (2001) Late Cenozoic drainage evolution in the Algoa Basin with special reference to the Sundays River Valley. Council for Geoscience, Bulletin 128: 141 pp

Haq BU, Hardenbol J, Vail PR (1987) Chronology of fluctuating sea levels since the Triassic. Science 235: 1156–1166

Helland-Hansen W, Gjelberg JG (1994) Conceptual basis and variability in sequence stratigraphy: a different perspective. Sed Geo 92: 31–52

Hodgson DM, Browning JV, Miller KG, Hesselbo SP, Poyatos-More M, Mountain G S (2018) Sedimentology, stratigraphic context, and implications of intrashelf bottomset deposits, offshore New Jersey. Geosphere 14: 95–114

Holz M, Vilas-Boas DB Troccoli EB, Santana VC, Vidigal-Souza PA (2017) Conceptual models for sequence stratigraphy of continental rift successions. Stratigraphy & Timescales 2: 119–186

Hong S, Bradshaw CJ, Brook BW (2015) Global zero-carbon energy pathways using viable mixes of nuclear and renewables. Appl Energy 143: 451–459

Hunt D, Tucker ME (1992) Stranded parasequences and the forced regressive wedge systems tract: deposition during base-level fall. Sed Geo 8: 1–9

Hunt D, Tucker ME (1995) Stranded parasequences and the forced regressive wedge systems tract: deposition during base-level fall – reply. Sed Geo 95: 147–160

Illenberger WK (1992) Lithostratigraphy of the Schlemm Hoek formation (Algoa Group). Inst Coastal Research, University of Port Elizabeth

Jungslager EHA (1996) Geological Evaluation of the Remaining Prospectivity for Oil and Gas of the Pre-1At1 "Synrift" Succession in Block 9, Republic of South Africa. Unpublished SOEKOR Rep, 63 pp

Johnson JG, Murphy MA (1984) Time-rock model for Siluro-Devonian continental shelf, western United States. Geol Soc Am Bull 95:1349–1359

Koopmann H, Franke D, Schreckenberger B, Schulz H, Hartwig A, Stollhofen H, di Primio R (2014) Segmentation and volcano-tectonic characteristics along the SW African continental margin, South Atlantic, as derived from multichannel seismic and potential field data. Mar Pet Geo 50: 22–39

Le Roux FG (1990) Palaeontological correlation of Cenozoic marine deposits of the southeastern, southern and western coasts, Cape Province. S Afr J Geo 93(3): 514–518

Le Roux FG (1989) The lithostratigraphy of Cenozoic deposits along the south-east Cape coast as related to sea-level changes. Doctoral dissertation, Stellenbosch: Stellenbosch University

Le Roux FG (1987) Lithostratigraphy of the Alexandria Formation. S Afr Committee Stratigraphy (SACS), Lithostratigraphic Series: 1, 1–18

Lovecchio JP, Rohais S, Joseph P, Bolatti ND, Ramos VA (2020) Mesozoic rifting evolution of SW Gondwana: A poly-phased, subduction-related, extensional history responsible for basin formation along the Argentinean Atlantic margin. Earth Sci Rev 203: 103138

Malan JA (1993) Geology, potential of Algoa, Gamtoos Basins of South Africa. Oil & Gas Journal. Soekor (Pty.) Ltd.

Malan JA, Martin AK, Cartwright JA (1990) The structural and stratigraphic development of the Gamtoos and Algoa Basins, offshore South Africa. Geol Soc of S Afr 90:328–331

Martin AK, Hartnady CJH, Goodlad SW (1981) A revised fit of South America and South-Central Africa. Earth Planet Sci Lett 54: 293-305

Martin AK, Hartnady CJH (1986) Plate tectonic development of the south west Indian Ocean: A revised reconstruction of East Antarctica and Africa. J Geophys Res 91: 4767-4786

Martins-Neto MA, Catuneanu O (2010) Rift sequence stratigraphy. Mar Pet Geo 27: 247–253

McLachlan IR, McMillan IK (1976) Review and stratigraphic significance of southern Cape Mesozoic palaeontology. Trans Geol Soc S Afr 79: 197–212

McMillan IK (2003) The Foraminifera of the Late Valanginian to Hauterivian (Early Cretaceous) Sundays River Formation of the Algoa Basin, Eastern Cape Province, South Africa. Ann S Afr Mus 106: 1–274

McMillan IK, Brink GJ, Broad DS, Maier JJ (1997) Late Mesozoic sedimentary basins off the south coast of South Africa. In Selly, R.C. (ed), African Basins, Sedimentary Basins of the World. Elsevier, Amsterdam, 319–376

McMillan IK (2010) The Foraminifera of the Portlandian (Late Jurassic) Bethelsdorp Formation of the Onshore Algoa Basin, Eastern Cape Province. Les Rosalines Press, Clovelly, 176

Miall AD (2015) Updating uniformitarianism: stratigraphy as just a set of 'frozen accidents'. In: Smith DG, Bailey RJ, Burgess PM, Fraser AJ (eds) Strata and time: Probing the gaps in our understanding. Geol Soc London Spec Publ 404: 11–36

Miall AD, Strasser A (2018) Standards for publications in the field of basin analysis. Earth Sci Rev: 177, 1

Muir RA (2019) Recalibrating the breakup history of SW Gondwana: the first U-Pb chronostratigraphy for the Uitenhage Group, South Africa

Muir R, Bordy EM, Prevec R (2015) Lower Cretaceous deposit reveals first evidence of a post-wildfire debris flow in the Kirkwood Formation, Algoa Basin, Eastern Cape, South Africa. Cret Res 56: 161–179

Muir R, Bordy EM, Reddering JSV, Viljoen JHA (2017a) Lithostratigraphy of the Enon Formation (Uitenhage Group), South Africa. Geol Soc of S Afr 120: 273–280

Muir R, Bordy EM, Reddering JSV, Viljoen JHA (2017b) Lithostratigraphy of the Kirkwood Formation (Uitenhage Group), including the Bethelsdorp, Colchester and Swartkops Members, South Africa. Geol Soc of S Afr 120: 281–293

Muir R, Bordy EM, Mundi R, Frei D (2020) Recalibrating the breakup history of SW Gondwana: U–Pb radioisotopic age constraints from the southern Cape of South Africa. Gondwana Res 84, 177–19.

Nádor A, Sztanó, O (2011) Lateral and vertical variability of channel belt stacking density as a function of subsidence and sediment supply: field evidence from the intramountaine Körös Basin, Hungary. SEPM Spec Publ 97: 75–392

Neal JE, Risch D, Vail P (1993) Sequence stratigraphy-a global theory for local success. Oilfield Rev 5: 51-62

Neal JE, Abreu V (2009) Sequence stratigraphy hierarchy and the accommodation succession method. Geology 37: 779–782

Neal JE, Abreu V, Bohacs K M, Feldman HR, Pederson KH (2016) Accommodation succession (δA/δS) sequence stratigraphy: observational method, utility and insights into sequence boundary formation. J Geol Soc 173: 803–816

Paton AD, Underhill JR (2004) Role of crustal anisotropy in modifying the structural and sedimentological evolution of extensional basins: the Gamtoos Basin, South Africa. Basin Res 16: 339–359

Platon C (2017) Guyana-Suriname Basin, South America: Hot Ultra-Deepwater Exploration Opportunities and Liza Field: Worldwide Largest 2015–2016 Hydrocarbon Discovery. AAPG Annual Convention and Exhibition, Houston, Texas, April 2-5, 2017

Plint AG, Nummedal D (2000) The falling stage systems tract: recognition and importance in sequence stratigraphic analysis. In: D. Hunt and R. Gawthorpe (eds) Sedimentary Responses to forced regressions. Geol Soc Spec Publ 172: 1–17.

Posamentier HW, Allen GP (1999) Siliciclastic sequence stratigraphy: concepts and applications. SEPM Concepts in Sedimentology and Paleontology 7: 210 pp

Posamentier HW, Jervey MT, Vail PR (1988) Eustatic controls on clastic deposition. I. Conceptual framework. In: Wilgus CK, Hastings BS, Kendall CGStC, Posamentier HW, Ross CA, Van Wagoner JC (eds) Sea Level Changes—An Integrated Approach. SEPM Spec Publ 42: 110-124

Prosser S (1993) Rift-related linked depositional systems and their seismic expression. In: Williams, G.D., Dobb, A. (eds) Tectonics and seismic sequence stratigraphy. Geol Soc London Spec Publ 71: 35–66

Schimschal C M Jokat, W (2019) The Falkland Plateau in the context of Gondwana breakup. Gondwana Res 68: 108-115

Shone RW (2006) Onshore post-Karoo Mesozoic deposits. In: Johnson MR, Anhaeusser CR, Thomas RJ (eds) The Geology of South Africa. Geol Soc of S Afr, Johannesburg and CGS, Pretoria: 541–571

Shone RW (1978) A case for lateral gradation between the Kirkwood and Sundays River Formations, Algoa Basin. Trans Geol Soc of S Afr 81: 319–326.

Shone RW (1976) The sedimentology of the Mesozoic Algoa Basin. Unpublished M.Sc. thesis, University of Port Elizabeth: 48p

Singh V, Brink, GJ and Winter HDLR (2005) New interpretation reveals potential in onshore Algoa basin, South Africa. Oil and Gas J 103(1): 34–39.

Stevenson IR, McMillan IK (2004) Incised valley fill stratigraphy of the Upper Cretaceous succession, proximal Orange Basin, Atlantic margin of southern Africa. J Geol Soc Lond 161: 185–208

Thompson JO, Moulin M, Aslanian D, de Clarens P, Guillocheau F (2019) New starting point for the Indian Ocean: Second phase of breakup for Gondwana. Earth-Sci. Rev. 191: 26–56

Thomson K (1999) Role of continental break-up, mantle plume development and fault reactivation in the evolution of the Gamtoos Basin, South Africa. Mar Pet Geo 16: 409–429

Vail PR, Todd RG, Sangree JB (1977) Seismic stratigraphy and Global Changes of Sea Level: Part 5. Chronostratigraphic Significance of Seismic Reflections: Section 2. Application of Seismic Reflection Configuration to Stratigraphic Interpretation 26: 99–116

Vail PR, Audemard F, Bowman SA, Eisner PN, Perez-Cruz C (1991) The stratigraphic signatures of tectonics, eustasy and sedimentology – an overview. In: Einsele G, Ricken W, Seilacher A (eds), Cycles and Events in Stratigraphy. Springer–Verlag: 617–659

Van Wagoner J C, Posamentier HW, Mitchum RM Jr, Vail PR, Sarg JF, Loutit TS, Hardenbol J (1988) An overview of sequence stratigraphy and key definitions. In Sea Level Changes–An Integrated Approach. In: Wilgus CK, Hastings BS, Kendall CGStC, Posamentier HW, Ross CA, Van Wagoner JC (eds) Sea Level Changes—An Integrated Approach. SEPM Spec Publ 42: 39–45

Van Wagoner JC, Mitchum RM Jr, Campion KM, Rahmanian VD (1990) Siliciclastic sequence stratigraphy in well logs, core, and outcrops: concepts for high-resolution correlation of time and facies. APPG Methods in Exploration Series 7: 55